Polymeric Particulate Systems for Immunotherapy of Cancer

Sima Rahimian

2015

Polymeric Particulate Systems for Immunotherapy of Cancer

Sima Rahimian

2015

Polymeric Particulate Systems for Immunotherapy of Cancer

The printing of this thesis was financially supported by

Utrecht Institute for Pharmaceutical Sciences, Utrecht, The Netherlands

Polymeric Particulate Systems for Immunotherapy of Cancer

ISBN: 978-903-93-6371-3

Cover photo: Sima Rahimian
Cover design: Sima Rahimian and Tomas E. Coomans

Printed by CPI Koninklijke Wöhrmann Print Service

This research was supported by Center for Translational Molecular Medicine (CTMM), Cancer Vaccine Tracking project (#030-302).

Polymeric Particulate Systems for Immunotherapy of Cancer

Polymere Deeltjessystemen voor Immunotherapie van Kanker
(met een samenvatting in het Nederlands)

Proefschrift

ter verkrijging van de graad van doctor aan de Universiteit Utrecht op gezag van de rector magnificus, prof. dr. G.J. van der Zwaan, ingevolge het besluit van het college voor promoties in het openbaar te verdedigen op woensdag 8 juli 2015 des middags te 12.45 uur

door

Sima Rahimian

geboren op 21 september 1982
te Sari, Iran

Promotoren:	Prof. dr. ir. W. E. Hennink
	Prof. dr. F. A. Ossendorp
Copromotor:	Dr. M. Amidi

To know and to die or not to know and to die?!

Aburayhan Biruni

Contents

CHAPTER 1

General Introduction

Cancer treatment

Conventional cancer treatment modalities such as chemotherapy target not only tumor cells but all rapidly dividing cells which causes toxicity and other adverse effects. Therefore, there is a great need for novel tumor-specific and potent cancer treatment strategies. Immunotherapy offers more specific and therefore potentially less toxic alternative approaches for the treatment of cancer. Immunotherapy relies on strategies to manipulate the immune system to enhance or block an immune response to fight cancer [1]. Immunotherapeutic strategies are not only employed to confront malignancies, but also for the treatment of allergies [2] and viral diseases such as HIV infection [3].

Numerous immunotherapy strategies have been investigated with promising clinical results including:

1-Peptide and protein based cancer vaccines [4,5] including dendritic cell(DC)-based vaccine e.g. the first FDA approved therapeutic cancer vaccine against prostate cancer (Provenge), where DCs of the patient are activated with the tumor antigen and re-administered to the patient [6].

2-Immunomodulatory antibodies such as immune check point blockers, (FDA approved ipilimumab (antiCTLA4) [7] and lambrolizumab (antiPD1) [8]) and immunostimulatory antibodies such as antiCD40 and antiOX40 [9].

3-Antibodies that target tumor cells such as antiHER2 [10]

4-Adoptive transfer of B/T/NK cells [11-14].

The potential of immunotherapy lies in the fact that our body's immune system is capable of identifying and killing foreign cells. Nevertheless cancer cells use several mechanisms to evade the immune system [15]. To oppose immune-evading mechanisms and induce a potent immune response, immunotherapeutic approaches in combination with well-defined adjvants have been used to achieve a potent immune response [16].

Currently in cancer immunotherapy clinical trials, mainly relatively simple adjuvant systems such as emulsions are used as delivery systems. These emulsions (such as incomplete Freund's adjuvant (IFA), Montanide and MF59) are based on mineral oils and form a depot at the injection site providing sustained release of their cargo [17-19]. However, these emulsions are pharmaceutically not well-defined formulations and suffer from stability issues and poor control over release kinetics [20-22]. Additionally, the administration of IFA and Montanide emulsions is accompanied with severe adverse and long-lasting side effects. Development of well-defined pharmaceutical formulations is therefore urgently needed and crucial for the success of immunothepy.

Particulate systems for immunotherapy

Delivery of biotherapeutics such as protein and peptides is challenging due to their low stability, including sensitivity of these macromolecules to degradation and the importance of their 3D structure for their function and biological activity. To address these challenges, it is important to develop biocompatible carrier systems that are capable of delivering an effective dose of the biotherapeutic at the desired site, while protecting the cargo from enzymatic degradation upon administration and therefore increasing the efficacy and reducing the side effects [23-25].

One of the extensively used systems are biodegradable polymers, particularly aliphatic polyesters such as poly(lactic-co-glycolic) acid (pLGA), poly lactic acid (pLA) and poly ε-caprolactone (pCL). Among these polymers, pLGA is one of the most frequently investigated biodegradable polymers that has been used for several applications from sutures to delivery of biotherapeutics, including peptides, proteins and nucleic acids [26-28] as well

as vaccine formulations [16,29-31].
Advantages of using particulate drug delivery systems based on polymers such as pLGA for immunotherapy include protection of the cargo, ability to decorate the surface of the particles with ligands for imaging and targeting purposes and co-delivery of multiple immunotherapeutics including adjuvants, as well as sustained and controlled delivery of the antigen. Moreover, the size of the particulate system can be optimized to achieve optimal uptake by the antigen presenting cells (APCs) especially DCs or even target certain subsets of DCs. Additionally, in some cases it is important that the particles are not taken up by APCs and this can be achieved by preparing particle with a size larger than 10 μm [32]. These features of pLGA-based particulate carriers as well as various examples of particulate based immunotherapeutic formulations are reviewed in **Chapter 2**.

pLGA vs pLHMGA

One of the main pitfalls of using pLGA as a delivery system is the incomplete release of the cargo [29,33]. Upon degradation of pLGA, lactic and glycolic acid as well as water-soluble oligomers of these monomers are formed. Accumulation of these acidic degradation products results in pH drop inside the polymeric matrix which in turn might result in aggregation, chemical modification such as acylation, loss of activity and incomplete release [24,34]. These drawbacks result in weak response and can cause unwanted immunogenic reactions and other adverse effects [23,35].
To overcome the disadvantages of pLGA and similar polymers, functionalized polyesters with enhanced hydrophilicity have been developed [36]. High water uptake results in relatively fast degradation rates. additionally, the acidic degradation products rapidly diffuse out resulting in a close-to-neutral pH inside the degrading particle matrix. One example is poly(lactide-co-hydroxymethyl glycolide) (pLHMGA) (**Figure 1**) developed in our group. This polymer has a similar backbone as pLGA, however, it possesses pendant hydroxyl groups which make it more hydrophilic than pLGA. Earlier studies showed that the degradation of pLHMGA with variable monomer ratios can be tailored from a few days to two months [37]. Nano- and microparticulate delivery systems based on this polymer loaded with peptide and proteins were prepared and exhibited tailorable degradation and release characteristics. In these studies, pLHMGA has shown better protein/peptide compatibility as well as complete release of proteins/peptides as compared to pLGA [38-40]. Additionally, good *in vitro* cytocompatibility and *in vivo* biocompatibility upon subcutaneous injection of pLHMGA particles have been observed [41].

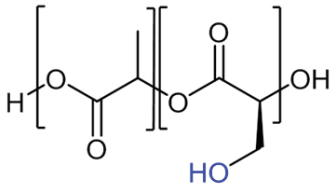

Figure 1. poly(lactic-co-hydroxymethyl glycolic acid) (pLHMGA)

Aim of the current thesis

Given the superior features of pLHMGA particles as delivery systems and the need for development of pharmaceutically-defined and safe alternatives for commonly used emulsion formulations, particulate systems based on pLHMGA were developed in this thesis as potential biocompatible carriers either as a **cancer vaccine** or for **delivery of immunomodulatory antibodies**.

This project was part of a bigger research program conducted by Center for Translational Molecular Medicine (CTMM) entitled "Cancer Vaccine Tracking". This project aimed at development of several immunotherapeutic formulations and tracking them *in vivo* using near-infrared labels as well as optimization of these formulations to achieve potent formulations for clinical translation.

Cancer vaccines aim to deliver tumor-specific antigens and adjuvants to APCs, particularly DCs. As a result, stimulated DCs activate tumor-specific CD8+ T cells which subsequently eradicate the tumor. To induce CD8+ T cell responses, the antigen should be processed and presented by mature DCs to T cells via MHC class I molecules (cross-presentation) [42]. Weak immunogenicity of soluble antigens and adjuvants, stability and toxicity issues encouraged the development of particulate cancer vaccines. Encapsulation in nanoparticles promotes cross-presentation and enables co-delivery of adjuvants to induce DC maturation [42,43]. In recent years several types of antigens have been studied for use in cancer vaccines ranging from short peptides consisting of MHC class I/II epitopes of tumor antigens to protein antigens, cell lysates and DNA encoding tumor antigens [44]. Recent studies have introduced a category of tumor antigens called synthetic long peptides (SLPs) [45] which are usually overlapping 15-35 amino acid peptides that cover the sequence of a tumor antigen. SLPs are more efficiently processed by DCs and induce a stronger T cell immune response as compared to protein antigens. Vaccination with SLPs based on human papillomavirus oncoproteins (HPV16 E6 and E7) has shown promising results in clinical trials [19,22,46].
In the current thesis, first, the model antigen ovalbumin was encapsulated in pLHMGA nanoparticles and the kinetics of the vaccine drainage to the lymph nodes and its immunogenicity were studied *in vivo* after subcutaneous (s.c.) administration. Following the promising results of human papillomavirus (HPV) SLPs in clinical trials, the therapeutic efficacy of pLHMGA nanoparticles as cancer vaccines was investigated by encapsulating a therapeutic peptide antigen, namely the human papillomavirus synthetic long peptide, and a TLR3 ligand (poly IC) in tumor-bearing mice.

Immunomodulatory antibodies regulate T cell immune response by either activation or inhibition of T cells/DCs [47]. One group of antibodies such as agonistic antiCD40, activates DCs, which in turn induces tumor-specific CD8+ T cell response [11]. Another group called immune check-point blockers such as antagonistic antiCTLA4 blocks inhibitory receptors on T cells [8-10]. Several classes of antibodies have been used in clinical trials with encouraging results [48,49]. However, systemic administration of these antibodies in their free form has been associated with systemic toxicity and momentary immune responses and autoimmunity [50,51].
To overcome these challenges, in the current study, sustained release microparticulate formulations loaded with an immune check point blocker (antiCTLA4) or a stimulatory antibody (antiCD40) were developed. These formulations were administered locally into tumor-bearing mice to provide controlled release of the antibody with the aim of achieving high therapeutic efficacy and preventing systemic toxicity and autoimmunity.

It was further hypothesized that these nano- and microparticulate carrier systems increase the efficacy of the treatment and limit the toxicity associated with administration of soluble therapeutics as well as with conventional adjuvant/delivery systems.

Outline of this thesis

Chapter 2 is an overview of particulate formulations based on aliphatic polyesters in cancer immunotherapy. To overcome challenges facing successful immunotherapy such as immunosuppression and tolerance, particulate systems have been suggested as a useful tool. It is shown in a number of publications that particulate systems indeed increase the therapeutic efficacy and reduce toxicity. In this review, we address the potential of pLGA-based particulate formulations for immunotherapy of cancer.

In **Chapter 3** the feasibility of pLHMGA nanoparticles loaded with ovalbumin as model vaccine was investigated. Ovalbumin and the polymer were labeled with two different near-infrared dyes to enable the *in vivo* tracking of both the antigen and the delivery system simultaneously. The ability of the formulation to enhance sentation and T cell proliferation was studied *in vitro* and *in vivo* and compared to soluble ovalbumin.

Chapter 4 describes preparation and preclinical evaluation of a cancer vaccine formulation for treatment of human papillomavirus (HPV)-induced malignancies. A synthetic long peptide (SLP) derived from HPV16 E7 oncoprotein with or without a toll like receptor 3 (TLR3) ligand (poly IC) was encapsulated in pLHMGA nanoparticles. The therapeutic efficacy of the nanoparticulate formulation was compared to that of HPV SLP and poly IC formulated in IFA in tumor-bearing mice. Finally the expansion of HPV-specific CD8+ T cells in the blood was studied in mice.

In **Chapter 5** the application of pLHMGA microparticles in local and sustained delivery of an immunostimulating antibody, antiCD40 and an immune check point blocker, antiCTLA4 was investigated. The antibody release profile of these microparticles was studied *in vitro* and the therapeutic efficacy of the particles was compared to the antitumor effect of antibody IFA emulsions in MC38 colon carcinoma tumor model. Moreover, the antibody serum levels and local reactions upon administration of these formulations were studied.

Chapter 6 studies the effect of particle size on uptake of the pLHMGA nano- and microparticles by DCs and localization of these particles within DCs. The uptake *in vitro* was compared between different particles sizes by flow cytometry analysis and the uptake rate and intracellular localization of the particles was studied by confocal microscopy. It was hypothesized that the nanoparticles are taken up to a higher extent as compared to microparticles.

Chapter 7 provides an overview of the results and discusses the major findings and conclusions of the research conducted in this thesis and provides suggestions and perspectives for the future of cancer immunotherapy with particulate systems.

References

[1] Couzin-Frankel J. Breakthrough of the year 2013. Cancer immunotherapy. Science 2013;342:1432-1433.
[2] Valenta R. The future of antigen-specific immunotherapy of allergy. Nat Rev Immunol 2002;2:446-453.
[3] Pett SL. Immunotherapies in HIV-1 infection. Current Opinion in HIV and AIDA 2009;4:188-193.
[4] Srivastava PK. Immunotherapy for human cancer using heat shock protein-peptide complexes. Curr Oncol Rep 2005;7:104-8.
[5] Tsuboi A, Oka Y, Osaki T, Kumagai T, Tachibana I, Hayashi S, et al. WT1 peptide-based immunotherapy for patients with lung cancer: Report of two cases. Microbiol Immunol 2004;48:175-184.
[6] Cheever MA, Higano CS. PROVENGE (Sipuleucel-T) in Prostate Cancer: The first FDA-approved therapeutic cancer vaccine. Clin Cancer Res 2011;17:3520-3526.
[7] Callahan MK, Wolchok JD. At the Bedside: CTLA-4-and PD-1-blocking antibodies in cancer immunotherapy. J Leukoc Biol 2013;94:41-53.
[8] McDermott J, Jimeno A. Pembrolizumab: PD-1 inhibition as a therapeutic strategy in cancer. Drugs of today 2015;51:7-20.
[9] Aranda F, Vacchelli E, Eggermont A, Galon J, Fridman WH, Zitvogel L, et al. Immunostimulatory monoclonal antibodies in cancer therapy. Oncoimmunol 2014;3:e27297.
[10] Sapra P, Shor B. Monoclonal antibody-based therapies in cancer: Advances and challenges. Pharmacol Ther 2013;138:452-469.
[11] Gattinoni L, Powell DJ, Rosenberg SA, Restifo NP. Adoptive immunotherapy for cancer: building on success. Nat Rev Immunol 2006;6:383-393.
[12] Kershaw MH, Westwood JA, Parker LL, Wang G, Eshhar Z, Mavroukakis SA, et al. A phase I study on adoptive immunotherapy using gene-modified T cells for ovarian cancer. Clin Cancer Res 2006;12:6106-6115.
[13] Kondo H, Hazama S, Kawaoka T, Yoshino S, Yoshida S, Tokuno K, et al. Adoptive immunotherapy for pancreatic cancer using MUC1 peptide-pulsed dendritic cells and activated T lymphocytes. Anticancer Res 2008;28:379-387.
[14] Cheng M, Chen Y, Xiao W, Sun R, Tian Z. NK cell-based immunotherapy for malignant diseases. Cell Mol Immunol2013;10:230-252.
[15] Kim R, Emi M, Tanabe K, Arihiro K. Tumor-driven evolution of immunosuppressive networks during malignant progression. Cancer Res 2006;66:5527-5536.
[16] Elamanchili P, Lutsiak CME, Hamdy S, Diwan M, Samuel J. "Pathogen-mimicking" nanoparticles for vaccine delivery to dendritic cells. J Immunother 2007;30:378-395.
[17] Yang M, Yan Y, Fang M, Wan M, Wu X, Zhang X, et al. MF59 formulated with CpG ODN as a potent adjuvant of recombinant HSP65-MUC1 for inducing anti-MUC1(+) tumor immunity in mice. Int Immunopharmacol 2012;13:408-416.
[18] Bijker MS, van den Eeden SJE, Franken KL, Melief CJM, van der Burg SH, Offringa R. Superior induction of anti-tumor CTL immunity by extended peptide vaccines involves prolonged, DC-focused antigen presentation. Eur J Immunol 2008;38:1033-1042.
[19] Welters MJP, Kenter GG, de Vos van Steenwijk,Peggy J., Löwik MJG, Berends-van der Meer DMA, Essahsah F, et al. Success or failure of vaccination for HPV16-positive vulvar lesions correlates with kinetics and phenotype of induced T-cell responses. Proc Natl Acad Sci U S A 2010;107:11895-11899.
[20] Murray R, Cohen P, Hardegre.MC. Mineral-oil adjuvants - biological and chemical studies. Ann Allergy 1972;30:146-&.
[21] Graham BS, McElrath MJ, Keefer MC, Rybczyk K, Berger D, Weinhold KJ, et al. Immunization with cocktail of HIV-derived peptides in montanide ISA-51 is immunogenic, but causes sterile abscesses and unacceptable reactogenicity. PLoS One 2010;5:e11995.
[22] Kenter GG, Welters MJP, Valentijn ARPM, Lowik MJG, Berends-van der Meer DMA, Vloon APG, et al. Vaccination against HPV-16 oncoproteins for vulvar intraepithelial neoplasia. N Engl J Med 2009;361:1838-1847.
[23] Hermeling S, Crommelin DJA, Schellekens H, Jiskoot W. Structure-immunogenicity relationships of therapeutic proteins. Pharm Res 2004;21:897-903.
[24] van de Weert M, Hennink WE, Jiskoot W. Protein instability in poly(lactic-co-glycolic acid) microparticles. Pharm Res 2000;17:1159-1167.
[25] Pisal DS, Kosloski MP, Balu-Iyer SV. Delivery of therapeutic proteins. J Pharm Sci 2010;99:2557-2575.
[26] Chen M, Ouyang H, Zhou S, Li J, Ye Y. PLGA-nanoparticle mediated delivery of anti-OX40 monoclonal antibody enhances anti-tumor cytotoxic T cell responses. Cell Immunol 2014;287:91-99.
[27] Mueller M, Schlosser E, Gander B, Groettrup M. Tumor eradication by immunotherapy with biodegradable PLGA microspheres-an alternative to incomplete Freund's adjuvant. Int J Cancer 2011;129:407-416.
[28] Hamdy S, Molavi O, Ma Z, Haddadi A, Alshamsan A, Gobti Z, et al. Co-delivery of cancer-associated antigen and Toll-like receptor 4 ligand in PLGA nanoparticles induces potent CD8(+) T cell-mediated anti-tumor immunity. Vaccine 2008;26:5046-5057.
[29] Jiang G, Woo BH, Kang FR, Singh J, DeLuca PP. Assessment of protein release kinetics, stability and protein polymer interaction of lysozyme encapsulated poly (D,L-lactide-co-glycolide) microspheres. J ControlRelease 2002;79:137-145.
[30] Elamanchili P, Diwan M, Cao M, Samuel J. Characterization of poly(D,L-lactic-co-glycolic acid) based nanoparticulate system for enhanced delivery of antigens to dendritic cells. Vaccine 2004;22:2406-2412.
[31] Jiang WL, Gupta RK, Deshpande MC, Schwendeman SP. Biodegradable poly(lactic-co-glycolic acid)

microparticles for injectable delivery of vaccine antigens. Adv Drug Deliv Rev 2005;57:391-410.
[32] Conniot J, Silva JM, Fernandes JG, Silva LC, Gaspar R, Brocchini S, et al. Cancer immunotherapy: nanodelivery approaches for immune cell targeting and tracking. Front Chem 2014;2:105-105.
[33] Kim HK, Park TG. Microencapsulation of human growth hormone within biodegradable polyester microspheres: Protein aggregation stability and incomplete release mechanism. Biotechnol Bioeng 1999;65:659-667.
[34] Ding AG, Schwendeman SP. Acidic microclimate pH distribution in PLGA microspheres monitored by confocal laser scanning microscopy. Pharm Res 2008;25:2041-2052.
[35] Jiskoot W, van Schie RMF, Carstens MG, Schellekens H. Immunological risk of injectable drug delivery systems. Pharm Res 2009;26:1303-1314.
[36] Seyednejad H, Ghassemi AH, van Nostrum CF, Vermonden T, Hennink WE. Functional aliphatic polyesters for biomedical and pharmaceutical applications. J Controlled Release 2011;152:168-176.
[37] Leemhuis M, Kruijtzer JAW, van Nostrurn CF, Hennink WE. In vitro hydrolytic degradation of hydroxyl-functionalized poly(alpha-hydroxy acid)s. Biomacromolecules 2007;8:2943-2949.
[38] Liu Y, Ghassemi AH, Hennink WE, Schwendeman SP. The microclimate pH in poly(D,L-lactide-co-hydroxymethyl glycolide) microspheres during biodegradation. Biomaterials 2012;33:7584-7593.
[39] Ghassemi AH, van Steenbergen MJ, Talsma H, van Nostrum CF, Jiskoot W, Crommelin DJA, et al. Preparation and characterization of protein loaded microspheres based on a hydroxylated aliphatic polyester, poly (lactic-co-hydroxymethyl glycolic acid). J Control Release 2009;138:57-63.
[40] Ghassemi AH, van Steenbergen MJ, Barendregt A, Talsma H, Kok RJ, van Nostrum CF, et al. Controlled release of octreotide and assessment of peptide acylation from poly(D,L-lactide-co-hydroxymethyl glycolide) compared to PLGA microspheres. Pharm Res 2012;29:110-120.
[41] Kazazi-Hyseni F, Zandstra J, Popa ER, Goldschmeding R, Lathuile AAR, Veldhuis GJ, et al. Biocompatibility of poly(d,l-lactic-co-hydroxymethyl glycolic acid) microspheres after subcutaneous and subcapsular renal injection. Int J Pharm 2015;482:99-109.
[42] Shen H, Ackerman AL, Cody V, Giodini A, Hinson ER, Cresswell P, et al. Enhanced and prolonged cross-presentation following endosomal escape of exogenous antigens encapsulated in biodegradable nanoparticles. Immunol 2006;117:78-88.
[43] Serda RE. Particle platforms for cancer immunotherapy. Int J Nanomedicine 2013;8:1683-1696.
[44] Aly HAA. Cancer therapy and vaccination. J Immunol Methods 2012;382:1-23.
[45] Zwaveling S, Mota S, Nouta J, Johnson M, Lipford G, Offringa R, et al. Established human papillomavirus type 16-expressing tumors are effectively eradicated following vaccination with long peptides. J Immunol 2002;169:350-358.
[46] Kenter GG, Welters M, Lowik M, Drijfhout J, Valentijn R, Ostendorp J, et al. Therapeutic HPV 16 vaccination with long E6 and E7 peptides shows immunological and clinical efficacy. Gynecol Oncol 2008;108:S19-S19.
[47] Peggs KS, Quezada SA, Allison JP. Cancer immunotherapy: co-stimulatory agonists and co-inhibitory antagonists. Clin Exp Immunol 2009;157:9-19.
[48] Brahmer JR, Tykodi SS, Chow LQM, Hwu W, Topalian SL, Hwu P, et al. Safety and activity of anti-PD-l1 antibody in patients with advanced cancer. N Engl J Med 2012;366:2455-2465.
[49] Mellman I, Coukos G, Dranoff G. Cancer immunotherapy comes of age. Nature 2011;480:480-489.
[50] Baldo BA. Adverse events to monoclonal antibodies used for cancer therapy Focus on hypersensitivity responses. Oncoimmunol 2013;2.
[51] Fransen MF, Ossendorp F, Arens R, Melief CJM. Local immunomodulation for cancer therapy Providing treatment where needed. Oncoimmunol 2013;2:e26493.

CHAPTER 2

Particulate systems based on poly(lactic-co-glycolic)acid (pLGA) for immunotherapy of cancer

Sima Rahimian

Marieke F. Fransen

Jan Willem Kleinovink

Maryam Amidi

Ferry Ossendorp

Wim E. Hennink

Current Pharmaceutical Design 2015

In Press

Abstract

Immunotherapy of cancer is a promising therapeutic approach which aims to eliminate malignancies by inducing or enhancing an immune response against the tumor. Immunotherapy, however, faces several challenges such as local immunosuppression in the tumor area leading to immunological tolerance. To overcome these challenges, particulate formulations such as nano- and microparticles containing immunotherapeutics have been developed to increase therapeutic efficacy and reduce toxicity of immunotherapy. Particulate formulations based on biodegradable aliphatic polyesters such as poly(lactic-co-glycolic acid) (pLGA) have been extensively used with promising results. In this review, we addressed the potential of pLGA-based particulate formulations for immunotherapy of cancer. The discussion was focused on cancer vaccines and delivery of immunomodulatory antibodies. Features and drawbacks of pLGA systems were discussed together with several examples of recently developed therapeutic cancer vaccines and antibody-loaded particulate systems. Various strategies to overcome the drawbacks and optimize the formulations were given. In conclusion, pLGA-based particulate systems are attractive carriers for development of clinically acceptable formulations in immunotherapy of cancer.

Keywords: Cancer immunotherapy, pLGA, Aliphatic polyesters, Cancer vaccine, Immunomodulatory antibody, Nanoparticles, Microparticles

1. Introduction

Cancer immunotherapy is a rapidly evolving branch of cancer treatment. It involves modulation of the host's immune response to fight cancer. This is achieved by either enhancing tumor-specific T cell responses [1,2] or inhibition of the tumor-induced immune suppression [3]. Compared to conventional cancer therapies, using immunotherapy to activate the immune system against tumors brings several advantages such as specificity (specific killing), minimal toxicity, systemic immune responses enabling the identification and eradication of possible metastases, and immunological memory [4].

Methods in cancer immunotherapy and current challenges

Various strategies are followed in immunotherapy of cancer, two of which are the focus of this review; Therapeutic vaccination (cancer vaccines) and administration of immunomodulatory antibodies. Cancer vaccines target antigen presenting cells resulting in uptake and processing of tumor-specific antigens and stimulation by adjuvants to induce a long-lasting and robust tumor-specific CD8+ T cell immune response [5]. Immunomodulatory antibodies promote the anti-tumor immune response by modifying the stimulatory or inhibitory signals on dendritic cells (DCs) and T cells [6].

1-Cancer vaccines aim to induce or enhance T cell-mediated immune responses against tumors by activation/stimulation of antigen presenting cells (APCs), more specifically DCs, with tumor-specific antigen and adjuvants. From the perspective of an APC, antigens can be presented according to two categories based on their origin: exogenous and endogenous. Endogenous antigens already intracellularly present in APCs such as viral antigens and normal cell proteins, are processed into peptide epitopes and presented to CD8+ T cells on major histocompatibility complex (MHC) class I molecules on the plasma membrane [7]. When CD8+ T cells attain their effector functions, they are referred to as cytotoxic T cells (CTL), capable of target cell killing [8]. Exogenous antigens such as bacterial antigens, allergens, proteins from transplanted organs and tumor antigens are internalized by the APCs, processed in the endosomes and classically presented to CD4+ T cells on MHC class II molecules. CD4+ T cells in a particular cytokine environment differentiate into one of several lineages of T helper (Th) cells. Th1 cells facilitate cellular immune responses against viruses and tumors and Th2 cells promote antibody production and initiation of a humoral immune response [9]. APCs have the unique ability to process both endogenous and exogenous antigens while normal nucleated cells in the body can only present endogenous antigens [7]. A strong CD8+ T cell response is known to be essential in the eradication of tumor cells [10]. CD8+ T cells are activated through ligation of the T cell receptor (TCR) by APCs presenting their specific antigen in MHC I molecules. Classically, only epitopes from intracellular proteins are presented in MHC I, while internalized exogenous material is presented in distinct MHC II molecules. As cancer antigens are from exogenous origin, they need to cross from the MHC II route to the MHC I route in order to induce a CD8+ T cell response. This process is called cross-presentation [8]. DCs are highly efficient in antigen internalization, processing and cross-presentation to specific CD8+ T cells which consequently differentiate to cytotoxic T cells [11]. A potent T cell response is achieved only when the antigen is presented by mature DCs, while antigen presentation by immature DCs results in tolerance [12,13]. Immature DCs have high antigen uptake and low antigen processing capabilities [14] and express low levels of MHC and co-stimulatory molecules [15]. DCs mature in the presence of danger signals derived from either microorganisms or from damaged tissue, which bind to sensing receptors expressed both on the plasma membrane and intracellularly [16,17]. Mature DCs lose their exceptional antigen uptake

properties and gain potent T cell priming capacity by expression of high levels of MHC class I and II and co-stimulatory molecules such as CD80 and CD86 and production of cytokines such as interleukin (IL)-12 [15,17,18]. Addition of adjuvants to a cancer vaccine formulation can provide the stimulatory signals necessary for DC maturation. However, administration of soluble antigens and adjuvants as such has several pitfalls, including weak immunogenicity, poor antigen cross-presentation as well as stability and toxicity concerns. These limitations can be overcome by particulate formulations. Particles can co-deliver multiple components such as several antigens and adjuvants. This co-delivery is crucial for induction of a robust CTL response [19,20] and to overcome tumor-induced immunosuppression [21]. Importantly, particles can also be decorated with targeting ligands. In this way, they mimic pathogens and cause less toxicity while the cargo will be more stable. Based on the type of antigen used, several particulate cancer vaccines can be distinguished including peptide, protein and cell lysate [22-24] cancer vaccines. These vaccines are either administered directly to the patient or used for *ex vivo* manipulation of DCs and are therefore called DC-based vaccines [25].

2-Immunomodulatory antibodies enhance the T cell immune response by 1-activation of T cells such as antiCD137 (4-1BB agonists) and 2-activation of DCs, such as CD40 agonists, or 3-blockade of inhibitory signals on T cells, like programmed cell death 1 (PD1) and cytotoxic T cell lymphocyte antigen 4 (CTLA4) blocking antibodies [26]. These antibodies have shown promising results in clinical trials [27,28] and some have even been approved for human use such as ipilimumab (antiCTLA4) and pembrolizumab (antiPD1). Nevertheless, there are certain drawbacks which limit their applications, such as increased systemic toxicity as a result of multiple (systemic) administrations, short-lived immune responses, lack of specificity and high costs [29,30]. The tumor environment is infiltrated with various types of immune cells and multiple immunosuppressive cells such as regulatory T cells (Tregs) [31] which facilitate the tumor growth by cytokine secretion as well as by suppressing tumor-specific T cell response. Facing this complex tumor environment calls for well-engineered formulations. Studies have shown that local and sustained delivery of antibodies can overcome these limitations. Controlled release of antibody results in high therapeutic efficacy and prevents systemic toxicity as well as autoimmunity [32,33]. Current strategies for sustained delivery of antibodies such as formulations based on incomplete Freund's adjuvant (IFA) cause certain adverese effects associated with the delivery vehicle [34] which will be further discussed in this review in **Section 4**. Therefore, it was hypothesized that encapsulation of antibodies in polymeric particles can face these challenges.

Besides these approaches, passive strategies including administration of tumor-targeting antibodies such as antiHER2 for breast cancer (Herceptin or Rituximab) [35] and adoptive transfer of activated T cells or natural killer (NK) cells (expansion of tumor-specific T cells or NK cells *in vitro* and re-administration to the patient) have been used in immunotherapy of cancer with promising results [36,37].

2. Particulate systems for immunotherapy of cancer

Recent advances in particulate delivery systems have given rise to multiple groups of synthetic particles including polymeric nano- and microparticles, liposomes, virus-like particles (VLPs) and immune-stimulating complexes (ISCOMs) [38]. The features of particulate carrier systems are summarized in **Table 1** and discussed further in detail.

Table 1. Advantages of particulate carrier systems for delivery of immunotherapeutics

Particles can
1-Protect their cargo against degradation
2-Be decorated with targeting ligands, dyes etc.
3-Mimic the pathogens
4-Co-deliver multiple antigens and adjuvants
5-Overcome poor bioavailability of the drug by encapsulation

1-Protection of the immunotherapeutic agent from premature degradation. Immunotherapeutics generally include biomolecules such as peptides/proteins, antibodies, DNA/RNA and lipopeptides, all of which are subjected to enzymatic degradation when injected in their free form into the body. However, when encapsulated in particles, these molecules will be protected against enzymatic attack and consequently have a longer half-life in the body [39].
2-Particles provide the possibility to co-encapsulate and co-deliver various molecules such as antigens, adjuvants and imaging tools.
As discussed in previous section, co-delivery of several immunotherapeutic agents is crucial for facing the tumor-induced immunosuppression [21].
3-Encapsulation of immunotherapeutics in particles enables us to conjugate certain molecules for targeting, labeling and shielding (with polyethylene glycol (PEG)) or in short "surface decoration". There are versatile ways to perform this conjugation such as click chemistry, NHS coupling and maleimide chemistry [39,40] which are reviewed in detail in [39].
4-Based on their size, particles can mimic certain pathogens (e.g. microparticles (MPs) can mimic bacteria and nanoparticles (NPs) mimic viruses). Other than size, the presence of adjuvants, targeting ligands and sustained release of the antigen and adjuvant help the particulate systems to act like an artificial pathogen [41].
5-Encapsulation of immunotherapeutics helps overcome poor solubility, low therapeutic indices and poor bioavailability of these agents; encapsulation results in a strong T cell response with low doses of the immunotherapeutics which in turn results in lower toxicity and lower costs [42,43].

Features of aliphatic polyester-based particulate systems for cancer immunotherapy

Particulate formulations based on aliphatic polyesters have been extensively used as drug delivery systems for small molecules as well as macromolecules [44-47] with several products in market [48,49]. Micro- and nanoparticles based on poly(lactic-co-glycolic acid) (pLGA) and similar polymers have been widely investigated as antigen delivery systems in preclinical studies with promising results [50,51].
General hallmarks of particulate carrier systems based on pLGA and related polymers in immunotherapy are outlined in **Table 2** and discussed further in detail.

Table 2. Features of pLGA particles in cancer immunotherapy

pLGA particles
1-Are commercially available
2-Are biodegradable and biocompatible
3-Provide sustained release of the cargo
4-Can be easily modified to obtain varying release profiles

1-These polymers are commercially available and are easy to synthesize.
2- pLGA is a biodegradable polymer composed of varying ratios of lactic and glycolic acid. The ester bond present in this polymer hydrolyzes in aqueous media and the degradation products can be metabolized via the Krebs cycle [52,53].
3-Sustained delivery of their payload. Encapsulation of a bioactive molecule can provide controlled release of the agent and limit the number of injections. This controlled release is especially important in case of cancer vaccines where a prolonged delivery of antigen and adjuvant is needed for a robust immune response [54]. It has been shown that administration of minimal peptide antigens in slow-delivery formulations (around 100 days) such as IFA can cause T cell tolerance. However, this does not seem to be solely related to the slow antigen release kinetics, but also other factors such as the type of the antigen (short peptide) and absence of co-stimulatory signals which were responsible for the loss of the T cell response [55,56]. Nevertheless, multiple studies have shown that prolonged antigen presentation is an important parameter in inducing a long-lasting CTL response. It can be argued that the duration of antigen presentation (few days to few months) could be of importance and should be further studied.
4-The possibility to tune the release/degradation rate and targeting by manipulation of pLGA. The release rate of a loaded "drug" from pLGA particles can be tailored by changing the monomer ratio and molecular weight of the polymer [57]. This has been shown in a recent *in vitro* study comparing commonly-used pLGA with 50:50 lactide/glycolide monomer ratio to pLGA with 75:25 lactide to glycolide ratio [58]. Moreover, chemical modifications on pLGA provide an array of versatile polymers. PEG is widely used to increase the hydrophilicity of pLGA [44]. Pegylation also eases the procedure of adding targeting ligands on the surface of the particle [59,60]. This has been shown in *in vitro* and *in vivo* studies using antibody-targeted pegylated pLGA NPs [40,61].

Drawbacks of commonly used aliphatic polyesters such as pLGA

Even though pLGA offers great opportunities in immunotherapy, pitfalls of this polymer come to sight when biotherapeutics are involved. Upon degradation, acidic degradation products such as lactic acid and glycolic acid as well as and short oligomers accumulate in the particle. This results in a pH drop inside the particle [62] which negatively affects the protein/peptide integrity and stability [63,64]. Physical changes (unfolding, denaturation, aggregation) and chemical modifications (acylation of lysine residues) of the entrapped macromolecules have been observed, resulting in incomplete release of the cargo and possible unwanted immunological reactions and toxic side effects [61]. This might not be very critical in case of antigen delivery (since antigens are degraded in the APCs) and peptide delivery (since denaturation is ruled out), but it is of utmost importance when the sustained and complete release of a macromolecule such as antibody is required.
Some strategies have focused on stabilization of peptides and proteins inside pLGA particles including pegylation of peptides/proteins and addition of urea to the formulation [62,63]. In addition, insoluble basic excipients such as magnesium hydroxide have been used to neutralize the acidic pH in the degrading particles [64]. Furthermore, dermatan sulfate, a glycosaminoglycan polymer, has been used to stabilize the model protein BSA in the pLGA particles [65]. Moreover, lysine, trehalose and sorbitol have been used to prevent aggregation and unfolding of proteins [66].
Other strategies to prevent acidification of PLGA particles encompassed the development of hydrophilic polymers with fast degradation rates. These polymers include pegylated aliphatic polyesters [67] as well as novel polyesters with a more hydrophilic backbone [68]. High water uptake of these polymers results in accelerated degradation (and release of the payload) and fast removal of the acidic degradation products and, thus prevents the pH drop [69]. Preparation of porous particles is another approach that facilitates the water diffusion and increases the degradation rate of the particles [70]. Strategies shortly discussed here are

reviewed in more detail in [71].
Another challenge limiting the use of pLGA particles is the costly aseptic scale-up preparation procedure. However, regarding the fact that several pLGA formulations are already available on the market [65] these issues can obviously be overcome. Drawbacks of pLGA-based delivery systems are summarized in **Table 3**.

Table 3. Drawbacks of pLGA particles for cancer immunotherapy

Drawbacks of pLGA delivery systems
1-Acidification of the polymer matrix upon degradation resulting in aggregation, chemical modifcation and incomplete release of the cargo
2-Low encapsulation efficiencies for hydrophilic molecules
3-Lack of functional groups for conjugaton of targeting ligands etc.
4-Costly aseptic production

3. Cancer vaccines

As mentioned earlier, cancer vaccines target DCs to initiate a T cell immune response. An ideal cancer vaccine should activate cellular and humoral immune responses and result in formation of memory T cells and memory B cells for a durable tumor-specific immunity [43]. Particulate formulations based on aliphatic polyesters such as pLGA and poly lactic acid (pLA) are specifically suitable as cancer vaccines because they are taken up efficiently by DCs and promote cross-presentation [11,66]. The depot effect of the particles provides another advantage of particulate cancer vaccines by prolongation of antigen presentation to T cells which is important for a strong T cell response and formation of immunological memory [43,67,68]. The action of a typical cancer vaccine is presented in **Figure 1.**

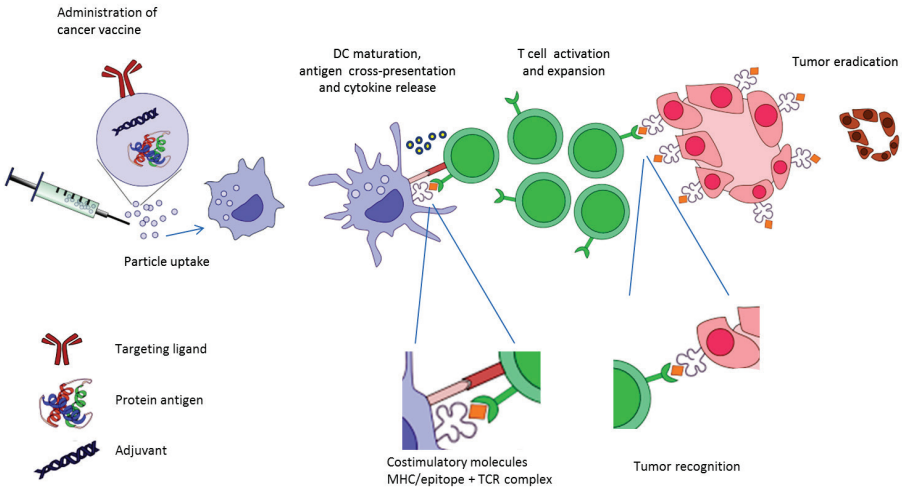

Figure 1. A particulate cancer vaccine in action. A particle loaded with protein antigen and adjuvant and decorated with a DC-specific antibody is administered to the body. The particle is taken up by an immature dendritic cell, the antigen is processed and presented on MHC I molecules. In the prescence of costimulatory molecules and cytokines, the now "mature" DC activates the T cells. Upon activation, the T cell population expands and migrates to tumor site where T cells recognize and destroy the tumor.

3.1. Physicochemical requirements for particulate cancer vaccines

3.1.1. Particle size

Many studies have focused on the effect of the size of the antigen-loaded particle on the T cell immune response. However, there is no consensus on the optimal size for a cancer vaccine. Conflicting data arise from the heterogeneous experiments studying different variables, such as route of administration, method of antigen loading, and type of antigen (Reviewed by Oyevumi et al.) [69]. Nevertheless, it is known that particle size is not only important for the uptake as such but also for the intracellular trafficking and processing of the antigen [43,45]. Various studies stress the advantages of NPs in the range of around 200 nm (and sometimes as small as 40-50 nm) [70] because of their ability to drain to the lymph nodes after subcutaneous administration for subsequent uptake by immature resident DCs [45]. When targeting lymph nodes, the size of the lymphoid capillaries should also be taken into account [71,72]. Only small NPs (< 200 nm) can drain freely to the lymph nodes and are found there shortly after administration (2 h). However, bigger particles need to be transported to the lymph nodes upon uptake by DCs. Particles bigger than 200-500 nm are deposited in the lymph nodes no sooner than 24 h after administration which might delay the immune response [72]. Other studies indicated that as a result of enhanced uptake, NPs containing CpG ODN (TLR9 ligand) more efficiently induce DC maturation and immune responses than MPs [73]. In a recent study by Silva et al., the effect of particle size on the type and extent of the immune response was evaluated. MPs (112 μm) and NPs (350 nm) loaded with ovalbumin (OVA) and poly IC (TLR3 ligand) were compared and it was shown that the NPs were efficiently taken up by DCs and showed stronger antigen cross-presentation *in vitro* and *in vivo* as compared to MPs. [58].

3.1.2. Surface characteristics (surface charge, hydrophobicity/hydrophilicity)

Effect of surface charge on particle uptake

Surface characteristics also affect the particle uptake and consequently the immune response. Studies showed that the electrostatic interaction between positively charged particles and negatively charged cellular membranes results in high and efficient particle uptake by human monocyte-derived DCs and macrophages *in vitro* [74]. As a result, strategies have been used to decorate the surface of commonly negative pLGA particles with positively-charged groups such as protamine [75] and chitosan or to shield the negative charge with PEG [76]. However, It has been shown that interaction of positively-charged particles with non-phagocytic cells [77,78] and endogenous proteins [79] is also higher than that of negatively-charged particles. Therefore, it can be argued that positively-charged particles exhibit high levels of non-specific binding and uptake and therefore possibly decreased efficacy.

Effect of hydrophilicity on cell uptake, lymph node drainage and immune response

In a study performed by Rao et al., the effect of particle hydrophilicity and surface charge on lymphatic drainage and retention was evaluated. (pLGA + PEG-pLA) NPs of various sizes (50-200 nm) were injected to foodpad of rats and the results were compared with that of polystyrene NPs. 1-pyrenemethylamine (PMA) was chemically conjugated to to pLGA to facilitate *in vivo* tracking of the particles. The results showed that an increased hydrophilicity of the particle surface (by increasing the PEG content) causes higher accumulation in the lymph nodes [80]. Additionally the kinetics of lymph node drainage of negatively charged pLGA NPs (with varying amount of COOH end groups) was studied. It was shown that the rate and extent of lymphatic drainage is directly related to the negative surface charge. It was suggested that this fast drainage is caused by triggering macrophage uptake and drainage as well as free diffusion of the NPs [80]. However, another study performed by Liu et al. using pLA, pLGA and PEG-pLA MPs (1 μm), showed that increased surface hydrophobicity resulted in increased antigen uptake by bone marrow-derived murine DCs *in vitro and* enhanced DC maturation and lymph node drainage after subcutaneous injection in mice.

Importantly, *in vivo* studies showed an elevated T cell response (but not antibody production) when more hydrophobic particles (pLA) were used. It was shown that the increased surface hydrophobicity results in a stronger interaction between the particles and the DCs [81].

3.1.3. Shape

Particle shape is important for the interaction between APCs and particles and this has been the subject of a few studies on particle uptake by macrophages and DCs. Rod-shaped gold NPs (40 by 10 nm) were taken up by bone marrow-derived murine DCs more efficiently than spherical (20 or 40 nm) or cubic NPs (40 nm). However, spherical NPs (40 nm) induced a more potent immune response than the other particles [82]. Uptake of particles larger than 1 μm was highly dependent on their shape. Macrophages were much more successful in the uptake of spherical polystyrene particles as compared to worm-shaped particles with >20 aspect ratios [83,84].

3.2. Components of a particulate cancer vaccine

3.2.1. Antigens

Antigens used in cancer vaccines are ideally expressed by the tumor cells exclusively (tumor antigens) or primarily (tumor-associated antigens), and are essential for the survival of the cells and as a result not able to evade the immune surveillance [4]. A wide array of antigens has been encapsulated in particles based on aliphatic polyesters, including tumor lysates, protein antigens, synthetic long peptides and minimal epitope peptides [51,85-87].

3.2.2. Adjuvants

The importance of adjuvants in cancer vaccines cannot be stressed enough because the presence of adjuvants is crucial for a successful cancer vaccine, regardless of the type of antigen used [1]. After antigen uptake, DCs only undergo maturation in the presence of adjuvants such as LPS, resulting in an effective T cell response.

Depending on the type of immune response needed, several adjuvants are available. As mentioned earlier, in promoting strong CD8+ T cell activation, CD4+ T helper cells (Th) play a key role. Th cells are responsible for activation of APCs, especially DCs. Of two Th cell subtypes, Th1 takes part in activation of CD8+ T cells and Th2 is responsible for humoral responses [1]. However, in cancer treatment, a Th1 immune response is needed while the classical adjuvants such as alum mainly cause a Th2 immune response [88].

Due to superior immunogenicity of pLGA-based vaccines compared to their soluble counterparts, pLGA particles are considered to exhibit intrinsic adjuvant properties. Multiple studies have shown that encapsulation of antigen and adjuvants in pLGA particles results in enhanced humoral and celluar immune response when compared to soluble forms [19,89-91]. This adjuvanticity is attributed to the high and efficient uptake of the particles and increased stability and sustained release of the antigen/adjuvant to result in more efficient cross-presentation [68]. In addition, a study by Zhang et al. has shown that even placebo pLGA MPs are able to induce upregulation of CD80 (a co-stimulatory molecule on DCs) on *in vitro* bone marrow-derived murine DCs [92]. However, another study using placebo pLGA MPs showed no MHC class I , II and CD86 upregulation in bone marrow-derived murine cells indicating that these particles are not capable of inducing DC maturation [19]. Similar results to the latter study have been reported using human monocyte-derived DCs [93].

Toll like receptor (TLR) ligands

In order to achieve a high extent of DC maturation and Th1 immune response, one can benefit from using TLR ligands. Toll like receptors recognize highly conserved pathogen-associated molecular patterns (PAMPs) from pathogens [94,95], and are well-defined and widely used adjuvants in preclinical as well as in clinical studies [20]. These molecules induce DC maturation and enhance the vaccine efficacy by increasing both cytokine secretion

and presentation of surface peptide/MHC and co-stimulatory molecules [43]. TLR ligands which have commonly been investigated in cancer immunotherapy include: TLR2/6 ligands (lipoproteins), TLR3 ligands (double stranded RNA such as poly IC), TLR4 ligands (LPS), TLR7 ligands (imidazoquinolines) and TLR9 ligands (CpG DNA) [96]. Some TLR ligands such as TLR3 and TLR9 ligands have been reported to enhance antigen cross-presentation [97]; the role and mechanism of action of TLR ligands are reviewed in more detail in [95].

Co-delivery of the antigen and adjuvant

As antigen uptake and processing in the absence of adjuvants and lack of proper activation of DCs, might result in immunological tolerance, several studies have reported about co-encapsulation of an antigen and an adjuvant in pLGA NPs [24,50,51,98]. The majority of studies showed that co-encapsulation of antigen and adjuvant resulted in superior antigen presentation and T cell activation as compared to separate administration. These studies suggest that the co-delivery of the vaccine components to the same cellular compartment (and not only to the same DC) is playing a major role in the induction of a potent cellular immune response. In a study conducted by Schlosser et al., OVA was co-encapsulated either with CpG (TLR9 ligand) or with poly IC (TLR3 ligand)) in pLGA MPs. Co-encapsulated MPs were more successful in inducing cross-presentation in immunized mice six days after injection when compared to co-administration of OVA MPs and TLR ligand MPs and soluble adjuvants. Single injection of co-encapsulated (OVA+CpG) MPs in mice resulted in 9% tetramer positive CD8+ T cells, high level of production of IFN-γ and protection from vaccinia virus infection [19]. Several examples of similar studies with a focus on co-delivery of antigens and TLR ligands are reviewed in [21,99].

3.2.3. Targeting ligands

Decoration of the NP surface with targeting ligands has two major aims: 1- increased uptake by specific cells [100,101] and 2-enhanced adjuvanticity [76]. Ligands with a receptor on the DCs are great candidates for targeting DCs, these targeting ligands include:

-DC-specific antibodies including:

C type lectin receptor (CLR) ligands (targeting mannose and DC-SIGN and DEC-205), antiCD40 (a TNF-α family receptor), antiCD11c (an integrin receptor) [23,40,61,102,103]

-Nucleotide-binding oligomerization domain (NOD) like receptor ligands and TLR ligands that facilitate intracellular transport [41,104]

TLR3, -7, -8 and -9 ligands can also be used as intracellular targeting ligands [105]. Other than enhanced uptake, binding of CLRs and TLRs to their ligands causes DC maturation which results in efficient immune cell activation and Th1 immune response. Particulate formulations utilizing targeting ligands are discussed in detail elsewhere [45].

A schematic overview of components of a cancer vaccine is given in **Figure 2**.

3.3. Particle preparation strategies

As discussed earlier, particulate formulations comprise of various types of molecules, including peptides, proteins (including antibodies), nucleic acids, lipids etc. Co-delivery of multiple antigens and adjuvants and introducing targeting ligands further complicates this procedure. In order to develop a stable and effective formulation, physico-chemical properties of each component should be considered and the interaction between several components of the formulation and its effect on stability and efficacy of the formulation should be studied.

Components of a formulation can either be loaded by encapsulation or by surface association. Encapsulation is more widely used for delivery of immunotherapeutics and has been reviewed in [106,107]. Encapsulation protects the payload from enzymatic degradation and provides sustained release of the cargo. However, some encapsulation methods such as the water-

in-oil-in-water emulsion method require organic solvents which increase the possibility of denaturation and aggregation of macromolecules such as antibodies. In addition, as discussed in the section "drawbacks of pLGA" biotherapeutics encapsulated in pLGA particles are

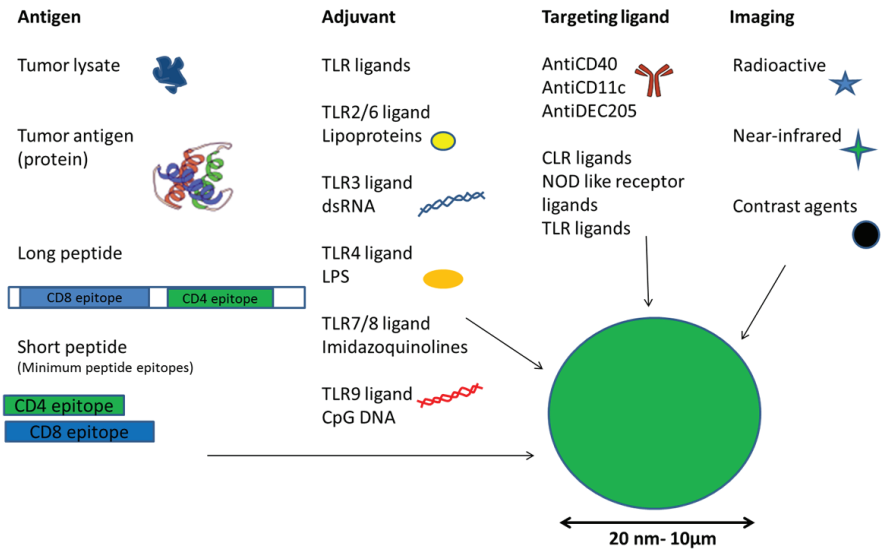

Figure 2. Schematic overview of components of a particulate cancer vaccine.

prone to chemical modification, aggregation and instability which drastically affect the immunogenicity of the formulation [108]. To increase the stability of the therapeutic agent and as an alternative to other options mentioned in the section "drawbacks of pLGA", various particle preparation methods have been investigated such as surface-binding [109] and encapsulation by self-healing [110,111].

3.4. Examples of particulate cancer vaccines based on polyesters

This section provides examples of recent particulate cancer vaccines being developed plus a brief discussion of the obtained results.

3.4.1. DC vaccines

This branch of cancer vaccines is based on *ex vivo* manipulation of DCs. First, the patient's DCs are isolated and exposed to antigens/adjuvants and subsequently the activated DCs are administered to the patient as a cancer vaccine. The first DC-based therapeutic cancer vaccine was approved by the FDA for prostate cancer (Provenge) [112] which encouraged various studies on the development of DC vaccines using pLGA particulate systems [113]. Promising results were reported, but the development of such vaccines is very labor-intensive and associated with high costs and regulatory complications [114]. Moreover, upon administration, DCs vaccines need to be transported to the lymph nodes which might affect the type and kinetics of the immune response [40]. These limitations can easily be overcome by using *in vivo* administered particulate cancer vaccines.

3.4.2. Cell lysate vaccines

Gross et al. recently encapsulated 4T1 cell lysate (adenocarcinoma breast cancer) in 2.3 µm pLGA MPs. These particles were injected subcutaneously as the prime dose into 4T1 tumor-bearing mice. Boost injection consisted of soluble tumor lysates and a cocktail of

TLR 3, 2/6 and 9 ligands in DOTAP liposomal transfection reagent (N-[1-(2,3-Dioleoyloxy) propyl]-N,N,N-trimethylammonium methyl-sulfate). This cancer vaccine efficiently reduced the number of lung metastases (up to 42%) as compared to untreated controls 25 days after tumor inoculation [115]. Another research team encapsulated a TRAMP prostate tumor lysate and TLR9 ligand (CpG) in pLGA MPs (size 1-10 µm). Co-encapsulated TRAMP + CpG MPs were co-administered subcutaneously with TLR3 ligand (poly IC) MPs in a TRAMP C2 prostate carcinoma tumor model in mice. TRAMP is a well-characterized transgenic mouse model of prostate cancer that expresses SV40 large T antigen [116]. Therapeutic vaccination resulted in a potent CD8+ T cell response and a significant decrease in tumor size [24].
Although tumor cell lysates have shown promising results, from a pharmaceutical point of view, these formulations are not well defined and lack specificity. Therefore, current research is more focused on protein and peptide formulations.

3.4.3. Protein and peptide vaccines

In various studies, model antigen OVA was used either as whole protein or as peptide (containing CD8+ T cell epitope) encapsulated in polyester-based NPs also co-encapsulated with TLR ligands such as TLR3, TLR4 and TLR9 to evaluate the effect of (co-) encapsulation of the antigen and adjuvants. Results showed that these particulate formulations are superior in antigen cross-presentation and in enhancing the CD8+ T cell response compared to the use of soluble antigen [113]. Moreover, the TLR ligands induced a strong maturation of the DCs characterized by an increase in DC surface markers and a very potent CD8+ T cell response. Furthermore, when decorated with targeting ligands such as antiCD40, particulate formulations show a superior antigen-specific T cell response (discussed in detail by Silva et al. [21]). As an example of targeted NP delivery, a recent study by Rosalia et al. used antiCD40 targeted pLGA NPs loaded either with OVA or with human papillomavirus (HPV) E7 oncoprotein and co-encapsulated with TLR2 and TLR3 ligands. Upon subcutaneous administration in mice, antiCD40 targeted NPs were taken up by DCs in an efficient and selective way. Antigen-specific T cell expansion was observed for both antigens *in vivo* and therapeutic vaccination against B16-OVA tumor-bearing mice enhanced tumor control and increased the survival of mice [23] (**Figure 3 and 4**).

Encouraged by the results obtained using model antigens, several therapeutic peptide epitopes were studied *in vitro* and *in vivo*. pLGA NPs loaded with tyrosinase-related peptide 2 ($TRP2_{180-188}$- a melanoma antigen) and with 7-acyl lipid A (TLR4 ligand) were administered to B16 melanoma tumor-bearing mice. These formulations showed a good anti-tumor effect, a strong T cell activation and increased secretion of pro-inflammatory cytokines in the tumor environment [98]. Similar results have been obtained using other clinically relevant peptides [22,117].
Recent studies have shown that the efficacy of vaccination is considerably enhanced by increasing the length of the peptide antigens [118]. These antigens are coined as synthetic long peptides (SLPs). It has been documented that administration of peptide vaccines consisting of minimum peptide epitopes in slow-release formulations results in a brief T cell response which consequently causes T cell tolerance and lack of immunological memory, mainly because of peptide presentation on many MHC I expressing somatic cells lacking co-stimulation [55,119-121]. The increase in peptide length in SLPs avoids its direct interaction with MHC I molecules. As a result, SLPs need to be taken up and processed by professional antigen presenting cells like DCs in order for the epitope to be presented to CD8+ T cells. Additionally, following administration of SLPs, longer antigen presentation was observed *in vivo* [122]. Moreover, DCs process SLPs more efficiently than whole proteins and cause long term antigen presentation [123] and efficient T cell activation as well as expansion [123,124]. Despite the promising results of SLPs in inducing strong T cell responses as compared to minimum peptide epitopes, if administered in free form, SLPs can be degraded by proteases

before being taken up and processed [125]. Encapsulation of SLPs therefore was considered to increase the stability and efficacy of the vaccine [51,126]. A model SLP based on OVA was encapsulated in pLGA NPs either alone or co-encapsulated with a TLR2 ligand. Importantly, SLP-loaded NPs (without any adjuvant) were superior to soluble SLPs in the induction of T cell responses *in vitro* [126]. Adoptive transfer of DCs loaded with SLP+TLR2 ligand NPs resulted in sustained CD8+ T cell proliferation. However, as opposed to previous studies, the co-encapsulation of antigen and adjuvant was not necessary but it was argued that the positively charged TLR2 ligand in soluble form has electrostatic and hydrophobic interactions with negatively charged pLGA NPs [127]. Following the promising results of a model SLP encapsulated in NPs *in vitro* and *in vivo* and success of human papillomavirus (HPV) SLPs in clinical trials [34,128,129], a recent study of our group used an HPV SLP derived from HPV16 E7 oncoprotein and a TLR3 ligand (poly IC) encapsulated in a hydrophilic polyester, poly(lactic-co-hydroxymethyl glycolic acid) (pLHMGA). pLHMGA has a similar backbone as pLGA but also carries pendant hydroxyl groups [130-132]. The therapeutic efficacy of NPs loaded with HPV SLP and poly IC in the TC1 tumor model in mice was equivalent to that of HPV SLP and poly IC formulated in incomplete Freund's adjuvant (IFA) emulsion -a commonly used vaccine adjuvant that forms a depot at the injection site [51]. Once again in this case the co-encapsulation of HPV SLP and poly IC was not required for an effective T cell response. A few examples of recent developments in particulate cancer vaccines based on aliphatic polyesters and the *in vitro*/preclinical results are provided in **Table 4**.

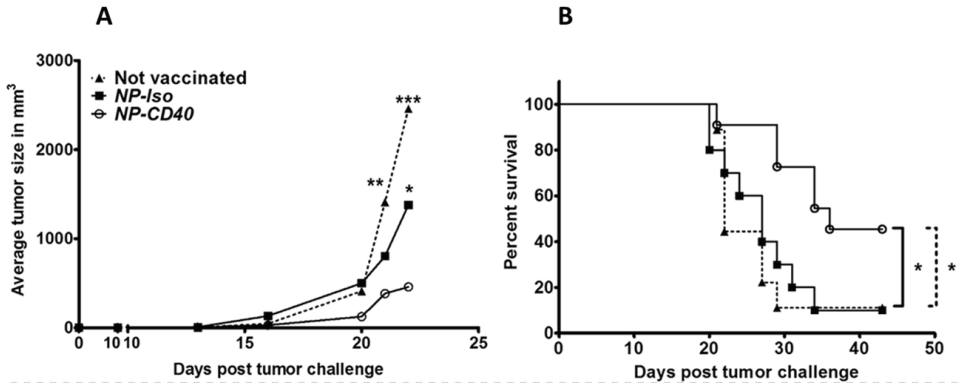

Figure 3. Seven days after tumor inoculation with B16-OVA cells, mice were vaccinated with antiCD40-targeted pLGA NPs loaded with OVA (10 μg) and TLR2+3 ligands followed by boost injection 10 days after the first vaccination. A) Average tumor size per group is plotted until the first mouse is sacrificed (day 22). Two-way ANOVA (with Bonferroni post-test) was used to determine the differences in average tumor size per group to calculate the difference in mean values at each time point. Targeted NPs significantly suppressed the tumor growth comparing to non targeted NPs. B) Animal survival is presented in Kalpan Meier plot and the differences between groups were assessed using Log-rank (Mantel-Cox) test, *** = $p < 0.001$, ** = $p < 0.01$ and * = $p < 0.05$. Targeted cancer vaccine significantly prolonged the survival of mice as compared to non targeted NPs. Reproduced with permission from [23].

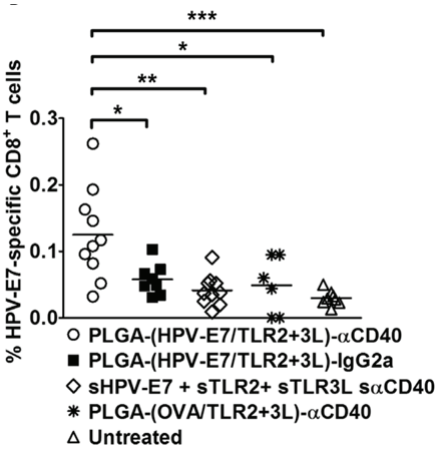

Figure 4. TC1 tumor-bearing mice were vaccinated with antiCD40-targeted pLGA NPs loaded with HPV E7 protein antigen (15 μg) and TLR2 and 3 ligands on day 7 after tumor inoculation. On day 15, the percentage of RAHYNIVTF/H2-Db specific CD8+ T cells in blood was significantly higher than the non targeted NPs and mixture of soluble HPV E7 antigen together with TLR ligands and antiCD40. Differences in percentage of Ag-specific CD8+T cells were analyzed by Mann Whitney tests, * = $p < 0.05$. Reproduced with permission from [23].

4. Immunomodulatory antibodies

Immunomodulatory antibodies activate the immune system either by blocking inhibitory signals or enhancing immunostimulatory signals on DCs and T cells. Immunomodulatory antibodies have been used in clinical trials as monotherapy for the treatment of malignancies with promising results [134]. A well-established category of antibodies is known as checkpoint blockers. The targets of these antibodies are inhibitory receptors such as CTLA4 and PD1. CTLA4 and PD1 are expressed on T cells to inhibit their activation or function. Successful clinical trials resulted in FDA approval of both antiCTLA4 and antiPD1 [135,136]. T cells also express stimulatory receptors from the TNFR superfamily including OX40 and 4-1BB, whose ligation by agonistic antibodies has a stimulatory effect on T cell survival and on memory T cells [137]. Finally, DCs and other APCs can be activated by agonistic antibodies against the stimulatory molecule CD40, resulting in DC maturation which is crucial for the induction of a potent immune response [138,139] (**Figure 5)**.

One of the major factors that limits the application of the immunomodulatory antibodies is the occurrence of immune-related adverse effects such as autoimmune and inflammatory reactions upon systemic/high dose administration [29,140,141]. In order to minimize adverse effects, several antibodies have been formulated in water-in-oil adjuvants such as IFA and Montanide [32,142] and have been administered locally mostly by subcutaneous injection. IFA and Montanide are mixtures of non-metabolizable mineral oils such as paraffin oil and surfactants such as mannide monooleate. The formulations are prepared by emulsification of a solution of antibodies in these mineral oils and surfactants to form a water-in-oil (W/O) emulsion [143]. However, these emulsions caused local inflammation and other adverse effects related to the W/O carrier system [144]. From a pharmaceutical point of view, these emulsions are not well-defined as the release kinetics of the antigen/adjuvant are not predictable and their stability profile is not well characterized [34,145]. Therefore, pharmaceutically acceptable formulations which provide sustained release of the antibody are preferred (**Figure 5**).

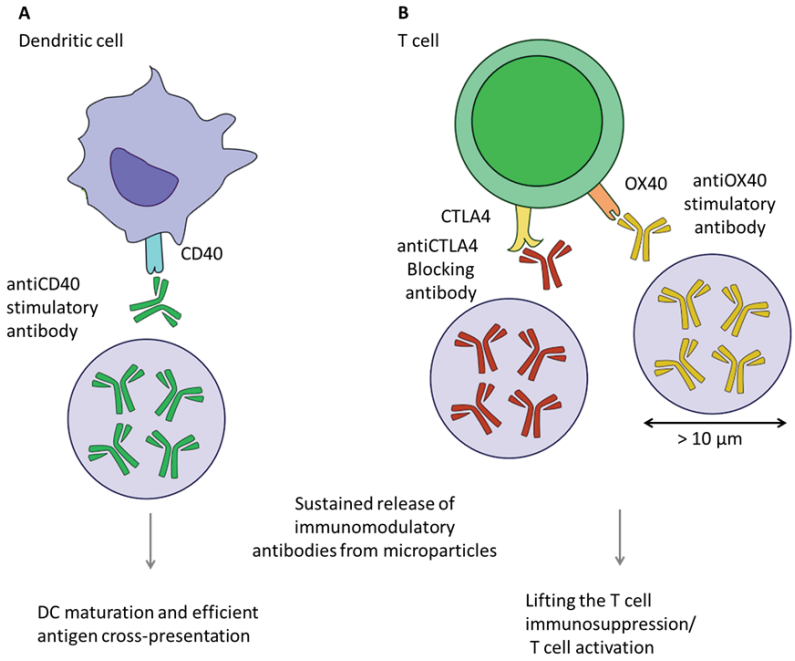

Figure 5. Sustained delivery of immunomodulatory antibodies results in activation of immune system. A) Immunomodulatory antibodies targeting DCs. CD40 is a stimulatory molecule expressed by DC and a member of TNF receptor superfamily. Interaction between CD40 and CD40 ligand expressed on activated T helper cells results in DC maturation by upregulation of co-stimulatory molecules and secretion of various cytokines, efficient cross-presentation and a potent T cell response. Agonistic CD40-specific antibodies can mimic this DC-T helper interaction and will strongly activate DC and thereby stimulate cellular immune responses. **B) Immunomodulatory antibodies targeting T cells.** CTLA4 expressed on T cells competes with CD28 (also on T cells) for binding to CD80 and CD86 (co-stimulatory molecules on DCs) resulting in immunosuppression. Blocking CTLA4 using antiCTLA4 antibodies released locally from the MPs, allows enhanced T cell stimulation by blocking the inhibitory signal of CTLA4. OX40 is also expressed on T cells but as opposed to CTLA4 has a stimulatory role in initiation of T cell immune response. AntiOX40 promotes co-stimulatory signals to T cells which result in enhanced T cell proliferation and effector function.

4.1. Physicochemical requirements of antibody-loaded particulate systems

4.1.1. Particle size

To provide sustained release of antibodies close to the tumor, antibody-loaded particles -as opposed to cancer vaccines- should not to be taken up by phagocytic cells such as macrophages and DCs. This can be achieved by choosing an appropriate particle size (larger than 10 µm) [146].

4.1.2. Stability of the antibody in the particle

As discussed in **Section 2,** upon degradation of pLGA, acidic byproducts are formed that cause instability and aggregation of the protein/peptide cargo. This might not be of concern for antigens since they are degraded upon uptake, but it is of great importance for delivery of large proteins especially antibodies where sustained release of a fully functional antibody is necessary. Instability of antibodies does not happen only during release but encapsulation methods and storage of the formulations can also result in aggregation and loss of activity [63,147].

In order to achieve a stable formulation, several encapsulation methods have been explored

for the preparation of antibody-loaded particles using aliphatic polyesters such as water-in-oil-in water (W/O/W) and solid-in-oil-in-water (S/O/W) encapsulation processes as well as stabilizers such as mannitol and trehalose. Examples of these formulations and *in vitro*/ preclinical results are discussed below as well as in **Table 5**.

As mentioned in **Section 2**, pLHMGA polymers are recently developed hydrophilic polyesters which have been used for encapsulation and release of peptides [148] and proteins [132]. pLHMGA particles have shown to be peptide/protein-friendly as they do not exhibit a pH drop upon degradation in the particles and release the cargo completely and without modification [149]. The degradation of the particles and the release of the entrapped peptides/proteins can be tailored by adjusting their copolymer composition. Moreover, upon subcutaneous administration these particles have shown good biocompatibility [150]. These advantages make pLHMGA polymers attractive candidates for antibody delivery.

4.2. Examples of antibody-loaded particulate systems based on polyesters

As opposed to several studies using pLGA as an antigen delivery vehicle, there are only a few studies covering the delivery of antibodies loaded in polyester particulate forms, which may be due to the drawbacks of pLGA as a protein carrier system as discussed earlier. The stability of monoclonal antibodies encapsulated in pLGA or similar polyesters was evaluated in a few studies. In a study by Wang et al., W/O/W and S/O/W particle preparation methods were compared using human IgG as model antibody and several stabilizers. Although the primary structure of the IgG was unchanged by ultrasonication, W/O/W resulted in 80% denaturation of IgG due to aggregation as well as unfolding at interface between water and the organic phase. Mannitol and trehalose could successfully stabilize IgG during spray freeze-drying. Nevertheless, the release of the antibody from MPs prepared by both methods was incomplete which was argued to be a result of aggregation and degradation of the antibody [151]. In a similar study, polyclonal bovine IgG was encapsulated by S/O/W method in pLGA MPs using ethyl acetate as organic phase. The integrity of the IgG was characterized by SEC-HPLC and was shown to be preserved using this method. These particles showed low burst release (20%) and complete release of the IgG *in vitro* in 8 weeks [152]. Polycaprolactone (pCL) and a triblock copolymer of PEG and pCL (mPEG-pCL-PEG) were used for encapsulation of human IgG using W/O/W method. It was shown that pegylation of the polymer provided more control over the release of the antibody *in vitro* as compared to pCL. However, only 57% of the released IgG kept structural integrity (measured by ELISA) after 90 days [153]. Marquette et al. studied the stability of antiTNF alpha in pLGA MPs with varying amount of lactic acid. Their results showed that the antibody was more stable in pLGA with higher content of lactic acid (75%) compared to pLGA with 50% lactic acid [154]. The effect of stabilizers was studied on the conformational stability of the antibody as well as the activity of the antibody as a DNA binding agent. Among several stabilizers (polyethylene glycol (PEG), trehalose, mannitol and heparin) mannitol was reported to be the best performing stabilizer. However, the release kinetics of the protein from the particles was not studied [155]. In another study, a relevant antibody for immunotherapy (antiOX40) was coated on pLGA NPs. The *in vitro* release kinetics of the antibody loaded NPs showed a low burst release of 12% at day one followed by sustained release up to 60% at day 20. *In vitro*, these NPs were capable of inducing a CD8+ T cell response and enhanced cytokine production which was stronger than their soluble counterpart (**Figure 6**). Nevertheless, the release of the antiOX40 from the NPs was not complete, which might point to the instability of the antibody inside the NPs. However, these particles were not examined *in vivo* where there is a high chance that the particles are taken up because of their small size [156].

In our recent study, two immunostimulatory antibodies (antiCD40 and antiCTLA4) were encapsulated in pLHMGA MPs. These particles were bigger than 10 µm to avoid uptake by macrophages. The *in vitro* release profile of antiCD40 and antiCTLA4 from MPs showed a burst release of about 20% of the loading and a sustained release of the content up to 80%

in approximately 30 days. Particles were administered locally into tumor-bearing mice and the therapeutic efficacy was compared to IFA W/O formulations. The antibody-loaded MPs showed comparable and as efficient therapeutic efficacy as the IFA formulation with no local adverse effects. The antibody levels in sera of mice were low, reducing the risk of systemic toxicity (manuscript submitted for publication). **Table 5** provides particulate formulations loaded with model/therapeutic antibodies in aliphatic polyesters.

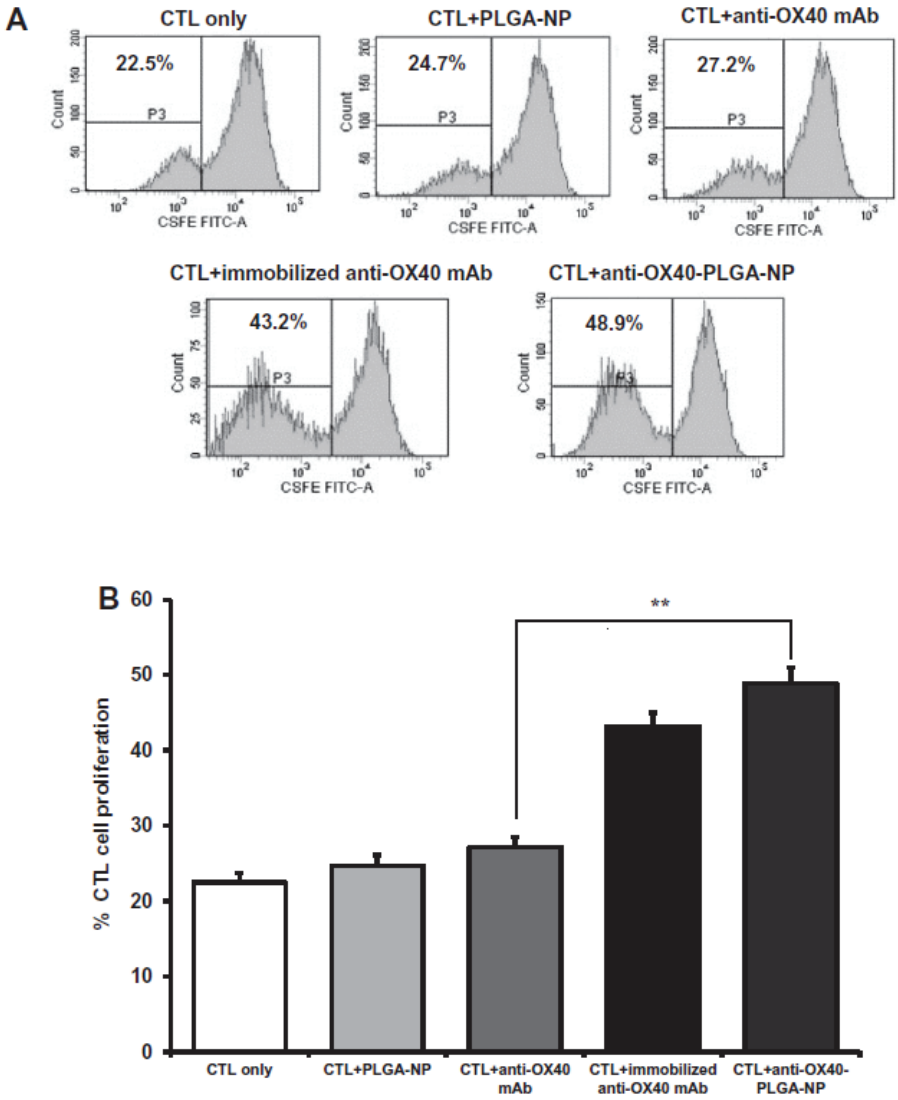

Figure 6. The effect of surface coated antiOX40 NPs on T cell expansion was studied by CFSE dilution assay followed by flow cytometric analysis. (A) An analysis of CFSE staining in the CTLs (CD8+ T cells) was performed after gating on viable cells, and the percentage of proliferating cells is indicated for each panel. (B) Data from three independent experiments were analyzed by student's *t* test $p < 0.01$, the antiOX40 NPs significantly enhanced the T cell proliferation *in vitro* compared to soluble antiOX40. Reproduced with permission from [156].

Table 4. pLGA-derived particulate systems for cancer immunotherapy

	Antigen type	Antigen	Adjuvant	Average particle size	Tumor model	Polymer	Result	Ref.
1	DC vaccine/ Tumor lysate	epithelial ovarian cancer line TARA R182	-	NPs 100-300 nm	-	pLGA	Increased cytokine production by CD8+ T cells and induced T cell expression of cell surface co-stimulatory molecules	[113]
2	Tumor lysate	4T1 tumor lysate (prime)	Cocktail of TLR ligands + free tumor lysate (boost)	MPs 2.3 µm	Mouse 4T1 breast adeno-carcinoma	pLGA	Reduced metastatic lung tumor by 42% in a prime-boost vaccination	[115]
3	Tumor lysate	TRAMP tumor lysate	TLR3ligand (Poly IC) TLR9 ligand (CpG) MPs	MPs 1-10 µm	Mouse TRAMP C2 prostate carcinoma	pLGA	Substantial CD8+ T cell responses and significant decrease in tumor growth	[24]
4	Protein and cell lysate	gp100 and B16-tumor lysate containing gp100	-	NPs 200-350 nm	-	pLGA	Increased IFN-γ and decreased immunoinhibitory IL-10 synthesis *in vitro*	[133]
5	Protein antigen	OVA	-	NPs 300-400 nm	-	pLHMGA	Enhanced antigen specific T cell proliferation *in vivo*	[130]
6	Protein antigen	OVA	TLR3 ligand (poly IC) and 7 ligand (R848) -CD40, DEC-205, CD11c targeted	NPs 200-250 nm		pLGA	Enhanced NP uptake and cytokine production *in vitro* by targeted NPs. Superior *in vivo* T cells proliferation and cell lysis following DC vaccination with targeted NPs	[40]
7	Protein antigen	OVA	TLR2 ligand (Pam3CSK4) TLR3 ligand (poly IC) -CD40 targeted	NPs 200-250 nm	Mouse B16-OVA	pLGA	Selective delivery to DC *in vivo* and enhanced tumor regression and increased survival *in vivo*	[23]
8	Protein antigen	HPV E7 Human papillomavirus	TLR2 ligand (Pam3CSK4) TLR3 ligand (poly IC) -CD40 targeted	NPs 240-260 nm	Mouse TC1	pLGA	Significant enhancement in HPV-specific CD8+ T cells in blood after administration of CD40 targeted- HPV E7 loaded NPs compared to HPV E7 NPs or a mixture of soluble HPV E7 and adjuvants.	[23]

Table 4. Continued

	Antigen type	Antigen	Adjuvant	Average particle size	Tumor model	Polymer	Result	Ref.
9	Peptide antigen	TRP2(180-188) melanoma tumor antigen	TLR4 ligand (7-acyl lipid)	NPs 350-410 nm	Mouse B16-F10 melanoma tumor model	pLGA	Significant tumor regression	[98]
10	Peptide antigen	WT1 (Wilms' tumor protein)	TLR9 ligand (CpG)	MPs 0.8-1.6 μm	NB4 leukemia	pLGA	Enhanced IFN-γ production *in vitro*	[117]
11	Peptide antigen	MUC-1	TLR4 ligand (MPLA)	NPs 60-100 nm	-	pLGA	Enhanced proliferation of MUC1 T cells demonstrating the break in tolerance to self-antigen MUC1 *in vitro*	[22]
12	Long peptide antigen	OVA SLP containing SIINFEKL	-	NPs 330 nm	-	pLGA	Enhanced antigen specific T cell activation in vitro	[126]
13	Long peptide antigen	OVA SLP containing SIINFEKL	TLR2 ligand (Pam3CSK4)	NPs 300-350 nm		pLGA	Continuous antigen-specific T cell expansion following adoptive transfer of OVA SLP loaded DCs	[127]
14	Long peptide antigen	HPV SLP containing RAHYNIVTF	TLR3 ligand (poly IC)	NPs 400-500 nm	Mouse TC1	pLHMGA	Efficient and comparable tumor regression to IFA emulsion after prime boost injections	[51]

Table 5. Antibody-loaded particles based on aliphatic polyesters

	Antibody	Average particle size	Tumor model	Polymer	Method of particle preparation	Result	Ref.
1	Model Human IgG	MPs 110-145 µm	-	pLGA	S/O/W and W/O/W	S/O/W method was superior to W/O/W in keeping the integrity of encapsulated IgG.Use of mannitol and trehalose resulted in 90% retention of IgG bioactivity during spray freeze drying..Incomplete release of IgG from S/O/W MPs likely due to degradation or aggregation of IgG.	[151]
2	Model Bovine IgG	MPs 110 µm	-	pLGA	S/O/W	Low burst release and complete release of IgG in 8 weeks	[152]
3	Anti-TNF alpha	MPs 40-70 µm	-	pLGA (two different pLGA polymers were used;One with 75% lactic acid and the other with 50% lactic acid)	S/O/W	Stability of the antibody formulations was studied under three conditions; 5, 25 and 40°C for12 weeks. Antibody-loaded pLGA MPs were stable when stored at 5°CHigher temperatures caused aggregation,fragmentation and loss of activity.	[154]
4	Model Human IgG	MPs 6 µm	-	mPEG-pCL-mPEG and pCL	W/O/W	mPEG-pCL-mPEG MPs showed a more controlled release profile compared to pCL and the 57 ± 3% of the released IgG was bioactive after 90 days of release as opposed to 30 ± 2% in pCL.	[153]
5	3D8 scFv -A DNA binding antibody	NPs 68 nm	-	pLGA	W/O/W	Good recovery of antibody using mannitol as stabilizer	[155]
6	Anti-OX40	NPs 86 nm	Mouse AFP-expressing HepG2	pLGA	Surface attachment to NPs	Strong CD8+ T cell proliferation and tumor antigen-specific cytotoxicity as well as cytokine production. more strongly than free antiOX40 mAb *in vitro*	[156]
7	AntiCTLA4	MPs 15 µm	Mouse MC38 Colon carcinoma tumor	pLHMGA	W/O/W	Tumor regression comparable to IFA formulation	Manuscript submitted for publication
8	AntiCD40	MPs 12 µm	Mouse MC38 Colon carcinoma tumor	pLHMGA	W/O/W	Tumor regression comparable to IFA formulation	Manuscript submitted for publication

5. Perspectives

Although some monotherapy approaches discussed in this review have shown encouraging results, the immunosuppressive tumor environment is a threat to the success of cancer immunotherapy. Tumor cells can escape from the immune system by employing several strategies including downregulation of MHC molecules (decrease in antigen presentation) and the induction of immunosuppressive cells and molecules leading to immune tolerance [157-160]. Combinatorial therapies including combination of chemotherapy and immunotherapy as well as utilizing multiple immunotherapy strategies are very attractive for overcoming the immunosuppression caused by tumors and is regarded as a feasible next step in immunotherapy of cancer.

From a pharmaceutical point of view future improvements can include co-encapsulation and/or surface decoration of cancer vaccine with multiple antigens, adjuvants, immunomodulatory antibodies and targeting ligands to provide an optimal immunotherapeutic agents resulting in induction of an efficient and potent immune response.

6. Conclusion

This review aimed to highlight recent advances in development of particulate formulation for cancer immunotherapy. Important parameters in design of a particulate carrier system such as nature of the polymers, particle size, hydrophobicity/hydrophilicity, surface charge etc. were discussed as well as various types of cancer vaccines (antigens, adjuvants and targeting ligands) and immunomodulatory antibodies (antiCD40, antiCTLA4, etc.). Various formulations have been discussed such as particulate cancer vaccines based on pLGA and pLHMGA containing SLPs and TLR ligands, and pLGA and pLHMGA loaded with immunomodulatory antibodies with promising results.

In summary, particulate formulations based on pLGA and related polymers are attractive systems for delivery of immunotherapeutics.

Acknowledgements

This research was conducted within the framework of the Cancer Vaccine Tracking project (#03O-302), Center for Translational Molecular Medicine (CTMM).

References

[1] Finn OJ. Cancer vaccines: Between the idea and the reality. Nat Rev Immunol 2003;3:630-641.
[2] Timmerman JM, Levy R. Dendritic cell vaccines for cancer immunotherapy. Annu Rev Med 1999;50:507-529.
[3] Couzin-Frankel J. Breakthrough of the year 2013. Cancer immunotherapy. Science 2013;342:1432-1433.
[4] Sheng W, Huang L. Cancer Immunotherapy and Nanomedicine. Pharm Res 2011;28:200-214.
[5] Gallois A, Bhardwaj N. A needle in the 'cancer vaccine' haystack. Nat Med 2010;16.
[6] Weiner LM, Surana R, Wang S. Monoclonal antibodies: versatile platforms for cancer immunotherapy. Nat Rev Immunol 2010;10:317-327.
[7] Trombetta ES, Mellman I. Cell biology of antigen processing in vitro and in vivo. Annu Rev Immunol 2005;23:975-1028.
[8]Heath WR, Belz GT, Behrens GMN, Smith CM, Forehan SP, Parish IA, et al. Cross-presentation, dendritic cell subsets, and the generation of immunity to cellular antigens. Immunol Rev 2004;199:9-26.
[9] Guermonprez P, Valladeau J, Zitvogel L, Thery C, Amigorena S. Antigen presentation and T cell stimulation by dendritic cells. Annu Rev Immunol 2002;20:621-667.
[10] Schuler G, Schuler-Thurner B, Steinman RM. The use of dendritic cells in cancer immunotherapy. Curr Opin Immunol 2003;15:138-147.
[11] Shen H, Ackerman AL, Cody V, Giodini A, Hinson ER, Cresswell P, et al. Enhanced and prolonged cross-presentation following endosomal escape of exogenous antigens encapsulated in biodegradable nanoparticles. Immunol 2006;117:78-88.
[12] Heath WR, Carbone FR. Cross-presentation, dendrttic cells, tolerance and immunity. Annu Rev Immunol 2001;19:47-64.
[13] Tan JKH, O'Neill HC. Maturation requirements for dendritic cells in T cell stimulation leading to tolerance versus immunity. J Leukoc Biol 2005;78:319-324.
[14] Wilson NS, El-Sukkari D, Villadangos JA. Dendritic cells constitutively present self antigens in their immature state in vivo and regulate antigen presentation by controlling the rates of MHC class II synthesis and endocytosis. Blood 2004;103:2187-2195.
[15] Cella M, Engering A, Pinet V, Pieters J, Lanzavecchia A. Inflammatory stimuli induce accumulation of MHC class II complexes on dendritic cells. Nature 1997;388:782-787.
[16] Sparwasser T, Koch ES, Vabulas RM, Heeg K, Lipford GB, Ellwart JW, et al. Bacterial DNA and immunostimulatory CpG oligonucleotides trigger maturation and activation of murine dendritic cells. Eur J Immunol 1998;28:2045-2054.
[17] Sallusto F, Schaerli P, Loetscher P, Schaniel C, Lenig D, Mackay CR, et al. Rapid and coordinated switch in chemokine receptor expression during dendritic cell maturation. Eur J Immunol 1998;28:2760-2769.
[18] Schuurhuis D, Laban S, Toes R, Ricciardi-Castagnoli P, Kleijmeer M, van der Voort E, et al. Immature dendritic cells acquire CD8(+) cytotoxic T lymphocyte priming capacity upon activation by T helper cell-independent or -dependent stimuli. J Exp Med 2000;192:145-150.
[19] Schlosser E, Mueller M, Fischer S, Basta S, Busch DH, Gander B, et al. TLR ligands and antigen need to be coencapsulated into the same biodegradable microsphere for the generation of potent cytotoxic T lymphocyte responses. Vaccine 2008;26:1626-1637.
[20] Lu H. TLR Agonists for Cancer Immunotherapy: Tipping the Balance between the Immune Stimulatory and Inhibitory Effects. Front Immunol 2014;5:83-83.
[21] Silva JM, Videira M, Gaspar R, Preat V, Florindo HF. Immune system targeting by biodegradable nanoparticles for cancer vaccines. J Control Release 2013;168:179-199.
[22] Zhang Z, Tongchusak S, Mizukami Y, Kang YJ, Ioji T, Touma M, et al. Induction of anti-tumor cytotoxic T cell responses through PLGA-nanoparticle mediated antigen delivery. Biomaterials 2011;32:3666-3678.
[23] Rosalia RA, Cruz LJ, van Duikeren S, Tromp AT, Silva AL, Jiskoot W, et al. CD40-targeted dendritic cell delivery of PLGA-nanoparticle vaccines induce potent anti-tumor responses. Biomaterials 2015;40:88-97.
[24] Mueller M, Reichardt W, Koerner J, Groettrup M. Coencapsulation of tumor lysate and CpG-ODN in PLGA-microspheres enables successful immunotherapy of prostate carcinoma in TRAMP mice. J Control Release 2012;162:159-166.
[25] Klippstein R, Pozo D. Nanotechnology-based manipulation of dendritic cells for enhanced immunotherapy strategies. Nanomedicine-Nanotechnology Biology and Medicine 2010;6:523-529.
[26] Peggs KS, Quezada SA, Allison JP. Cancer immunotherapy: co-stimulatory agonists and co-inhibitory antagonists. Clin Exp Immunol 2009;157:9-19.
[27] Brahmer JR, Tykodi SS, Chow LQM, Hwu W, Topalian SL, Hwu P, et al. Safety and Activity of Anti-PD-L1 Antibody in Patients with Advanced Cancer. N Engl J Med 2012;366:2455-2465.
[28] Mellman I, Coukos G, Dranoff G. Cancer immunotherapy comes of age. Nature 2011;480:480-489.
[29] Baldo BA. Adverse events to monoclonal antibodies used for cancer therapy Focus on hypersensitivity responses. Oncoimmunol 2013;2.
[30] Fransen MF, Ossendorp F, Arens R, Melief CJM. Local immunomodulation for cancer therapy Providing treatment where needed. Oncoimmunol 2013;2:e26493.
[31] Moon JJ, Huang B, Irvine DJ. Engineering nano- and microparticles to tune immunity. Adv Mater 2012;24:3724-3746.
[32] Fransen MF, Sluijter M, Morreau H, Arens R, Melief CJ. Local activation of CD8 T cells and systemic tumor eradication without toxicity via slow release and local delivery of agonistic CD40 antibody. Clin Cancer Res

2011;17:2270-2280.
[33] Fransen MF, Arens R, Melief CJM. Local targets for immune therapy to cancer: Tumor draining lymph nodes and tumor microenvironment. Int J Cancer 2013;132:1971-1976.
[34] Kenter GG, Welters MJP, Valentijn ARPM, Lowik MJG, Berends-van der Meer DMA, Vloon APG, et al. Vaccination against HPV-16 Oncoproteins for Vulvar Intraepithelial Neoplasia. N Engl J Med 2009;361:1838-1847.
[35] Chen H, Gao J, Lu Y, Kou G, Zhang H, Fan L, et al. Preparation and characterization of PE38KDEL-loaded anti-HER2 nanoparticles for targeted cancer therapy. J Control Release 2008;128:209-216.
[36] Cheng M, Chen Y, Xiao W, Sun R, Tian Z. NK cell-based immunotherapy for malignant diseases. Cell Mol Immunol 2013;10:230-252.
[37] Steenblock ER, Fahmy TM. A comprehensive platform for ex vivo T-cell expansion based on biodegradable polymeric artificial antigen-presenting cells. Mol Ther 2008;16:765-772.
[38] Foged C, Hansen J, Agger EM. License to kill: Formulation requirements for optimal priming of CD8(+) CTL responses with particulate vaccine delivery systems. Eur J Pharm Sci 2012;45:482-491.
[39] Conniot J, Silva JM, Fernandes JG, Silva LC, Gaspar R, Brocchini S, et al. Cancer immunotherapy: nanodelivery approaches for immune cell targeting and tracking. Frontiers in chemistry 2014;2:105-105.
[40] Cruz LJ, Rosalia RA, Kleinovink JW, Rueda F, Lowik CWGM, Ossendorp F. Targeting nanoparticles to CD40, DEC-205 or CD11c molecules on dendritic cells for efficient CD8(+) T cell response: A comparative study. J Control Release 2014;192:209-218.
[41] Elamanchili P, Lutsiak CME, Hamdy S, Diwan M, Samuel J. "Pathogen-mimicking" nanoparticles for vaccine delivery to dendritic cells. Journal of Immunotherapy 2007;30:378-395.
[42] Ahmed KK, Geary SM, Salem AK. Applying biodegradable particles to enhance cancer vaccine efficacy. Immunol Res 2014;59:220-228.
[43] Serda RE. Particle platforms for cancer immunotherapy. Int J Nanomedicine 2013;8:1683-1696.
[44] Mundargi RC, Babu VR, Rangaswamy V, Patel P, Aminabhavi TM. Nano/micro technologies for delivering macromolecular therapeutics using poly(D,L-lactide-co-glycolide) and its derivatives. J Control Release 2008;125:193-209.
[45] Danhier F, Ansorena E, Silva JM, Coco R, Le Breton A, Preat V. PLGA-based nanoparticles: An overview of biomedical applications. J Control Release 2012;161:505-522.
[46] Wischke C, Schwendeman SP. Principles of encapsulating hydrophobic drugs in PLA/PLGA microparticles. Int J Pharm 2008;364:298-327.
[47] Ye M, Kim S, Park K. Issues in long-term protein delivery using biodegradable microparticles. J Control Release 2010;146:241-260.
[48] Bala I, Hariharan S, Kumar MNVR. PLGA nanoparticles in drug delivery: The state of the art. Crit Rev Ther Drug Carrier Syst 2004;21:387-422.
[49] Mundargi RC, Babu VR, Rangaswamy V, Patel P, Aminabhavi TM. Nano/micro technologies for delivering macromolecular therapeutics using poly(D,L-lactide-co-glycolide) and its derivatives. J Control Release 2008;125:193-209.
[50] Zhang Z, Tongchusak S, Mizukami Y, Kang YJ, Ioji T, Touma M, et al. Induction of anti-tumor cytotoxic T cell responses through PLGA-nanoparticle mediated antigen delivery. Biomaterials 2011;32:3666-3678.
[51] Rahimian S, Fransen M, Kleinovink J, Christensen J, Amidi M, Hennink W, et al. Polymeric nanoparicles for co-delivery of synthetic long peptide antigen and poly IC as therapeutic cancer vaccine formulation. J Control Release 2015.
[52] Anderson JM, Shive MS. Biodegradation and biocompatibility of PLA and PLGA microspheres. Adv Drug Deliv Rev 1997;28:5-24.
[53] Vert M, Schwach G, Engel R, Coudane J. Something new in the field of PLA/GA bioresorbable polymers? J Control Release 1998;53:85-92.
[54] Demento SL, Cui W, Criscione JM, Stern E, Tulipan J, Kaech SM, et al. Role of sustained antigen release from nanoparticle vaccines in shaping the T cell memory phenotype. Biomaterials 2012;33:4957-4964.
[55] Bijker MS, van den Eeden SJF, Franken KL, Melief CJM, Offringa R, van der Burg SH. CD8(+) CTL priming by exact peptide epitopes in incomplete Freund's adjuvant induces a vanishing CTL response, whereas long peptides induce sustained CTL reactivity. J Immunol 2007;179:5033-5040.
[56] den Boer A, Diehl L, van Mierlo G, van der Voort E, Fransen M, Krimpenfort P, et al. Longevity of antigen presentation and activation status of APC are decisive factors in the balance between CTL immunity versus tolerance. J Immunol 2001;167:2522-2528.
[57] Eldridge JH, Staas JK, Meulbroek JA, Mcghee JR, Tice TR, Gilley RM. Biodegradable microspheres as a vaccine delivery system. Mol Immunol 1991;28:287-294.
[58] Silva AL, Rosalia RA, Varypataki E, Sibuea S, Ossendorp F, Jiskoot W. Poly-(lactic-co-glycolic-acid)-based particulate vaccines: Particle uptake by dendritic cells is a key parameter for immune activation. Vaccine 2015;33:847-854.
[59] Locatelli E, Franchini MC. Biodegradable PLGA-b-PEG polymeric nanoparticles: synthesis, properties, and nanomedical applications as drug delivery system. J Nanoparticle Res 2012;14:1316.
[60] Zhang K, Tang X, Zhang J, Lu W, Lin X, Zhang Y, et al. PEG-PLGA copolymers: Their structure and structure-influenced drug delivery applications. J Control Release 2014;183:77-86.
[61] Cruz LJ, Tacken PJ, Fokkink R, Joosten B, Stuart MC, Albericio F, et al. Targeted PLGA nano- but not microparticles specifically deliver antigen to human dendritic cells via DC-SIGN in vitro. J Controlled Release 2010;144:118-126.

[62] Ding AG, Schwendeman SP. Acidic Microclimate pH distribution in PLGA microspheres monitored by confocal laser scanning microscopy. Pharm Res 2008;25:2041-2052.
[63] van de Weert M, Hennink WE, Jiskoot W. Protein instability in poly(lactic-co-glycolic acid) microparticles. Pharm Res 2000;17:1159-1167.
[64] Houchin ML, Topp EM. Chemical degradation of peptides and proteins in PLGA: A review of reactions and mechanisms. J Pharm Sci 2008;97:2395-2404.
[65] Pisal DS, Kosloski MP, Balu-Iyer SV. Delivery of therapeutic proteins. J Pharm Sci 2010;99:2557-2575.
[66] Johansen P, Men Y, Merkle HP, Gander B. Revisiting PLA/PLGA microspheres: an analysis of their potential in parenteral vaccination. Eur J Pharm Biopharm 2000;50:129-146.
[67] Slutter B, Bal S, Keijzer C, Mallants R, Hagenaars N, Que I, et al. Nasal vaccination with N-trimethyl chitosan and PLGA based nanoparticles: Nanoparticle characteristics determine quality and strength of the antibody response in mice against the encapsulated antigen. Vaccine 2010;28:6282-6291.
[68] Krishnamachari Y, Geary SM, Lemke CD, Salem AK. nanoparticle delivery systems in cancer vaccines. Pharm Res 2011;28:215-236.
[69] Oyewumi MO, Kumar A, Cui Z. Nano-microparticles as immune adjuvants: correlating particle sizes and the resultant immune responses. Exp Rev Vaccines 2010;9:1095-1107.
[70] Park Y, Lee SJ, Kim YS, Lee MH, Cha GS, Jung ID, et al. Nanoparticle-based vaccine delivery for cancer immunotherapy. Immune network 2013;13:177-83.
[71] Reddy ST, van der Vlies AJ, Simeoni E, Angeli V, Randolph GJ, O'Neill CP, et al. Exploiting lymphatic transport and complement activation in nanoparticle vaccines. Nat Biotechnol 2007;25:1159-1164.
[72] Manolova V, Flace A, Bauer M, Schwarz K, Saudan P, Bachmann MF. Nanoparticles target distinct dendritic cell populations according to their size. Eur J Immunol 2008;38:1404-1413.
[73] Joshi VB, Geary SM, Salem AK. Biodegradable Particles as Vaccine Delivery Systems: Size Matters. Aaps Journal 2013;15:85-94.
[74] Foged C, Brodin B, Frokjaer S, Sundblad A. Particle size and surface charge affect particle uptake by human dendritic cells in an in vitro model. Int J Pharm 2005;298:315-322.
[75] Han R, Zhu J, Yang X, Xu H. Surface modification of poly(D,L-lactic-co-glycolic acid) nanoparticles with protamine enhanced cross-presentation of encapsulated ovalbumin by bone marrow-derived dendritic cells. J Biomed Mat Res Part a 2011;96A:142-149.
[76] Fernandez-Megia E, Novoa-Carballal R, Quinoa E, Riguera R. Conjugation of bioactive ligands to PEG-grafted chitosan at the distal end of PEG. Biomacromolecules 2007;8:833-842.
[77] Vasir JK, Labhasetwar V. Quantification of the force of nanoparticle-cell membrane interactions and its influence on intracellular trafficking of nanoparticles. Biomaterials 2008;29:4244-4252.
[78] Froehlich E. The role of surface charge in cellular uptake and cytotoxicity of medical nanoparticles. Int J Nanomedicine 2012;7:5577-5591.
[79] Aggarwal P, Hall JB, McLeland CB, Dobrovolskaia MA, McNeil SE. Nanoparticle interaction with plasma proteins as it relates to particle biodistribution, biocompatibility and therapeutic efficacy. Adv Drug Deliv Rev 2009;61:428-437.
[80] Rao DA, Forrest ML, Alani AWG, Kwon GS, Robinson JR. Biodegradable PLGA Based Nanoparticles for Sustained Regional Lymphatic Drug Delivery. J Pharm Sci 2010;99:2018-2031.
[81] Liu Y, Yin Y, Wang L, Zhang W, Chen X, Yang X, et al. Surface hydrophobicity of microparticles modulates adjuvanticity. J Mat Chem B 2013;1:3888-3896.
[82] Niikura K, Matsunaga T, Suzuki T, Kobayashi S, Yamaguchi H, Orba Y, et al. Gold Nanoparticles as a Vaccine Platform: Influence of Size and Shape on Immunological Responses in Vitro and in Vivo. ACS Nano 2013;7:3926-3938.
[83] Champion JA, Mitragotri S. Role of target geometry in phagocytosis. Proc Natl Acad Sci U S A 2006;103:4930-4934.
[84] Champion JA, Mitragotri S. Shape Induced Inhibition of Phagocytosis of Polymer Particles. Pharm Res 2009;26:244-249.
[85] Prasad S, Cody V, Saucier-Sawyer JK, Saltzman WM, Sasaki CT, Edelson RL, et al. Polymer nanoparticles containing tumor lysates as antigen delivery vehicles for dendritic cell-based antitumor immunotherapy. Nanomedicine-Nanotech Biol Med 2011;7:1-10.
[86] Clawson C, Huang C, Futalan D, Seible DM, Saenz R, Larsson M, et al. Delivery of a peptide via poly(D,L-lactic-co-glycolic) acid nanoparticles enhances its dendritic cell-stimulatory capacity. Nanomedicine-Nanotech Biol Med 2010;6:651-661.
[87] Solbrig CM, Saucier-Sawyer JK, Cody V, Saltzman WM, Hanlon DJ. Polymer nanoparticles for immunotherapy from encapsulated tumor-associated antigens and whole tumor cells. Mol Pharm 2007;4:47-57.
[88] Petrovsky N, Aguilar JC. Vaccine adjuvants: Current state and future trends. Immunol Cell Biol 2004;82:488-496.
[89] Mueller M, Schlosser E, Gander B, Groettrup M. Tumor eradication by immunotherapy with biodegradable PLGA microspheres-an alternative to incomplete Freund's adjuvant. Int J Cancer 2011;129:407-416.
[90] Florindo HF, Pandit S, Goncalves LM, Videira M, Alpar O, Almeida AJ. Antibody and cytokine-associated immune responses to S. equi antigens entrapped in PLA nanospheres. Biomaterials 2009;30:5161-5169.
[91] Demento SL, Eisenbarth SC, Foellmer HG, Platt C, Caplan MJ, Saltzman WM, et al. Inflammasome-activating nanoparticles as modular systems for optimizing vaccine efficacy. Vaccine 2009;27:3013-3021.
[92] Zhang X, Dahle CE, Baman NK, Rich N, Weiner GJ, Salem AK. Potent antigen-specific immune responses

stimulated by codelivery of CpG ODN and antigens in degradable microparticles. Journal of Immunother 2007;30:469-478.
[93] Fischer S, Uetz-von Allmen E, Waeckerle-Men Y, Groettrup M, Merkle HP, Gander B. The preservation of phenotype and functionality of dendritic cells upon phagocytosis of polyelectrolyte-coated PLGA microparticles. Biomaterials 2007;28:994-1004.
[94] Kawai T, Akira S. TLR signaling. Semin Immunol 2007;19:24-32.
[95] Steinhagen F, Kinjo T, Bode C, Klinman DM. TLR-based immune adjuvants. Vaccine 2011;29:3341-3355.
[96] Adams S. Toll-like receptor agonists in cancer therapy. Immunother 2009;1:949-964.
[97] Leleux J, Roy K. Micro and nanoparticle-based delivery systems for vaccine immunotherapy: an immunological and materials perspective. Adv Healthcare Mat 2013;2:72-94.
[98] Hamdy S, Molavi O, Ma Z, Haddadi A, Alshamsan A, Gobti Z, et al. Co-delivery of cancer-associated antigen and Toll-like receptor 4 ligand in PLGA nanoparticles induces potent CD8(+) T cell-mediated anti-tumor immunity. Vaccine 2008;26:5046-5057.
[99] Hamdy S, Haddadi A, Hung RW, Lavasanifar A. Targeting dendritic cells with nano-particulate PLGA cancer vaccine formulations. Adv Drug Deliv Rev 2011;63:943-955.
[100] Alexis F, Pridgen E, Molnar LK, Farokhzad OC. Factors affecting the clearance and biodistribution of polymeric nanoparticles. Mol Pharm 2008;5:505-515.
[101] Burgdorf S, Kurts C. Endocytosis mechanisms and the cell biology of antigen presentation. Curr Opin Immunol 2008;20:89-95.
[102] Ghotbi Z, Haddadi A, Hamdy S, Hung RW, Samuel J, Lavasanifar A. Active targeting of dendritic cells with mannan-decorated PLGA nanoparticles. J Drug Target 2011;19:281-292.
[103] Hamdy S, Haddadi A, Shayeganpour A, Samuel J, Lavasanifar A. Activation of antigen-specific T cell-responses by mannan-decorated PLGA nanoparticles. Pharm Res 2011;28:2288-2301.
[104] Kwon Y, James E, Shastri N, Frechet J. In vivo targeting of dendritic cells for activation of cellular immunity using vaccine carriers based on pH-responsive microparticles. Proc Natl Acad Sci U S A 2005;102:18264-18268.
[105] Steinhagen F, Kinjo T, Bode C, Klinman DM. TLR-based immune adjuvants. Vaccine 2011;29:3341-3355.
[106] Tamber H, Johansen P, Merkle HP, Gander B. Formulation aspects of biodegradable polymeric microspheres for antigen delivery. Adv Drug Deliv Rev 2005;57:357-376.
[107] Jiang WL, Gupta RK, Deshpande MC, Schwendeman SP. Biodegradable poly(lactic-co-glycolic acid) microparticles for injectable delivery of vaccine antigens. Adv Drug Deliv Rev 2005;57:391-410.
[108] Hafner AM, Corthesy B, Merkle HP. Particulate formulations for the delivery of poly(I:C) as vaccine adjuvant. Adv Drug Deliv Rev 2013;65:1386-1399.
[109] O'Hagan DT, Singh M, Ulmer JB. Microparticle-based technologies for vaccines. Methods 2006;40:10-19.
[110] Reinhold SE, Schwendeman SP. Effect of polymer porosity on aqueous self-healing encapsulation of proteins in plga microspheres. Macromol Biosci 2013;13:1700-1710.
[111] Desai KG, Schwendeman SP. Active self-healing encapsulation of vaccine antigens in PLGA microspheres. J Control Release 2013;165:62-74.
[112] Cheever MA, Higano CS. PROVENGE (Sipuleucel-T) in Prostate Cancer: The first FDA-approved therapeutic cancer vaccine. Clin Cancer Res 2011;17:3520-3526.
[113] Hanlon DJ, Aldo PB, Devine L, Alvero AB, Engberg AK, Edelson R, et al. Enhanced stimulation of anti-ovarian cancer CD8+t cells by dendritic cells loaded with nanoparticle encapsulated tumor antigen. Am J ReproducImmunol 2011;65:597-609.
[114] Jaehnisch H, Fuessel S, Kiessling A, Wehner R, Zastrow S, Bachmann M, et al. Dendritic Cell-Based Immunotherapy for Prostate Cancer. Clin Develop Immunol 2010:517493.
[115] Gross BP, Wongrakpanich A, Francis MB, Salem AK, Norian LA. A therapeutic microparticle-based tumor lysate vaccine reduces spontaneous metastases in murine breast cancer. Aaps Journal 2014;16:1194-1203.
[116] Greenberg NM, Demayo F, Finegold MJ, Medina D, Tilley WD, Aspinall JO, et al. Prostate-Cancer in a Transgenic Mouse. Proc Natl Acad Sci U S A 1995;92:3439-3443.
[117] Zhang L, Zhao S, Duan J, Hu Y, Gu N, Xu H, et al. Enhancement of DC-mediated anti-leukemic immunity in vitro by WT1 antigen and CpG co-encapsulated in PLGA microparticles. Protein & Cell 2013;4:887-889.
[118] Zwaveling S, Mota S, Nouta J, Johnson M, Lipford G, Offringa R, et al. Established human papillomavirus type 16-expressing tumors are effectively eradicated following vaccination with long peptides. J Immunol 2002;169:350-358.
[119] Bennett SRM, Carbone FR, Toy T, Miller JFAP, Heath WR. B cells directly tolerize CD8(+) T cells. J Exp Med 1998;188:1977-1983.
[120] Toes REM, Blom RJJ, Offringa R, Kast WM, Melief CJM. Enhanced tumor outgrowth after peptide vaccination - Functional deletion of tumor-specific CTL induced by peptide vaccination can lead to the inability to reject tumors. J Immunol 1996;156:3911-3918.
[121] Toes REM, Offringa R, Blom RJJ, Melief CJM, Kast WM. Peptide vaccination can lead to enhanced tumor growth through specific T-cell tolerance induction. Proc Natl Acad Sci U S A 1996;93:7855-7860.
[122] Melief CJM, van der Burg SH. Immunotherapy of established (pre) malignant disease by synthetic long peptide vaccines. Nat Rev Cancer 2008;8:351-360.
[123] Rosalia RA, Quakkelaar ED, Redeker A, Khan S, Camps M, Drijfhout JW, et al. Dendritic cells process synthetic long peptides better than whole protein, improving antigen presentation and T-cell activation. Eur J Immunol

2013;43:2554-2565.
[124] Bijker MS, van den Eeden SJE, Franken KL, Melief CJM, van der Burg SH, Offringa R. Superior induction of anti-tumor CTL immunity by extended peptide vaccines involves prolonged, DC-focused antigen presentation. Eur J Immunol 2008;38:1033-1042.
[125] Falo LD, Colarusso LJ, Benacerraf B, Rock KL. Serum proteases alter the antigenicity of peptides presented by class-i major histocompatibility complex-molecules. Proc Natl Acad Sci U S A 1992;89:8347-8350.
[126] Silva AL, Rosalia RA, Sazak A, Carstens MG, Ossendorp F, Oostendorp J, et al. Optimization of encapsulation of a synthetic long peptide in PLGA nanoparticles: Low-burst release is crucial for efficient CD8(+) T cell activation. Eur J Pharm Biopharms 2013;83:338-345.
[127] Rosalia R. Particulate based vaccines for cancer immunotherapy. 2014:95-128.
[128] Kenter GG, Welters MJP, Valentijn ARPM, Lowik MJG, Berends-van der Meer DMA, Vloon APG, et al. Vaccination against HPV-16 oncoproteins for vulvar intraepithelial neoplasia. N Engl J Med 2009;361:1838-1847.
[129] Welters MJP, Kenter GG, de Vos van Steenwijk, Peggy J., Löwik MJG, Berends-van der Meer DMA, Essahsah F, et al. Success or failure of vaccination for HPV16-positive vulvar lesions correlates with kinetics and phenotype of induced T-cell responses. Proc Natl Acad Sci U S A 2010;107:11895-11899.
[130] Rahimian S, Kleinovink JW, Fransen MF, Mezzanotte L, Gold H, Wisse P, et al. Near-infrared labeled, ovalbumin loaded polymeric nanoparticles based on a hydrophilic polyester as model vaccine: In vivo tracking and evaluation of antigen-specific CD8+ T cell immune response. Biomaterials 2015;37:469-477.
[131] Leemhuis M, van Nostrum C, Kruijtzer J, Zhong Z, ten Breteler M, Dijkstra P, et al. Functionalized poly(alpha-hydroxy acid)s via ring-opening polymerization: Toward hydrophilic polyesters with pendant hydroxyl groups. Macromolecules 2006;39:3500-3508.
[132] Ghassemi AH, van Steenbergen MJ, Talsma H, van Nostrum CF, Jiskoot W, Crommelin DJA, et al. Preparation and characterization of protein loaded microspheres based on a hydroxylated aliphatic polyester, poly (lactic-co-hydroxymethyl glycolic acid). J Control Release 2009;138:57-63.
[133] Prasad S, Cody V, Saucier-Sawyer JK, Fadel TR, Edelson RL, Birchall MA, et al. Optimization of stability, encapsulation, release, and cross-priming of tumor antigen-containing PLGA nanoparticles. Pharm Res 2012;29:2565-2577.
[134] Weiner LM, Surana R, Wang S. Monoclonal antibodies: versatile platforms for cancer immunotherapy. Nat Rev Immunol 2010;10:317-327.
[135] Hamid O, Robert C, Daud A, Hodi FS, Hwu W, Kefford R, et al. Safety and Tumor Responses with Lambrolizumab (Anti-PD-1) in Melanoma. N Engl J Med 2013;369:134-144.
[136] Kyi C, Postow MA. Checkpoint blocking antibodies in cancer immunotherapy. FEBS Lett 2014;588:368-376.
[137] Peggs KS, Quezada SA, Allison JP. Cancer immunotherapy: co-stimulatory agonists and co-inhibitory antagonists. Clin Exp Immunol 2009;157:9-19.
[138] van Mierlo G, den Boer A, Medema J, van der Voort E, Fransen M, Offringa R, et al. CD40 stimulation leads to effective therapy of CD40(-)tumors through induction of strong systemic cytotoxic T lymphocyte immunity. Proc Natl Acad Sci U S A 2002;99:5561-5566.
[139] Todryk S, Tutt A, Green M, Smallwood J, Halanek N, Dalgleish A, et al. CD40 ligation for immunotherapy of solid tumours. J Immunol Methods 2001;248:139-147.
[140] Attia P, Phan G, Maker A, Robinson M, Quezado M, Yang J, et al. Autoimmunity correlates with tumor regression in patients with metastatic melanoma treated with anti-cytotoxic T-lymphocyte antigen-4. J Clin Oncol 2005;23:6043-6053.
[141] Sanderson K, Scotland R, Lee P, Liu D, Groshen S, Snively J, et al. Autoimmunity in a phase I trial of a fully human anti-cytotoxic T-lymphocyte antigen-4 monoclonal antibody with multiple melanoma peptides and montanide ISA 51 for patients with resected stages III and IV melanoma. J Clin Oncol 2005;23:741-750.
[142] Fransen MF, van der Sluis TC, Ossendorp F, Arens R, Melief CJM. Controlled local delivery of CTLA-4 blocking antibody induces CD8(+) T-cell-dependent tumor eradication and decreases risk of toxic side effects. Clin Cancer Res 2013;19:5381-5389.
[143] Guy B. The perfect mix: recent progress in adjuvant research. Nat Rev Microbiol 2007;5:505-517.
[144] Kenter GG, Welters M, Lowik M, Drijfhout J, Valentijn R, Ostendorp J, et al. Therapeutic HPV 16 vaccination with long E6 and E7 peptides shows immunological and clinical efficacy. Gynecol Oncol 2008;108:S19-S19.
[145] Murray R, Cohen P, Hardegre.MC. Mineral-oil adjuvants - biological and chemical studies. Ann Allergy 1972;30:146-&.
[146] Doshi N, Mitragotri S. Macrophages Recognize Size and Shape of Their Targets. Plos One 2010;5:e10051.
[147] Frokjaer S, Otzen DE. Protein drug stability: A formulation challenge. Nat Rev Drug Discovery 2005;4:298-306.
[148] Ghassemi AH, van Steenbergen MJ, Barendregt A, Talsma H, Kok RJ, van Nostrum CF, et al. Controlled release of octreotide and assessment of peptide acylation from poly(D,L-lactide-co-hydroxymethyl glycolide) compared to PLGA microspheres. Pharm Res 2012;29:110-120.
[149] Liu Y, Ghassemi AH, Hennink WE, Schwendeman SP. The microclimate pH in poly(D,L-lactide-co-hydroxymethyl glycolide) microspheres during biodegradation. Biomaterials 2012;33:7584-7593.
[150] Kazazi-Hyseni F, Zandstra J, Popa E, Goldschmeding R, Lathuile A, Veldhuis G, et al. Biocompatibility of poly(d,l-lactic-co-hydroxymethyl glycolic acid) microspheres after subcutaneous and subcapsular renal injection. Int J Pharm 2015;482:99-109.
[151] Wang JJ, Chua KM, Wang CH. Stabilization and encapsulation of human immunoglobulin G into biodegradable

microspheres. J Colloid Interface Sci 2004;271:92-101.
[152] Marquette S, Peerboom C, Yates A, Denis L, Goole J, Amighi K. Encapsulation of immunoglobulin G by solid-in-oil-in-water: Effect of process parameters on microsphere properties. Eur J Pharm Biopharm 2014;86:393-403.
[153] Erdemli O, Usanmaz A, Keskin D, Tezcaner A. Characteristics and release profiles of MPEG-PCL-MPEG microspheres containing immunoglobulin G. Colloids Surf B Biointerfaces 2014;117:487-496.
[154] Marquette S, Peerboom C, Yates A, Denis L, Langer I, Amighi K, et al. Stability study of full-length antibody (anti-TNF alpha) loaded PLGA microspheres. Int J Pharm 2014;470:41-50.
[155] Son S, Lee WR, Joung YK, Kwon MH, Kim YS, Park KD. Optimized stability retention of a monoclonal antibody in the PLGA nanoparticles. Int J Pharm 2009;368:178-185.
[156] Chen M, Ouyang H, Zhou S, Li J, Ye Y. PLGA-nanoparticle mediated delivery of anti-OX40 monoclonal antibody enhances anti-tumor cytotoxic T cell responses. Cell Immunol 2014;287:91-99.
[157] Gabrilovich DI, Nagaraj S. Myeloid-derived suppressor cells as regulators of the immune system. Nat Rev Immunol 2009;9:162-174.
[158] Drake CG, Jaffee E, Pardoll DM. Mechanisms of immune evasion by tumors. Adv Immunol, Vol 90: Cancer Immunother 2006;90:51-81.
[159] Poggi A, Zocchi MR. Mechanisms of tumor escape: role of tumor microenvironment in inducing apoptosis of cytolytic effector cells. Arch Immunol Ther Exp (Warsz) 2006;54:323-333.
[160] Seliger B. Strategies of tumor immune evasion. Biodrugs 2005;19:347-354.

CHAPTER 3

Near-infrared labeled, ovalbumin-loaded polymeric nanoparticles based on a hydrophilic polyester as model vaccine: *In vivo* tracking and evaluation of antigen-specific CD8+ T cell immune response

Sima Rahimian*
Jan Willem Kleinovink*
Marieke F. Fransen
Laura Mezzanotte
Henrik Gold
Patrick Wisse
Hermen Overkleeft
Maryam Amidi
Wim Jiskoot
Clemens W. Löwik
Ferry Ossendorp
Wim E. Hennink

Biomaterials 2015, 37;469-477

*** authors contributed equally**

Abstract

Particulate antigen delivery systems aimed at the induction of antigen-specific T cells form a promising approach in immunotherapy to replace pharmacokinetically unfavorable soluble antigen formulations. In this study, we developed a delivery system using the model protein antigen ovalbumin (OVA) encapsulated in nanoparticles based on the hydrophilic polyester poly(lactide-co-hydroxymethylglycolic acid) (pLHMGA). Spherical nanoparticles with size 300-400 nm were prepared and characterized and showed a strong ability to deliver antigen to dendritic cells for cross-presentation to antigen-specific T cells *in vitro*. Using near-infrared (NIR) fluorescent dyes covalently linked to both the nanoparticle and the encapsulated OVA antigen, we tracked the fate of this formulation in mice. We observed that the antigen and the nanoparticles are efficiently co-transported from the injection site to the draining lymph nodes, in a more gradual and durable manner than soluble OVA protein. OVA-loaded pLHMGA nanoparticles efficiently induced antigen cross-presentation to OVA-specific CD8+ T cells in the lymph nodes, superior to soluble OVA vaccination. Together, these data show the potential of pLHMGA nanoparticles as attractive antigen delivery vehicles.

Keywords: Antigen delivery, *In vivo* tracking, Nanoparticles, Near-infrared imaging, pLHMGA

1. Introduction

Immunotherapy aims at the induction or enhancement of cellular immune responses against the target of interest, and has the advantage of a high efficacy and low side effects based on antigen specificity [1]. One of the challenging aspects in the development of effective strategies for immunotherapy is to secure efficient antigen presentation by dendritic cells (DCs) in a targeted and sustained manner to subsequently result in activation of antigen-specific T cells [2]. DCs are professional antigen presenting cells (APCs) and have a pivotal role in the initiation and orchestration of T cell immune responses [3-6]. Immature DCs constantly engulf and process soluble and particulate antigens, as well as necrotic and apoptotic cells via various mechanisms [7]. Upon maturation, DCs migrate to draining lymph nodes and present the processed protein antigens in the form of linear peptide epitopes to CD4+ and CD8+ T cells through major histocompatibility complex (MHC) class I and class II molecules to initiate a proper immune response against the antigens [6,8,9]. The crucial role of DCs in adaptive immunity makes them an important target for the development of vaccines. The weak immunogenicity of soluble protein antigens has led to the development of carrier systems that aim for DC targeting and intracellular antigen delivery [2,10-17]. Particulate delivery systems have several advantages such as protection of antigen against enzymatic degradation and enhanced uptake by DCs, the possibility of co-delivery of antigen and adjuvants to DCs, and the possibility of introducing targeting ligands on the surface of the particle as well as prolonged antigen delivery for sustained antigen-presentation by DCs [2,3,7,15,18-22]. Especially biodegradable polymeric nanoparticles (NPs) have been used extensively as antigen delivery vehicles [3,15,19,23]. In particular, particles based on poly(lactic-co-glycolic acid) (pLGA), a biodegradable polyester, have been widely investigated for diverse pharmaceutical applications including protein and antigen delivery [24-29]. Several studies have shown the efficacy of antigen-loaded pLGA particulate systems in the induction of immune responses both *in vitro* and in animal models [18,30,31]. pLGA particles are far more efficient in generating long lasting CD8+ T cell immunity than soluble antigen and antigen in incomplete Freund's adjuvant (IFA) formulations [32]. Nevertheless, pLGA systems have several drawbacks as peptide/protein-releasing formulations. Upon degradation, acidification inside the particles results in aggregation and denaturation of the loaded peptide/protein [33]. Moreover, peptide/protein encapsulated in pLGA are prone to chemical modifications such as acylation [34,35]. Altogether these drawbacks lead to incomplete release [36] of the content from the particles and possible undesired immunogenicity and other adverse reactions [37]. To overcome pLGA pitfalls, functionalized polyesters such as poly(lactic-co-glycolic-hydroxymethyl glycolic acid) (pLGHMGA) and poly(lactic-co-hydroxymethyl glycolic acid) (pLHMGA) have been developed. These polymers are more hydrophilic than pLGA and therefore degrade faster, do not show a pH drop inside the degrading particles [38] and cause much lower acylation. Moreover, they show complete and faster release in comparison to pLGA particles [39-41].

The fate of vaccines after administration has been investigated in several *in vivo* imaging studies [42-46]. Fluorescence imaging has received considerable attention during the past few years because of its advantages such as the ease of translation from *in vitro* imaging studies and being non-invasive, fast and cost-effective [47-51]. Several *in vivo* near-infrared (NIR) fluorescent dyes have been developed with excitation/emission maxima between 700 and 900 nm to minimize tissue absorbance and light scattering, resulting in increased depth of penetration, low fluorescence background, and high intensity signals [45]. These dyes can be modified or conjugated to antigens or NPs/polymers [50]. A considerable number of vaccine tracking studies with NIR fluorescent dyes focuses on tracking of DCs rather than the vaccine. Moreover, the fluorescent dye is often encapsulated in the particles which brings the risk of dye leakage from the particles [46,52], or is attached to other contrast agents such

as superparamagnetic iron oxide particles [53,54]. The use of NIR fluorescent dyes coupled both to the antigen of interest and to the delivery system may therefore be preferred.
In this study, we evaluate the feasibility of polymeric pLHMGA NPs as a protein antigen delivery system. The particulate antigen showed a superior ability to induce antigen cross-presentation to antigen-specific T cells compared to soluble antigen, both *in vitro* and *in vivo*. Using NIR dyes covalently linked to both the NP and the model protein antigen, we visualized the delivery system and its content in real-time, showing gradual relocation from the injection site to the draining lymph nodes. This shows the potential of pLHMGA NPs as an efficient antigen delivery system for the induction of antigen-specific cellular immune responses and suggests its experimental application in cancer research.

2. Materials and methods

2.1. Materials

Ovalbumin Low Endo™ (OVA, batch X2N13844) was purchased from Worthington, USA. IRDye680RD and IRDye800CW N-hydroxysuccinimide ester (NHS ester) were purchased from LI-COR Biosciences, USA. Alexa647-labeled ovalbumin was obtained from Molecular probes, the Netherlands. 5-Hexyn-1-ol, polyvinyl alcohol (PVA; Mw 30,000-70,000; 88% hydrolyzed), palladium on carbon (Pd/C; 10% wt. loading dry support), tin(II) 2-ethylhexanoate ($Sn(Oct)_2$), copper(I) acetate, dimethyl sulfoxide (DMSO) and tris[(1-benzyl-1H-1,2,3-triazol-4-yl)methyl]amine (TBTA) were obtained from Sigma Aldrich, USA. Benzyl alcohol, sodium dihydrogen phosphate (NaH_2PO_4) and disodium hydrogen phosphate (Na_2HPO_4) were obtained from Merck, Germany. D,L-Lactide was from Purac, the Netherlands. N,N dimethylformamide (DMF), chloroform, dichloromethane (DCM), n-propanol, methanol, tetrahydrofuran (THF) and toluene were from Biosolve, the Netherlands. Sodium azide (NaN_3, 99%), sodium hydroxide (NaOH) and sodium dodecyl sulphate 20% (SDS) were purchased from Fluka, the Netherlands. Micro-BCA protein assay kit was obtained from Thermo Fisher Scientific Inc., USA. Pyrogen-free water was purchased from Carl Roth, Germany. Phosphate buffered saline (1.8 mM NaH_2PO_4, 8.7 mM Na_2HPO_4, 163.9 mM Na^+, 140.3 mM Cl^-) (PBS) was obtained from B Braun, Germany. Toluene and DMF were dried on 3Å molecular sieves prior to use. Chemicals were used as received without further purification, unless otherwise stated. Azide-functionalized water-soluble near-infrared fluorescent dye 10 (azide- NIR10) (**Supplementary Figure S1**) was prepared as described elsewhere [55] (Experimental details are provided in supplementary data).

2.2. Synthesis of polymers

2.2.1. Synthesis of copolymers of 3S-(benzyloxymethyl)-6S-methyl-1,4-dioxane-2,5-dione with D,L-lactide (pLHMGA)

3S-(benzyloxymethyl)-6S-methyl-1,4-dioxane-2,5-dione (benzyloxymethylmethylglycolide) (BMMG) was synthesized as described before [56]. A copolymer of D,L-lactide and BMMG (50:50 molar ratio) was synthesized via ring opening polymerization at 130°C using benzyl alcohol as initiator with a 100/1 monomer-to-initiator molar ratio and $Sn(Oct)_2$ as catalyst (**Figure 1**) [39,56]. In a typical procedure, vacuum dried monomers (BMMG (2840 mg, 11.35 mmol) and D,L-lactide (1630 mg, 11.35 mmol)) were introduced into a dry schlenk tube under a nitrogen atmosphere. Next, benzyl alcohol (24.5 mg, 0.226 mmol; 223.1 mL from a 109.8 mg/mL stock solution in toluene) and $Sn(Oct)_2$ (45.9 mg, 0.113 mmol; 409.8 mL from a 112 mg/mL stock solution in toluene) were added. Toluene was evaporated under vacuum for 2 h, the tube was closed and immersed into a preheated 130°C oil bath for 16 h while stirring. Next, the obtained polymer was dissolved in 10 mL chloroform and subsequently precipitated in 500 mL cold methanol to remove the unreacted monomers and to precipitate the polymer, which was collected by filtration and vacuum dried to yield 4.5 g (90%) poly(D,L-lactic-co-benzyloxymethylglycolic acid) (pLBMGA). Subsequently, pLBMGA was dissolved in 500 mL THF, and 5 g of 10% w/w Pd/C catalyst was added. The flask was

filled with hydrogen in three consecutive steps of subsequent evacuation and refilling with H_2 and the reaction mixture was stirred for 16 h under a H_2 pressure. Next, Pd/C was removed using a glass filter and THF was removed by evaporation. The obtained polymer was then dissolved in 5 mL chloroform and precipitated in 200 mL n-propanol and vacuum dried after filtration to yield 3 g of pLHMGA (84%).

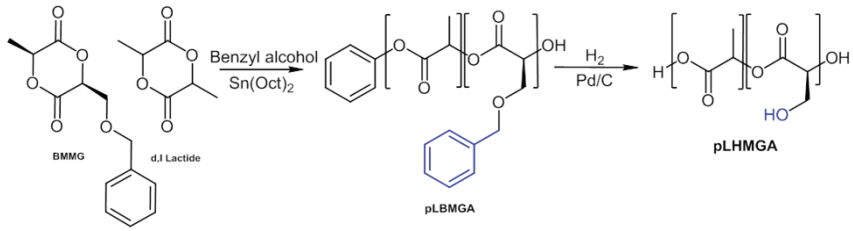

Figure 1. Synthesis of poly(lactic-co-hydroxymethylglycolic acid) (pLHMGA) in two steps; synthesis of poly(lactic-co-benzyloxymethylglycolic acid) (pLBMGA) via ring opening polymerization of BMMG and D,L-lactide, followed by removing the benzyl group by hydrogenation to yield pLHMGA.

2.2.2. Synthesis of hexyn-poly(D,L-lactide) (hexyn-pDLLA) to couple to azide-NIR10 via click chemistry

Hexyn-pDLLA was synthesized via ring opening polymerization similar to the method described in **Section 2.2.1**. Briefly, vacuum dried D,L-lactide (396 mg, 2.75 mmol) was transferred into a dry schlenk tube under a nitrogen atmosphere. Next, the initiator, 5-hexyn-1-ol (monomer-to-initiator molar ratio was 70 to 1, 3.85 mg, 0.039 mmol; 75.5 mL from a 51 mg/mL stock solution in toluene) and $Sn(Oct)_2$ (7.9 mg, 0.020 mmol; 71.2 mL from a 112 mg/mL stock solution in toluene) were introduced into the schlenk tube. The tube was evacuated for 2 h, sealed, and immersed in an oil bath thermostated at 130°C. The polymerization was performed for 16 h and the formed polymer was purified by dissolution in chloroform and precipitation in n-propanol followed by filtration and vacuum drying to yield 370 mg of hexyn-pDLLA (**Supplementary Figure S2**) (Yield: 92%).

2.3. Conjugation of azide-NIR10 to hexyn-pDLLA by click chemistry

Conjugation of the azide-NIR10 to hexyn-pDLLA was performed using copper catalyzed azide-alkyne cycloaddition [57-60] (**Supplementary Figure S3**). In a typical procedure, 30.4 mg hexyn-pDLLA (1.84 mmol) and 2 mg azide-NIR10 (1.84 mmol) were transferred into a vial. Then copper (I) acetate (0.2 mol per mole of polymer) and TBTA (0.05 mol per mole of polymer) were added to the vial from their stock solution in dried DMF and the volume was adjusted with DMF to 250 mL. The system was flushed with nitrogen for 20 min and the reaction was performed at 40°C overnight. The obtained conjugate (NIR10-pDLLA) was purified by precipitation in water. The obtained precipitate was washed with water and freeze-dried at -50°C and 0.7 mbar overnight (Chris Alpha 1-2 freeze-drier, Germany). The conjugation efficiency was calculated using GPC analysis by dividing the area under the curve of the conjugated polymer using UV detection by the area under the curve of reaction mixture (Yield: 76%).

2.4. Polymer characterization

2.4.1. NMR spectroscopy

A Gemini 300 MHz spectrometer (Varian Associates Inc., USA) was used to conduct ^1H NMR measurements at 298 K. Chemical shifts are reported in ppm with reference to the solvent peak (δ) 7.26 ppm for $CDCl_3$.

2.4.2. Gel permeation chromatography (GPC)

Molecular weight and molecular weight distribution (polydispersity index (PDI); weight average molecular weight/number average molecular weight) of the synthesized pLHMGA was measured by using a Waters Alliance system (Waters, USA) with a Waters 2695 separating module equipped with Waters 2414 refractive index detector. Fifty µL of 5 mg/mL sample was injected onto two PL-gel 5 mm mixed-D columns fitted with a guard column (Polymer Laboratories, Mw range 0.2-400 kDa). Polystyrene standards were used to calibrate the columns and AR grade THF was used as eluent at a flow rate of 1 mL/min and a run time of 30 min. For hexyn-pDLLA and NIR10-pDLLA, DMF containing LiCl 10 mM was used as eluent and a Waters 2478 UV detector was connected to the system and the UV absorbance of the dye was measured at 700 nm. Polyethylene glycol (PEG) standards were used to calibrate the column. The flow rate was set at 0.7 mL/min with a run time of 40 min. The results were analyzed using Empower software v. 2 (Waters, USA).

2.4.3. Differential scanning calorimetry (DSC)

The thermal properties of the polymers were established by using differential scanning calorimetry (Discovery DSC, TA instrument, USA). Two to five mg of polymer sample was loaded into an aluminum pan which was subsequently heated from room temperature to 120°C, with a heating rate of 5°C/min, followed by cooling down to -50°C. Thereafter, the sample was heated to 120°C with a temperature modulation of ±1°C and a ramping rate of 2°C/min. The glass transition temperature (T_g) was recorded as the midpoint of the heat capacity change in the second heating run.

2.5. Labeling OVA with NIR fluorescent dyes

OVA was labeled with either IRDye680RD (IR680) or IRDye800CW (IR800) by coupling the NHS ester of the dyes to the protein. In a typical procedure, 20 mg of OVA was dissolved in 1 mL PBS (B Braun, Germany) pH 7.4 and the pH was adjusted to 8.5 by adding 0.1 mL of K_2HPO_4 1 M pH 9. The IRDye680RD NHS ester was dissolved in DMSO (4 mg/mL) and 0.25 mL of the stock solution containing 1 mg of the dye was added to the OVA solution at a 2:1 molar ratio. The reaction was carried out at room temperature for 2 h. The unreacted dye was subsequently removed with pyrogen-free water by using Zeba™ spin desalting columns equilibrated with pyrogen-free water in two consecutive steps and IR680-OVA was collected after freeze-drying (yield: 85%). IR800CW was conjugated and purified by using the same procedure with a dye/OVA feed molar ratio of 1.7 to 1 (Yield: 79%).

2.6. Characterization of labeled OVA

IR680-OVA was characterized by GPC using a Waters UPLC Acquity system equipped with a fluorescence detector. Two channels were used: channel 1 for detection of the protein (excitation at 280 nm and emission at 340 nm) and channel 2 for detection of the IR680 signal (excitation at 672 nm and emission at 694 nm). Seven and a half µL of IR680-OVA (10 mg/mL in PBS) was injected onto a BEH450 SEC 2.5 mm column (Waters, USA). PBS was used as elution buffer and the flow rate was set at 0.25 mL/min. To calculate the dye/OVA molar ratio, the UV spectrum of the freeze-dried labeled OVA was recorded (Shimadzu 2450, Japan) and the absorbance values at 280 nm (A280) and 672 nm (A672) were used to calculate the degree of conjugation according to the following formula:

$$\frac{\text{Dye}}{\text{OVA}} = \left[\!\left[\frac{A_{672}}{\varepsilon_{Dye}}\right]\!\right] \div \left[\!\left[\frac{A_{280} - 0.07 \times A_{672}}{\varepsilon_{OVA}}\right]\!\right]$$

Dye/OVA is the molar ratio of IR680 to OVA and the molar extinction coefficient of IR680 (εDye) is 165,000 M^{-1} cm^{-1} (according to the manufacturer) and the molar extinction coefficient of OVA (εOVA) is 30590 M^{-1} cm^{-1} [61]. IR800-OVA was characterized similarly by using the corresponding wavelengths suitable for IR800.

2.7. Preparation of NPs

OVA-loaded NPs were prepared by using a double emulsion solvent evaporation method essentially as described before [62]. In brief, 50 µL of 30 mg/mL OVA solution in pyrogen-free water was emulsified by sonication (30 s, 20 W-ultrasonic homogenizer (Labsonic P, B. Braun Biotech, Germany)) in a solution of 50 mg of pLHMGA in 1 mL of DCM to obtain a water-in-oil emulsion (W1/O). Next, 2 mL of PVA 1% w/v solution in pyrogen-free water (filtered through a 0.2 µm filter) was added to this first emulsion and a water-in-oil-in-water emulsion was formed by a second round of sonication for 30 s. The double emulsion ($W_1/O/W_2$) was then added dropwise to 25 mL of PVA 0.3% w/v in pyrogen-free water at 40°C while stirring for rapid removal of DCM. After 1 h, the particles were collected by centrifugation for 30 min at 20,000 g, washed with PBS and consecutively with water, resuspended in pyrogen-free water, and freeze-dried overnight. Dual labeled NPs containing NIR10-labeled pLHMGA and IR680-OVA were prepared using the same method by addition of 4 mg of NIR10-pDLLA to 50 mg of pLHMGA and using IR680-OVA (20 mg/mL) as internal water phase. For preparation of empty NPs or NPs loaded with Alexa 647-OVA, 50 µL pyrogen-free or 50 µL of Alexa 647-OVA 20 mg/mL was used as internal water phase.

2.8. NP characterization

2.8.1. Size and morphology analysis

2.8.1.1. Dynamic light scattering

The size of NPs was measured with dynamic light scattering (DLS) on an ALV CGS-3 system (Malvern Instruments, Malvern, UK) equipped with a JDS Uniphase 22mW He-Ne laser operating at 632.8 nm, an optical fiber-based detector, and a digital LV/LSE-5003 correlator. Freeze-dried NPs were suspended in deionized water (RI = 1.332 and viscosity 0.8898 cP) and measurements were done at 25°C at an angle of 90°.

2.8.1.2. Transmission electron microscopy (TEM)

The size and morphology of NPs were analyzed by using transmission electron microscopy (TEM, Philips-FEI Tecnai T10, USA). A droplet of NP suspension in water was placed on a carbon coated copper grid and the sample was stained with 2% uranyl acetate. NPs were visualized with 7-73 k fold magnification and analyzed by MeasureIT software.

2.8.2. OVA content and loading efficiency of NPs

OVA loading efficiency of the NPs was determined by measuring the protein content of digested NPs essentially as described before [63]. In short, about 5 mg of particles (accurately weighed) was dissolved in 0.5 mL of DMSO followed by addition of 2.5 mL of 50 mM NaOH containing 0.5% (w/v) SDS. After complete degradation of the particles, the resulting solution was analyzed by using the Micro-BCA Protein Assay Kit, a calorimetric method that quantifies protein concentration based on peptide bonds and specific amino acid residues. Calibration was performed using 2-40 µg/mL of OVA solution in DMSO:NaOH 50 mM/SDS 0.5% (1:5). Loading efficiency (LE%) is defined as the amount of OVA encapsulated in the NPs divided by the amount of protein added × 100%. Loading percentage (L%) is reported as the amount of OVA entrapped in the particles per total dry mass of the NPs × 100%. In case of dual labeled NPs (containing IR680-OVA) the solution containing the degraded particles was analyzed for its OVA content based on the NIR label by using an Odyssey scanner (LI-COR Biosciences, USA) at the 700 nm channel for IR680-OVA and the calibration was done using IR680-OVA.

2.8.3. *In vitro* release of OVA from NPs

About 5 mg of freeze-dried dual labeled NPs (containing IR680-OVA) was accurately weighed and suspended in 5 mL phosphate buffered saline (pH 7.4, 49 mM NaH_2PO_4, 99 mM Na_2HPO_4, 6 mM NaCl and 0.05% (w/v)). The particle suspension was incubated at 37°C under mild agitation. At different time points, 300 µL was removed and centrifuged at 24000 g for 15 min. The amount of protein released and present in the supernatant was quantified by using an Odyssey scanner using the 700 nm channel for visualization of IR680-OVA. Calibration was done using IR680-OVA in PBS.

2.9. Mice and cells

WT C57BL/6 (CD45.2/Thy1.2; H2-K^b) mice were obtained from Charles River Laboratories (France). Albino BL/6 mice (B6(Cg)-Tyr^{c-2J}/J tyrosinase-deficient immunocompetent BL/6 mice) were bred in the animal breeding facility of the Leiden University Medical Center, the Netherlands. All experiments were approved by the animal experimental committee of Leiden University, the Netherlands. D1 cells are a DC line of BL/6 background [64], and B3Z is a CD8+ T cell hybridoma specific for the SIINFEKL epitope from OVA and carrying the *lacZ* (Escherichia coli β-galactosidase) reporter gene induced by NFAT (nuclear factor of activated T cells) [65]. Antigen-specific activation of B3Z cells leads to T cell receptor-mediated triggering of NFAT, and the subsequent production of β-galactosidase can be quantified by addition of CPRG, a substrate for the β-galactosidase, as a measure of antigen cross-presentation [66]. Cells were cultured in Iscove's Modified Dulbecco's Medium (IMDM, Lonza) containing 8% fetal calf serum (FCS, Greiner), supplemented with 2 mM GlutaMax (Gibco) and 80 IU/mL sodium-penicillin G (Astellas, the Netherlands) for D1 cells, or supplemented with 100 IU/mL penicillin/streptomycin (Gibco), 2 mM glutamin (Gibco), 25 µM 2-mercaptoethanol and 500 µg/mL Hygromycin B (AG Scientific) for B3Z cells. OT-I * Thy1.1 mice are TCR-transgenic mice on B6 background whose CD8+ T cells recognize the OVA epitope SIINFEKL presented in H2-K^b, crossed to Thy1.1 mice to obtain a congenic marker for distinction from endogenous CD8+ T cells in transfer experiments. Naïve OT-I CD8+ T cells were obtained by creating single-cell suspensions from spleens and lymph nodes of OT-I * Thy1.1 mice and subsequent purification of CD8+ cells.

2.10. DC viability assay

D1 DCs (50,000 cells/well in 96-well plates) were incubated with dispersions of unlabeled and labeled NPs (7.8-1000 µg/mL) overnight at 37°C, and cell viability was measured by flow cytometry using the DNA-binding fluorescent dye 7-amino-actinomycin-D (7-AAD) to stain the dead cells.

2.11. Analysis of cellular uptake

D1 cells (100,000 cells/well in 96-well plates) were incubated with Alexa647-OVA NPs (final concentration of OVA in the medium was 6 µg/mL) overnight. D1 cells were subsequently transferred onto a confocal slide without washing or fixation. The intracellular localization of NPs was studied by confocal laser scanning microscopy imaging using inverted Leica SP2 confocal microscope and the samples were analyzed using the corresponding Leica confocal software in DIC mode.

2.12. *In vitro* antigen cross-presentation assay

In vitro cross-presentation of OVA by DCs was studied by incubating titrated amounts of OVA encapsulated in NPs or in soluble form with 50,000 D1 cells (100 µL of OVA 0.2-25 µg/mL in PBS corresponding to 0.12-1.5 mg/mL of NPs) for two hours at 37°C followed by addition of 50,000 B3Z cells and incubation overnight at 37°C in 96-well plates. The cells were then incubated with a lysis buffer containing the CPRG substrate for *lacZ* (PBS +1% 9

mg/mL CPRG + 0.9% 1M $MgCl_2$ + 0.125% NP40 + 0.71% 14.3 M 2-mercaptoethanol) at 37°C until the color reaction had progressed sufficiently for readout in a plate reader measuring the optical density at 590 nm. The direct MHC-binding minimal epitope SIINFEKL (100 ng/mL in PBS) was used as a positive control, and unstimulated D1 cells were negative controls.

2.13. *In vivo* tracking of labeled NPs

Albino BL/6 mice were vaccinated subcutaneously with 50 µg OVA encapsulated in dual labeled NPs dispersed in 100 µL PBS or 50 µg IR800-OVA in 100 µL PBS. Vaccine kinetics were then studied at several time points after administration by using the IVIS spectrum preclinical *in vivo* imaging system (PerkinElmer). Kinetics were measured by quantifying the fluorescent intensity in pre-set regions of interest (ROI) at the injection site and the two vaccine-draining inguinal lymph nodes, expressed as the total radiant efficiency in [p/s]/[mW/cm^2]. The fluorescent signal in the injection site at each time point is presented as the as percentage of the maximum recorded value, to show percentual decrease in time. In the lymph nodes the data is presented as the signal to background ratio and it is calculated by dividing the fluorescence signal of the lymph nodes by the background signal at each time point [67].

2.14. *In vivo* antigen cross-presentation

To establish antigen presentation *in vivo*, BL/6 mice were vaccinated with OVA encapsulated in NPs or in its soluble form. Mice were injected subcutaneously with 200 µL of a 2 mg/mL suspension of NPs in PBS containing 50 µg of encapsulated OVA or 50 µg of soluble OVA. One day after vaccination, 500,000 OVA-specific OT-I CD8+ T cells were injected intravenously in the tail vein in 200 µL PBS. Mice were sacrificed four days after T cell transfer to analyze the expansion of the transferred OVA-specific T cells caused by presentation of the OVA antigen. Vaccine-draining inguinal lymph nodes and the spleen were taken out, mashed on 70 mm cell strainers (Becton Dickinson) and the cells were stained with fluorescently labeled antibodies for CD8β and the OT-I congenic marker CD90.1 (Thy1.1), and analyzed by flow cytometry. T cell expansion is expressed as the number of transferred (OT-I) T cells as a percentage from total CD8+ T cells [68].

2.15. Statistical analysis

GraphPad Prism software was used for statistical analysis. Two groups were compared by unpaired two-tailed Student's *t*-test with alpha = 0.05. Statistical significance was considered when $p < 0.05$.

3. Results and discussion

3.1. Synthesis and characterization of pLHMGA

A random copolymer of BMMG and D,L-lactide was synthesized by using BnOH and $Sn(Oct)_2$ as initiator and catalyst, respectively, via ring opening polymerization (**Figure1**) and the polymer was obtained in high yield (~100%). The protective benzyl groups were subsequently removed overnight by hydrogenation to yield pLHMGA (83%). The structures of the synthesized polymers were confirmed by ^{1}H NMR spectroscopy and this analysis showed that the molar ratio of BMMG and D,L-lactide in pLBMGA (protected polymer) was 48/52, which is close to feed ratio (50/50). Both pLBMGA and pLHMGA were amorphous with T_g values of 39°C and 57°C, respectively, which were similar to values reported earlier[39] and confirmed the random structure of the polymers. GPC analysis showed that the number average molecular weight of pLHMGA (16.2 kDa) was close to the aimed molecular weight based on monomer-to initiator molar ratio (15.8 kDa) and the PDI was 1.6 (**Supplementary Table S1**). Based on previous studies using the same polymers, we selected a polymer with a relatively low molecular weight in order to achieve small NPs with high loading and fast release.

3.2. Synthesis and characterization of hexyn-pDLLA and NIR10-pDLLA

An alkyne-bearing homopolymer of D,L-lactide (hexyn-pDLLA) was synthesized by using 1 hexyn-6-ol as initiator and $Sn(Oct)_2$ as catalyst. The alkyne functionality in this polymer provides the possibility to conjugate azide-bearing molecules via click chemistry. The obtained polymer was amorphous with a T_g of 50°C, similar to values reported in the literature [69]. GPC analysis showed that the number average molecular weight of hexyn-pDLLA (11.0 kDa) was close to that of the aimed molecular weight based on monomer-to-initiator molar ratio (10.1 kDa) (**Supplementary Table S2**). To obtain a NIR fluorescent-labeled polymer, the azide-NIR10 was coupled to hexyn-pDLLA by click reaction. Analysis of the reaction mixture after 16 h by GPC with UV detection confirmed the presence of labeled polymer at a retention time of 20 min corresponding to that of the polymer, while a peak was also observed at 23.5 min, which corresponds to the retention time of the free dye. Based on the chromatogram a coupling efficiency of 85% was calculated. After purification, GPC analysis showed that the polymer contained 8% of free dye. GPC analysis of the freeze-dried particles containing NIR10-pDLLA showed that only a negligible amount of free dye was present in the particles indicating that most of the free dye was removed during particle preparation process (**Supplementary Figure S4, and supplementary Table S3**).

3.3. Characterization of IR680-OVA and IR800-OVA

In order to prepare a traceable OVA for *in vivo* imaging, the NHS ester of IRdye680RD was conjugated to OVA and the obtained IR680-OVA was analyzed by GPC. Overlapping peaks corresponding to OVA (excitation 280 and emission 340 nm) and IR680 (excitation 672 and emission 694 nm) in the GPC chromatogram of the purified IR680-OVA confirmed that the IR680 was indeed conjugated to OVA (**Supplementary Figure S5**). No additional peaks (fluorescence detection) were observed, indicating that the free dye was completely removed by purification. Conjugation efficiency calculated by UV measurements showed an average molar dye/protein ratio of 1.7. IR800-OVA was successfully prepared and purified as described for IR680-OVA. The average molar dye/protein ratio was 1.0 (**Supplementary Table S4**).

3.4. Preparation and characterization of empty and OVA-loaded NPs

Empty and OVA-loaded NPs particles were prepared by a double emulsion-solvent evaporation method, which is a well-known procedure and has been used frequently for encapsulation of hydrophilic drugs as well as biotherapeutics [70-73]. Empty and OVA-loaded NPs with NIR fluorescent dyes on the polymer and/or the protein antigen had comparable characteristics in terms of morphology and size. DLS analysis showed that the mean hydrodynamic diameter of the NPs ranged from 290 to 370 nm with a PDI of 0.15-0.33 (**Table 1**).

Table 1. Characteristics of NPs. Representative data are presented as average ± SD (N=3)

NPs	Size (nm) (DLS)	PDI (DLS)	Loading (L)%	LE% (Loading efficiency)
Empty NPs	364 ± 40	0.22 ± 0.08	-	-
OVA NPs	340 ± 4	0.19 ± 0.04	1.71 ± 0.01	57.4 ± 0.4
Dual labeled NPs	293 ± 3	0.15 ± 0.02	1.38 ± 0.01	69.0 ± 0.4
Alexa-OVA NPs	384 ± 20	0.33 ± 0.05	1.15 ± 0.02	57.6 ± 0.4

The particle preparation procedure was optimized in order to obtain NPs with a size of around 300 nm because NPs of this size were most efficient in activation of DCs and inducing a systemic immune response as compared to bigger particles [74]. Analysis of freeze-dried samples with TEM showed spherical NPs with a size ranging from 150 to 250 nm (**Figure 2**), which is smaller than the sizes obtained with DLS. This is due to the fact that DLS reports the hydrodynamic diameter of the particles based on scattering intensity which is proportional to the 6th power of the particle diameter, and therefore in polydisperse samples, relatively low scattering intensities of small particles are overshadowed by high scattering intensities of big particles, resulting in a skewed average size [75,76]. The loading efficiency of unlabeled as well as labeled OVA in NPs was about 60%. The *in vitro* release of OVA from pLHMGA particles was studied by using dual labeled NPs (containing IR680-OVA). **Figure 3** shows that the particles had a low burst release of about 5%, followed by sustained release up to 70% for 30 days. These data are in line with previous studies of pLHMGA particles with the same copolymer composition and loaded with bovine serum albumin [77]. Considering slight variations in the loading efficiency of the NPs and in order to allow a fair comparison in functional experiments, a fixed amount of OVA was used in various *in vitro* and *in vivo* studies.

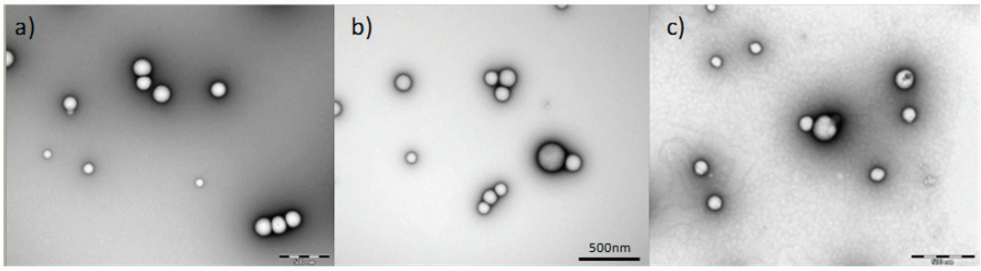

Figure 2. TEM images of NPs a) Empty NPs, b) Unlabeled OVA NPs, c) Dual labeled NPs. The bar scale indicates 500 nm.

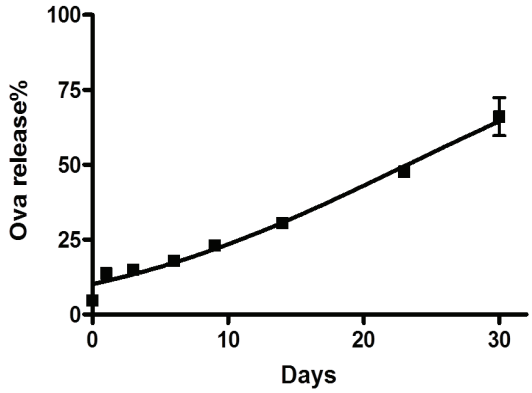

Figure 3. *In vitro* release of IR680-OVA from pLHMGA NPs. Dual labeled NPs were dispersed in PBS (1 mg/mL) and kept at 37°C under mild agitation. Following a low burst release of about 5%, IR680-OVA was release in a sustained manner in 30 days up to 70%.

3.5. Cytocompatibility of empty and OVA-loaded NPs

To assess the cytocompatibility of NPs, DCs were incubated with empty and OVA NPs as well as dual labeled NPs for 16 h at 37°C. Dead cells were quantified by using 7-AAD, a

DNA binding fluorescent dye which stains cells that have lost membrane integrity [78]. DCs incubated with LPS and soluble OVA corresponding to the amounts of OVA in the loaded NPs were used as controls. Cell viability was about 90% for DCs incubated with empty and OVA-loaded NPs (concentration of NPs ranging from 7.8 to 1000 µg/mL). These data show the cytocompatibility of these particles.

3.6. NP uptake by DCs

To verify that OVA NPs are taken up by DCs, D1 cells were incubated with Alexa647-OVA NPs overnight and the fluorescent Alexa647 signal was visualized by confocal microscopy. As shown in **Figure S6**, DCs efficiently take up NPs carrying OVA protein.

3.7. Antigen cross-presentation *in vitro*

Subsequently, we wanted to test whether the uptake of OVA NPs by DCs leads to processing and cross-presentation of the OVA antigen to OVA-specific T cells. To this end, DCs were incubated with OVA NPs and co-cultured with OVA-specific B3Z hybridoma T cells. **Figure 4** shows that OVA NPs induced antigen-specific T cell activation in a dose-dependent manner, while soluble OVA failed to activate T cells even at high doses. Since this assay is based on the immunological principles of antigen-specificity of T cells, any T cell activation is the result of uptake, processing and cross-presentation of the antigen by DCs to T cells. Furthermore, the dual labeled NPs were equally efficient in T cell activation as the unlabeled NPs (data not shown), showing that labeling did not affect the ability of NPs to induce *in vitro* cross-presentation.

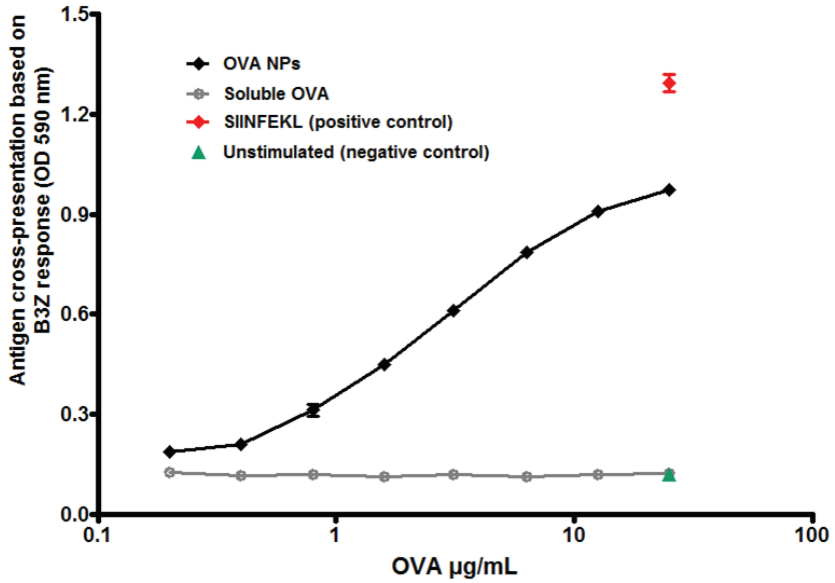

Figure 4. *In vitro* protein cross-presentation of OVA-encapsulated NPs. DCs were incubated with 0.2-25 mg OVA/mL encapsulated in NPs or in soluble form, and co-cultured with OVA-specific B3Z hybridoma T cells overnight. The B3Z cells contain a construct in which triggering of the T cell receptor, by cross-presentation of their specific OVA epitope SIINFEKL by DCs, leads to the production of the enzyme β-galactosidase that mediates a color reaction upon addition of the substrate CPRG. This color reaction, measured as the optical density (OD) at 590 nm, therefore forms a measure for antigen cross-presentation by DCs to specific T cells. The SIINFEKL minimal peptide epitope (100 ng/mL in PBS) was used as a positive control, and unstimulated DCs with B3Z cells formed the negative control. N = 3 samples per condition, representative graph of 5 independent experiments.

3.8. *In vivo* tracking of labeled NPs

As our aim was to develop an antigen delivery system that ensures a prolonged supply of antigen to the immune system, we visualized the presence of OVA NPs in the injection site and in the draining lymph nodes, where immune responses are initiated. The tail-base injection site was chosen as it drains specifically to the inguinal lymph nodes which are located at sufficient distance in the mouse to be able to distinguish the injection site from the lymph nodes, and to visualize and quantify their respective signals accurately. Using a dual-color *in vivo* imaging setup based on two distinct NIR fluorescent dyes, we were able to visualize the antigen and the delivery vehicle simultaneously. The NIR fluorescent dye IR680 (excitation 675 nm, emission 720 nm) was coupled to the OVA antigen and the dye NIR10 (excitation 745 nm and emission 840 nm) was coupled to the polymer to track the delivery vehicle. **Figure 5(a)** shows the presence of the double-labeled OVA NPs at the injection site in time, compared to a soluble formulation of NIR-labeled OVA protein in PBS. As expected, the vast majority of soluble OVA antigen leaves the injection site within the first day, leading to a short peak presence in the lymph nodes immediately after injection that rapidly decreases (**Figure 5(b)**). In contrast, OVA encapsulated in NPs was cleared from the injection site more gradually, corresponding with gradual accumulation in the draining lymph nodes and remaining there for several days. **Figure 6** shows examples of the presence of OVA NPs at the injection site and in the draining lymph nodes. Interestingly, the signals from the NP vehicle and its OVA content show similar patterns in the injection site and lymph nodes, suggesting that the OVA antigen arrives in the lymph nodes in encapsulated form. The increasing fluorescent signal of encapsulated IR680-OVA in the first day after injection may be caused by initial quenching of the signal, for example by the hydrophobic environment in the NPs or by self-aggregation and stacking of the dye at high concentrations [79]. Hydration of the NPs and a decreased stacking of NPs at the injection site during the first day would relieve the IR680 dye from both these quenching effects.

3.9. *In vivo* antigen cross-presentation

The efficient and prolonged delivery of antigen to the draining lymph nodes by OVA NPs led us to test their ability to induce antigen cross-presentation *in vivo*. To test this hypothesis, we administered OVA NPs to mice, followed after one day by an adoptive transfer of OVA-specific CD8+ T cells (OT-I cells). By transferring these high numbers of OT-I T cells, we increase the precursor frequency of OVA-specific T cells to artificially high levels, which allows us to detect subtle effects in terms of cross-presentation of OVA antigen. Four days after T cell transfer, the proliferation of these transferred OT-I T cells as a result of *in vivo* cross-presentation of the OVA antigen was assessed in the vaccine draining lymph nodes and the spleen (**Figure 7 and Supplementary Figure S7**). A strong expansion of OT-I cells was found in the lymph nodes and spleen of mice treated with OVA NPs, which proved far superior to the administration of soluble OVA. The absence of T cell proliferation after injection of equal amounts of empty NPs shows that the delivery system itself plays no role and emphasizes the antigen-specific nature of T cell activation. These results correspond with the superior ability of OVA NPs over soluble OVA to induce *in vitro* antigen cross-presentation to OVA-specific CD8+ T cells (**Figure 4**).

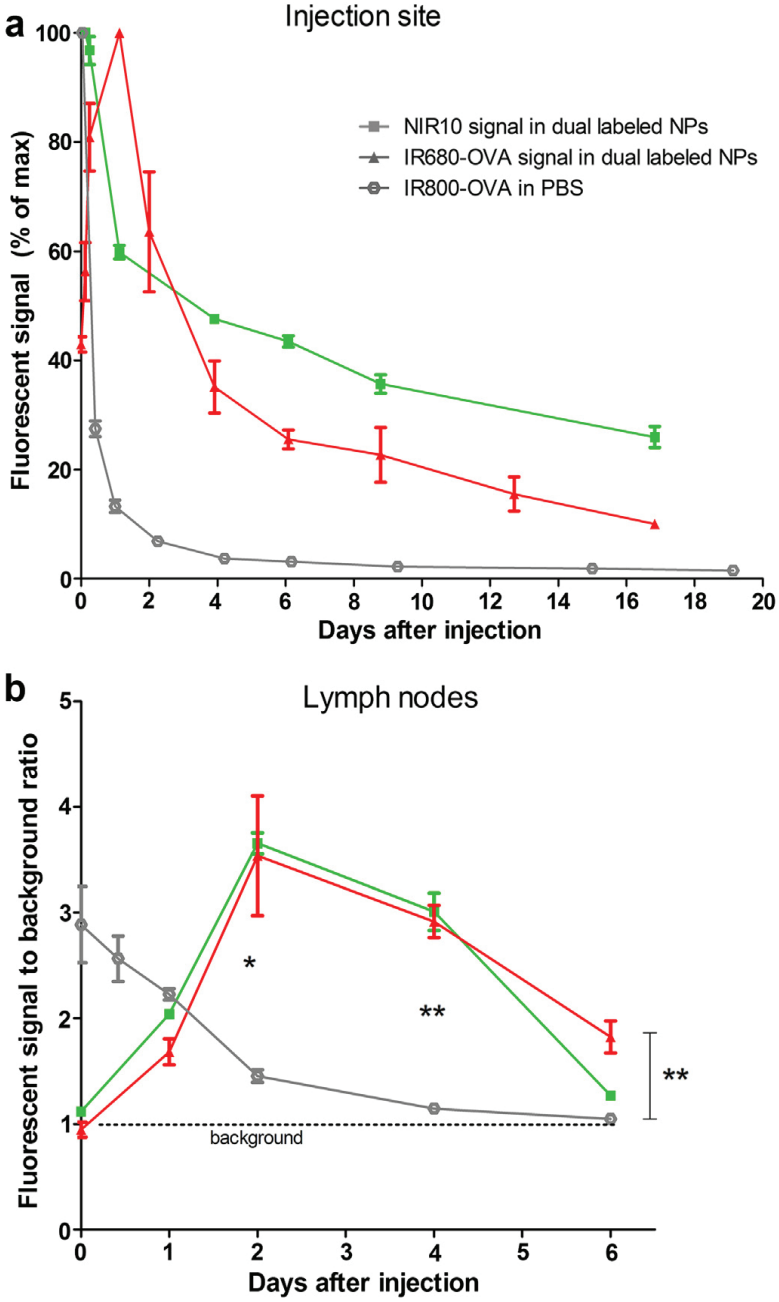

Figure 5. *In vivo* tracking of NPs and OVA antigen. Quantification of the fluorescent signal of IR680 and NIR10 in dual labeled NPs (containing NIR10 dye on the polymer and IR680 on the OVA), and IR800 signal of soluble antigen (IR800-OVA in PBS) after s.c. injection of 50 μg OVA in NPs or in soluble form. a) Fluorescent signal at the injection site expressed as a percentage of maximum signal. b) Fluorescent signal in the draining lymph nodes expressed as signal to background ratio. Statistical significance is indicated by asterisks comparing IR680 signal in NPs vs. soluble IR800-OVA. Statistical analysis was performed by unpaired Student's *t*-test, * = $p < 0.05$, ** = $p < 0.01$. N = 3 mice per group.

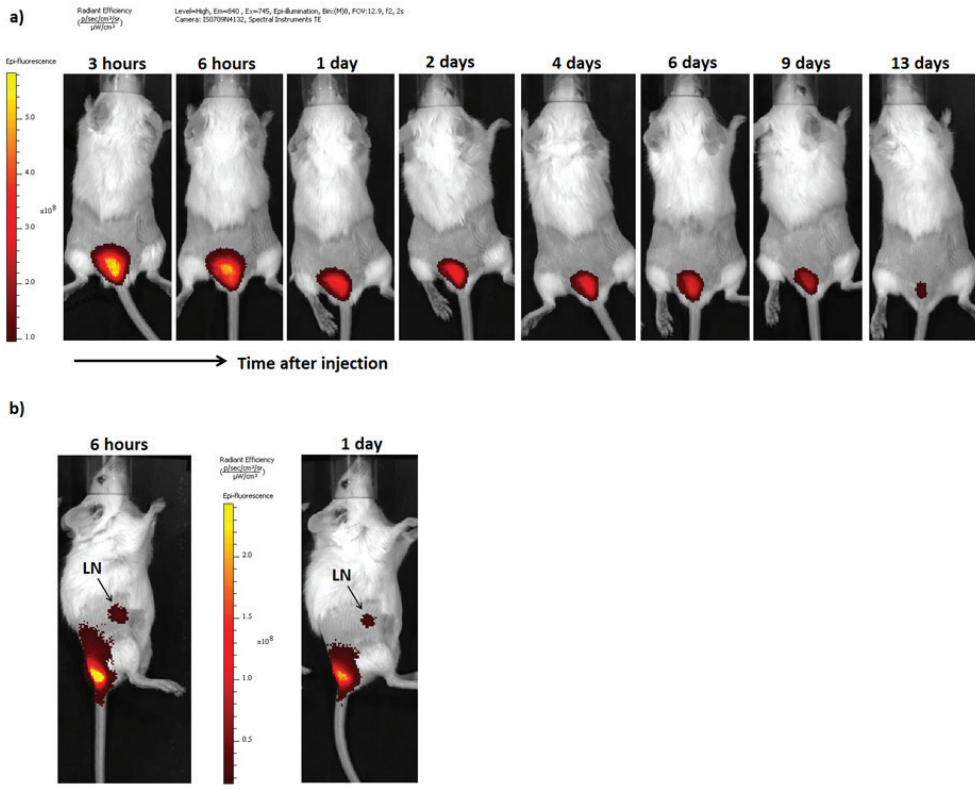

Figure 6. *In vivo* visualization of OVA NPs in the injection site and draining lymph nodes. Presence of OVA NPs in a) the injection site and b) the right inguinal draining lymph node, based on quantification of the fluorescent signal of NIR10 coupled to the NP polymer. Repeated measurements in time plotted on the same scale of fluorescence. The lymph node (LN) is indicated by an arrow. All images are overlays of grayscale photographs with fluorescence intensity measurements indicated on the color scale. (For interpretation of the references to color in this figure legend, the reader is referred to the web version of this article.)

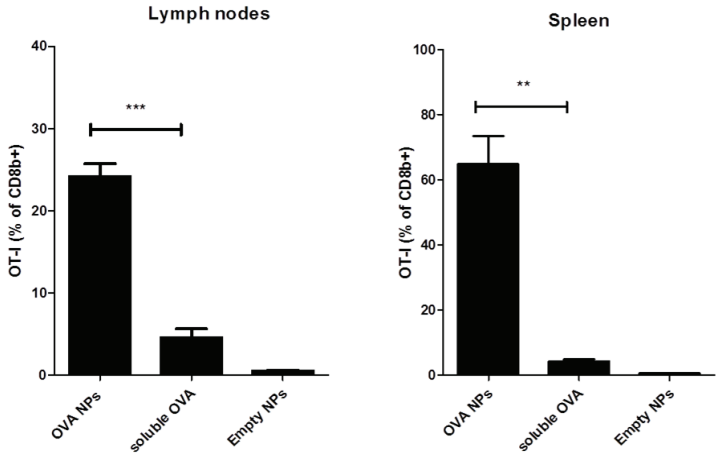

Figure 7. *In vivo* cross-presentation of OVA antigen to OVA-specific CD8+ T cells. Expansion of TCR-transgenic OVA-specific CD8+ T cells (OT-I) in the draining lymph nodes and spleen, 4 days after transfer into recipients mice. One day before the OT-I transfer, mice were treated subcutaneously with 50 µg OVA either in soluble form or in 400 µg of NPs or with 400 µg of empty NPs. *In vivo* expansion of the transferred OT-I T cells was quantified by ex vivo flow cytometry and expressed as the percentage of the total CD8+ T cell pool (CD8β staining). N = 3-4 mice per group, representative of 2 independent experiments. Unpaired Student's *t*-test showed significant difference in OT-I T cell expansion between mice treated with OVA NPs versus soluble OVA, ** = $p < 0.01$, *** = $p < 0.001$. N = 3-4 mice per group.

4. Conclusion

We developed an antigen delivery system based on pLHMGA NPs encapsulating the model protein antigen OVA. The NPs showed sustained release of antigen *in vitro* and were able to induce *in vitro* antigen cross-presentation by DCs to antigen-specific T cells. Using our non-invasive double-label approach, we visualized the delivery vehicle and the antigen simultaneously in real-time and showed that the antigen is carried to the lymphoid organs by the delivery vehicle. This finding is in line with the results of *in vivo* antigen presentation in the lymph nodes, where the OVA NPs exhibited a strong capacity to induce antigen-specific CD8+ T cell proliferation through cross-presentation of the antigen. In conclusion, pLHMGA NPs are attractive vehicles for protein antigen delivery for effective stimulation of the cellular immune system.

Acknowledgments

We thank Ana Luisa Silva, Paul Werkhoven, Nataschja Ho and Joep van den Dikkenberg for technical assistance and useful suggestions.

This research was conducted within the framework of the Cancer Vaccine Tracking project (#03O-302), Center for Translational Molecular Medicine (CTMM).

Appendix. Supplementary data

References

[1] Silva JM, Videira M, Gaspar R, Preat V, Florindo HF. Immune system targeting by biodegradable nanoparticles for cancer vaccines. J Control Release 2013;168:179-99.
[2] Reddy ST, Swartz MA, Hubbell JA. Targeting dendritic cells with biomaterials: developing the next generation of vaccines. Trends Immunol 2006;27:573-9.
[3] Akagi T, Baba M, Akashi M. Biodegradable nanoparticles as vaccine adjuvants and delivery systems: regulation of immune responses by nanoparticle-based vaccine. Polym Nanomedicine 2012;247:31-64.
[4] Banchereau J, Briere F, Caux C, Davoust J, Lebecque S, Liu YJ, et al. Immunobiology of dendritic cells. Annu Rev Immunol 2000;18:767-811.
[5] Banchereau J, Palucka A. Dendritic cells as therapeutic vaccines against cancer. Nat Rev Immunol 2005;5:296-306.
[6] Banchereau J, Steinman RM. Dendritic cells and the control of immunity. Nature 1998;392:245-52.
[7] Lanzavecchia A. Mechanisms of antigen uptake for presentation. Curr Opin Immunol 1996;8:348-54.
[8] Vyas JM, Van der Veen AG, Ploegh HL. The known unknowns of antigen processing and presentation. Nat Rev Immunol 2008;8:607-18.
[9] Schuurhuis D, Laban S, Toes R, Ricciardi-Castagnoli P, Kleijmeer M, van der
Voort E, et al. Immature dendritic cells acquire CD8(+) cytotoxic T lymphocyte priming capacity upon activation by T helper cell-independent or –dependent stimuli. J Exp Med 2000;192:145-50.
[10] Elamanchili P, Diwan M, Cao M, Samuel J. Characterization of poly(D,L-lactic co- glycolic acid) based nanoparticulate system for enhanced delivery of antigens to dendritic cells. Vaccine 2004;22:2406-12.
[11] Elamanchili P, Lutsiak CME, Hamdy S, Diwan M, Samuel J. "Pathogenmimicking" nanoparticles for vaccine delivery to dendritic cells. J Immunother 2007;30:378-95.
[12] Gregory AE, Titball R, Williamson D. Vaccine delivery using nanoparticles. Front Cell Infect Microbiol 2013;3.
[13] Bolhassani A, Safaiyan S, Rafati S. Improvement of different vaccine delivery systems for cancer therapy. Mol Cancer 2011;10(3).
[14] Joshi MD, Unger WJ, Storm G, van Kooyk Y, Mastrobattista E. Targeting tumor antigens to dendritic cells using particulate carriers. J Control Release 2012;161:25-37.
[15] Krishnamachari Y, Geary SM, Lemke CD, Salem AK. Nanoparticle delivery systems in cancer vaccines. Pharm Res 2011;28:215-36.
[16] Mahapatro A, Singh DK. Biodegradable nanoparticles are excellent vehicle for site directed *in vivo* delivery of drugs and vaccines. J Nanobiotechnol 2011;9:55.
[17] Park YM, Lee SJ, Kim YS, Lee MH, Cha GS, Jung ID, et al. Nanoparticle-based vaccine delivery for cancer immunotherapy. Immune Netw 2013;13:177-83.
[18] Zhang Z, Tongchusak S, Mizukami Y, Kang YJ, Ioji T, Touma M, et al. Induction
of anti-tumor cytotoxic T cell responses through PLGA-nanoparticle mediated antigen delivery. Biomaterials 2011;32:3666-78.
[19] Hamdy S, Haddadi A, Hung RW, Lavasanifar A. Targeting dendritic cells with nano-particulate PLGA cancer vaccine formulations. Adv Drug Deliv Rev 2011;63:943-55.
[20] Demento SL, Cui W, Criscione JM, Stern E, Tulipan J, Kaech SM, et al. Role of sustained antigen release from nanoparticle vaccines in shaping the T cell memory phenotype. Biomaterials 2012;33:4957-64.
[21] Melief CJM. Cancer immunotherapy by dendritic cells. Immunity 2008;29: 372-83.
[22] van Montfoort N, Camps MG, Khan S, Filippov DV, Weterings JJ, Griffith JM, et al. Antigen storage compartments in mature dendritic cells facilitate prolonged cytotoxic T lymphocyte cross-priming capacity. Proc Natl Acad Sci U S A 2009;106:6730-5.
[23] Ma W, Chen M, Kaushal S, McElroy M, Zhang Y, Ozkan C, et al. PLGA nanoparticle-mediated delivery of tumor antigenic peptides elicits effective immune responses. Int J Nanomedicine 2012;7:1475-87.
[24] Ye M, Kim S, Park K. Issues in long-term protein delivery using biodegradable microparticles. J Control Release 2010;146:241-60.
[25] Giteau A, Venier-Julienne MC, Aubert-Pouessel A, Benoit JP. How to achieve sustained and complete protein release from PLGA-based microparticles? Int J Pharm 2008;350:14-26.
[26] Sinha V, Trehan A. Biodegradable microspheres for protein delivery. J Control Release 2003;90:261-80.
[27] van de Weert M, Hennink WE, Jiskoot W. Protein instability in poly(lactic-coglycolic acid) microparticles. Pharm Res 2000;17:1159-67.
[28] Brannon-Peppas L, Blanchette J. Nanoparticle and targeted systems for cancer therapy. Adv Drug Deliv Rev 2004;56:1649-59.
[29] Jain R. The manufacturing techniques of various drug loaded biodegradable poly(lactide-co-glycolide) (PLGA) devices. Biomaterials 2000;21:2475-90.
[30] O'Hagan D, Singh M, Gupta R. Poly(lactide-co-glycolide) microparticles for the development of single-dose controlled-release vaccines. Adv Drug Deliv Rev 1998;32:225-46.
[31] Rosalia RA, Silva AL, Camps M, Allam A, Jiskoot W, van der Burg SH, et al. Efficient *ex vivo* induction of T cells with potent anti-tumor activity by protein antigen encapsulated in nanoparticles. Cancer Immunol Immunother 2013;62:1161-73.
[32] Mueller M, Schlosser E, Gander B, Groettrup M. Tumor eradication by immunotherapy with biodegradable PLGA microspheres-an alternative to incomplete Freund's adjuvant. Int J Cancer 2011;129:407-16.
[33] Ding AG, Schwendeman SP. Acidic microclimate pH distribution in PLGA microspheres monitored by confocal

laser scanning microscopy. Pharm Res 2008;25:2041-52.
[34] Sophocleous AM, Zhang Y, Schwendeman SP. A new class of inhibitors of peptide sorption and acylation in PLGA. J Control Release 2009;137:179-84.
[35] Houchin ML, Topp EM. Chemical degradation of peptides and proteins in PLGA: a review of reactions and mechanisms. J Pharm Sci 2008;97:2395-404.
[36] Kim HK, Park TG. Microencapsulation of human growth hormone within biodegradable polyester microspheres: protein aggregation stability and incomplete release mechanism. Biotechnol Bioeng 1999;65:659-67.
[37] Hermeling S, Crommelin DJA, Schellekens H, Jiskoot W. Structure-immunogenicity relationships of therapeutic proteins. Pharm Res 2004;21:897-903.
[38] Liu Y, Ghassemi AH, Hennink WE, Schwendeman SP. The microclimate pH in poly(D,L-lactide-co-hydroxymethyl glycolide) microspheres during biodegradation. Biomaterials 2012;33:7584-93.
[39] Ghassemi AH, van Steenbergen MJ, Talsma H, van Nostrum CF, Jiskoot W, Crommelin DJA, et al. Preparation and characterization of protein loaded microspheres based on a hydroxylated aliphatic polyester, poly(lactic-cohydroxymethyl glycolic acid). J Control Release 2009;138:57-63.
[40] Ghassemi AH, van Steenbergen MJ, Barendregt A, Talsma H, Kok RJ, van Nostrum CF, et al. afs controlled release of octreotide and assessment of peptide acylation from poly(D,L-lactide-co-hydroxymethyl glycolide) compared to PLGA microspheres. Pharm Res 2012;29:110-20.
[41] Samadi N, van Nostrum CF, Vermonden T, Amidi M, Hennink WE. Mechanistic studies on the degradation and protein release characteristics of poly(lactic-co-glycolic-co-hydroxymethylglycolic acid) nanospheres. Biomacromolecules 2013;14:1044-53.
[42] Srinivas M, Cruz LJ, Bonetto F, Heerschap A, Figdor CG, de Vries IJM. Customizable,
multi-functional fluorocarbon nanoparticles for quantitative *in vivo* imaging using F-19 MRI and optical imaging. Biomaterials 2010;31: 7070-7.
[43] Verdijk P, Scheenen TWJ, Lesterhuis WJ, Gambarota G, Veltien AA, Walczak P, et al. Sensitivity of magnetic resonance imaging of dendritic cells for *in vivo* tracking of cellular cancer vaccines. Int J Cancer 2007;120:978-84.
[44] Long CM, van Laarhoven HWM, Bulte JWM, Levitsky HI. Magneto vaccination as a novel method to assess and quantify dendritic cell tumor antigen capture and delivery to lymph nodes. Cancer Res 2009;69:3180-7.
[45] Yang Z, Zheng S, Harrison WJ, Harder J, Wen X, Gelovani JG, et al. Long circulating near-infrared fluorescence core-cross-linked polymeric micelles: synthesis, characterization, and dual nuclear/optical imaging. Biomacromolecules2007;8:3422-8.
[46] Heo MB, Lim YT. Programmed nanoparticles for combined immunomodulation, antigen presentation and tracking of immunotherapeutic cells. Biomaterials 2014;35:590-600.
[47] Christian NA, Benencia F, Milone MC, Li G, Frail PR, Therien MJ, et al. *In Vivo* dendritic cell tracking using fluorescence lifetime imaging and near-infrared emissive polymersomes. Mol Imaging Biol 2009;11:167-77.
[48] Frangioni J. *In vivo* near-infrared fluorescence imaging. Curr Opin Chem Biol 2003;7:626-34.
[49] Escobedo JO, Rusin O, Lim S, Strongin RM. NIR dyes for bioimaging applications.
Curr Opin Chem Biol 2010;14:64-70.
[50] Key J, Leary JF. Nanoparticles for multimodal in vivo imaging in nanomedicine. Int J Nanomedicine 2014;9:711-26.
[51] Rao J, Dragulescu-Andrasi A, Yao H, Yao H. Fluorescence imaging in vivo: recent advances. Curr Opin Biotechnol 2007;18:17-25.
[52] Mou Y, Hou Y, Chen B, Hua Z, Zhang Y, Xie H, et al. In vivo migration of dendritic cells labeled with synthetic superparamagnetic iron oxide. Int J Nanomedicine 2011;6:2633-40.
[53] Su H, Mou Y, An Y, Han W, Huang X, Xia G, et al. The migration of synthetic magnetic nanoparticle labeled dendritic cells into lymph nodes with optical imaging. Int J Nanomedicine 2013;8:3737-44.
[54] Chen YC, Wen S, Shang SA, Cui Y, Luo B, Teng GJ. Magnetic resonance and near-infrared imaging using a novel dual-modality nano-probe for dendritic cell tracking *in vivo*. Cythotherapy 2014;16:699-710.
[55] Lee H, Mason JC, Achilefu S. Heptamethine cyanine dyes with a robust CeC bond at the central position of the chromophore. J Org Chem 2006;71: 7862-5.
[56] Leemhuis M, van Nostrum C, Kruijtzer J, Zhong Z, ten Breteler M, Dijkstra P, et al. Functionalized poly(alpha-hydroxy acid)s via ring-opening polymerization: toward hydrophilic polyesters with pendant hydroxyl groups. Macromolecules 2006;39:3500-8.
[57] Kolb H, Finn M, Sharpless K. Click chemistry: diverse chemical function from a few good reactions. Angew Chemie Int Ed 2001;40:2004.
[58] van Dijk M, Rijkers DTS, Liskamp RMJ, van Nostrum CF, Hennink WE. Synthesis and applications of biomedical and pharmaceutical polymers via click chemistry methodologies. Bioconjug Chem 2009;20:2001-16.
[59] Moses JE, Moorhouse AD. The growing applications of click chemistry. Chem Soc Rev 2007;36:1249-62.
[60] Binder WH, Sachsenhofer R. 'Click' chemistry in polymer and material science: an update. Macromol Rapid Commun 2008;29:952-81.
[61] Gill SC, von Hippel PH. Calculation of protein extinction coefficients from amino acid sequence data. Anal Biochem 1989;182:319-26.
[62] Silva AL, Rosalia RA, Sazak A, Carstens MG, Ossendorp F, Oostendorp J, et al. Optimization of encapsulation of a synthetic long peptide in PLGA nanoparticles: low-burst release is crucial for efficient CD8(+) T cell activation. Eur J Pharm Biopharm 2013;83:338-45.

[63] Sah H. A new strategy to determine the actual protein content of poly(lactideco- glycolide) microspheres. J Pharm Sci 1997;86:1315-8.
[64] Winzler C, Rovere P, Rescigno M, Granucci F, Penna G, Adorini L, et al. Maturation stages of mouse dendritic cells in growth factor-dependent longterm cultures. J Exp Med 1997;185:317-28.
[65] Karttunen J, Sanderson S, Shastri N. Detection of rare antigen-presenting cells by the lacZ T-cell activation assay suggests an expression cloning strategy for T-cell antigens. Proc Natl Acad Sci U S A 1992;89:6020-4.
[66] Shastri N, Gonzalez F. Endogenous generation and presentation of the ovalbumin peptide/k(b) complex to T-cells. J Immunol 1993;150:2724-36.
[67] Filonov GS, Piatkevich KD, Ting L, Zhang J, Kim K, Verkhusha VV. Bright and stable near-infrared fluorescent protein for in vivo imaging. Nat Biotechnol 2011;29:757-61.
[68] Hogquist KA, Jameson SC, Heath WR, Howard JL, Bevan MJ, Carbone FR. T cell receptor antagonist peptides induce positive selection. Cell 1994;76:17-27.
[69] Perego G, Cella GD, Bastioli C. Effect of molecular weight and crystallinity on poly(lactic acid) mechanical properties. J Appl Polym Sci 1996;59:37-43.
[70] Cohen S, Yoshioka T, Lucarelli M, Hwang L, Langer R. Controlled delivery systems for proteins based on poly(lactic glycolic acid) microspheres. Pharm Res 1991;8:713-20.
[71] Mundargi RC, Babu VR, Rangaswamy V, Patel P, Aminabhavi TM. Nano/micro technologies for delivering macromolecular therapeutics using poly(D,L-lactide- co-glycolide) and its derivatives. J Control Release 2008;125:193-209.
[72] Zambaux M, Bonneaux F, Gref R, Maincent P, Dellacherie E, Alonso M, et al. Influence of experimental parameters on the characteristics of poly(lactic acid) nanoparticles prepared by a double emulsion method. J Control Release 1998;50:31-40.
[73] Couvreur P, Puisieux F. Nanoparticles and microparticles for the delivery of polypeptides and proteins. Adv Drug Deliv Rev 1993;10:141-62.
[74] Joshi VB, Geary SM, Salem AK. Biodegradable particles as vaccine delivery systems: size matters. Aaps J 2013;15:85-94.
[75] Dhawan A, Sharma V. Toxicity assessment of nanomaterials: methods and challenges. Anal Bioanal Chem 2010;398:589-605.
[76] Patterson JP, Robin MP, Chassenieux C, Colombani O, O'Reilly RK. The analysis of solution self-assembled polymeric nanomaterials. Chem Soc Rev 2014;43: 2412-25.
[77] Ghassemi AH, van Steenbergen MJ, Talsma H, van Nostrum CF, Crommelin DJA, Hennink WE. Hydrophilic polyester microspheres: effect of molecular weight and copolymer composition on release of BSA. Pharm Res 2010;27:2008-17.
[78] Zembruski NCL, Stache V, Haefeli WE, Weiss J. 7-Aminoactinomycin D for apoptosis staining in flow cytometry. Anal Biochem 2012;429:79-81.
[79] Zhegalova NG, He S, Zhou H, Kim DM, Berezin MY. Minimization of self-quenching fluorescence on dyes conjugated to biomolecules with multiple labeling sites via asymmetrically charged NIR fluorophores. Contrast Media Mol Imaging 2014;9:355-62.

Appendix A
Supplementary Data

Synthesis of azide-NIR dye 10

Azide-functionalized water-soluble near-infrared fluorescent dye **10** was prepared as follows: indolenine **1** was N-alkylated with a sulfopropyl group **2**, giving indolinium salt **3** in 90% yield. The iminium salt **5** was synthesized by Vilsmeier-Haack formylation of cyclohexanone **4**. NIR dye **6** was synthesized by condensation of indolinium salt **3** and iminium salt **5** using NaOAc in dry MeOH. The mixture was refluxed for 3 hours, cooled down and the dye **6** was precipitated from diethyl ether. The chloride in **6** was substituted with benzoic acid by a Suzuki-reaction using boronic acid **7** and $Pd(Ph)_4$. The reaction was followed by LCMS, which showed formation of NIR-acid dye **8**, but also partial hydrolysis of C-Cl bond. The H_2N-PEG_3-N_3 and NIR-acid dye **8** were condensed using EDC.HCl to give the desired azide-NIR dye **10** (azide-NIR10) in 33% over two steps (**Figure S1**).

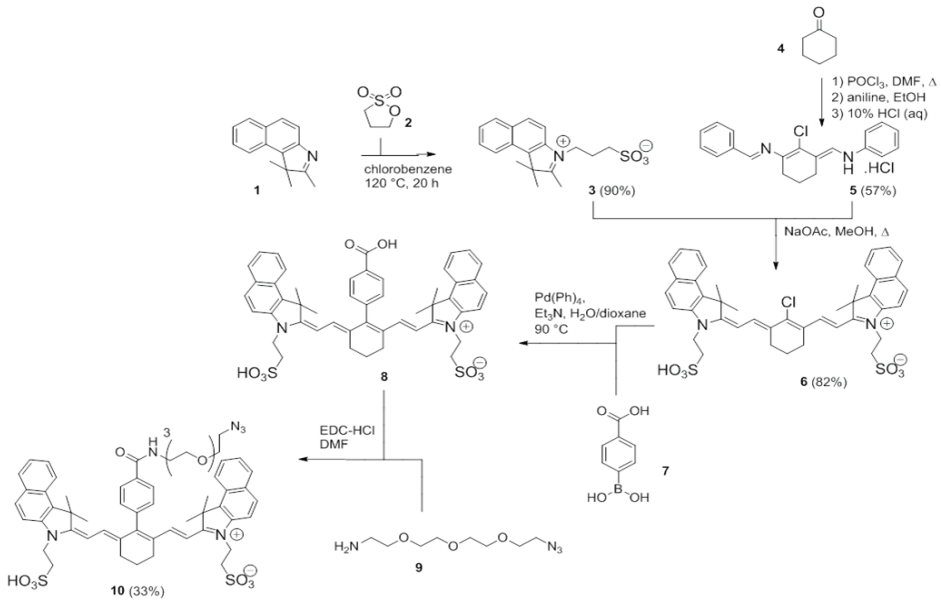

Figure S1. Synthesis of azide-NIR10.

2,3,3-Trimethyl -1-(3-sulfopropyl)-3H-indolium (3). 2,3,3-Trimethylbenz[e]indole **1** (6.7 g, 32 mmol, 1.05 eq) and 1,3-propanesultone **2** (3.71 g, 30.4 mmol, 1.0 eq) were dissolved in chlorobenzene (15 mL) and capped in a microwave vial after filling the tube with Argon. The reaction was heated to 120°C overnight. The chunks were suspended in acetone and filtered giving the target compound as light blue crystals (9.76 g, 29.4 mmol, 92%). ^{1}H NMR (400 MHz, MeOD-d_4): 8.31 (dd, 1 H, J = 8.3, 1.1 Hz, H_{arom}), 8.20 (d, 1 H, J = 9.0 Hz, H_{arom}), 8.13 (m, 2 H, H_{arom}), 7.79 (ddd, 1 H, J = 8.4, 6.9, 1.3 Hz, H_{arom}), 7.70 (m, 1 H, H_{arom}), 4.88 (s, 3 H, H_{methyl}), 4.86 (m, 2 H, H_{propyl}), 3.06 (t, 2 H, J = 6.5 Hz, H_{propyl}), 2.44 (m, 2 H, H_{propyl}), 1.83 (s, 6 H, 2x H_{methyl}); ^{13}C NMR (100 MHz, MeOD-d_4); 198.06, 139.85, 138.66, 135.20, 132.45, 131.03, 129.61, 129.09, 128.62, 124.35, 113.94, 57.30, 48.14, 24.84, 22.35. HRMS Calculated for $[C_{18}H_{21}NO_3S + H]^+$: 332.1320, found 332.1315

***N*-[5-Anilino-3chloro-2,4-(propane-1,3-diyl)-2,4-pentadiene-1-ylidine]anilinium chloride (5).** At 0°C, phosphorus oxychloride (11 mL, 0.12 mol, 2.25 eq) was added dropwise to anhydrous DMF (13 mL, 0.17 mmol, 3.2 eq) at 0°C and after 30 min cyclohexanone 4 (5.5 mL, 53 mmol, 1.0 eq) was added and the mixture was reflux for 1 h. At room temperature, an aniline/ethanol (1:1, 18 mL) (106 mmol aniline, 2 eq) was added and the reaction was stirred for 1 h. The deep purple mixture was poured into 110 mL cold HCl aqueous solution (10%). The mixture was allowed to crystallize overnight in the fridge. The crystals were filtered and washed twice with cold water, washed twice with ether and then dried under vacuum. Product was obtained as purple crystals (10.8 g, 30.2 mmol, 57%); ^{1}H NMR (400 MHz, MeOD-d_4); 8.68 (s, 2 H), 7.60-7.30 (m, 10 H, H_{arom}), 2.66 (t, 4 H, *J* = 6.4 Hz, 2x $CH_{2\text{-cyclohexanone}}$), 2.00 (m, 2 H, $CH_{2\text{-cyclohexanone}}$); ^{13}C NMR (100 MHz, MeOD-d_4); 150.50, 140.67, 131.32, 128.00, 11988, 116.36, 25.56, 21.07. HRMS Calculated for $[C_{20}H_{19}ClN_2 + H]^+$: 323.1315, found 323.1310.

NIR-dye (6). Compound **3** (3.31 g, 10.0 mmol, 2.0 eq) and aniline **5** (1.80 g, 5.00 mmol, 1.0 eq) was dissolved in dry MeOH (100 mL). Anhydrous NaOAc (1.64 g, 20.0 mmol, 4 eq) was added and the mixture refluxed for 3 h. The reaction was cooled down and the poured into ether (200 mL) giving green solid (3.3 g, 4.12 mmol, 82%). ^{1}H NMR (400 MHz, DMF-d_7): 8.50 (d, 2 H, *J* = 13.9 Hz, 2x =CH), 8.38 (d, 2 H, *J* = 8.9 Hz, 2x H_{arom}), 8.14 (d, 2 H, *J* = 8.9 Hz, 2x H_{arom}), 8.11 (d, 2 H, *J* = 8.5, 2x H_{arom}), 7.70 (m, 2 H, H_{arom}), 7.55 (t, 2 H, *J* = 7.5 Hz, 2x =CH), 4.71 (m, 4 H, 2x $CH_{2\text{-propyl}}$), 2.82-2.76 (m, 8 H, 2x $CH_{2\text{-propyl}}$ and 2x $CH_{2\text{-cyclohexanone}}$) 2.28 (m, 4 H, 2x $CH_{2\text{-propyl}}$), 2.07 (s, 12 H, 4x CH_3), 1.91 (m, 2 H, $CH_{2\text{-cyclohexanone}}$); ^{13}C NMR (100 MHz, DMF-d_7): 174.16, 162.54, 143.06, 140.52, 134.23, 132.22, 130.89, 130.29, 129.16, 128.21, 127.90, 127.34, 125.14, 122.68, 118.56, 112.23, 102.05, 51.33, 49.02, 48.08, 43.68, 27.17, 24.23. HRMS Calculated for $[C_{44}H_{47}ClN_2O_6S_2 + H]^+$: 799.2642, found 799.2638.

NIR-PEG$_3$-Azide (10). NIR-dye **6** (0.4 g, 0.5 mmol, 1.0 eq) was dissolved in water/dioxane (1:1, 5 mL) in a microwave vial. To the solution were added $Pd(Ph)_4$ (12 mg, 0.01 mmol, 0.02 eq), boronic acid 7 (0.1 g, 0.6 mmol, 1.2 eq) and Et_3N (0.28 mL, 2.0 mmol, 4.0 eq). The mixture was flushed with argon and the microwave vial was closed. The mixture was heated to 90°C for two hours, concentrated in vacuo and co-evaporated twice with toluene. The crude acid (0.5 mmol) was dissolved in dry DMF (5 mL) and N_3-PEG_4-NH_3Cl **9** (140 mg, 0.55 mmol, 1.1 eq) was added followed by EDC-Cl (0.24 g, 1.25 mmol, 2.5 eq). The reaction was stirred at room temperature overnight and full conversion was confirmed with HPLC-MS. The reaction was concentrated and purified by HPLC-MS giving **10** as a green powder (180 mg, 0.16 mmol, 33%). ^{1}H NMR (400 MHz, DMF-d_7); 8.94 (t, 1 H, *J* = 5.4 Hz, NH), 8.33 (d, 2 H, *J* = 8.1 Hz, H_{arom}), 8.05-7.98 (m, 6 H, H_{arom}), 7.89 (d, 2 H, *J* = 8.9 Hz, H_{arom}), 7.62 (ddd, 2 H, *J* = 8.3, 6.8, 1.3 Hz, H_{arom}), 7.52 (d, 2 H, *J* = 8.1 Hz, H_{arom}), 7.48 (dd, 2 H, *J* = 8.2, 6.9 Hz, H_{arom}), 7.29 (d, 2 H, *J* = 14.1 Hz, 2x =CH), 6.64 (d, 2 H, *J* = 14.1 Hz, 2x =CH), 4.60 (m, 4 H, 2x $CH_{2\text{-propyl}}$), 3.78 (t, 2 H, *J* = 6.3 Hz, $CH_{2\text{-PEG}}$), 3.72-3.68 (m, 4 H, 2x $CH_{2\text{-PEG}}$), 3.67-3.63 (m 4 H, 2x $CH_{2\text{-PEG}}$), 3.42 (m, 2 H, $CH_{2\text{-PEG}}$), 2.85 (t, 4 H, *J* = 5.7 Hz, 2x $CH_{2\text{-cyclohexanone}}$), 2.76 (m, 4 H, 2x $CH_{2\text{-propyl}}$), 2.20 (m, 4 H, $CH_{2\text{-propyl}}$), 1.98 (m, 2 H, $CH_{2\text{-cyclohexanone}}$), 1.51 (s, 12 H, 4x CH_3); ^{13}C NMR (100 MHz, DMF-d_7); 173.02, 166.62, 162.52, 160.40, 146.68, 142.63, 140.57, 134.88, 133.31, 131.95, 130.74, 130.24, 130.05, 128.17, 127,94, 127.81, 124.84, 122.37, 111.98, 100.69, 70.55, 70.53, 70.40, 70.35, 69.95, 69.63, 50.71, 50.54, 48.17, 43.35, 39.92, 26.64, 24.94, 24.10. HRMS Calculated for $[C_{59}H_{68}N_6O_{10}S_2 + H]^+$: 1085.4517, found 1085.4512.

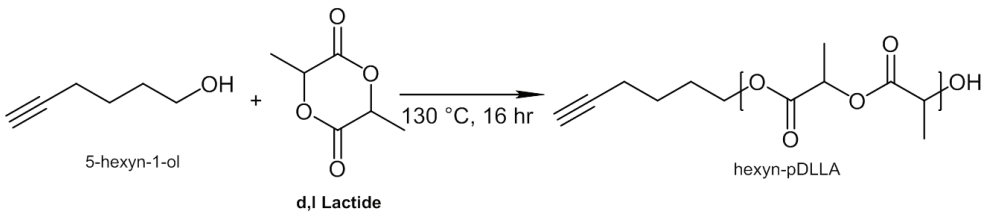

Figure S2. Synthesis of hexyn-pDLLA by ring opening polymerization.

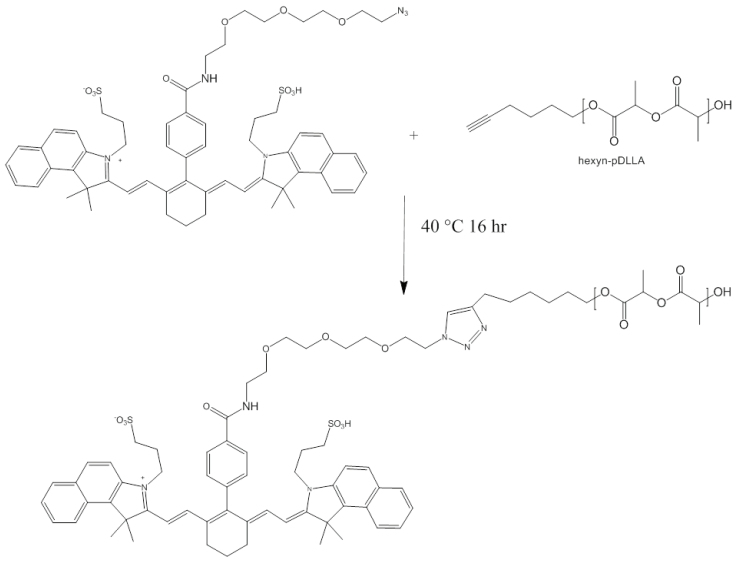

Figure S3 . Click reaction between azide-NIR10 and hexyn-pDLLA.

Table S1. Characteristics of pLBMGA and pLHMGA.

pLBMGA							**pLHMGA**				
Monomer /initiator molar ratio	BMMG/ d,l-lactide molar ratio in feed	NMR	GPC		DSC	Yield (%)	Target M_n (kDa)	GPC		DSC	Yield (%)
		BMMG /d,l-lactide molar ratio	M_n (kDa)	PDI	T_g (°C)			M_n (kDa)	PDI	T_g (°C)	
100	50/50	48/52	13.4	1.99	39	100	15.8	16.2	1.57	57	83

Table S2. Characteristics of hexyn-pDLLA.

Hexyn-pDLLA					
Monomer/ Initiator molar ratio	Target M_n (kDa)	GPC		DSC	Yield (%)
		M_n (kDa)	PDI	T_g(°C)	
70	10.1	11.0	1.62	50	75

Table S3. Characteristics of NIR10-pDLLA.

Polymer	Polymer/ dye molar ratio in the feed	Yield (%)	Conjugation efficiency (%)	Free dye in polymer after reaction (%)	Free dye present after precipitation in water (%)	M_n (kDa)	PDI
NIR10-pDLLA	1	76	85	15	8	12.8	1.40

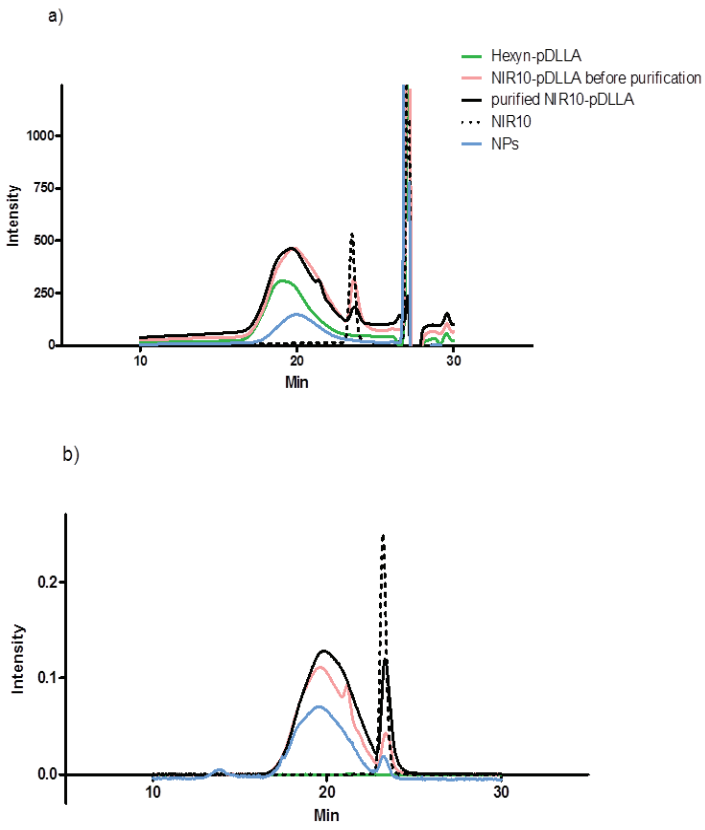

Figure S4. GPC chromatograms of hexyn-pDLLA, NIR 10-pDLLA before purification and NIR10-pDLLA after purification and dual labeled NPs a) RI detection, b) UV detection at 700 nm.

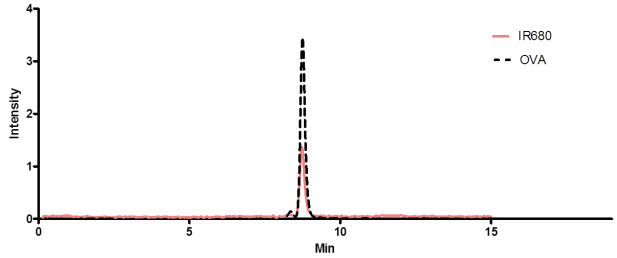

Figure S5. GPC chromatogram of IR680-OVA after purification with a Zeba spin column (see **Section 2.6**).

Table S4. Characteristics of IR680-OVA and IR800-OVA.

IR-OVA	Dye/protein molar ratio in the feed	Dye/protein molar ratio in the freeze-dried product	Conjugation efficiency (%)	Yield (%)
IR680-OVA	2.0	1.7	80	85
IR800-OVA	1.7	1.0	58	84

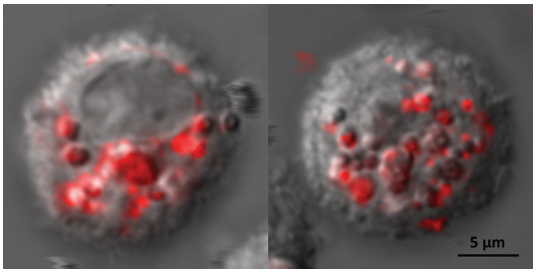

Figure S6. Uptake of OVA loaded NPs by D1 cells. Confocal microscopic images showing the uptake of OVA NPs by D1 dendritic cells. NPs loaded with Alexa 647 OVA (red) were incubated with D1 dendritic cells overnight, and NP uptake was visualized based on the red fluorescent signal of Alexa647. The shown cells are representative for the whole sample.

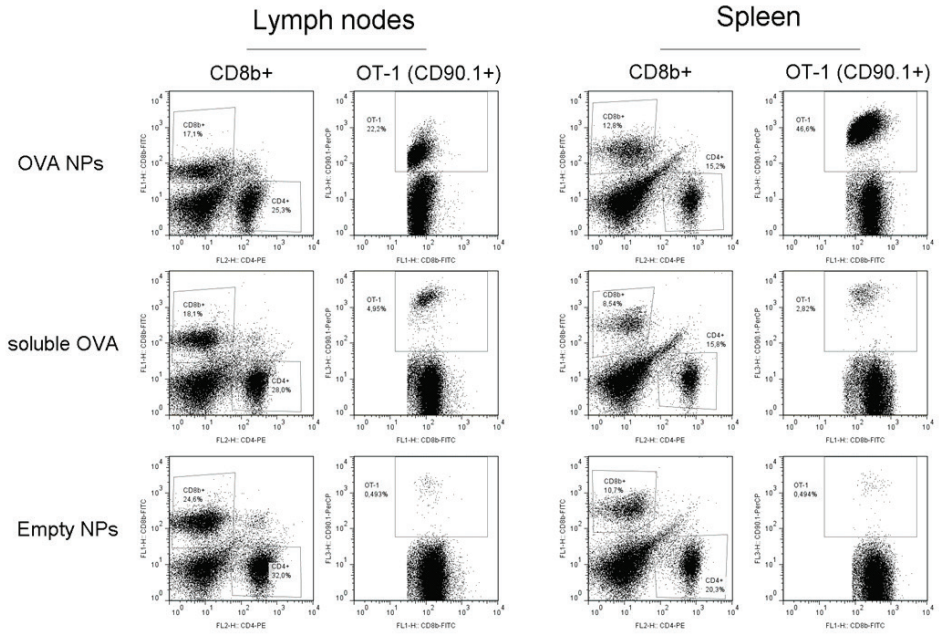

Figure S7. Flow cytometry plots for quantification of *in vivo* OT-I proliferation. Expansion of transferred OT-I cells after administration of OVA NPs to mice was quantified by *ex vivo* flow cytometry analysis. Inguinal lymph nodes (both draining the injection site) and the spleen were harvested and single-cell suspensions were stained with fluorescently labeled antibodies to identify the total CD8+ T cell pool (CD8β staining) and the transferred OT-I cells (CD90.1 staining). Shown examples are representative plots from N=4 mice, as shown in **Figure 8**.

CHAPTER 4

Polymeric nanoparticles for co-delivery of synthetic long peptide antigen and poly IC as therapeutic cancer vaccine formulation

Sima Rahimian

Marieke F. Fransen

Jan Willem Kleinovink

Jonatan Riis Christensen

Maryam Amidi

Wim E. Hennink

Ferry Ossendorp

Journal of Controlled Release 2015; 203: 16-22

Abstract

The aim of the current study was to develop a cancer vaccine formulation for treatment of human papillomavirus (HPV)-induced malignancies. Synthetic long peptides (SLPs) derived from HPV16 E6 and E7 oncoproteins have been used for therapeutic vaccination in clinical trials with promising results. In preclinical and clinical studies adjuvants based on mineral oils (such as incomplete Freund's adjuvant (IFA) and Montanide) are used to create a sustained release depot at the injection site. While the depot effect of mineral oils is important for induction of robust immune responses, their administration is accompanied with severe and long lasting side effects. In order to develop an alternative for IFA family of adjuvants, polymeric nanoparticles (NPs) based on hydrophilic polyester (poly(D,L lactic-co-hydroxymethyl glycolic acid) (pLHMGA)) were prepared. These NPs were loaded with a synthetic long peptide (SLP) derived from HPV16 E7 oncoprotein and a toll like receptor 3 (TLR3) ligand (poly IC) by double emulsion solvent evaporation technique. The therapeutic efficacy of the nanoparticulate formulations was compared to that of HPV SLP + poly IC formulated in IFA. Encapsulation of HPV SLP antigen in NPs substantially enhanced the population of HPV-specific CD8+ T cells when combined with poly IC either co-encapsulated with the antigen or in its soluble form. The therapeutic efficacy of NPs containing poly IC in tumor eradication was equivalent to that of the IFA formulation. Importantly, administration of pLHMGA NPs was not associated with adverse effects and therefore these biodegradable NPs are excellent substitutes for IFA in cancer vaccines.

Keywords: Therapeutic cancer vaccine, Human papillomavirus (HPV), Synthetic long peptide (SLP), TLR3 ligand, Poly IC, Nanoparticles, pLHMGA, Incomplete Freund's adjuvant (IFA)

1. Introduction

Infection with human papillomavirus (HPV) is the main cause of cervical cancer and is associated with other anogenital malignancies such as vaginal and anal cancer [1]. More than 99% of cervical cancer cases - the second most common cancer in women worldwide [2] - are attributed to infection with high risk oncogenic HPV types [3]. The predominant high risk type is HPV16 [4] which accounts for approximately 50% of the cervical tumors [5]. Known etiology of the disease provides an appealing opportunity to develop vaccines against the high risk HPV types. The registered prophylactic vaccines are highly successful in prevention of cancer [6] but have no therapeutic efficacy [7]. Therefore, there is great need for therapeutic vaccines to treat HPV-induced malignancies. HPV16 encodes two major oncoproteins, namely E6 and E7 which are expressed in all HPV16-induced cervical cancer cells [5] and are responsible for interference in the cell cycle [8]. Several clinical studies have used E6 and E7 proteins as targets in immunotherapy of HPV-induced cancer using different strategies such as peptide and protein based vaccines, virus like particles and DC-based vaccines [9–12]. Although these studies showed activation of CD8+ T cells - the immune cells capable of killing tumor cells - the majority exhibited limited tumor regression and therapeutic efficacy [13–15]. Vaccination with minimal peptide epitopes of oncoproteins has been a popular approach in several studies for treatment of HPV-induced malignancies [16–18]. Nevertheless, it has not been very successful due to several reasons, including direct binding of the peptide epitope to MHC molecules on the surface of cells, which results in tolerization of T cells [15,18] and failure to develop a long-term memory [19]. Increasing the length of the peptide antigens has substantially improved the efficacy of the peptide vaccines [19,20]. As synthetic long peptides (SLPs) are too large to be able to directly bind to MHC molecules on the surface of cells, their epitope can only be presented by professional antigen presenting cells (APCs) which are able to take up and process the peptide for subsequent presentation to T cells. This restriction to professional APCs is essential as only these cells can provide the co-stimulatory signals necessary for adequate T cell activation. DCs are the most efficient professional APCs. These cells process SLPs more efficiently than whole proteins [21] and provide long-term antigen presentation in the draining lymph nodes which is crucial for T cell activation and expansion [22].

Vaccination with SLPs overlapping the whole sequence of HPV16 E6 and E7 oncoproteins formulated in Montanide ISA 51 has proven the immunogenicity of the vaccine in clinical trials [23–26]. Incomplete Freund's adjuvant (IFA) and similar adjuvants such as Montanide ISA 51 act as depots that deliver the peptide antigen in water-in-oil emulsions [27,28]. However, their adjuvanticity is not sufficient for initiation of a strong T cell response [19,24,25]. An effective cancer vaccine is capable of activating the adaptive as well as the innate immune system which results in efficient targeting and elimination of cancer cells by eliciting a strong T cell-mediated immune response [29]. IFA formulations fail to cause strong DC maturation and as a result, are not capable of inducing a strong CD8+ T cell response [30,31]. DC maturation bridges between innate and adaptive immune system and can be mediated by triggering a family of receptors on DCs (as well as other cells), called toll-like receptors (TLRs) [32,33]. Some TLR ligands such as TLR3 ligands bind to their receptors in the endosome, where the antigens are processed [34]. An advantage of using TLR3 ligands such as poly IC in cancer vaccines is that upon triggering, these ligands are able to enhance antigen cross-presentation to CD8+ T cells, therefore expanding the cytotoxic T cell population to induce cellular immune response [35]. However poly IC - a double stranded RNA construct, is degraded rapidly by nucleases in the body. This demands a high administered dose which consequently might result in toxicity and autoimmune responses [36]. Studies have demonstrated that the

co-delivery of TLR ligands and peptide antigens in carrier systems can considerably enhance T cell response [37–40] while decreasing the risk of toxicity [36].
Another drawback of IFA other than its weak immunogenicity is adverse effects at the injection site such as painful granulomas, inflammation and swelling, sterile abscesses and cysts [41,42]. Hence, development of a delivery system to replace IFA in cancer vaccines is of great interest. The present study, aimed to 1) to increase the efficacy and safety of the HPV SLP cancer vaccine by designing a particulate cancer vaccine, and 2) to study the effect of co-delivery of HPV SLP and TLR3 ligand (poly IC) in nanoparticles (NPs). We have developed a nanoparticulate cancer vaccine based on a biodegradable polymer, poly(D,L lactic-co-hydroxymethyl glycolic acid) (pLHMGA) [43,44] and loaded with a 27 amino acid synthetic long peptide and poly IC (TLR3 ligand). This SLP contains both a CD8+ epitope (RAHYNIVTF) and a CD4+ epitope (DRAHYNI) of the HPV16 E7 protein. Previous studies have shown the advantages of pLHMGA over the well-known and frequently investigated pLGA, such as better compatibility with proteins and peptides [45,46]. In a recent study, ovalbumin-loaded pLHMGA NPs were used as a model vaccine. These particles showed prolonged presence in the lymph nodes upon subcutaneous administration and excellent *in vivo* T cell expansion which proved their potential as antigen delivery systems [47]. pLHMGA particles have shown good cytocompatibility *in vitro* [47,48] and are biocompatible *in vivo* after subcutaneous administration [48]. In the current study, we examined the therapeutic efficacy of HPV SLP-loaded pLHMGA NPs in a prime-boost vaccination regimen in TC-1 tumor-bearing mice and compared it with IFA formulation.

2. Materials and methods

2.1. Materials

Poly(D,L lactic-co-hydroxymethyl glycolic acid) (pLHMGA) with initial monomer ratios of 65/35 (d,l lactide/benzyloxy methyl methylglycolide (BMMG)) was synthesized and characterized as described before [43, 47] (**Supplementary Figure S1**-details are provided in the supplementary data). Polyvinyl alcohol (PVA; Mw 30,000–70,000; 88% hydrolyzed), dimethyl sulfoxide (DMSO), tetrafluoroacetic acid (TFA), poly IC (sodium salt, gamma irradiated) and 4-(2-hydroxyethyl) piperazine-1-ethanesulfonic acid (HEPES 1 M) were obtained from Sigma-Aldrich, USA. Dichloromethane (DCM) and acetonitrile (ACN) were obtained from Biosolve, the Netherlands. Sodium hydroxide (NaOH) and sodium dodecyl sulfate 20% (SDS) were purchased from Fluka, The Netherlands. Pyrogen-free water was obtained from Carl Roth, Germany. Phosphate buffered saline (1.8 mM NaH_2PO_4, 8.7 mM Na_2HPO_4, 163.9 mM Na^+, 140.3 mM Cl^- , pH 7.4) (PBS) was obtained from B Braun, Germany. IFA was purchased from Difco, USA. Synthetic long peptide 27-mer HPV SLP (GQAEPDRAHYNIVTF(Abu)(Abu)K(Abu)DSTLRL(Abu)V), containing the cytotoxic T lymphocyte (CTL) epitope RAHYNIVTF of HPV E7 oncoprotein (E743–69) was synthesized in interdepartmental GMP facility of the Department of Clinical Pharmacy and Toxicology of Leiden University Medical Center. In this SLP, cysteines were replaced by the unnatural amino acid, aminobutyric acid (Abu). Chemicals were used as received without further purification, unless otherwise stated.

2.2. Preparation of HPV SLP loaded NPs with/without poly IC

HPV SLP-loaded pLHMGA NPs with/without poly IC (HPV SLP ± poly IC NPs) were prepared using a double emulsion solvent evaporation technique essentially as described before [49] with a few adjustments. In brief, 200 µL of 10 mg/mL HPV SLP (100 µL of ACN and 100 µL of TFA 0.1% in pyrogen-free water) ± 50 µL of 20 mg/mL poly IC in pyrogen-free water were emulsified by sonication (30 s, 20% amplitude-ultrasonic homogenizer (Labsonic P, B. Braun Biotech, Germany)) in 50 mg of pLHMGA dissolved in 1 mL of DCM to prepare

a water-in-oil emulsion (W_1/O). Next 2 mL of an aqueous PVA 1% w/v solution (filtered through 0.2 µm cellulose acetate sterile filter) was added to this first emulsion and the mixture was emulsified again by sonication forming the double emulsion (W_1/O/W_2). This double emulsion was then added drop-wise to 25 mL of PVA 0.3% w/v at 40°C while stirring for rapid removal of DCM. After 1 h, the particles were harvested by centrifugation for 30 min at 20,000 g, washed with pyrogen-free water, resuspended in pyrogen-free water and freeze-dried overnight.

2.3. NP characterization

2.3.1. Size, zeta-potential and morphology of the NPs

2.3.1.1. Dynamic light scattering

The size of NPs was measured by dynamic light scattering (DLS) on an ALV CGS-3 system (Malvern Instruments, Malvern, UK) equipped with a JDS Uniphase 22 mW He–Ne laser operating at 632.8 nm, an optical fiber-based detector, and a digital LV/LSE-5003 correlator. Freeze-dried NPs were suspended in deionized water (RI = 1.332 and viscosity of 0.8898 cP) and measurements were done at 25°C at an angle of 90°.

2.3.1.2. Transmission electron microscopy (TEM)

The size and morphology of NPs were analyzed using transmission electron microscopy (TEM, Philips-FEI Tecnai T10, USA). Twenty microliter of particle suspension in water was placed on parafilm. A glow discharged Formvar carbon film on copper grid (Agar scientific, UK) was placed on the particle suspension to absorb the NPs. After 2 min the excess liquid was removed using a filter paper. The sample was stained with 20 µL of 2% uranyl acetate in water for 1 min and consecutively dried with filter paper and was left for 5 min to dry completely. NPs were visualized with 7–73 k fold magnification and analyzed by Olympus MeasureIT software.

2.3.1.3. Zeta potential

The zeta-potential (ζ) of the NPs was measured using a Malvern Zetasizer Nano-Z (Malvern Instruments, Malvern, UK) with disposable folded capillary cells. NPs were dispersed in 10 mM HEPES pH 7.0 and zeta potential was measured at 25°C and analyzed using DTS Nano 4.20 software.

2.3.2. Loading efficiency measurements

2.3.2.1. HPV SLP content

The HPV SLP loading efficiency of the NPs was determined by measuring the peptide content of digested NPs as previously described [61]. Approximately 5 mg of freeze-dried NPs was carefully weighed and dissolved in 0.25 mL of DMSO. After complete dissolution of NPs (60°C, 1 h) 375 µL of ACN and 375 µL of TFA 0.1% in water was added to precipitate the polymer. After 2 h at 60°C, samples were centrifuged at 14,000 g for 15 min and 100 µL of the supernatant was injected into an HPLC system equipped with a C18 column (Dr. Maisch Reprosil-Pur C18-AQ, 3 µm, 150 × 4.6 mm) and an ultraviolet detector (Waters 2487). Mobile phases were 5% ACN in water with 0.1% TFA (solvent A), and 95% ACN in water with 0.1% TFA (solvent B). HPV SLP was separated by applying a linear gradient from 0% to 100% solvent B over 15 min, at a flow rate of 1 mL/min, and peptide detection was at 210 nm. Calibration was done using 100 µL of HPV SLP (1.5–200 µg/mL).

2.3.2.2. Poly IC content

The amount of poly IC encapsulated in the NPs was determined as previously described [50] with some modifications. In detail, approximately 5 mg of freeze-dried NPs was accurately

weighed and dissolved in 1 mL of DCM. Then 3 mL of Tris EDTA (TE-provided with the Quantifluor kit, (Promega Corporation, USA)) buffer was added and the tube was vortexed for 30 s. The two immiscible layers were separated by centrifugation at 5000 g for 5 min. Next, 2.5 mL of the upper layer containing poly IC in TE buffer was removed and replaced by 2.5 mL of fresh TE buffer and the extraction was repeated 4-5 times until the amount of poly IC extracted was less than 1% of the initial loading. The amount of poly IC in the extraction medium was measured by using Quantifluor RNA quantification assay kit and calibration was done using poly IC in TE buffer (4.8–2500 ng/mL). HPV SLP NPs and empty NPs as well as empty NPs plus known amount of poly IC were used as controls. These samples were treated similar to (HPV SLP + poly IC) NPs. Loading efficiency (LE%) is reported as the amount of HPV SLP/poly IC encapsulated in the NPs divided by the amount of HPV SLP/poly IC added × 100%. Loading percentage (L%) is reported as the amount of HPV SLP/poly IC entrapped in the NPs per total dry mass of the NPs × 100%.

2.4. Mice and cells

Female C57BL/6 (H-2b) mice were purchased from Charles River laboratories (France) and kept in specified pathogen-free facility. The experiments were approved by the Animal Experimental Committee of the Leiden University Medical Center. TC-1 cells (growth factor independent and highly oncogenic in immunocompetent mice) are primary lung epithelial cells of C57BL/6 mice transformed with HPV16 E6 and E7 and c-Ha-Ras oncogenes [51]. TC-1 cells were cultured at 37°C with 5% CO_2 in IMDM containing 8% FCS (Greiner), 2 mM glutamine, and 100 IU/mL penicillin, 400 µg/mL geneticin (G418; Life Technologies), non-essential amino acids (Life Technologies), and 1 mM sodium pyruvate (Life Technologies).

2.5. Therapeutic vaccination

2.5.1. Vaccination regimen

TC-1 tumor cells (10^5) dispersed in 200 µL of PBS were injected subcutaneously (s.c.) in the right flank of mice (age 8-10 weeks). Tumor size was measured with calipers two times per week in three dimensions and the tumor volume was calculated using this formula: tumor length × width × height. Only mice with palpable tumors (0.5-3 mm^3) were enrolled in the experiment. Therapeutic vaccination was given in a prime-boost fashion; when the tumors were palpable, on day 8 after tumor inoculation the prime dose was injected and the boost was given on day 22 after tumor inoculation. Mice (5-10 in each group) were vaccinated s.c. in the left flank with 100 µg of HPV SLP NPs with or without 50 µg of poly IC either co-encapsulated in NPs or in soluble form. IFA formulation containing HPV SLP and poly IC was used as control. This IFA formulation was prepared on the vaccination day by mixing 100 µg HPV SLP and 50 µg poly IC in PBS/IFA with a volume ratio of 1:1 and vortexing for 30 min [52]. As we aimed to compare the effect of NPs to IFA formulations used previously, the doses of HPV SLP and poly IC were chosen according to the previous treatments which showed good T cell response and tumor regression [52]. Empty pLHMGA NPs were excluded from this experiment. Earlier studies showed that empty pLHMGA NPs do not elicit a T cell response [47]. Furthermore, empty pLHMGA microparticles have been used as control in tumor therapy (unpublished data) where no delay in tumor growth and survival of mice was observed. Mice were sacrificed for ethical reasons when tumors exceeded 1000 mm^3 or in case of tumor ulceration. The experiment was ended when none of the mice had a palpable tumor. Tumor growth for each group is presented as relative tumor volume (RTV) calculated using this formula: RTV_t=Tumor volume at time t/initial tumor volume. Data were fitted using non-linear regression and survival of mice is presented in Kaplan-Meier plot.

2.5.2. Detection of HPV16 E7-specific CD8+ T cells in peripheral blood of tumor-bearing mice by tetramer staining

Peripheral blood was collected from the tail-vein of the mice 9 days after the prime dose (17 days after tumor inoculation). After lysis of erythrocytes, the blood samples were stained for cell surface markers CD3ε, CD8α and the allophycocyanine-conjugated H-2Db E749–57 tetramer which binds to the T cell receptor recognizing RAHYNIVTF epitope [53].

2.6. Statistical analyses

All data were analyzed using GraphPad Prism 5.02 software. For tumor experiments Kaplan-Meier survival curves were applied and the differences between survival curves were analyzed by log-rank test ($p < 0.05$ was considered statistically significant). Expansion of HPV-specific CD8+ T cells in the blood of tumor-bearing mice 9 days after the prime vaccination in mice treated with HPV SLP and poly IC formulations was compared to untreated mice by Dunn's multiple comparisons test. Statistical significance of total experiment ($p < 0.001$) was calculated by Kruskal-Wallis test.

3. Results and discussion

3.1. Preparation and characterization of (HPV SLP ± poly IC) NPs

HPV SLP loaded NPs and (HPV SLP + poly IC) loaded NPs were prepared by a double emulsion solvent evaporation technique. This method has been extensively used for encapsulation of peptides and nucleic acids as well as other biomacromolecules in nano- and microparticles based on aliphatic polyesters [54–58]. The obtained NP formulations showed comparable characteristics in terms of size and morphology and HPV SLP loading efficiency. The mean hydrodynamic diameter of the NPs measured by DLS ranged between 400 and 500 nm with a PDI of approximately 0.20-0.29. Analysis of freeze-dried samples with TEM showed spherical NPs with a smooth surface and a particle size of approximately 100-200 nm (**Figure 1**). The difference between the observations from TEM and results of DLS measurements can be explained by the algorithms used for calculation of hydrodynamic diameter of the NPs by DLS which results in overestimation of the average population [59]. The HPV SLP loaded NP exhibited negative zeta potential (approximately -14 mV). The negative zeta potential of the HPV loaded NPs could be ascribed to the carboxylic (COOH) end groups present in the pLHMGA polymer (**Supplementary Figure S1**). These COOH groups are deprotonated in HEPES buffer and therefore causing a negative zeta potential. The isoelectric point (pI) of HPV SLP is 7.7 and therefore it bears very low charge in HEPES buffer pH 7.0 (**Supplementary Figure S2**) which is unlikely to contribute to the negative zeta potential values. The zeta potential values of (HPV SLP + poly IC) NPs were approximately -25 mV which can be attributed to negatively-charged poly IC molecules that are associated with/close to the surface of the NPs. The loading efficiency of HPV SLP for both NP formulations was approximately 60% and independent of presence of poly IC in the formulations. The loading efficiency of poly IC in (HPV SLP + poly IC) NPs was approximately 65% and the ratio between HPV SLP and poly IC was close to the target ratio (2 to 1 (w/w)). For the ease of comparison, the ratio between HPV SLP and poly IC was chosen according to the previous studies in which HPV SLP was used in soluble form or emulsified in Montanide [52]. Analysis of HPV SLP NPs and empty NPs using Quantifluor kit showed the baseline signal for empty and HPV SLP NPs formulations. Additionally poly IC was completely recovered when added to the empty NPs, Therefore it was concluded that neither HPV SLP in the particles nor the particles as such affect the quantification of poly IC. The HPV SLP has a poor solubility in aqueous solutions. As it has been studied by Silva et al., the *in vitro* release of long peptides from pLGA NPs could not be accurately followed for more than 24 h, likely due to the precipitation of peptide during release. However in the

abovementioned study, pLGA NPs with low burst release showed superior T cell activation *in vitro,* when compared to pLGA NPs with high burst release [49]. The *in vitro* release of HPV SLP from pLHMGA NPs in PBS was followed up to 48 h and not more than 5-7% of the encapsulated peptide was detected. Moreover, there is no good model system to investigate the release of peptides from carriers in DCs. The characteristics of the NPs are summarized in **Table 1**.

Table 1. Characteristics of NPs. Results are representative of two independent formulations.

NP formulation	Theoretical Loading % HPV SLP/ poly IC	Size (nm)	PDI	Zeta potential (mV)	HPV SLP loading efficiency (%)	Poly IC loading efficiency (%)	µg HPV SLP/ µg poly IC in 1 mg of NP formulation
HPV SLP	4/0	423 ± 49	0.21 ± 0.03	-14.9 ± 0.3	58.3 ± 9.9	-	-
HPV SLP + poly IC	4/2	491 ± 16	0.29 ± 0.08	-25.0 ± 1.3	58.8 ± 5.9	63.0 ± 10.0	1.92 ± 0.06

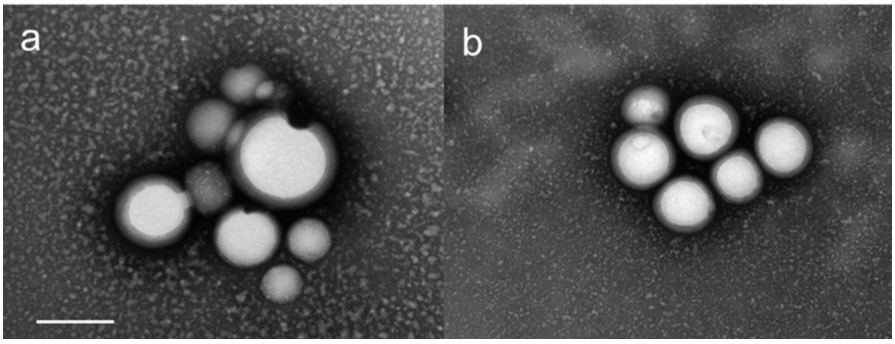

Figure 1. TEM photographs of a) (HPV SLP + poly IC) NPs and b) HPV SLP NPs. Scale bar represents 200 nm.

3.2. Tumor growth following treatment with NP and IFA formulations

To assess the anti-tumor efficacy of nanoparticulate cancer vaccines in comparison to commonly used IFA formulations in a mouse model of HPV-induced cervical cancer, mice were inoculated subcutaneously with TC-1 tumor cells expressing HPV16 oncogenes E6 and E7. When the tumors were palpable, at day 8 after tumor inoculation, the mice were s.c. vaccinated with various formulations and received the boost dose at day 21 after tumor inoculation. In order to evaluate the necessity of using poly IC in co-encapsulated form with HPV SLP, one group of mice was vaccinated with HPV SLP NPs and poly IC in PBS. Control mice were either treated with poly IC in PBS or left untreated. Tumor growth curves in the different groups of mice are presented in **Figure 2a** and **Supplementary Figure S3**. All untreated mice developed tumors larger than 1000 mm^3 and were euthanized no later than 28 days post inoculation. In the groups of mice which received poly IC in soluble form, tumors grew out similarly to untreated mice. This confirms previous observations showing that a TLR ligand per se does not cause regression in pre-established tumors [52]. HPV

SLP NPs increased the overall survival of mice but their inhibitory effect was limited, in agreement with previous studies in which the administration of the HPV SLP in IFA was able to delay the tumor growth, but did not completely eradicate tumors [20]. In contrast, NPs loaded with HPV SLP and poly IC strongly delayed the tumor growth with approximately 20 days, comparable to the effect after administration of HPV SLP NPs in combination with soluble poly IC. Treatment with HPV and poly IC in IFA emulsion showed similar tumor regression to NP formulations administered with poly IC (either encapsulated or in soluble form). The anti-tumor efficacy of the various HPV SLP formulations in tumor-bearing mice is presented in the Kaplan-Meier plot (**Figure 2b**). Neither poly IC in soluble form (median survival: 22 days) nor HPV SLP NPs (median survival: 25 days) were able to significantly prolong the survival of mice as compared to untreated mice (median survival: 22 days), whereas vaccination with NP formulations containing HPV SLP in combination with a TLR3 ligand (poly IC) significantly increased the survival time of mice ($p < 0.001$) (median survival 43 days). There were no differences in survival proportion and median survival of mice which received (HPV SLP + poly IC) NPs and the group which received HPV SLP NP co-administered with poly IC in soluble form. Although previous studies suggested that the co-encapsulation of the antigen and the adjuvant substantially enhances the T cell response, our data did not support this notion [36]. This can likely be ascribed to the relatively high dose of soluble poly IC that was administered. It can be expected that at lower doses, co-encapsulation will have a beneficial effect. The favorable aspect of co-encapsulation over soluble administration is the lower risk of systemic immune activation by spread of the soluble TLR ligand. Upon vaccination of mice with HPV SLP + poly IC in IFA, the vaccine formed a lump at the injection site which persisted until the end of the experiment, whereas in mice treated with NPs, no residue (remainder) of NPs was observed. This is in line with previous observations where upon local administration of pLHMGA NPs of similar size in mice, NPs were cleared from the injection site in a sustained manner [47]. Moreover, pLHMGA particles when injected subcutaneously have shown biocompatibility with no toxicity [48]. In an earlier study, a postmortem examination of the injection site 60 days after administration of both pLHMGA microparticles and IFA formulation showed that the IFA depot was still present while no remainders of pLHMGA particles were observed (unpublished data) which confirms previous observations on *in vitro* degradation of pLHMGA particles in 30–50 days [45].

3.3. HPV-specific T cell expansion in peripheral blood of tumor-bearing mice after treatment with NP and IFA formulations

Earlier studies have shown that the ability of a peptide vaccine to induce a systemic CD8+T cell response predicts the anti-tumor efficacy of the vaccine [20,52]. Therefore, the population of HPV-specific CD8+T cells in blood was measured by tetramer staining 9 days after the prime vaccination. Mice treated with poly IC containing NP formulations and HPV SLP + poly IC in IFA showed high and comparable frequencies of HPV-specific CD8+ T cells whereas this effect was not observed for mice treated with the HPV SLP NP formulation (**Figure 2c**). In agreement with previous observations [60–62], TLR3 ligand alone (poly IC in PBS) did not induce any HPV-specific T cell expansion. Importantly, the height of the HPV-specific CD8+ T cell response in blood correlated with the delay in tumor growth, suggesting an important role for CD8+ T cells in the anti-tumor effect of the vaccines.

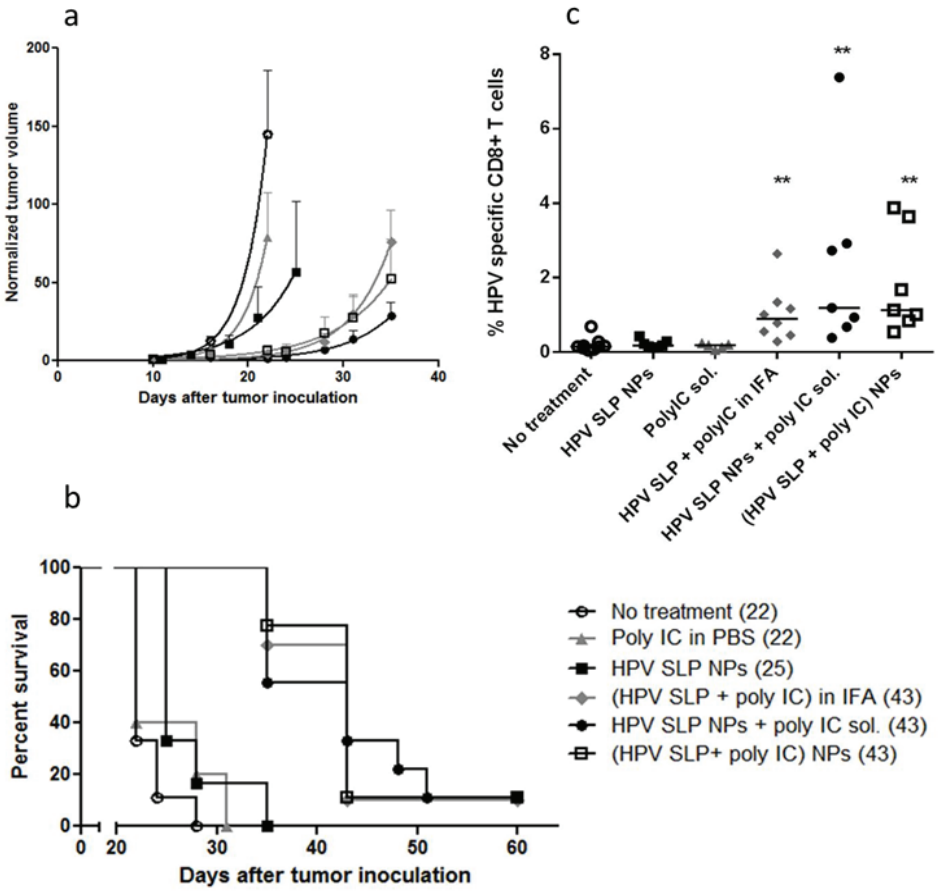

Figure 2. a) Relative tumor growth in tumor bearing mice. Seven days after TC-1 tumor inoculation in wild-type C57BL/6 mice, and when tumors were palpable, mice were either left untreated or were s.c. vaccinated in the opposite flank with formulations consisting of HPV SLP with or without poly IC formulated in NPs or in IFA followed by a boost injection 14 days after the prime dose. The mice were sacrificed when the tumor volume reached 1000 mm^3 or in case of tumor ulceration. The relative TC-1 tumor volume is plotted against time and fitted using non-linear regression. For each group, line is only plotted until the first mouse is sacrificed. 5-10 mice per group were used. Data is representative of two independent experiments. b) Survival of mice per group presented in Kaplan-Meier plot. The differences between the groups were calculated using log-rank (Mantel-Cox) test. The survival of mice vaccinated with HPV SLP NPs with poly IC (either co-encapsulated or in soluble form) and HPV SLP + poly IC in IFA was significantly longer compared to the non-treated mice ($p < 0.001$). Numbers in the legends represent median survival in days. Data is representative of two independent experiments. c) Expansion of HPV-specific CD8+ T cells in the blood of tumor-bearing mice 9 days after the prime vaccination. Each dot represents one mouse. HPV-specific CD8+T cell expansion in tumor-bearing mice 9 days after the prime vaccination in mice treated with HPV SLP and poly IC formulations is compared to untreated mice by Dunn's multiple comparisons test. Statistical significance of total experiment ($p < 0.001$) is calculated by Kruskal-Wallis test. Statistical significance between groups is shown by asterisks, ** = $p < 0.01$.

4. Conclusion

This study highlights the potential of pLHMGA NPs as substitute for IFA-based cancer vaccines. Vaccination with NPs comprising a synthetic long peptide derived from HPV E7 oncoprotein and poly IC as a TLR3 ligand substantially prolonged the survival of mice (three weeks) in a therapeutic tumor setting. There was no difference between the effects of using poly IC in encapsulated NP form or in a soluble form when the HPV SLP was encapsulated in pLHMGA NPs. Importantly, the anti-tumor effect of these NP formulations was comparable to that of IFA, while as opposed to IFA, subcutaneous administration of pLHMGA NPs was not associated with local adverse effects. Moreover, the HPV-specific CD8+ T cell expansion following administration of NPs could predict their therapeutic efficacy in tumor-bearing mice. Although the efficacies of the studied vaccine formulations; HPV SLP + poly IC in IFA, (HPV SLP + poly IC) NPs and HPV SLP NPs + poly IC were similar, safety concerns are considerably distinct for each formulation. Encapsulation of poly IC prevents autoimmunity caused by high systemic concentrations of poly IC. Additionally NPs do not exhibit the local adverse effects associated with administration of IFA. In conclusion, the (HPV SLP + poly IC) NPs provide equal efficacy and are superior in terms of safety and therefore the preferred formulation in cancer immunotherapy as alternatives for IFA in immunotherapy of cancer.

Acknowledgments

This research was conducted within the framework of Cancer Vaccine Tracking project (#03O-302), Center For Translational Molecular Medicine (CTMM).

Appendix. Supplementary data

References

[1] F. Bosch, A. Lorincz, N. Munoz, C. Meijer, K. Shah, The causal relation between human papillomavirus and cervical cancer. J Clin Pathol 2002;55:244–265.

[2] H. zur Hausen, Papillomaviruses and cancer: from basic studies to clinical application. Nat. Rev. Cancer 2002;2:342–350.

[3] J.M.M. Walboomers, M.V. Jacobs, M.M. Manos, F.X. Bosch, J.A. Kummer, K.V. Shah, P.J.F. Snijders, J. Peto, C.J.L.M. Meijer, N. Munoz, Human papillomavirus is a necessary cause of invasive cervical cancer worldwide. J Pathol 1999;189:12–19.

[4] N.Munoz, F. Bosch, X. Castellsague, M. Diaz, S. De Sanjose, D. Hammouda, K. Shah, C. Meijer, Against which human papillomavirus types shall we vaccinate and screen? The international perspective. Int J Cancer 2004;111:278–285.

[5] N. Munoz, F.X. Bosch, S. de Sanjose, R. Herrero, X. Castellsague, K.V. Shah, P.J.F. Snijders, C.J.L.M. Meijer, Epidemiologic classification of human papillomavirus types associated with cervical cancer, N Engl J Med 2003;348:518–527.

[6] C.M.Wheeler, Advances in primary and secondary interventions for cervical cancer: human papillomavirus prophylactic vaccines and testing. Nat Clin Pract Oncol. 2007;4:224–235.

[7] A. Hildesheim, R. Herrero, S. Wacholder, A.C. Rodriguez, D. Solomon, M.C. Bratti, J.T. Schiller, P. Gonzalez, G. Dubin, C. Porras, S.E. Jimenez, D.R. Lowy, Effect of human papillomavirus 16/18 L1 virus-like particle vaccine among young women with pre-existing infection - a randomized trial, JAMA 2007;298:743–753.

[8] S. Tyring, Human papillomavirus infections: epidemiology, pathogenesis, and host immune response. J Am Acad Dermatol 2000:43:S18–S26.

[9] N.P. Tran, C. Hung, R. Roden, T.C. Wu, Control of HPV infection and related cancer through vaccination. Recent Results Cancer Res 2014;193:149–171.

[10] B.Ma, B.Maraj, NamPhuongTran, J. Knoff, A. Chen, R.D.Alvarez, C. Hung, T.Wu, Emerging human papillomavirus vaccines. Expert Opin Emerg Drugs 2012;17:469–492.

[11] T. Liu, W.M. Hussein, I. Toth, M. Skwarczynski, Advances in peptide-based human papillomavirus therapeutic vaccines. Curr Top Med Chem 2012;12:1581–1592.

[12] A. Bolhassani, E. Mohit, S. Rafati, Different spectra of therapeutic vaccine development against HPV infections. Hum Vaccin 2009;5:671–689.

[13] M. Ressing, W. van Driel, R. Brandt, G. Kenter, J. de Jong, T. Bauknecht, G. Fleuren, P. Hoogerhout, R. Offringa, A. Sette, E. Celis, H. Grey, B. Trimbos, W. Kast, C. Melief, Detection of T helper responses, but not of human papillomavirus-specific cytotoxic T lymphocyte responses, after peptide vaccination of patients with cervical carcinoma. J Immunother 2000;23:255–266.

[14] L. Muderspach, S. Wilczynski, L. Roman, L. Bade, J. Felix, L. Small, W. Kast, G. Fascio, V. Marty, J. Weber, A phase I trial of a human papillomavirus (HPV) peptide vaccine for women with high-grade cervical and vulvar intraepithelial neoplasia who are HPV 16 positive. Clin Cancer Res 2000;6:3406–3416.

[15] R.E.M. Toes, R. Offringa, R.J.J. Blom, C.J.M. Melief, W.M. Kast, Peptide vaccination can lead to enhanced tumor growth through specific T-cell tolerance induction, Proc. Natl. Acad. Sci. U. S. A. 1996;93:7855–7860.

[16] S.H. van der Burg, M.S. Bijker, M.J.P. Welters, R. Offringa, C.J.M. Melief, Improved peptide vaccine strategies, creating synthetic artificial infections to maximize immune efficacy. Adv Drug Deliv Rev 2006;58:916–930.

[17] M.S. Bijker, C.J. Melief, R. Offringa, S.H. van der Burg, Design and development of synthetic peptide vaccines: past, present and future. Expert Rev Vaccines 2007;6:591–603.

[18] R.E.M. Toes, R.J.J. Blom, R. Offringa, W.M. Kast, C.J.M. Melief, Enhanced tumor outgrowth after peptide vaccination — functional deletion of tumor-specific CTL induced by peptide vaccination can lead to the inability to reject tumors. J Immunol 1996; 156:3911–3918.

[19] M.S. Bijker, S.J.F. van den Eeden, K.L. Franken, C.J.M. Melief, R. Offringa, S.H. van der Burg, CD8(+) CTL priming by exact peptide epitopes in incomplete Freund's adjuvant induces a vanishing CTL response, whereas long peptides induce sustained CTL reactivity. J Immunol 2007;179:5033–5040.

[20] S. Zwaveling, S.Mota, J. Nouta, M. Johnson, G. Lipford, R. Offringa, S. van der Burg, C. Melief, Established human papillomavirus type 16-expressing tumors are effectively eradicated following vaccination with long peptides. J Immunol 2002;169:350–358.

[21] R.A. Rosalia, E.D. Quakkelaar, A. Redeker, S. Khan, M. Camps, J.W. Drijfhout, A.L. Silva, W. Jiskoot, T. van Hall, P.A. van Veelen, G. Janssen, K. Franken, L.J. Cruz, A. Tromp, J. Oostendorp, S.H. van derBurg, F. Ossendorp, C.J.M. Melief, Dendritic cells process synthetic long peptides better than whole protein, improving antigen presentation and T-cell activation. Eur J Immunol 2013:43;2554–2565.

[22] M.S. Bijker, S.J.E. van den Eeden, K.L. Franken, C.J.M. Melief, S.H. van der Burg, R. Offringa, Superior induction of anti-tumor CTL immunity by extended peptide vaccines involves prolonged, DC-focused antigen presentation. Eur J Immunol 2008;38:1033–1042.

[23] C.J.M. Melief, S.H. van der Burg, Immunotherapy of established (pre) malignant disease by synthetic long peptide vaccines. Nat Rev Cancer 2008;8:351–360.

[24] M.J.P. Welters, G.G. Kenter, S.J. Piersma, A.P.G. Vloon, M.J.G. Lowik, D.M.A. Berendsvan der Meer, J.W. Drijfhout, A.R.P.M. Valentijn, A.R. Wafelman, J. Oostendorp, G.J. Fleuren, R. Offringa, C.J.M. Melief, S.H. van der Burg, Induction of tumor-specific CD4+ and CD8+ T-cell immunity in cervical cancer patients by a human papillomavirus type 16 E6 and E7 long peptides vaccine. Clin Cancer Res 2008;14:178–187.

[25] G.G. Kenter, M. Welters, M. Lowik, J. Drijfhout, R. Valentijn, J. Ostendorp, F. Gertjan, S. Van de Burg, C. Melief, Therapeutic HPV 16 vaccination with long E6 and E7 peptides shows immunological and clinical efficacy. Gynecol

Oncol 2008;108:S19-S19.
[26] G.G. Kenter, M.J.P. Welters, A.R.P.M. Valentijn, M.J.G. Lowik, D.M.A. Berends-van der Meer, A.P.G. Vloon, F. Essahsah, L.M. Fathers, R. Offringa, J.W. Drijfhout, A.R. Wafelman, J. Oostendorp, G.J. Fleuren, S.H. van der Burg, C.J.M. Melief, Vaccination against HPV-16 oncoproteins for vulvar intraepithelial neoplasia. N Engl J Med 2009;361:1838–1847.
[27] J. Aucouturier, L. Dupuis, S. Deville, S. Ascarateil, V. Ganne, Montanide ISA 720 and 51: a new generation ofwater in oil emulsions as adjuvants for human vaccines. Expert Rev Vaccines 2002;1:111–118.
[28] J. Aucouturier, S. Ascarateil, L. Dupuis, The use of oil adjuvants in therapeutic vaccines, Vaccine (Suppl. 2) 2006;24:S2-44-5.
[29] J.M. Silva, M. Videira, R. Gaspar, V. Preat, H.F. Florindo, Immune system targeting by biodegradable nanoparticles for cancer vaccines. J Control Release 2013; 168:179–199.
[30] D.E. Speiser, D. Lienard, N. Rufer, V. Rubio-Godoy, D. Rimoldi, F. Lejeune, A.M. Krieg, J.C. Cerottini, P. Romero, Rapid and strong human CD8+T cell responses to vaccination with peptide, IFA, and CpG oligodeoxynucleotide 7909. J Clin Invest 2005;115:739–746.
[31] A. Shibaki, S. Katz, Induction of skewed Th1/Th2 T-cell differentiation via subcutaneous immunization with Freund's adjuvant. Exp Dermatol 2002;11:126–134.
[32] S. Akira, K. Takeda, T. Kaisho, Toll-like receptors: critical proteins linking innate and acquired immunity. Nat Immunol 2001;2:675–680.
[33] C.Melief, S. van der Burg, R. Toes, F. Ossendorp, R. Offringa, Effective therapeutic anticancer vaccines based on precision guiding of cytolytic T lymphocytes. Immunol Rev 2002;188:177–182.
[34] B. Salaun, S. Lebecque, S. Matikainen, D. Rimoldi, P. Romero, Toll-like receptor 3 expressed by melanoma cells as a target for therapy? Clin. Cancer Res. 2007;13:4565–4574.
[35] F. Steinhagen, T. Kinjo, C. Bode, D.M. Klinman, TLR-based immune adjuvants. Vaccine 2011;29:3341–3355.
[36] A.M. Hafner, B. Corthesy, H.P. Merkle, Particulate formulations for the delivery of poly(I:C) as vaccine adjuvant. Adv Drug Deliv Rev 2013;64:1386–1399.
[37] E. Schlosser, M.Mueller, S. Fischer, S. Basta, D.H. Busch, B. Gander, M. Groettrup, TLR ligands and antigen need to be coencapsulated into the same biodegradable microsphere for the generation of potent cytotoxic T lymphocyte responses. Vaccine 2008;26:1626–1637.
[38] S. Hamdy, O.Molavi, Z.Ma, A. Haddadi, A. Alshamsan, Z. Gobti, S. Elhasi, J. Samuel, A. Lavasanifar, Co-delivery of cancer-associated antigen and Toll-like receptor 4 ligand in PLGA nanoparticles induces potent CD8(+) T cell-mediated anti-tumor immunity. Vaccine 2008;26:5046–5057.
[39] C. Wischke, J. Zimmermann, B. Wessinger, A. Schendler, H. Borchert, J.H. Peters, T. Nesselhut, D.R. Lorenzen, Poly(I:C) coated PLGA microparticles induce dendritic cell maturation. Int J Pharm 2009; 365:61–68.
[40] S. De Koker, B.N. Lambrecht, M.A. Willart, Y. van Kooyk, J. Grooten, C. Vervaet, J.P. Remon, B.G. De Geest, Designing polymeric particles for antigen delivery. Chem Soc Rev 2011;40:320–339.
[41] H.Toledo, A. Baly, O. Castro, S. Resik, J. Laferte, F. Rolo, L. Navea, L. Lobaina, O. Cruz, J. Miguez, T. Serrano, B. Sierra, L. Perez, M.E. Ricardo, M. Dubed, A.L. Lubian, M. Blanco, J.C. Millan, A. Ortega, E. Iglesias, E. Penton, Z. Martin, J. Perez, M. Diaz, C.A. Duarte, A phase I clinical trial of a mufti-epitope polypeptide TAB9 combined with Montanide ISA 720 adjuvant in non-HIV-1 infected human volunteers. Vaccine 2001;19:4328–4336.
[42] R. Gupta, E. Relyveld, E. Lindblad, B. Bizzini, S. Benefraim, C. Gupta, Adjuvants - a balance between toxicity and adjuvanticity. Vaccine 1993;11:293–306.
[43] M. Leemhuis, C. van Nostrum, J. Kruijtzer, Z. Zhong, M. ten Breteler, P. Dijkstra, J. Feijen, W. Hennink, Functionalized poly(alpha-hydroxy acid)s via ring-opening polymerization: toward hydrophilic polyesters with pendant hydroxyl groups. Macromolecules 2006;39:3500–3508.
[44] M. Leemhuis, J.A.W. Kruijtzer, C.F. van Nostrurn, W.E. Hennink, In vitro hydrolytic degradation of hydroxyl-functionalized poly(alpha-hydroxy acid)s. Biomacromolecules 2007;8:2943–2949.
[45] A.H. Ghassemi, M.J. van Steenbergen, A. Barendregt, H. Talsma, R.J. Kok, C.F. van Nostrum, D.J.A. Crommelin, W.E. Hennink, Controlled release of octreotide and assessment of peptide acylation from poly(D, L-lactide-co-hydroxymethyl glycolide) compared to plga microspheres. Pharm Res 2012;29:110–120.
[46] Y. Liu, A.H. Ghassemi, W.E. Hennink, S.P. Schwendeman, The microclimate pH in poly(D, L-lactide-co-hydroxymethyl glycolide) microspheres during biodegradation. Biomaterials 2012;33:7584–7593.
[47] S. Rahimian, J.W. Kleinovink, M.F. Fransen, L. Mezzanotte, H. Gold, P. Wisse, H. Overkleeft, M. Amidi, W. Jiskoot, C.W. Löwik, F. Ossendorp, W.E. Hennink, Near-infrared labeled, ovalbumin loaded polymeric nanoparticles based on a hydrophilic polyester as model vaccine: *in vivo* tracking and evaluation of antigen-specific CD8+ T cell immune response. Biomaterials 2015;37:469–477.
[48] F. Kazazi-Hyseni, J. Zandstra, E. Popa, R. Goldschmeding, A. Lathuile, G. Veldhuis, C. Van Nostrum, W. Hennink, R. Kok, Biocompatibility of poly(D, L-lactic-co-hydroxymethyl glycolic acid) microspheres after subcutaneous and subcapsular renal injection. Int J Pharm 2015;482:99-109.
[49] A.L. Silva, R.A. Rosalia, A. Sazak, M.G. Carstens, F. Ossendorp, J. Oostendorp, W. Jiskoot, Optimization of encapsulation of a synthetic long peptide in PLGA nanoparticles: low-burst release is crucial for efficient CD8(+) T cell activation. Eur J Pharm Biopharm 2013;83:338–345.
[50] Y. Krishnamachari, PLGA microparticle based vaccine carriers for an improved and efficacious tumor therapy, PhD thesis University of Iowa, 2011. (http://ir.uiowa.edu/ etd/2922).
[51] K. Lin, F. Guarnieri, K. Staveley OCarroll, H. Levitsky, J. August, D. Pardoll, T. Wu, Treatment of established tumors with a novel vaccine that enhances major histocompatibility class II presentation of tumor antigen. Cancer Res

1996;56:21–26.
[52] S. van Duikeren, M.F. Fransen, A. Redeker, B. Wieles, G. Platenburg, W. Krebber, F. Ossendorp, C.J.M. Melief, R. Arens, Vaccine-induced effector-memory CD8(+) T cell responses predict therapeutic efficacy against tumors. J Immunol 2012;189:3397–3403.
[53] J. Altman, P. Moss, P. Goulder, D. Barouch, M. McHeyzerWilliams, J. Bell, A. McMichael, M. Davis, Phenotypic analysis of antigen-specific T lymphocytes, Science 1996;274:94–96.
[54] R.C. Mundargi, V.R. Babu, V. Rangaswamy, P. Patel, T.M. Aminabhavi, Nano/micro technologies for delivering macromolecular therapeutics using poly(D, L-lactideco- glycolide) and its derivatives. J Control Release 2008;125:193–209.
[55] P. Couvreur, F. Puisieux, Nanoparticles and microparticles for the delivery of polypeptides and proteins. Adv Drug Deliv Rev 1993;10:141–162.
[56] W. Ma, M. Chen, S. Kaushal, M. McElroy, Y. Zhang, C. Ozkan, M. Bouvet, C. Kruse, D. Grotjahn, T. Ichim, B. Minev, PLGA nanoparticle-mediated delivery of tumor antigenic peptides elicits effective immune responses. Int J Nanomedicine 2012;7:1475–1487.
[57] Z. Zhang, S. Tongchusak, Y. Mizukami, Y.J. Kang, T. Ioji, M. Touma, B. Reinhold, D.B. Keskin, E.L. Reinherz, T. Sasada, Induction of anti-tumor cytotoxic T cell responses through PLGA-nanoparticle mediated antigen delivery. Biomaterials 2011;32:3666–3678.
[58] A.M. Tinsley-Bown, R. Fretwell, A.B. Dowsett, S.L. Davis, G.H. Farrar, Formulation of poly(D, L-lactic-co-glycolic acid) microparticles for rapid plasmid DNA delivery. J Control Release 2000;66:229–241.
[59] V. Filipe, A. Hawe, W. Jiskoot, Critical evaluation of nanoparticle tracking analysis (NTA) by nanosight for the measurement of nanoparticles and protein aggregates. Pharm Res 2010;27:796–810.
[60] D.A. Wick, J.R. Webb, A novel, broad spectrum therapeutic HPV vaccine targeting the E7 proteins of HPV16, 18, 31, 45 and 52 that elicits potent E7-specific CD8T cell immunity and regression of large, established, E7-expressing TC-1 tumors. Vaccine 2011;29:7857–7866.
[61] S. Chen, R. Ou, J. Tang, X. Deng, Y. Wu, J.C. van Velkinburgh, B. Ni, Y. Xu, Enhanced anti-tumor effects of HPV16E7(49–57)-based vaccine by combined immunization with poly(I:C) and oxygen-regulated protein 150. Cancer Epidemiol 2013;37:172–178.
[62] Z.R. Cui, F. Qiu, Synthetic double-stranded RNA poly(I:C) as a potent peptide vaccine adjuvant: therapeutic activity against human cervical cancer in a rodent model. Cancer Immunol Immunother 2006;55:1267–1279.

Appendix
Supplementary Data

Synthesis of poly(d,l lactic-co- hydroxymethylglycolic acid) (pLHMGA)

3S-(benzyloxymethyl)-6S-methyl-1,4-dioxane-2,5-dione (benzyloxymethyl-methylglycolide) (BMMG) was synthesized as described in detail elsewhere [1]. A random copolymer of BMMG and d,l-lactide (35:65 molar ratio) was synthesized via ring opening polymerization in melt using benzyl alcohol as initiator with a 100/1 monomer-to-initiator molar ratio and $Sn(Oct)_2$ as catalyst (**Figure S1**).

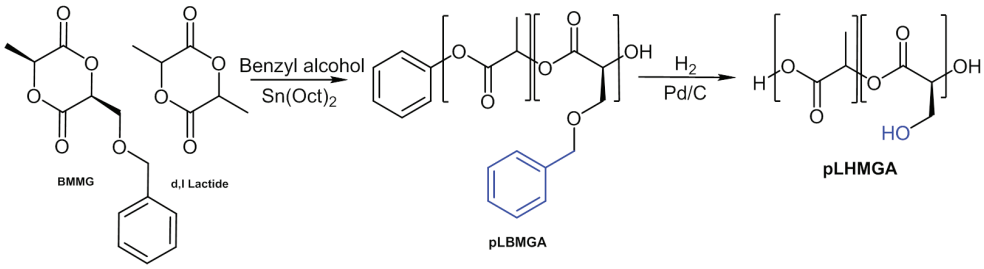

Figure S1. Synthesis of poly(lactic-co-hydroxymethyl-glycolic acid) (pLHMGA) in two consecutive steps; synthesis of poly(lactic-co-benzyloxymethyl-glycolic acid) (pLBMGA) via ring opening polymerization of BMMG and d,l lactide, followed by removal of the benzyl group by hydrogenation to yield pLHMGA.

In a typical procedure, vacuum-dried monomers (BMMG (1920 mg, 7.68 mmol) and d,l-lactide (2060 mg, 14.27 mmol)) were transferred into a dried schlenk tube under a nitrogen atmosphere. Benzyl alcohol (23.7 mg, 0.219 mmol; 215.8 µL from a 109.8 mg/mL stock solution in toluene)) and $Sn(Oct)_2$ (44.4 mg, 0.109 mmol; 396.1 µL from a 112 mg/mL stock solution in toluene) were added. Next, toluene was evaporated under vacuum for 2 h and the tube was closed and immersed into a preheated 130°C oil bath while stirring. After an overnight reaction, the obtained polymer was dissolved in 10 mL chloroform and purified by precipitation in 400 mL methanol. The precipitated polymer was collected by filtration and vacuum dried to yield 3.6 g (91%) poly(d,l-lactic-co-benzyloxymethylglycolic acid) (pLBMGA). Thereafter, pLBMGA was dissolved in 500 mL THF, and 4 g of 10 % w/w Pd/C catalyst was added. The flask was filled with hydrogen (H_2) in three consecutive steps of subsequent evacuation and refilling with H_2 and the reaction mixture was stirred overnight under an H_2 pressure. Next, Pd/C was removed by filtration and THF was removed by evaporation. The obtained polymer was then dissolved in 5 mL chloroform and precipitated in 200 mL n-propanol and vacuum dried after filtration to yield 3.0 g of pLHMGA (90%).
The molar ratio of BMMG and d,l-lactide in pLBMGA (protected polymer) was calculated from the NMR spectrum and was 34/66, which is close to feed ratio (35/65). In pLHMGA (deprotected polymer), the ratio remained the same, (34/66). DSC analysis showed that both pLBMGA and pLHMGA were fully amorphous with a T_g of 39°C and 50°C, respectively, in agreement with previously published data [2]. Molecular weight analysis by GPC showed that the number average molecular weight of pLHMGA (13.3 kDa) was close to the aimed molecular weight based on monomer-to-initiator molar ratio (14.8 kDa) implying that the backbone of the polymer was kept intact after hydrogenation. The polymer characteristics are summarized in **Table S1**.

Table S1. Characteristics of pLHMGA

pLBMGA							pLHMGA					
Monomer /initiator Molar ratio	BMMG/ d,l-lactide molar ratio in feed	NMR	GPC		DSC	Yield (%)	Target M_n (kDa)	NMR	GPC		DSC	Yield (%)
		BMMG/ d,l-lactide molar ratio	M_n (kDa)	PDI	T_g (°C)			HMG*/ d,l-lactide molar ratio	M_n (kDa)	PDI	T_g (°C)	
100	35/65	34±1/ 66±1	13.6± 0.8	2.00± 0.06	39±1	95±4	14.8	34±1/ 66±1	13.3± 2.2	1.90± 0.19	50±1	87±12

*HMG: Hydroxymethylglycolide; BMMG after removal of benzyl groups.

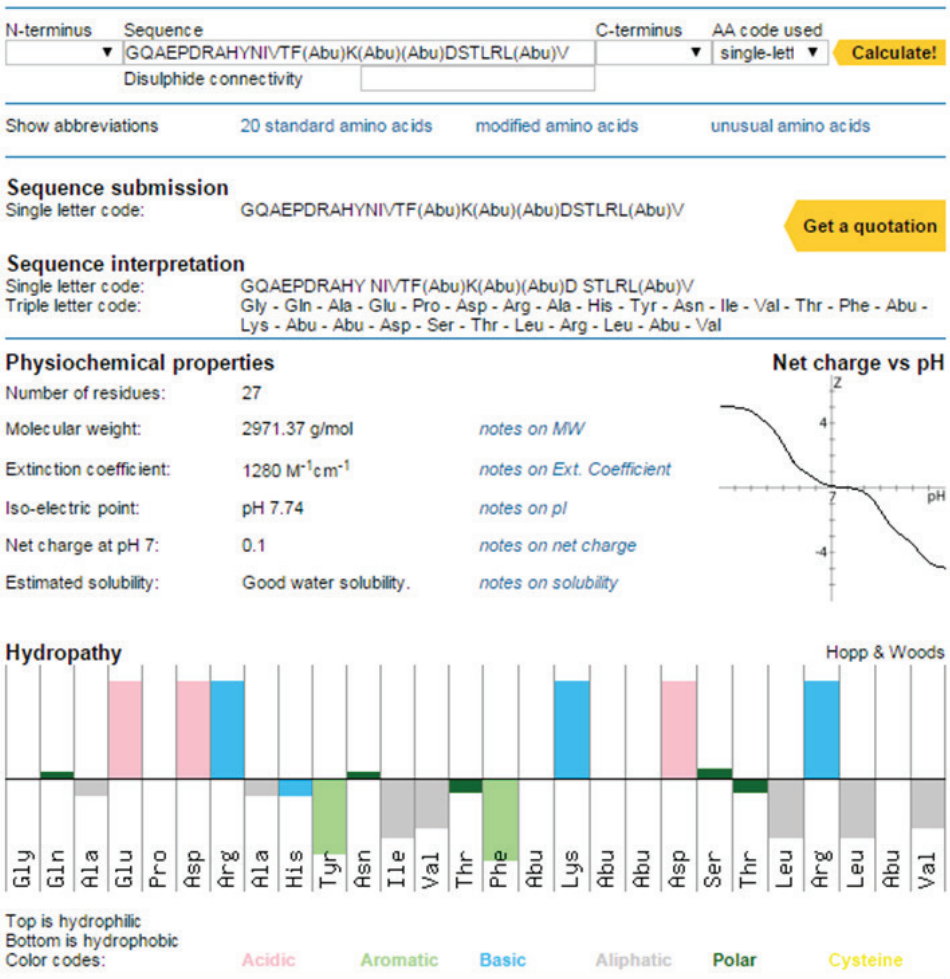

Figure S2. The isoelectric point (pI) of the HPV SLP was obtained from the following website: **http://pepcalc.com/peptide-solubility-calculator.php**

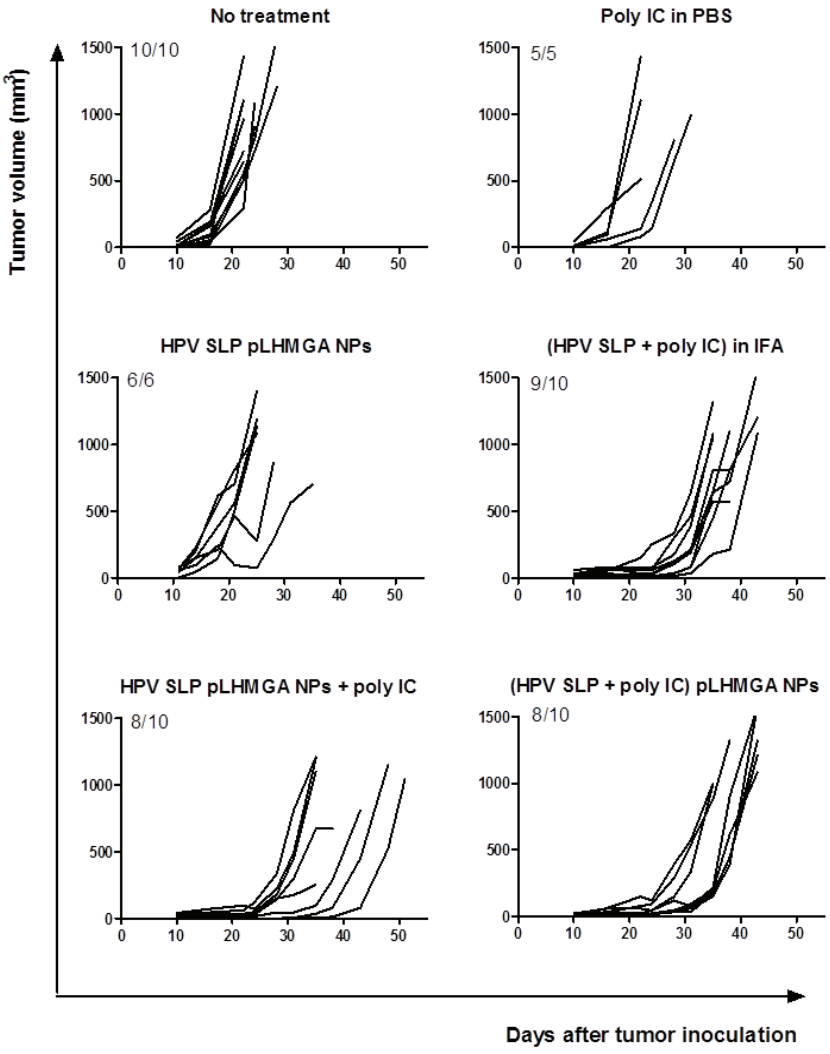

Figure S3. Tumor growth curves in tumor bearing mice receiving different therapeutic treatments. Wild-type C57BL/6 mice were inoculated with TC-1 cells and when tumors were palpable (0.5-3 mm^3), mice were either left untreated or were s.c. vaccinated in the opposite flank with formulations consisting of HPV SLP with or without TLR3 ligand (poly IC) formulated in NPs or in IFA and boosted 14 days later. The mice were sacrificed when the tumor volume reached 1000 mm^3 or in case of ulceration. Each line represents one mouse. Numbers in the top left corner indicate mice succumbed to tumor burden of all mice in that group at end of experiment. 5-10 mice per group were used. Data is representative of two independent experiments.

References

[1] Leemhuis M, van Nostrum C, Kruijtzer J, Zhong Z, ten Breteler M, Dijkstra P, et al. Functionalized poly(alpha-hydroxy acid)s via ring-opening polymerization: toward hydrophilic polyesters with pendant hydroxyl groups. Macromolecules 2006;39:3500-8.

[2] Rahimian S, Kleinovink JW, Fransen MF, Mezzanotte L, Gold H, Wisse P, Overkleeft H, Amidi M, Jiskoot W, Löwik CW, Ossendorp F, Hennink WE. Near-infrared labeled, ovalbumin loaded polymeric nanoparticles based on a hydrophilic polyester as model vaccine: *in vivo* tracking and evaluation of antigen-specific CD8+ T cell immune response, Biomaterials 2015;7:469–477.

CHAPTER 5

Polymeric microparticles for sustained and local delivery of antiCD40 and antiCTLA4 in immunotherapy of cancer

Sima Rahimian*

Marieke F. Fransen*

Jan Willem Kleinovink

Maryam Amidi

Ferry Ossendorp

Wim E. Hennink

Biomaterials, 2015; 61:33-40

* authors contributed equally

Abstract

This study investigated the feasibility of the use of polymeric microparticles for sustained and local delivery of immunomodulatory antibodies in immunotherapy of cancer. Local delivery of potent immunomodulatory antibodies avoids unwanted systemic side effects while retaining their anti-tumor effects. Microparticles based on poly(lactic-co-hydroxymethyl-glycolic acid) (pLHMGA) and loaded with two distinct types of immunomodulatory antibodies (CTLA4 antibody blocking inhibitory receptors on T cells or CD40 agonistic antibody stimulating dendritic cells) were prepared by double emulsion solvent evaporation technique. The obtained particles had a diameter of 12-15 μm to avoid engulfment by phagocytes and were slightly porous as shown by SEM analysis. The loading efficiency of the antibodies in the microparticles was >85%. The *in vitro* release profile of antiCD40 and antiCTLA4 from microparticles showed a burst release of about 20% followed by a sustained release of the content up to 80% of the loading in around 30 days. The therapeutic efficacy of the microparticulate formulations was studied in colon carcinoma tumor model (MC-38). Mice bearing subcutaneous MC-38 tumors were treated with the same dose of immunomodulatory antibodies formulated either in incomplete Freund's adjuvant (IFA) or in microparticles. The antibody-loaded microparticles showed comparable therapeutic efficacy to the IFA formulation with no local adverse effects. The biodegradable microparticles were fully resorbed *in vivo* and no remnants of inflammatory depots as observed with IFA were present in the cured mice. Moreover the microparticles exhibited lower antibody serum levels in comparison with IFA formulations which lowers the probability of systemic adverse effects. In conclusion, pLHMGA microparticles are excellent delivery systems in providing long-lasting and non-toxic antibody therapy for immunotherapy of cancer.

Keywords: pLHMGA, Immunomodulatory antibody, CTLA4-blocking antibody, AntiCD40, Cancer immunotherapy, Sustained release, Local delivery, Incomplete Freund's adjuvant (IFA)

1. Introduction

Immunotherapy has been established as a groundbreaking approach to treat cancer [1]. As opposed to conventional cancer treatment strategies which employ methods to eliminate all rapidly proliferating tumor cells, immunotherapy aims to use the immune system to attack the target of interest with high specificity and low toxicity [2-4]. Immunotherapy of cancer embraces several strategies, including application of immunomodulatory antibodies as monotherapy in the treatment of malignancies [5,6]. These antibodies do not directly target cancer cells but instead aim to induce and enhance immune responses against the tumor, particularly by CD8+ T cells which are crucial for tumor eradication [7]. The mode of action of such indirectly acting or immunomodulatory antibodies can be inhibitory or stimulatory, depending on the role of their target in the anti-tumor immune response. Check-point blocking antibodies such as antagonistic antiCTLA4 have been developed to block inhibitory receptors expressed on T cells [8-10]. Other antibodies such as agonistic antiCD40 function at an earlier phase of the immune response by activating antigen presenting cells (APCs) including dendritic cells (DCs) which are responsible for the activation of tumor-specific CD8+ T cells by cross-presentation of tumor antigens [11].

The cytotoxic T lymphocyte-associated antigen 4 (CTLA4) is one of the key inhibitory receptors expressed by activated CD4+ and CD8+ T cells as well as by memory and regulatory T cells [12], and is responsible for "pushing the brake" of the immune system [13,14]. CTLA4 has a high affinity for CD80 and CD86 on APCs and competes with CD28, a major co-stimulatory signal required for T cell activation, for binding to these ligands. Binding of CTLA4 to its natural ligands, CD80 and CD86 on APCs, results in decreased cytokine production and T cell proliferation [15]. The inhibitory role of CTLA4 is crucial to maintain the balance of the immune system and to prevent autoimmunity, whereas cancer immunotherapy aims to reverse the CD8+ T cell inactivation [16]. To overcome the effect of inhibitory immune regulators, CTLA4 blocking antibodies have been developed as potential anticancer agents [9,17-20].

CD40 is a receptor on APCs as well as on several other cells and binds to its ligand (CD154-also called CD40L) on activated CD4+ Th cells [21]. The CD40-CD40L interaction is essential for maturation of DCs (up-regulation of co-stimulatory molecules, increased secretion of cytokines) and consequently for CD8+ T cell priming and induction of CD8+ T cell response [22]. Earlier studies have shown that the CD40L signal from CD4+ Th cells can also be provided by agonistic antiCD40, encouraging their use for the induction of a robust T cell response [23]. Despite the promising results obtained with clinical trials using immunomodulatory antibodies in advanced stage cancer patients [18,24], after systemic administration, immune related adverse effects such as autoimmune and inflammatory reactions and cytokine release syndrome have been observed [20,25-30]. To minimize these adverse effects, Fransen et al. used Montanide ISA 51 to prepare a sustained-release water-in-oil emulsion for local delivery of an agonistic CD40 antibody in a preclinical mouse model. Unlike systemic antibody administration, this allowed local treatment with a lower dose of antibody, abrogating systemic toxicity while remaining effective in activating T cells [31,32].

In a study the effect of different administration methods on anti-tumor efficacy and toxicity of antiCD40 was evaluated in adenovirus protein E1A-expressing tumor-bearing mice. It was shown that the antitumor efficacy of 30 μg antiCD40 administered locally either in saline or Montanide was comparable to 3 consecutive intravenous injections of 100 μg antiCD40 (survival 70-80%) while single intravenous injection of 30 μg antiCD40 showed minimal tumor growth reduction (survival 30%). In addition, local treatment with low dose of antiCD40 resulted in lower toxicity than high dose intravenous treatment and sustained release formulation of antiCD40 in Montanide caused the lowest adverse effects, which was

characterized by organ histology and liver enzymes in the blood [32].
Montanide ISA 51 is a commercially available mixture of light mineral oils (similar to incomplete Freund's adjuvant (IFA)) with mannide monooleate (as surfactant) and has been used extensively in clinical trials [30,33]. Nevertheless, administration of Montanide ISA 51–based emulsion and similar formulations has been associated with several side effects such as inflammation and swelling, painful granulomas at the injection site, fever, cysts and sterile abscesses [34]. In order to provide a safe formulation for local delivery of immunomodulatory antibodies, microparticulate formulations loaded with CTLA4 blocking antibody and CD40 agonistic antibody were developed in this study using the biodegradable polymer (poly(d,l lactic-co-hydroxymethylglycolic acid) (pLHMGA)). Although similar in backbone to pLGA, pLHMGA possesses pendant hydroxyl groups which increase the hydrophilicity of the polymer. This results in less acidification inside the particles upon degradation and protects the protein/peptide from chemical modification [35,36]. As a result pLHMGA and similar hydrophilic polymers have shown better protein/peptide compatibility and complete release of encapsulated proteins/peptides as compared to pLGA [36-38]. Moreover, these polymers have been successfully used locally as antigen or drug delivery systems *in vivo* without showing toxicity [39,40]. In the present study, first, pLHMGA microparticles were optimized using - for economic reasons - polyclonal human IgG, to obtain a formulation with the desired particle size and antibody release profile. Because these particles were intended for local and sustained release of the antibody and not to be taken up by e.g. macrophages, the desired particle size should be larger than 10 µm [41]. Next, based on experience with the IgG formulations, antiCD40 and antiCTLA4 loaded microparticles were prepared and characterized. The anti-tumor efficacy of the obtained microparticles was compared with that of IFA formulations in tumor-bearing mice. Antibody serum levels were monitored during treatment for potential systemic toxicity and the site of injection was studied for local reactions.

2. Materials and Methods

2.1. Materials

Poly(lactic-co-hydroxymethyl glycolic acid) (pLHMGA) with a copolymer ratio of 50/50 was synthesized and characterized as described previously [40,42] (**Supplementary Figure S1 and Table S1**). IRDye680RD N-hydroxysuccinimide ester (NHS ester) was obtained from LI-COR Biosciences, USA. Polyclonal human IgG (50 mg/mL in glucose 5%) was a gift from Sanquin, the Netherlands. Polyvinyl alcohol (PVA; Mw 30,000-70,000; 88% hydrolyzed) and dimethyl sulfoxide (DMSO) were obtained from Sigma-Aldrich, USA. Sodium dihydrogen phosphate (NaH_2PO_4) and disodium hydrogen phosphate (Na_2HPO_4) were obtained from Merck, Germany. Dichloromethane (DCM) was from Biosolve, the Netherlands. Sodium azide (NaN_3, 99%), sodium hydroxide (NaOH), dipotassium hydrogen phosphate (K_2HPO_4) and sodium dodecyl sulfate 20% (SDS) were purchased from Fluka, the Netherlands. Bicinchoninic acid assay (MicroBCA) reagents were obtained from Thermo Fisher Scientific, USA. Phosphate buffered saline (1.8 mM NaH_2PO_4, 8.7 mM Na_2HPO_4, 163.9 mM Na^+, 140.3 mM Cl^-, pH 7.4) (PBS) was obtained from B Braun, Germany. Pyrogen-free water was obtained from Carl Roth, Germany. Polyclonal anti-rat antibody (BD biosciences, USA) was used for analysis of antiCD40 by ELISA and antiCTLA4 was analyzed by biotin-labeled mouse anti-hamster antibody (clone 192-1) (BD biosciences, USA). Chemicals were used as received without further purification, unless otherwise stated.

2.2. Labeling IgG with NIR fluorescent dyes

Given the limited availability of immunomodulatory antibodies, human IgG was used as a model antibody to optimize the pLHMGA microparticle formulations. In order to accurately

characterize the release kinetics of the formulations, IgG was labeled with IRDye680RD (IR680) by coupling the NHS ester of the dye to the protein. In a typical procedure, the medium in which the IgG was provided (50 mg/mL in glucose 5%) was exchanged to PBS (B Braun, Germany, pH 7.4) using a Zeba™ spin desalting column (7 kDa, Thermo Fisher Scientific, USA). Next, the pH of the antibody solution was adjusted to 8.5 by adding 0.1 mL of K_2HPO_4 1 M pH 9.0 to 1 mL of IgG in PBS. The IRDye680RD NHS ester was dissolved in DMSO (4 mg/mL) and 0.67 mL of this solution (2.7 mg of the dye) was added to the IgG solution yielding 2:1 molar ratio of dye/IgG. The reaction was carried out at room temperature for 2 h. The unreacted dye was subsequently removed using Zeba™ spin desalting columns (7 kDa) equilibrated with HEPES buffer 50 mM pH 7.0 in two consecutive steps and IR680-IgG was collected in HEPES buffer and kept at 4°C. IR680-IgG was characterized by gel permeation chromatography (GPC) as described previously [40].

2.3. Preparation of the microparticles

IR680-IgG loaded microparticles were prepared using a double emulsion solvent evaporation method [37,43]. One hundred and twenty five µL of 5 mg/mL IR-IgG in HEPES 50 mM pH 7.0 was emulsified in 0.5 ml of solution of pLHMGA (10%, 15%, 20% and 30%) in DCM by homogenization (IKA® T10 basic Ultra-Turrax, Germany) at 20,000 rpm for 45 s. This primary emulsion was subsequently emulsified in 1 mL aqueous solution of PVA 1% (20,000 rpm for 45 s) and transferred into 5 mL of PVA 0.5% in 0.9% NaCl in water. After evaporation of DCM (3 h, RT), the particle suspension was centrifuged at 3000 g for 3 min and the pellet was washed twice with pyrogen-free water and freeze-dried overnight. Immunomodulatory antibody loaded microparticles were prepared by the same method using 125 µL antiCD40 (5 mg/mL in HEPES 50 mM pH 7.0) or antiCTLA4 (3 mg/mL in HEPES 50 mM pH 7.0) and polymer concentration of 15%. Empty microparticles were prepared using polymer concentration of 15% and by replacing the antibody solution with pyrogen-free water.

2.4. Characterization of the microparticles

2.4.1. Size and morphology of the microparticles

The average size of the microparticles dispersed in water was measured using a light obscuration particle counter (Accusizer 780, USA).

The morphology of the microparticles was studied by scanning electron microscopy (SEM) (Phenom, FEI, the Netherlands). Freeze-dried microparticles were transferred onto 12-mm diameter aluminum specimen stubs (Agar Scientific Ltd., England) using double-sided adhesive tape and prior to analysis were coated with a 6 nm platinum layer using sputter coater.

2.4.2. Antibody loading in the microparticles

The loading efficiency of antibodies in the microparticles was determined by measuring the antibody content of digested microparticles [44]. In brief, around 5 mg of microparticles (accurately weighed) was dissolved in 0.5 mL DMSO. After complete dissolution, 2.5 mL of 50 mM NaOH containing 0.5% (w/v) SDS was added and the samples were incubated at 37°C overnight to accelerate the degradation process. For IR680-IgG loaded microparticles, the amount of antibody in the resulting solution was determined based on the IR680 label using an Odyssey™ scanner (LI-COR Biosciences, USA) at the 700 nm channel for IR680 and calibration was done using IR680-IgG (0.4-12.5 µg/mL) in DMSO:NaOH 50 mM/SDS 0.5% (1:5). The amount of antiCD40 and antiCTLA4 in microparticles was quantified by MicroBCA protein assay kit and calibration was done using 2-40 µg/mL of antibody solution in DMSO:NaOH 50 mM/SDS 0.5% (1:5).

2.4.3. *In vitro* release of antibodies from microparticles

Ten to twenty mg of freeze-dried antibody-loaded microparticles was accurately weighed and suspended in 1.5 mL of phosphate buffered saline pH 7.4 (49 mM NaH_2PO_4, 99 mM Na_2HPO_4, 6 mM NaCl and 0.05% (w/v) NaN_3). Samples were incubated at 37°C under mild agitation. At different time points, samples were centrifuged (2000 g for 2 min) and 0.75 mL of the supernatant was replaced by 0.75 mL of buffer. The supernatants were kept at 4°C before quantification. The protein content in the supernatant of samples containing IR680-IgG loaded MPs was measured with an Odyssey™ scanner using the 700 nm channel to detect IR680-IgG. Calibration was done using IR680-IgG in PBS (0.19-25 µg/mL). Quantification of antiCD40 and antiCTLA4 was done using the intrinsic fluorescence of the antibody (excitation 280 nm and emission 345 nm) and calibration was done with the corresponding antibody in PBS (1.5-50 µg/mL).

2.5. Experimental animals and cell lines

The experiments were approved by the Animal Experimental Committee of the University of Leiden. C57BL/6 mice were purchased from The Jackson Laboratory, USA. The FGK-45 hybridoma cells producing antiCD40 (a rat IgG2a provided by A. Rolink, Basel Institute for Immunology, Basel, Switzerland) [45] and hybridoma cells producing antiCTLA4 (a Syrian hamster IgG, clone 9H10) [13] were cultured in Protein-Free Hybridoma Medium (Gibco), and antibodies were purified using a Protein G column. Antibody purity was checked by SDS-PAGE.

2.6. Detection of IgG in sera of mice following administration of IR680-IgG loaded microparticles

IR680-IgG loaded microparticles (Formulation 2) were administered subcutaneously to non-tumor bearing mice and at several time points after injection, blood samples were drawn from mice and IgG was detected by ELISA using Protein A coating (Sigma-Aldrich, USA) and HRP conjugated goat-anti human IgG (Southern Biotech, USA).

2.7. Tumor experiments with immunomodulatory antibody- loaded microparticles and serum analysis

MC-38 tumor cells (murine colon carcinoma cell line) [46] were cultured in Iscove's Modified Dulbecco's Medium (IMDM; BioWhittaker) supplemented with 4% fetal calf serum (FCS), 50 mM 2-mercaptoethanol, and 100 IU/mL penicillin/streptomycin. MC-38 tumor cells (10^5 dispersed in 100 µL PBS) were injected subcutaneously into the right flank of 8 to12 week-old female mice. Treatment was started when the tumors were palpable (6-10 days after tumor inoculation; tumor size 0.5-3 mm^3), the tumor size was measured with calipers in three dimensions and mice were sacrificed when tumors size exceeded 1 cm^3. Mice (14-18 per group) were either left untreated or were injected subcutaneously close to the tumor with 30 µg antiCD40 or 50 µg antiCTLA4 in IFA (Dibco, USA) or encapsulated in microparticles. A group of 5 mice was treated with empty microparticles. IFA formulations were prepared by mixing the antibody in PBS at a concentration of 0.3 mg/mL for antiCD40 and 0.5 mg/mL for antiCTLA4 with IFA (1:1), and vortexing for 30 minutes to form a water-in-oil emulsion. The injected volume was 200 µL [34]. At several time points after administration of the formulations, blood samples were drawn from mice and antiCD40 and antiCTLA4 levels in serum were analyzed by ELISA.

2.8. Statistical analyses

All data were analyzed using GraphPad Prism 5.02 software. For tumor experiments Kaplan-Meier survival curves were applied and the differences between survival curves were

analyzed by log-rank test. Antibody serum levels in different groups of mice were compared using two-tailed unpaired Student's *t* test and $p < 0.05$ was considered statistically significant.

3. Results and Discussion

3.1. Characterization of IR680-IgG

To ensure accurate and sensitive detection of released antibody in *in vitro* studies, human IgG was labeled with IR680. IR680-IgG was obtained by coupling IR680 to IgG and was analyzed by GPC. Overlapping peaks corresponding to IgG (excitation 280 and emission 340 nm) and IR680 (excitation 672 and emission 694 nm) in the GPC chromatogram (**supplementary Figure S2**) of the purified IR680-IgG confirmed that the IR680 was indeed conjugated to IgG. No additional peaks (fluorescence detection) were observed, indicating that the free dye was completely removed by purification. Conjugation efficiency calculated by UV measurements showed an average molar dye/protein ratio of 1.4.

3.2. Optimization of pLHMGA microparticulate formulations

Preparation and characterization of IR680-IgG microparticles

IR680-IgG loaded microparticles were prepared using a double emulsion solvent evaporation process as described in **Section 2.3**. In the current study, these antibody-loaded particles were designed for sustained delivery. Because the antibody must be released in the extracellular matrix and not inside the cells where it can be degraded in the lysosomes, the particles were designed to be large enough to prevent uptake by the mononuclear phagocyte system, which is able to uptake particles ranging from 0.5 to10 µm, with its most efficient uptake of around 2-3 µm [41,47]. Besides particle size, sustained and complete release of the antibody is essential in the development of an optimal formulation [48,49]. High burst release might result in high local and systemic concentrations which in turn might cause toxicity [50,51]. The particle preparation was therefore optimized to obtain particles that are larger than 10 µm and provide sustained release of the antibody. Among several parameters involved in particle preparation, polymer concentration is a critical one which affects multiple characteristics of the microparticles, such as size, burst release, loading efficiency and duration of release [52]. The optimal formulation, with an appropriate particle size and fast release profile, was selected from 4 different IR680-IgG loaded pLHMGA microparticles, prepared by varying the polymer concentration from 10% to 30% w/v. The characteristics of these IR680-IgG loaded microparticles are summarized in **Table 1**.

Table 1. Characteristics of the IR680-IgG loaded pLHMGA microparticles.

Formulation	Polymer concentration (%)	Volume-average particle size (µm)	Loading efficiency (%)	Loading %
1	10	12	86	1.09
2	15	15	74	0.62
3	20	18	86	0.54
4	30	25	100	0.42

For all formulations, volume-average particle size was > 10 µm. Further, when the polymer concentration in the DCM solution was increased from 10% to 30%, the average particle size increased from 12 to 25 µm. Particle size determinations obtained by light obscuration (**Table 1**) were confirmed through SEM analysis (**Figure 1**), which also revealed that microparticles were spherical and slightly porous. IR680-IgG was encapsulated in the microparticles with high loading efficiency (~80%). The loading efficiency increased with

increasing polymer concentration in the oil phase. Formulation1, prepared with the lowest polymer concentration (10%), showed a burst IR680-IgG release of around 35% followed by sustained release of antibody up to 90% by day 7. Formulation 2 and 3 exhibited a burst release (12% and 8% respectively) and a sustained release of IR680-IgG up to 75% of the loading in 35 days. Formulation 4 prepared with the highest polymer concentration (30%), showed very low burst release (1%) and at day 35, 50% of the loaded IR680-IgG was released **(Figure 2)**. These observations are in agreement with earlier studies which showed that an increasing polymer concentration in the DCM solution and consequently a high viscosity of polymer solution resulted in an increase in both the particle size and the loading efficiency as well as retardation in release kinetics [52,53]. The burst release of IgG from the pLHMGA microparticles can be ascribed to the porosity of the microparticles. The burst release decreased with increasing polymer concentration **(Figure 2)**. The high burst release of particles of Formulation 1, can be attributed to the high surface to volume ratio of these particles and low polymer density inside the microparticles which result in fast hydration of the particles and consequently rapid diffusion of protein from water-filled pores [53]. Nevertheless all formulations showed sustained release of the IR680-IgG due to polymer degradation [37]. The characteristics of the obtained microparticles are presented in **Table 1**. Formulation 2 was chosen for further characterization because of its low burst as well as sustained release (up to 75% for 35 days *in vitro*) and relatively higher loading percentage comparing to Formulation 3 which showed similar release kinetics.

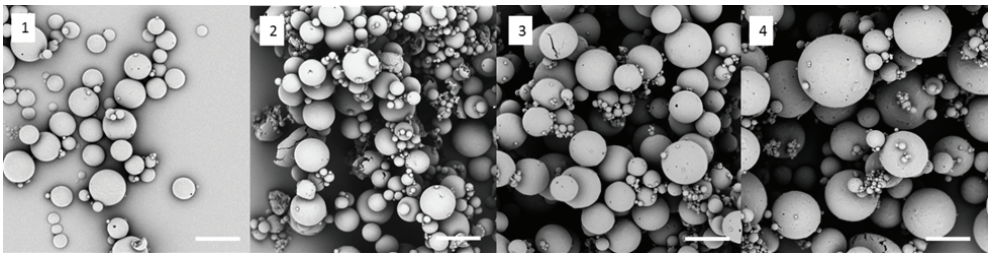

Figure 1. SEM images of the IR680-IgG microparticles. Scale bar represents 10 μm.

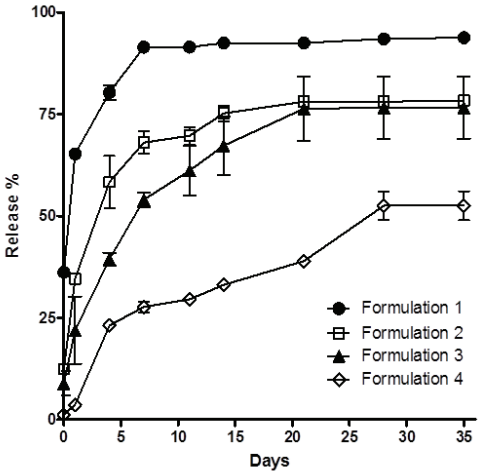

Figure 2. *In vitro* release of IR680-IgG from microparticle formulations. The characteristics of the formulations are given in Table 1. Values shown are the average ± SD of three measurements.

IR680-IgG serum levels in mice

After subcutaneous injection of equal doses of IgG whether in PBS, emulsified in IFA or encapsulated in microparticles (Formulation 2), sera of mice were collected at several time points and the antibody levels were quantified by ELISA. As depicted in **Figure 3**, subcutaneous injection of IgG dissolved in PBS resulted in high levels of serum IgG. Administration of IFA formulation resulted initially in lower concentrations than the PBS formulation but increased in time, resulting in comparable levels at day 6 post injection. Administration of IgG in microparticles was associated with at least 10 times lower serum concentrations than observed after administration of the soluble protein. This is likely due to the antibody being released locally in a controlled and sustained manner from the microparticles, reducing the risk of systemic toxicity. In the present study we were able to analyze the serum levels only for a limited time because on day 6 the levels were close to the detection limit of the ELISA assay (0.05 µg of human IgG/ml). It is therefore possible that the antibody was still released from the microparticles but it was below the detection limit.

Possible formed mice anti-human antibodies were not analyzed since **Figure 2** shows that most of the human IgG is released within the first two weeks which is too short for development of anti-human antibodies.

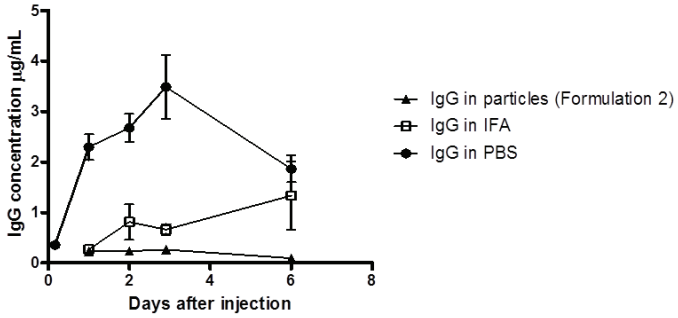

Figure 3. Antibody levels in serum after s.c. administration of 75 µg of IgG in various formulations in non-tumor-bearing mice. Samples were taken at regular intervals and the antibody levels in mice were measured by ELISA, N = 3 mice per group.

3.4. Preparation and characterization of antiCD40 and antiCTLA4 loaded microparticles

Based on the results obtained with the microparticles using the IR680-IgG as model antibody (section **3.3**), immunomodulatory antibodies were encapsulated in microparticles using polymer concentration of 15% (Formulation 2, **Table 1**). This formulation was chosen because of its low burst release, high encapsulation efficiency and sustained release of the cargo in 21 days. The characteristics of the prepared microparticles are summarized in **Table 2**. AntiCD40 and antiCTLA4 loaded microparticles were respectively around 12 and 15 µm in diameter, as measured by light obscuration. As shown by SEM, they were spherical and slightly porous (**Figure 4**). The loading efficiency of antiCD40 was 86% and of antiCTLA4, 89%. As **Figure 5** indicates, both microparticle formulations showed a 20% burst release (0.5 h) followed by sustained release, up to 80% of the loading in around 30 days. Though high burst release might be unfavorable in some sustained release formulations, the burst release observed with these formulations may be favorable in our study, achieving optimal therapeutic efficacy by providing a minimum therapeutic antibody level promptly after administration.

Table 2. Characteristics of empty, antiCD40 and antiCTLA4 loaded pLHMGA microparticles. Data shown is the result of several (8-15) pooled batches.

Microparticle formulations	Volume-average particle size (μm)	Loading efficiency (%)	Loading %
AntiCTLA4	15 ± 3	89	0.50
AntiCD40	13 ± 1	86	0.83
Empty	11 ± 4	-	-

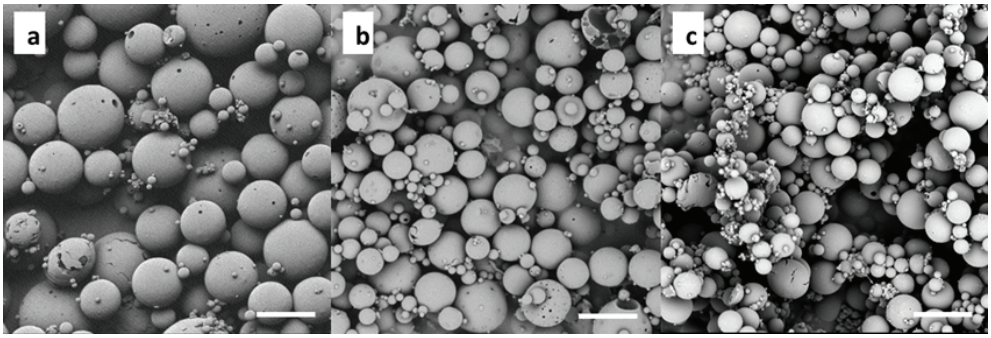

Figure 4. SEM images of the microparticles a) antiCTLA4, b) antiCD40 c) empty. Scale bar represents 10 μm.

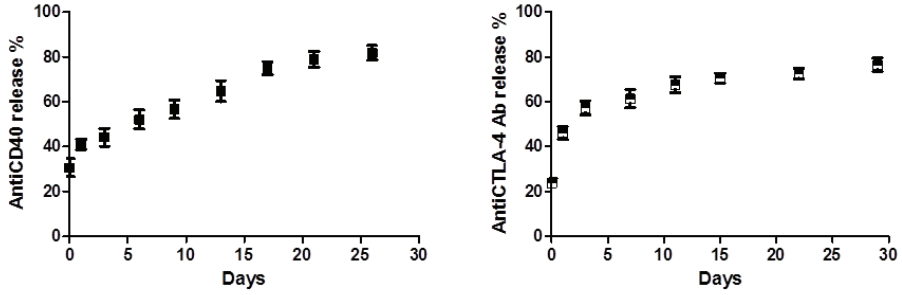

Figure 5. Sustained *in vitro* release of antibody from AntiCD40 microparticles and antiCTLA4 microparticles. Antibody-loaded microparticles were dispersed in PBS and incubated at 37°C while agitated. At various time points, samples were taken and the released antibody was measured by intrinsic fluorescence of the antibody. Mean ± SD of three measurements is presented.

3.5. Serum levels in tumor-bearing mice after treatment with antiCD40 and antiCTLA4 formulations

Sera of mice were collected at certain time points up to day 8 after administration of the immunomodulatory antibody formulations and quantified by ELISA. Following injection of antiCD40 loaded microparticles, a peak was reached in serum at day 3. Nevertheless, at all time points the level of antiCD40 antibody in the serum was lower than the antibody level detected following administration of IFA formulations. In case of antiCTLA4 microparticles, no peak was detected and antibody concentrations in blood were significantly lower (5-10 times) than the levels detected after injection of antiCTLA4 IFA formulation up to day

6 (**Figure 6**). This is in agreement with the results obtained from administration of IgG microparticles in serum (**Figure 3**), indicating that subcutaneous injection of microparticles causes low antibody serum levels and thus likely prevents systemic adverse effects. To test the hypothesis that biodegradable sustained-release formulations can be used as an alternative to IFA, we assessed the injection site of pLHMGA microparticles and IFA emulsions at the end of the experiment in mice cured of their tumor. Sixty days after administration of the different antibody formulations, mice treated with IFA had a palpable lump at the injection site, which was confirmed by post-mortem examination (**Figure 7a**). In contrast, cured mice treated with pLHMGA microparticles showed no apparent remainder of the antibody formulation (**Figure 7b**).

As mentioned in section **3.4**, these microparticles were completely degraded after 30 days *in vitro*; thus it is reasonable to assume that the same would be true 60 days following subcutaneous injection, and indeed no residues were found. These finding are in agreement with previous studies, which have shown that the microparticles based on pLHMGA with similar characteristics degrade in 30-60 days both *in vitro* [43,54] and *in vivo* [39].

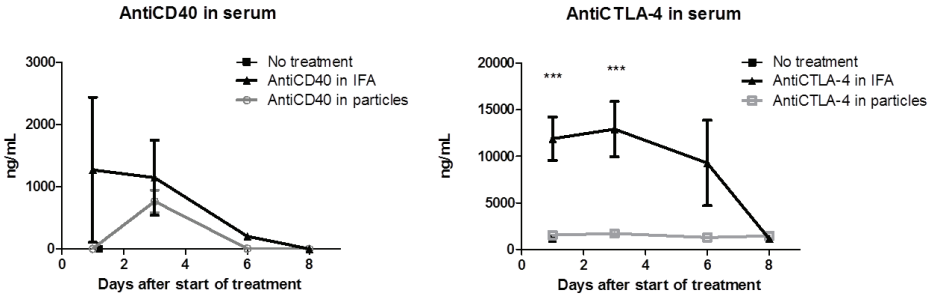

Figure 6. Antibody levels in serum after s.c. administration of various formulations in tumor-bearing mice. Samples were taken at regular intervals after treatment and the antibody levels in mice were detected by ELISA (*** $p<0.001$), N = 3 mice per group. Values shown are the average ± SD of three measurements.

3.6. Anti-tumor efficacy of antiCD40 and antiCTLA4 formulations

To evaluate the therapeutic efficacy of the microparticulate formulations, mice were inoculated with MC-38 tumor cells and the antibody treatment was started when the tumors were palpable (0.5-3 mm^3) and tumor outgrowth was monitored for 42-54 days after initiation of the treatment. Survival proportions of mice that received the different formulations are given in Kaplan-Meier plots **(Figure 8)**. The majority (about 90%) of untreated mice were sacrificed before day 30 after antibody treatment while in mice treated with antiCD40, 50% survival was observed at the end of the tumor experiment (day 54). The survival rate was comparable for both groups receiving antiCD40 encapsulated in microparticles or formulated in IFA as we have reported before [32]. A 40% survival rate was seen in mice treated with antiCTLA4 microparticles, and 30% survival was observed in mice treated with antiCTLA4 in IFA emulsion. Here again the therapeutic efficacy of microparticles and IFA formulation were comparable [31]. Treatment with empty microparticles showed no effect on tumor outgrowth and the survival of the mice treated with these microparticles was comparable with that of untreated mice **(Supplementary Figure S3)**. This supports earlier studies which have shown the advantages of local and sustained delivery of antiCD40 and antiCTLA4 as well as other immunomodulatory molecules in cancer treatment in comparison with systemic administration [31,32,55]. It has been shown that low doses of immunomodulatory antibodies are capable of inducing CD8+ T cell immune responses that

are as effective as systemic high doses without leading to the adverse effects associated with high antibody serum levels, such as autoimmune and inflammatory conditions. Therefore, local delivery of these antibodies is plausible and sustained-release formulations were developed to provide sustained delivery of the antibodies locally where they are needed [56]. IFA and similar vehicles have been widely used in preclinical studies as well as in clinical trials [57]. Though these vehicles differ in characteristics, they are used to formulate an emulsion (w/o in case of IFA and Montanide, or o/w in case of MF-59) containing the immunotherapeutic agent. This emulsion forms a depot and provides sustained release of the cargo. The challenges that emerge from using these formulations are the local and systemic adverse effects associated with the IFA formulations (as well as Montanide ISA 51) [58]. Alternatively, dextran microparticles containing antiCD40 have been used for this purpose in a preclinical study. These particles were successful in providing a sustained antibody release *in vitro* and *in vivo*, although they caused increased tumor outgrowth and local inflammation as well as ulcerating subcutaneous swelling [59]. Importantly, as the present study shows, pLHMGA microparticles loaded with antiCD40 or antiCTLA4 can result in efficient antitumor efficacy in a therapeutic setting in tumor-bearing mice comparable to IFA formulation but without causing adverse effects. This was expected because microparticles showed low antibody serum levels at early and late time points following administration in mice.

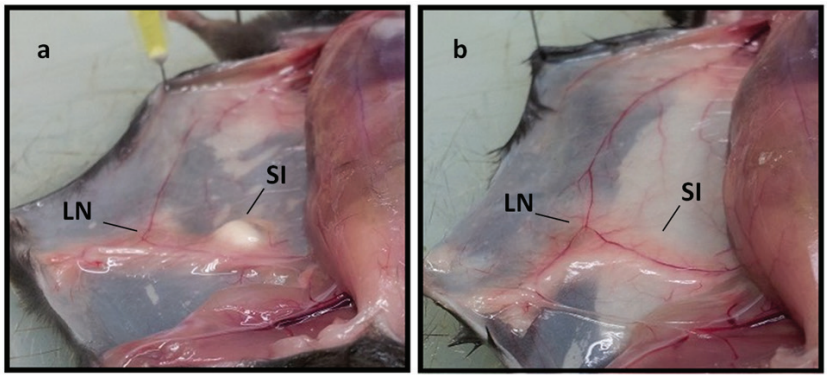

Figure 7. Post mortem examination of mice two months after treatment with immunomodulatory antibodies formulated in a) IFA or b) microparticles. LN: inguinal lymph node. SI: site of injection, Representative images of N = 4 mice per group injections.

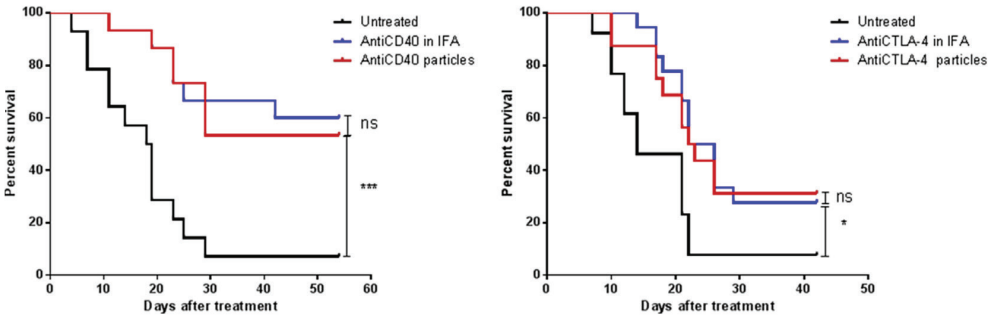

Figure 8. Kaplan-Meier plot presenting the survival proportions of MC-38 tumor bearing-mice treated with different formulations containing antiCD40 or antiCTLA4. Pooled data from two experiments (N = 14-18 mice) are shown.

4. Conclusion

This study shows that polymeric microparticles based on pLHMGA are capable of providing sustained delivery of encapsulated antibodies, and when administered locally and close to the tumor microenvironment, exhibit equal and efficient therapeutic efficacy as compared to IFA formulations. These biodegradable particles importantly display no local adverse effects. Moreover, low antibody serum levels at different time points suggest a strong limitation of systemic adverse effects. In conclusion, pLHMGA microparticles are attractive systems for local and sustained delivery of biotherapeutics.

Acknowledgements

This research was conducted within the framework of the Cancer Vaccine Tracking project (#03O-302), Center for Translational Molecular Medicine (CTMM).

Appendix. Supplementary data

References

[1] Couzin-Frankel J. Breakthrough of the year 2013. Cancer immunotherapy. Science 2013;342:1432-1433.
[2] Weir GM, Liwski RS, Mansour M. Immune modulation by chemotherapy or immunotherapy to enhance cancer vaccines. Cancers 2011;3:3114-3142.
[3] Dimberu PM, Leonhardt RM. Cancer immunotherapy takes a multi-faceted approach to kick the immune system into gear. Yale J Biol Med 2011;84:371-80.
[4] Vatsan RS, Bross PF, Liu K, Theoret M, De Claro AR, Lu J, et al. Regulation of immunotherapeutic products for cancer and FDA's role in product development and clinical evaluation. J Immunother Cancer 2013;1:5-5.
[5] Scott AM, Wolchok JD, Old LJ. Antibody therapy of cancer. Nat Rev Cancer 2012;12:278-287.
[6] Weiner LM, Surana R, Wang S. Monoclonal antibodies: versatile platforms for cancer immunotherapy. Nat Rev Immunol 2010;10:317-327.
[7] Peggs KS, Quezada SA, Allison JP. Cancer immunotherapy: co-stimulatory agonists and co-inhibitory antagonists. Clin Exp Immunol 2009;157:9-19.
[8] Korman AJ, Peggs KS, Allison JP. Checkpoint blockade in cancer immunotherapy. Adv Immunol 2006;90:297-339.
[9] Pardoll DM. The blockade of immune checkpoints in cancer immunotherapy. Nat Rev Cancer 2012;12:252-264.
[10] Brahmer JR, Pardoll DM. Immune checkpoint inhibitors: making immunotherapy a reality for the treatment of lung cancer. Cancer Immunol Res 2013;1:85-91.
[11] Todryk S, Tutt A, Green M, Smallwood J, Halanek N, Dalgleish A, et al. CD40 ligation for immunotherapy of solid tumours. J Immunol Methods 2001;248:139-147.
[12] Rudd CE. The reverse stop-signal model for CTLA4 function. Nat Rev Immunol 2008;8:153-160.
[13] Krummel MF, Allison JP. CD28 and CTLA-4 have opposing effects on the response of t-cells to stimulation. J Exp Med 1995;182:459-465.
[14] Ascierto PA, Marincola FM, Ribas A. Anti-CTLA4 monoclonal antibodies: the past and the future in clinical application. J Transl Med 2011;9:196-5876-9-196.
[15] Egen JG, Kuhns MS, Allison JP. CTLA-4: new insights into its biological function and use in tumor immunotherapy. Nat Immunol 2002;3:611-618.
[16] Quezada SA, Peggs KS, Simpson TR, Allison JP. Shifting the equilibrium in cancer immunoediting: from tumor tolerance to eradication. Immunol Rev 2011;241:104-118.
[17] Sandin LC, Eriksson F, Ellmark P, Loskog ASI, Totterman TH, Mangsbo SM. Local CTLA4 blockade effectively restrains experimental pancreatic adenocarcinoma growth in vivo. Oncoimmunol 2014;3:e27614.
[18] Grosso JF, Jure-Kunkel MN. CTLA-4 blockade in tumor models: an overview of preclinical and translational research. Cancer Immunity 2013;13:5.
[19] Camacho LH. Novel therapies targeting the immune system: CTLA4 blockade with tremelimumab (CP-675,206), a fully human monoclonal antibody. Exp Opin Investig Drugs 2008;17:371-385.
[20] Lens M, Ferrucci PF, Testori A. Anti-CTLA4 monoclonal antibody ipilimumab in the treatment of metastatic melanoma: Recent findings. Recent Pat Anticancer Drug Discov 2008;3:105-113.
[21] Morel Y, Truneh A, Sweet R, Olive D, Costello R. The TNF superfamily members LIGHT and CD154 (CD40 ligand) costimulate induction of dendritic cell maturation and elicit specific CTL activity. J Immunol 2001;167:2479-2486.
[22] van Mierlo G, den Boer A, Medema J, van der Voort E, Fransen M, Offringa R, et al. CD40 stimulation leads to effective therapy of CD40(-)tumors through induction of strong systemic cytotoxic T lymphocyte immunity. Proc Natl Acad Sci USA 2002;99:5561-5566.
[23] Schoenberger S, Toes R, van der Voort E, Offringa R, Melief C. T-cell help for cytotoxic T lymphocytes is mediated by CD40-CD40L interactions. Nature 1998;393:480-483.
[24] Vonderheide RH, Flaherty KT, Khalil M, Stumacher MS, Bajor DL, Hutnick NA, et al. Clinical activity and immune modulation in cancer patients treated with CP-870,893, a novel CD40 agonist monoclonal antibody. J Clin Oncol 2007;25:876-883.
[25] Attia P, Phan G, Maker A, Robinson M, Quezado M, Yang J, et al. Autoimmunity correlates with tumor regression in patients with metastatic melanoma treated with anti-cytotoxic T-lymphocyte antigen-4. J Clin Oncol 2005;23:6043-6053.
[26] Fransen MF, Arens R, Melief CJM. Local targets for immune therapy to cancer: Tumor draining lymph nodes and tumor microenvironment. Int J Cancer 2013;132:1971-1976.
[27] Vonderheide RH, Glennie MJ. Agonistic CD40 antibodies and cancer therapy. Clin Cancer Res 2013;19:1035-1043.
[28] Maker A, Yang J, Sherry R, Topalian S, Kannula U, Royal R, et al. Intrapatient dose escalation of anti-CTLA-4 antibody in patients with metastatic melanoma. J Immunother 2006;29:455-463.
[29] Baldo BA. Adverse events to monoclonal antibodies used for cancer therapy Focus on hypersensitivity responses. Oncoimmunol 2013;2.
[30] Sanderson K, Scotland R, Lee P, Liu D, Groshen S, Snively J, et al. Autoimmunity in a phase I trial of a fully human anti-cytotoxic T-lymphocyte antigen-4 monoclonal antibody with multiple melanoma peptides and

montanide ISA 51 for patients with resected stages III and IV melanoma. J Clin Oncol 2005;23:741-750.
[31] Fransen MF, van der Sluis TC, Ossendorp F, Arens R, Melief CJM. Controlled local delivery of CTLA-4 blocking antibody induces cd8(+) t-cell-dependent tumor eradication and decreases risk of toxic side effects. Clin Cancer Res 2013;19:5381-5389.
[32] Fransen MF, Sluijter M, Morreau H, Arens R, Melief CJ. Local activation of CD8 T cells and systemic tumor eradication without toxicity via slow release and local delivery of agonistic CD40 antibody. Clin Cancer Res 2011;17:2270-2280.
[33] Aucouturier J, Ascarateil S, O'Neill S. A review of some cancer clinical trials with montanide ISA 51 vaccine adjuvant. J Immunother 2003;26:S45-S46.
[34] Graham BS, McElrath MJ, Keefer MC, Rybczyk K, Berger D, Weinhold KJ, et al. Immunization with cocktail of HIV-derived peptides in montanide ISA-51 is immunogenic, but causes sterile abscesses and unacceptable reactogenicity. PLoS One 2010;5:e11995.
[35] Ghassemi AH, van Steenbergen MJ, Barendregt A, Talsma H, Kok RJ, van Nostrum CF, et al. Controlled release of octreotide and assessment of peptide acylation from poly(d,l-lactide-co-hydroxymethyl glycolide) compared to plga microspheres. Pharm Res 2012;29:110-120.
[36] Liu Y, Ghassemi AH, Hennink WE, Schwendeman SP. The microclimate pH in poly(D,L-lactide-co-hydroxymethyl glycolide) microspheres during biodegradation. Biomaterials 2012;33:7584-7593.
[37] Ghassemi AH, van Steenbergen MJ, Talsma H, van Nostrum CF, Jiskoot W, Crommelin DJA, et al. Preparation and characterization of protein loaded microspheres based on a hydroxylated aliphatic polyester, poly (lactic-co-hydroxymethyl glycolic acid). J Control Release 2009;138:57-63.
[38] Samadi N, van Nostrum CF, Vermonden T, Amidi M, Hennink WE. Mechanistic studies on the degradation and protein release characteristics of poly(lactic-co-glycolic-co-hydroxymethylglycolic acid) nanospheres. Biomacromolecules 2013;14:1044-1053.
[39] Kazazi-Hyseni F, Zandstra J, Popa E, Goldschmeding R, Lathuile A, Veldhuis G, et al. Biocompatibility of poly(d,l-lactic-co-hydroxymethyl glycolic acid) microspheres after subcutaneous and subcapsular renal injection. Int J Pharm 2015 In Press.
[40] Rahimian S, Kleinovink JW, Fransen MF, Mezzanotte L, Gold H, Wisse P, et al. Near-infrared labeled, ovalbumin loaded polymeric nanoparticles based on a hydrophilic polyester as model vaccine: In vivo tracking and evaluation of antigen-specific CD8+ T cell immune response. Biomaterials 2015;37: 469-477.
[41] Doshi N, Mitragotri S. Macrophages recognize size and shape of their targets. PloS One 2010;5:e10051.
[42] Leemhuis M, van Nostrum C, Kruijtzer J, Zhong Z, ten Breteler M, Dijkstra P, et al. Functionalized poly(alpha-hydroxy acid)s via ring-opening polymerization: Toward hydrophilic polyesters with pendant hydroxyl groups. Macromolecules 2006;39:3500-3508.
[43] Ghassemi AH, van Steenbergen MJ, Talsma H, van Nostrum CF, Crommelin DJA, Hennink WE. Hydrophilic polyester microspheres: effect of molecular weight and copolymer composition on release of BSA. Pharm Res 2010;27:2008-2017.
[44] Sah H. A new strategy to determine the actual protein content of poly(lactide-co-glycolide) microspheres. J Pharm Sci 1997;86:1315-1318.
[45] Rolink A, Melchers F, Andersson J. The SCID but not the RAG-2 gene product is required for S mu-S epsilon heavy chain class switching. Immunity 1996;5:319-330.
[46] Clarke P, Mann J, Simpson JF, Rickard-Dickson K, Primus FJ. Mice transgenic for human carcinoembryonic antigen as a model for immunotherapy. Cancer Res 1998;58:1469-1477.
[47] Champion JA, Walker A, Mitragotri S. Role of particle size in phagocytosis of polymeric microspheres. Pharm Res 2008;25:1815-1821.
[48] Giteau A, Venier-Julienne MC, Aubert-Pouessel A, Benoit JP. How to achieve sustained and complete protein release from PLGA-based microparticles? Int J Pharm 2008;350:14-26.
[49] Sinha V, Trehan A. Biodegradable microspheres for protein delivery. J Control Release 2003;90:261-280.
[50] Allison SD. Analysis of initial burst in PLGA microparticles. Exp Opin Drug Deliv 2008;5:615-628.
[51] Huang X, Brazel CS. On the importance and mechanisms of burst release in matrix-controlled drug delivery systems. J Control Release 2001;73:121-136.
[52] Yang Y, Chung T, Bai X, Chan W. Effect of preparation conditions on morphology and release profiles of biodegradable polymeric microspheres containing protein fabricated by double-emulsion method. Chem Eng Science 2000;55:2223-2236.
[53] Yang Y, Chung T, Ping Ng N. Morphology, drug distribution, and in vitro release profiles of biodegradable polymeric microspheres containing protein fabricated by double-emulsion solvent extraction/evaporation method. Biomaterials 2001;22:231-241.
[54] Leemhuis M, Kruijtzer JAW, van Nostrurn CF, Hennink WE. In vitro hydrolytic degradation of hydroxyl-functionalized poly(alpha-hydroxy acid)s. Biomacromolecules 2007;8:2943-2949.
[55] Sharon E, Streicher H, Goncalves P, Chen HX. Immune checkpoints in cancer clinical trials. Chin J Cancer 2014;33:434-444.
[56] Fransen MF, Ossendorp F, Arens R, Melief CJM. Local immunomodulation for cancer therapy Providing treatment where needed. Oncoimmunol 2013;2:e26493.
[57] Aucouturier J, Ascarateil S, Dupuis L. The use of oil adjuvants in therapeutic vaccines. Vaccine 2006;24 Suppl 2:S2-44-5.

[58] Alving CR. Design and selection of vaccine adjuvants: animal models and human trials. Vaccine 2002;20 Suppl 3:S56-64.
[59] Fransen MF, Cordfunke RA, Sluijter M, van Steenbergen MJ, Drijfhout JW, Ossendorp F, et al. Effectiveness of slow-release systems in CD40 agonistic antibody immunotherapy of cancer. Vaccine 2014;32:1654-1660.

Appendix
Supplementary data

Synthesis of copolymers of 3S-(benzyloxymethyl)-6S-methyl-1,4-dioxane-2,5-dione with D,L-lactide (pLHMGA)

3S-(benzyloxymethyl)-6S-methyl-1,4-dioxane-2,5-dione (benzyloxymethyl-methylglycolide) (BMMG) was synthesized as described before [1]. A copolymer of D,L-lactide and BMMG (50:50 molar ratio) was synthesized via ring opening polymeriztion at 130°C using benzyl alcohol as initiator with a 100/1 monomer-to-initiator molar ratio and $Sn(Oct)_2$ as catalyst **(Figure S1)**. In a typical procedure, vacuum dried monomers (BMMG (2840 mg, 11.35 mmol) and D,L-lactide (1630 mg, 11.35 mmol)) were introduced into a dry schlenk tube under a nitrogen atmosphere. Next, benzyl alcohol (24.5 mg, 0.226 mmol; 223.1 µL from a 109.8 mg/mL stock solution in toluene) and $Sn(Oct)_2$ (45.9 mg, 0.113 mmol; 409.8 µL from a 112 mg/mL stock solution in toluene) were added. Toluene was evaporated under vacuum for 2 hours, the tube was closed and immersed into a preheated 130°C oil bath for 16 h while stirring. Next, the obtained polymer was dissolved in 10 mL chloroform and subsequently precipitated in 500 mL cold methanol to remove the unreacted monomers and to precipitate the polymer, which was collected by filtration and vacuum dried to yield 4.5 g (93%) poly (D,L-lactic-co-benzyloxymethylglycolic acid) (pLBMGA). Subsequently, pLBMGA was dissolved in 500 mL THF, and 5 g of 10 % w/w Pd/C catalyst was added. The flask was filled with hydrogen in three consecutive steps of subsequent evacuation and refilling with H_2 and the reaction mixture was stirred for 16 hours under a H_2 pressure. Next, Pd/C was removed using a glass filter and THF was removed by evaporation (Yield 90%).

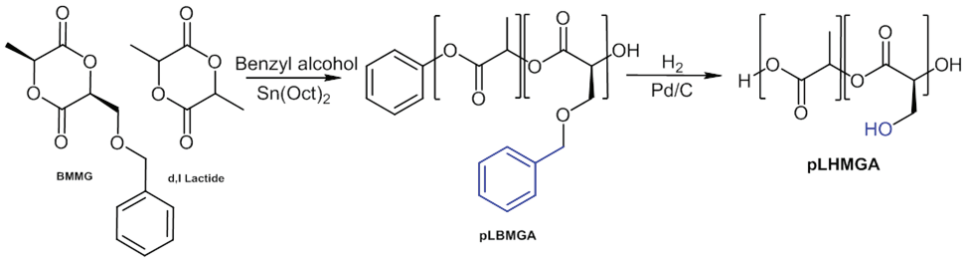

Figure S1. Synthesis of pLHMGA

The structure of the polymer was confirmed by ^{1}H NMR spectroscopy and the ratio between the monomers (BMMG/D,L lactide) was calculated to be 46/54, closely matching the feed ratio. Next, the benzyl groups in pLBMGA were removed by hydrogenation in an overnight reaction with H_2, to yield pLHMGA. The structure of pLHMGA and removal of protective benzyl groups were validated by ^{1}H NMR spectroscopy. Random structure in pLBMGA and pLHMGA was confirmed by DSC. Both polymers were amorphous, with a T_g value of 36°C and 52°C, respectively, similar to values reported earlier [2]. The molecular weight of the synthesized polymers was analyzed by GPC, the number average molecular weight of pLHMGA was 10.2 kDa and the PDI was 1.75 which verified that there were no chain sessions in the hydrogenation step. The characteristics of the obtained polymers are summarized in **Table S1**.

Table S1. Characteristics of synthesized polymers.

pLBMGA							pLHMGA					
Monomer/ initiator Molar ratio	BMMG/ D,L-lactide molar ratio in feed	NMR	GPC		DSC	Yield (%)	Target M_n (kDa)	NMR	GPC		DSC	Yield (%)
		BMMG/ D,L-lactide molar ratio	M_n (kDa)	PDI	T_g (°C)			HMG*/ D,L-lactide molar ratio	M_n (kDa)	PDI	T_g (°C)	
100	50/50	46/54	14.3	1.89	36	93	14.8	48/52	10.2	1.75	52	90

* HMG: Hydroxymethylglycolide; BMMG after removal of benzyl groups.

Characterization of IR680-IgG

IR680-IgG was characterized by gel permeation chromatography (GPC) using a Waters UPLC Acquity system equipped with a fluorescence detector. Two channels were used: channel 1 for detection of the protein (excitation at 280 nm and emission at 340 nm) and channel 2 for detection of the IR680 signal (excitation at 672 nm and emission at 694 nm). Seven and a half µL of IR680-IgG (10 µg/mL in PBS) was injected onto a BEH450 SEC 2.5 µm column (Waters, USA). PBS was used as elution buffer and the flow rate was set at 0.25 mL/min. To calculate the dye/IgG molar ratio, the UV spectrum of the freeze-dried labeled IgG was recorded (Shimadzu 2450, Japan) and the absorbance values at 280 nm (A280) and 672 nm (A672) were used to calculate the degree of conjugation according to the following formula:

$$\frac{\text{Dye}}{\text{IgG}} = \left[\!\left[\frac{A_{672}}{\varepsilon_{\text{Dye}}}\right]\!\right] \div \left[\!\left[\frac{A_{280} - 0.07 \times A_{672}}{\varepsilon_{\text{IgG}}}\right]\!\right]$$

Dye/IgG is the molar ratio of IR680 to IgG and the molar extinction coefficient of IR680 (εDye) is 165,000 M^{-1} cm^{-1} and the molar extinction coefficient of IgG (εIgG) is 210,000 M^{-1} cm^{-1}(according to the manufacturer)) .

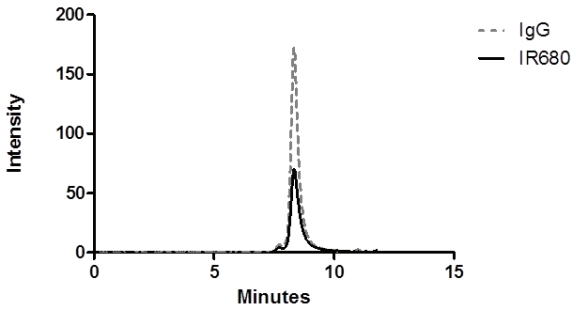

Figure S2. GPC chromatogram of IR680-IgG after purification with a Zeba spin column (see section 2.3).

Effect of administration of empty particles on survival of MC-38 tumor-bearing mice

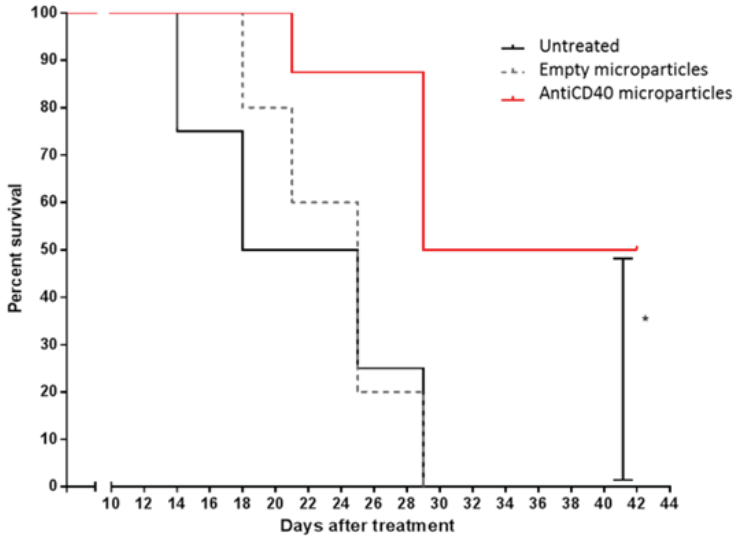

Figure S3. Kaplan-Meier plot presenting the survival proportions of MC-38 tumor bearing-mice treated with empty versus antiCD40-loaded microparticles. N = 4-8 mice per group, * = $p < 0.05$.

References

[1] Leemhuis M, van Nostrum C, Kruijtzer J, Zhong Z, ten Breteler M, Dijkstra P, et al. Functionalized poly(alpha-hydroxy acid)s via ring-opening polymerization: Toward hydrophilic polyesters with pendant hydroxyl groups. Macromolecules 2006;39:3500-3508.

[2] Ghassemi AH, van Steenbergen MJ, Talsma H, van Nostrum CF, Jiskoot W, Crommelin DJA, et al. Preparation and characterization of protein loaded microspheres based on a hydroxylated aliphatic polyester, poly (lactic-co-hydroxymethyl glycolic acid). J Control Release 2009;138:57-63.

CHAPTER 6

Effect of particle size on internalization of pLHMGA particles by dendritic cells: An introductory study

Sima Rahimian

Dandan Li

Bo Lou

Dusan Popov-Celeketic

Rachid El Khoulati

Joep van den Dikkenberg

Sabrina Oliveira

Maryam Amidi

Ferry Ossendorp

Wim E. Hennink

Abstract

The efficiency of a vaccine largely relies on its effective targeting to the antigen presenting cells (APCs), particularly to dendritic cells (DCs) as the most professional APCs. Additionally, the vaccine should provide continuous delivery of antigens to achieve a strong immune response. To achieve this, various strategies have focused on encapsulation of antigens in particulate delivery systems. To evaluate the effect of particle size on internalization of particles *in vitro*, biodegradable nanoparticles (average size 300 nm) and microparticles (size 1 and 2 μm) based on a hydrophilic polyester, poly(lactic-co-hydroxymethylglycolic acid) (pLHMGA) were prepared. These particles were compared for their ability to deliver a fluorescently labeled model antigen (Alexa488-ovalbumin) to murine dendritic cells *in vitro*. Flow cytometry studies revealed that nanoparticles showed higher cell binding and uptake upon incubation with DCs than microparticles. Co-localization studies using confocal laser scanning microscopy showed that upon incubation of DCs with nanoparticles, ovalbumin was released in the cytosol after 24 hours while microparticles mainly co-localized with the lysosomes. Our hypothesis is that in case of nanoparticles, the presence of ovalbumin in the cytosol suggests that the antigen can be cross-presented via MHC class I molecules to CD8+ T cells, to induce a cellular immune response. For cancer immunotherapy, cellular T cell responses are particularly desired. On the other hand, co-localization of microparticles with lysosomes can result in MHC class II antigen presentation and as a consequence in a weak cellular immune response. This introductory study shows the potential of pLHMGA particles for antigen delivery and suggests that future studies should focus on comparison of these particles *in vitro* and *in vivo* for their ability to present the antigen and induce antigen-specific immune responses.

Keywords: Particle uptake, pLHMGA, Dendritic cells, Microparticles, Nanoparticles

1. Introduction

Efficient antigen presentation is one of the key initial steps in achieving an effective immune response. Antigen presenting cells (APCs) have an important role in mediating between the innate and adaptive immune system. Dendritic cells (DCs), as the most professional APCs, are the primary targets of vaccine formulations [1]. Immature DCs constantly sample their environment for self- and foreign antigens including soluble antigens, particulate antigens as well as apoptotic cells which are internalized via several mechanisms. Antigen uptake and processing in the presence of co-stimulatory signals and cytokines result in maturation of DCs. Mature DCs subsequently migrate to the draining lymph nodes where the naïve T cells reside. The processed antigen is presented to CD8+ and CD4+ T cells through MHC class I and class II molecules, respectively, to establish an antigen-specific immune response [2]. Because of the essential role of DCs in the initiation of the immune response, many studies have focused on optimization of strategies to deliver vaccines by targeting DCs [3,4]. Particulate vaccine delivery systems have been developed to face the weak immunogenicity of soluble protein antigens [5-7]. Particles are internalized more efficiently and are able to promote/enhance antigen presentation via major histocompatibility complex (MHC) class I (also known as cross-presentation) which is essential for initiation of a T cell mediated immune response especially to fight cancer and viral infections [8]. Particles based on aliphatic polyesters such as poly(lactic-co-glycolic acid)(pLGA) are commonly used for delivery of different types of antigens such as proteins, peptides and nucleic acids with promising results *in vivo* [9]. However, there are some challenges facing the delivery systems based on pLGA as antigen delivery systems. Accumulation of acidic products of pLGA degradation (lactic acid and glycolic acid and their soluble oligomers) in the particles results in denaturation and aggregation of the loaded peptide/protein [10]. Additionally, peptides/proteins encapsulated in pLGA particles are susceptible to chemical modifications such as acylation [11]. These issues eventually result in incomplete release of the cargo from the particles, and immunogenicity against the loaded peptide/protein and other adverse reactions. In order to overcome these drawbacks, hydrophilic polyesters such as poly(lactic-co-hydroxymethyl glycolic acid) (pLHMGA) (**Figure 1**) have been developed [12].

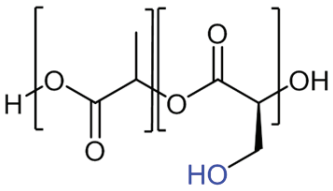

Figure 1. Structure of pLHMGA

During degradation, no pH drop was observed inside the particles which protected the cargo against denaturation and chemical modifications [13,14]. Importantly, these polymers have shown good biocompatibility *in vitro* and *in vivo* upon subcutaneous injection [15]. pLHMGA NPs have been recently used as antigen delivery systems with ovalbumin as the model antigen. These particles drained to lymph nodes and efficiently presented the antigen both *in vitro* and *in vivo* [16]. In another study, pLHMGA NPs were used as a therapeutic cancer vaccine encapsulating human papilloma virus synthetic long peptide as antigen. These particles could significantly prolong the survival of TC1 tumor-bearing mice [17]. In vaccine delivery, the challenge is to develop a vehicle with optimal size that efficiently targets the antigen presenting cells and provides controlled and sustained intracellular release of the

antigen. Studies suggest that the size of the particles affects the mechanism via which DCs process the antigen, which in turn affects the immunological outcome of the antigen [18]. Therefore, it is of great interest to study the uptake and internalization of antigen-loaded particles with different sizes by the DCs, to design optimal vaccine delivery systems. In this study, pLHMGA was used for encapsulation of a fluorescently labeled model antigen ovalbumin (Alexa488-OVA) and nano- and microparticles with different sizes were prepared and compared *in vitro* in terms of binding and internalization, as well as localization in the DCs.

2. Materials and Methods

2.1. Materials

Poly(d,l lactic-co-hydroxymethyl glycolic acid) (pLHMGA) with a copolymer ratio of 65/35 (d,l lactide/benzyloxy methyl methylglycolide (BMMG)) was synthesized and characterized as described before [12]. Hexyn-poly d,l lactic acid (hexyn-pDLLA) was synthesized and diSulfo-Cy5 azide dye (Cyandye, USA) was coupled to this polymer as previously described [16]. Alexa488-OVA and Lysotracker red DND-99 were obtained from Molecular Probes, Life Technologies USA. Ovalbumin (Low endo) was purchased from Worthington, USA.3-(4,5-Dimethylthiazol-2-yl)-5-(3-carboxymethoxyphenyl)-2-(4-sulfophenyl)-2H-tetrazolium) (MTS) was purchased from Promega, USA. Polyvinyl alcohol (PVA; Mw 30000-70000; 88% hydrolyzed), 4-(2-hydroxyethyl)piperazine-1-ethanesulfonic acid (HEPES) and 2-(4-amidinophenyl)-6-indolecarbamidine dihydrochloride (DAPI), paraformaldehyde (PFA) were obtained from Sigma-Aldrich, USA. Dichloromethane (DCM) was purchased from Biosolve, the Netherlands. Bicinchoninic acid assay (Micro BCA) reagents were obtained from Thermo Scientific Fischer, USA. Pyrogen-free water was purchased from Carl Roth, Germany. Phosphate buffered saline (1.8 mM NaH_2PO_4, 8.7 mM Na_2HPO_4, 163.9 mM Na^+, 140.3 mM Cl^-) (PBS) was obtained from B Braun, Germany. Chemicals were used as received without further purification, unless otherwise stated.

2.2. Preparation of the particles

OVA-loaded nano- and microparticles were prepared by a double emulsion- solvent evaporation technique as described before [16]. Preparation of particles was optimized in order to achieve three distinct sizes of nano- and microparticles.

Nanoparticles

Fifty µL of OVA 10 mg/mL (containing 30% Alexa488 OVA) in pyrogen-free water was emulsified in 1 mL pLHMGA 5% w/v in DCM for 30 s (Labsonic P, B. Braun Biotech, Germany, 20% amplitude) followed by sonication of this first emulsion in 2 mL PVA 1% in pyrogen-free water for 30 s. Next, the obtained double emulsion was transferred into 25 mL PVA 0.3% in pyrogen-free water and stirred for 2 h. After evaporation of DCM, the particles were harvested by centrifugation (20,000 g, 30 minutes) and washed with PBS and subsequently with pyrogen free water and freeze-dried overnight.

Microparticles

For preparation of 2 µm particles, 100 µL of 10 mg/mL OVA (containing 30% Alexa488-OVA) in pyrogen-free water was emulsified in 1 ml of solution of 10% pLHMGA in DCM using a homogenizer (IKA® T10 basic Ultra-Turrax, Germany) at 30,000 rpm for 60 s. This primary emulsion was subsequently emulsified in 10 mL of PVA 2.5% to form the double emulsion. After evaporation of DCM, the particle suspension was centrifuged at 3000 g for 3 minutes and the pellet washed with PBS and subsequently with pyrogen-free water and freeze-dried overnight.

One µm particles were prepared using 5% pLHMGA in DCM and the primary emulsion was prepared by addition of 50 µL of 10 mg/mL OVA (containing 30% Alexa488-OVA) in pyrogen-free water and mixing with ultra-turrax at 30,000 rpm for 60 s. To this first emulsion, 1 mL of PVA 1% in pyrogen free water was added and the double emulsion was prepared by mixing at 30,000 rpm for another 60 s. The double emulsion was subsequently transferred into 5 mL of PVA 0.5% in NaCl 0.9% and after evaporation of DCM, centrifugation was done at 5000 g for 3 minutes and the pellet was washed similarly as described for the other particles and freeze-dried overnight.
Dual labeled NPs and MPs were prepared using the same method by addition of 1% w/w of Cy5-pDLLA (from a 10 mg/mL polymer solution in DCM) to the pLHMGA.

2.3. Characterization of the particles

2.3.1. Size, zeta potential and morphology of the particles

Dynamic light scattering

The size of nanoparticles was measured with dynamic light scattering (DLS) on an ALV CGS-3 system (Malvern Instruments, Malvern, UK) equipped with a JDS Uniphase 22 mW He-Ne laser operating at 632.8 nm, an optical fiber-based detector, and a digital LV/LSE-5003 correlator. Freeze-dried nanoparticles were suspended in deionized water (RI = 1.332 and viscosity 0.8898 cP) and measurements were done at 25°C at an angle of 90°.

Light obscuration particle counter

The average size and size distribution of the freeze-dried microparticles were measured using a light obscuration particle counter (Accusizer 780, USA).

Zeta potential

The zeta-potential (ζ) of the particles was measured using a Malvern Zetasizer Nano-Z (Malvern Instruments, Malvern, UK) with disposable folded capillary cells. Freeze-dried particles were dispersed in 10 mM HEPES pH 7.0 and zeta potential was measured at 25°C and analyzed using DTS Nano 4.20 software.

Scanning electron microscopy (SEM)

The morphology of the particles was studied by SEM (FEI, XL30SFEG, USA for nanoparticles and Phenom, FEI, USA for microparticles). Freeze-dried particles were transferred onto 12-mm diameter aluminum specimen stubs (Agar Scientific Ltd., England) using double-sided adhesive tape and were coated with 6 nm platinum prior to analysis.

2.3.2. Loading efficiency and loading percentage in the particles

The OVA loading efficiency of the microparticles was determined indirectly by measuring the non-encapsulated OVA in the external water phase and washing liquids. Calibration was done using 2-40 µg/mL of OVA in PVA and in water. Loading efficiency (LE%) is defined as the amount of OVA encapsulated in the NPs divided by the amount of protein added × 100%. Loading percentage (L%) is reported as the amount of OVA entrapped in the particles per total dry mass of the NPs × 100%.

2.3.3. Experimental cell lines

D1 cells are GM-CSF dependent immature dendritic cell line derived from spleen of WT C57BL/6 (H-2b) mice [19]. Cells were cultured in Iscove's Modified Dulbecco's Medium (IMDM, Lonza) containing 8% fetal calf serum (FCS, Greiner), supplemented with 2 mM GlutaMax (Gibco) and 80 IU/mL sodium-penicillin G (Astellas, the Netherlands) for D1 cells, or supplemented with 100 IU/mL penicillin/streptomycin (Gibco), 2 mM glutamin (Gibco),

25 mM 2-mercaptoethanol.

2.3.4. Cytocompatibility (MTS assay)

CellTiter 96W AQueous Non-Radioactive Cell Proliferation Assay (Promega) was used to assess the cytocompatibility of Alexa488-OVA labeled and dual labeled particles. D1 cells were seeded into a 96-well plate at a density of 10^4 cell/well (100 µL in each well). Cells were allowed to attach by incubation in a CO_2 incubator at 37°C overnight. Various formulations were added to the cells in triplicate with concentrations ranging from 7.8 to 500 µg/mL of particles. The cells were incubated for 24 h. Then, 20 µL of MTS reagent (combined MTS/PMS solution at a ratio of 20 to 1- reagents provided in the assay kit) was added to each well and incubated for 2 h at 37°C in the cell incubator. Finally, the absorbance at 490 nm was measured using a microplate reader (Formazan bio-reduction by live cells).

2.3.5. *In vitro* binding and internalization study

D1 cells were plated at a density of 10^5 cells per well in 96-well plates and grown overnight. The cells were incubated for different time points with Alexa488-OVA particles at a concentration of 100 µg/mL of particles at 4°C (for binding assay) or at 37°C (for binding and internalization assay). Soluble OVA (containing 30% Alexa488-OVA) was used as control. After incubation, the cells were washed thrice with cold medium and once with PBS to remove unbound particles. Samples were analyzed by a FACScalibur (Becton Dickinson, USA). A minimum of 10,000 events was collected and the data were analyzed by Cell Quest Pro analysis software (Becton Dickinson) by gating on the live cell populations. For technical reasons, Alexa488-OVA (single-labeled) particles were used for flow cytometry studies.

2.3.6.Confocal microscopy analysis of internalization and intracellular distribution of particles

D1 cells were plated at a density of 50,000 per dish in a Fluorodish (tissue culture dish with a 10 mm glass coverslip (WPI, USA)) and were incubated overnight. Dual labeled nano- and 2 µm microparticles were added to the cells at a final concentration of 20 µg/mL and incubated for different times. Next, cells were washed 2 times with cold PBS and fixed in PFA 4% for 30 min. After washing with PBS, the cells were stained with DAPI for 5 min and washed with PBS. Fluorescence images were acquired using Zeiss LSM 700 and analyzed with ZEN lite software.

Co-localization studies

D1 cells were plated at a density of 50,000 per dish in a Fluorodish and incubated for 2 h to adhere**.** Dual labeled nano- and microparticles were added to the cells at a final concentration of 20 µg/mL and incubated for 2 h or 24 h at 37°C. Lysotracker red and DAPI were added 2 h before imaging. Cells were washed 2 times with cold PBS and fluorescence images were acquired using Leica SPE II and analyzed by LAF AF Lite software.

3. Results and discussion

3.1. Particle characterization

Particulate systems are extensively used as vaccine delivery systems and do offer great advantages over soluble antigens [8]. Nevertheless several variables (size, surface hydrophilicity and charge, the presence of targeting ligands, release characteristics etc.) need to be optimized for the development of particulate vaccine carrier systems. Particularly, several studies have reported on the effect of particle size on the vaccine-induced immune response without consensus on the optimal size [20]. These conflicting results are probably due to different design of studies using varying cell types [21-24] route of administration [7,25] and

antigen release kinetics [26,27]. Many studies have shown that nanoparticles smaller than 500 nm are responsible for CD8+ T cell responses, whereas MPs (of 1 μm and larger) cause activation of CD4+ T cells that consequently results in a humoral immune response [7,20]. On the other hand there are reports that MPs of size 0.5-5 μm are successful in inducing a CD8+ T cell response [28,29]. In this study we prepared nano- and microparticles and compared their uptake by D1 cells. pLHMGA NPs and MPs loaded with Alexa488 OVA were prepared by a double emulsion-solvent evaporation method. This method has been widely used for encapsulation of hydrophilic molecules including protein antigens in polyester based particles [9,30-32]. Particles with or without the labeled polymer (Cy5-pDLLA) had comparable characteristics in terms of morphology, size and loading efficiency. Mean hydrodynamic diameter of the NPs measured by DLS was 380 nm with a PDI of 0.16-0.17 (**Table 1**). The number average size of the MPs was approximately 1 and 2 μm with standard deviation of around 1.1-1.4. The SEM images revealed that the particles were spherical with a smooth surface (**Figure 2**). The loading efficiency of OVA in NPs was approximately 70%. For the 1 μm MPs the loading efficiency was higher and around 85%. Larger MPs of 2 μm showed a loading efficiency of 65%. The NPs showed a negative zeta potential of -24 mV. The zeta potential values of the 1 and 2 um MPs were -31 and-36 mV, respectively. These negative zeta potential values can be attributed to the carboxylic (COOH) end groups in pLHMGA (**Figure 1**) which are deprotonated in the HEPES buffer of pH 7.4.

Table 1. Characteristics of the OVA loaded particle

# Batch	Labels	Polymer concentration %	Size (nm) PDI (DLS)	Size (μm) ± STD DEV Number-average (Accusizer)	Zeta potential (mV)	Loading efficiency (%)
1	Alexa488	5	378-0.16	-	-23	70
2	Alexa + Cy5	5	382-0.17	-	-24	68
3	Alexa488	10	-	1.2 ± 1.0	-36	85
4	Alexa + Cy5	10	-	1.3 ± 1.1	-36	83
5	Alexa488	10	-	2.5 ± 1.6	-36	66
6	Alexa + Cy5	10	-	2.1 ± 1.4	-31	61

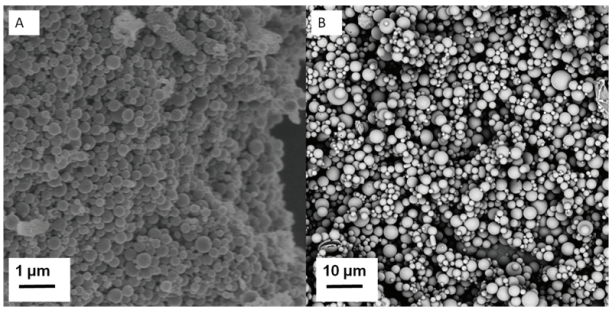

Figure 2. NPs and MPs (2 μm) loaded with OVA

3.2. Cytocompatibility

To assess the cytocompatibility of various particles, D1 cells were incubated with Alexa488-OVA and dual labeled particles (concentration from 7.8 to 500 μg/mL) for 24 h at 37°C. Control groups consisted of D1 cells and D1 cells incubated with soluble OVA corresponding

to the amounts of OVA in the particles (50- 4250 ng/mL). **Figure 3** shows that the viability of D1 cells incubated with NPs and MPs was comparable to the controls (approximately 90%) which showed the good cytocompatibility of these particles. These results are in line with previous studies confirming the cytocompatibility of pLHMGA particles [15-17].

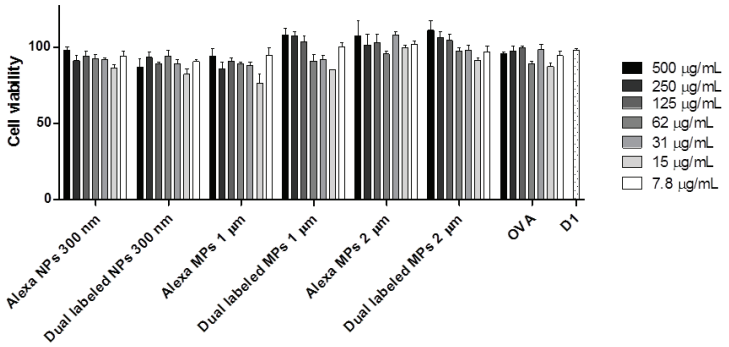

Figure 3. Cell viability of the D1 cells after 24 h incubation with NPs or MPs (7.8-500 µg/mL) using MTS assay.

3.3. Study of Binding and uptake of NPs and MPs by DCs

Binding of the NPs and 1 and 2 µm MPs to D1 cells and their subsequent internalization was studied using flow cytometry (**Figure 4**) and confocal microscopy (**Figure 5**). Soluble Alexa488-OVA used as control showed negligible binding at 4°C as well as very limited binding/internalization at 37°C. This result is in agreement with various studies demonstrating that soluble antigens are poorly taken up by the DCs [33-36]. In flow cytometry studies, 7% of D1 cells were positive for Alexa488-OVA after 4 h incubation with NPs incubated at 4°C while MPs showed negligible cell binding up to 4 h. The binding and uptake study performed at 37°C showed that almost all the D1 cells were associated with / had taken up the NPs after 24 h while MPs of 1 and 2 µm exhibited less cell association/uptake. Interestingly, DCs showed less internalizing of the 2 µm MPs than the 1 µm MPs. These results are in agreement with previous studies of pLGA particles which showed that 300 nm NPs were more efficiently taken up by DCs as compared to 1 µm MPs [7].

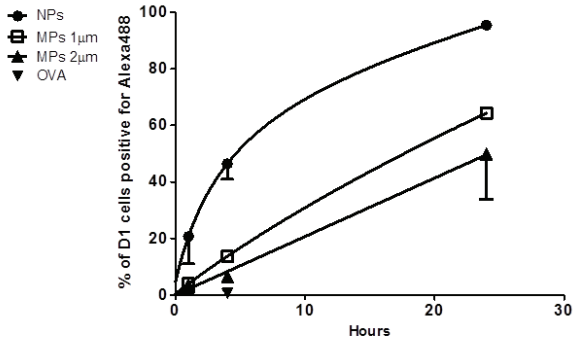

Figure 4. Binding and uptake of NPs / MPs by D1 cells. D1 cells were incubated at 37°C for 1, 4 and 24 h with 100 µg/mL of NPs and MPs followed by extensive washing. The Alexa488 signal (representative of OVA) was analyzed by flow cytometry. The percentage of Alexa-488 positive D1 cells is presented.

Confocal microscopy studies were performed using dual labeled NPs and 2 µm MPs as it was observed that there was no considerable difference between the binding and cell uptake of 1 and 2 µm MPs (**Figure 4**). Limited numbers of internalized NPs were observed after 10 min of incubation while no MPs were taken up. After 1 h incubation both the Alexa488 and Cy5 signals of NPs and MPs were visible inside the cells (**Figure 5**). Co-localization of the two signals was visible as yellow to orange points, however there was no complete co-localization of the two labels, which can be explained by the weak signal of Alexa488. Further, increasing uptake by D1 cells was observed with longer incubation time for both NPs and MPs. The fluorescence signals (both Cy5 and Alexa488) were monitored in time for NPs and MPs. Since the dye density on NPs was different from that of MPs, the signals of MPs could not be compared with those of NPs; instead the kinetics of the particle uptake was studied. MPs showed a more gradual trend in their uptake process by D1 cells during the 24 h as compared to NPs (**Figure 6**). Importantly, after 24 h of incubation with MPs, the Alexa488 (green) and Cy5 (red) signal were mainly co-localized (**Figure 4A**) showing that a small dose of the loaded amount Alexa488-OVA was released from the MPs. In contrast, in case of NPs, the Alexa488 signal was detectable all over the D1 cell and it co-localized with Cy5 (**Figure 4B**) which suggests that OVA was (at least partially) released from NPs. This was also confirmed when D1 cells were incubated with Alexa488-OVA-loaded NPs and 2 µm MPs and the co-localization with lysosomes was studied using Lysotracker Red (**Figure 7**). After 24 h incubation, staining with Lysotracker Red showed distinct lysosomes. Overlay of the red (lysosome) and green (OVA) signals showed a high level of co-localization of the two colors (yellow color) in DCs incubated with MPs, while NPs were detected both in the lysosomes and the cytosol which confirmed that the part of the released antigen was indeed present in the cytosol. This shows that the OVA was released from the NPs and had escaped from the lysosomes.

Perspectives and future studies

Upon internalization (mainly by endocytosis or micropinocytosis), antigen-loaded particles can be processed and presented via different pathways. If they remain in the endo-lysosomes, the particles can release the loaded antigen which after processing will be presented on MHC class II to CD4+ T cells. Upon activation, CD4+ T cells differentiate into Th cells [37]. On the other hand, the particle/antigen can escape from the endosomes resulting in their presence in the cytosol where the antigen will be processed by proteosomes and mount on MHC class I molecules and be presented to CD8+ T cells and initiate a cellular immune response [38]. However endosomal escape is not the only mechanism that can result in cross-presentation. Vacuolar pathway of cross-presentation involves localization of antigen/particles with endosomal compartments containing cathepsin S. Upon degradation of antigen by catepsin S, the processed antigen will be cross-presented to CD8+ T cells [39]. Some studies have investigated the effect of particle size on the cross-presentation pathways. One study showed that cross-presentation of 800 nm NPs was proteosome-dependent and governed by endosomal escape, while cross-presentation of bigger particles (3 µm) was via vacuolar pathway [40]. In another study, 300 nm NPs strongly induced cross-presentation and directed the immune response towards cellular (CD8+ T cell) responses while particles in the micrometer range were unsuccessful in inducing cross-presentation and caused humoral responses [7]. Interestingly, the NPs in our study escaped the endosome and were found in the cytosol (**Figure 5 and 7**). This suggests that pLHMGA NPs are more likely to cause antigen cross-presentation via MHC class I and induce a CD8+ T cell immune response. In contrast, the MPs were mainly in the lysosomes, where they are most probably to be presented via MHC class II which favors a humoral response. This should be evaluated in future studies by *in vitro* and *in vivo* antigen (cross-)presentation and T cell

proliferation assays. Further, *in vitro* particle degradation and antigen release as well as antigen co-localization studies in DCs would provide more insight into the role of particle size in antigen cross-presentation and immune response.

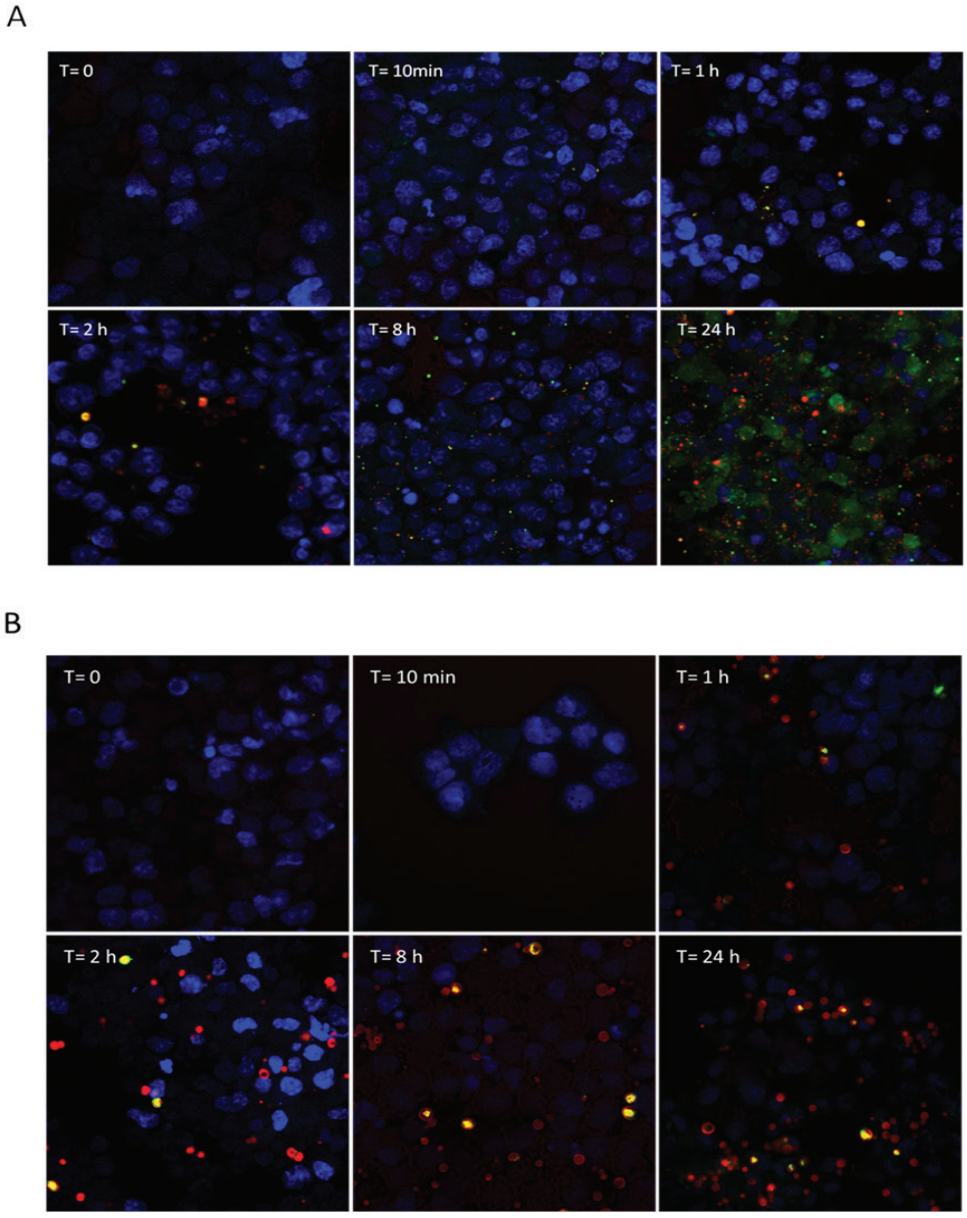

Figure 5. Confocal microscopy for assessment of particle uptake by D1 cells. D1 cells were incubated with 20 µg/mL of A) NPs and B) 2 µm MPs. After fixation with PFA and staining with DAPI, confocal images were obtained at various time points between 0 and 24 h.

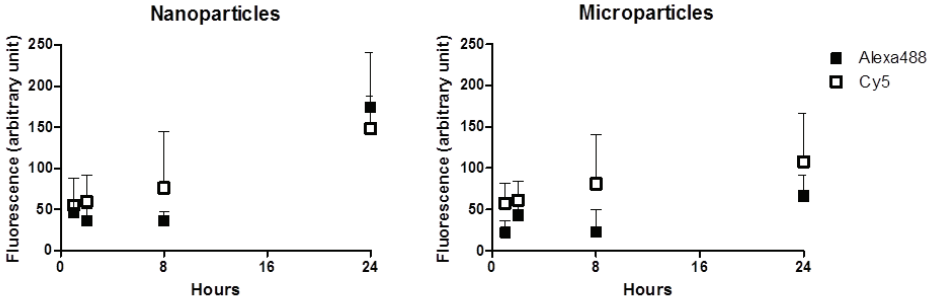

Figure 6. Average fluorescence intensity in D1 cells upon incubation with double labeled NPs and (2 µm) MPs obtained from confocal images.

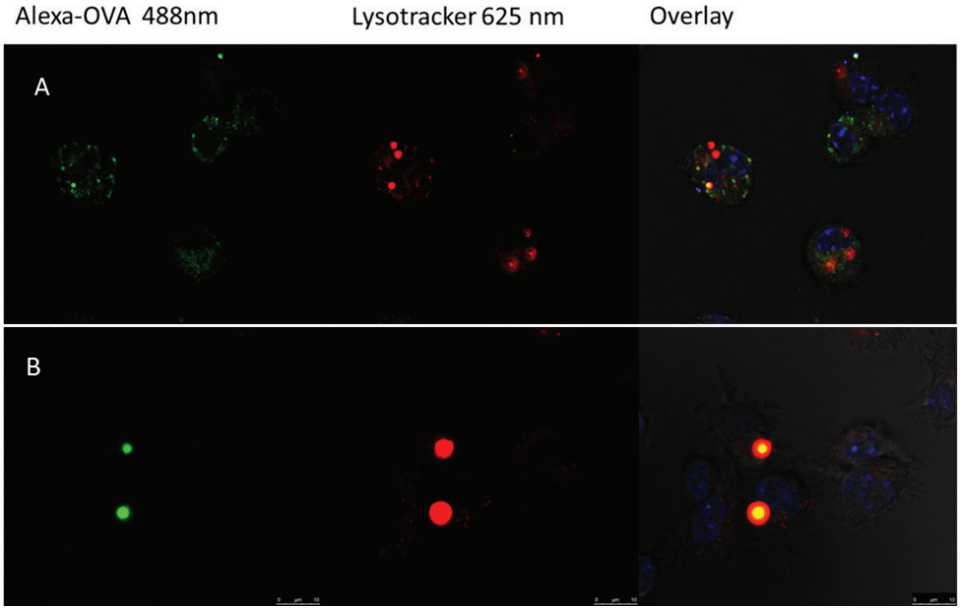

Figure 7. Confocal images of D1 cells incubated with 20 µg/mL of A) NPs and B) 2 µm MPs (loaded with Alexa488-OVA) for 24 h and stained with Lysotracker Red to visualize the lysosomes and DAPI (Blue) to visualize the nucleus (scale bar, 10 µm).

The charge of particles also affects their uptake and it has been shown that positively charged particles are more efficiently taken up by the cells *in vitro* [41], nevertheless negatively charged particles are more successful in draining to the lymph nodes upon subcutaneous administration [42,43] where large populations of DCs reside in lymph nodes. This could likely be due to the fact that negatively charged particles are not taken up by other (non-professional antigen presenting) cells and therefore freely drain to the lymph nodes [43]. Additionally, it has been reported that pLGA particles with a negative zeta potential could facilitate the endosomal escape [44]. Future work should focus on *in vitro* co-localization studies using pLHMGA particles with different surface charges.

Finally, comparing the volume and loading of the MPs and the NPs, and the results of the present study, the dose of antigen delivered to the D1 cells by one MP is considerably higher (~300 times) than for a single NP. It should however be noted that 1- the amount of antigen delivered does not affect the cross-presentation pathway [40] and 2- Upon *in vivo* administration, the MPs do not drain freely to the lymph nodes but instead need to be taken up by DCs at the injection site and then transferred to the lymph nodes which will affect both the kinetics and the type of the immune response. Small NPs on the other hand, are capable of free drainage to the lymph nodes [45]. Lymph nodes are home to a great population of DCs and play a significant role in induction of T cell immune response [46,47] as well as T cell tolerance [48] and therefore have been suggested and an attractive target for cancer vaccination [49]. Altogether, it is speculated that the overall response of the MPs might be hampered by the weak uptake by the DCs and drainage to the lymph nodes. Yet, future studies are necessary to further evaluate the role of particle size on the antigen-specific immune response.

4. Conclusion

pLHMGA NPs and MPs loaded with Alexa488-OVA were prepared and characterized for their cytocompatibility as well as *in vitro* binding and internalization by murine dendritic cells. The particles were incubated 24 h with D1 cells and showed no cytotoxicity even at the highest concentration tested. Binding and uptake studies showed that NPs are more efficiently taken up by the D1 cells after 24 h as compared to MPs. Confocal co-localization studies showed that after 24 h incubation of NPs with D1 cells, the antigen is detectable in the cytosol as well as in the lysosomes. This suggests that the antigen could possibly be presented in MHC class I to induce a CD8+ T cell immune response. In contrast MPs were co-localized mainly with lysosomes where they could most likely be processed and presented in context of MHC class II molecules, which does not *per se* result in a cellular immune response. This introductory study shows the potential and flexibility of particulate delivery systems as vaccine formulations. Future work should focus on *in vitro* and *in vivo* functional studies for characterization of type and strength of the immune responses.

Acknowledgments

Authors would like to thank Nahid Givi, Marcel Camps and Nataschja Ho for their useful suggestions and practical help.

This research was conducted within the framework of the Cancer Vaccine Tracking project (#03O-302), Center for Translational Molecular Medicine (CTMM).

References

[1] Banchereau J, Briere F, Caux C, Davoust J, Lebecque S, Liu Y, et al. Immunobiology of dendritic cells. Annu Rev Immunol 2000;18:767-811.
[2] Figdor C, de Vries I, Lesterhuis W, Melief C. Dendritic cell immunotherapy: mapping the way. Nat Med 2004;10:475-480.
[3] Banchereau J, Palucka A. Dendritic cells as therapeutic vaccines against cancer. Nat Rev Immunol 2005;5:296-306.
[4] Fong L, Engleman E. Dendritic cells in cancer immunotherapy. Annu Rev Immunol 2000;18:245-273.
[5] Shen H, Ackerman A, Cody V, Giodini A, Hinson E, Cresswell P, et al. Enhanced and prolonged cross-presentation following endosomal escape of exogenous antigens encapsulated in biodegradable nanoparticles. Immunol 2006;117:78-88.
[6] Zhang W, Wang L, Liu Y, Chen X, Liu Q, Jia J, et al. Immune responses to vaccines involving a combined antigen-nanoparticle mixture and nanoparticle-encapsulated antigen formulation. Biomaterials 2014;35:6086-6097.
[7] Joshi VB, Geary SM, Salem AK. Biodegradable Particles as Vaccine Delivery Systems: Size Matters. Aaps Journal 2013;15:85-94.
[8] Joshi VB, Geary SM, Salem AK. Biodegradable particles as vaccine antigen delivery systems for stimulating cellular immune responses. Human Vaccines & Immunotherapeutics 2013;9:2584-2590.
[9] Danhier F, Ansorena E, Silva JM, Coco R, Le Breton A, Preat V. PLGA-based nanoparticles: An overview of biomedical applications. J Control Release 2012;161:505-522.
[10] van de Weert M, Hennink WE, Jiskoot W. Protein instability in poly(lactic-co-glycolic acid) microparticles. Pharm Res 2000;17:1159-1167.
[11] Ding AG, Schwendeman SP. Acidic microclimate pH distribution in PLGA microspheres monitored by confocal laser scanning microscopy. Pharm Res 2008;25:2041-2052.
[12] Leemhuis M, van Nostrum C, Kruijtzer J, Zhong Z, ten Breteler M, Dijkstra P, et al. Functionalized poly(alpha-hydroxy acid)s via ring-opening polymerization: Toward hydrophilic polyesters with pendant hydroxyl groups. Macromolecules 2006;39:3500-3508.
[13] Liu Y, Ghassemi AH, Hennink WE, Schwendeman SP. The microclimate pH in poly(D,L-lactide-co-hydroxymethyl glycolide) microspheres during biodegradation. Biomaterials 2012;33:7584-7593.
[14] Ghassemi AH, van Steenbergen MJ, Talsma H, van Nostrum CF, Jiskoot W, Crommelin DJA, et al. Microspheres of hydrophilic PLGA highly atractive for protein delivery. J Control Release 2010;148:E39-E40.
[15] Kazazi-Hyseni F, Zandstra J, Popa E, Goldschmeding R, Lathuile A, Veldhuis G, et al. Biocompatibility of poly(d,l-lactic-co-hydroxymethyl glycolic acid) microspheres after subcutaneous and subcapsular renal injection. Int J Pharm 2015;482:99-109.
[16] Rahimian S, Kleinovink JW, Fransen MF, Mezzanotte L, Gold H, Wisse P, et al. Near-infrared labeled, ovalbumin loaded polymeric nanoparticles based on a hydrophilic polyester as model vaccine: In vivo tracking and evaluation of antigen-specific CD8+ T cell immune response. Biomaterials 2015;37:469-477.
[17] Rahimian S, Fransen MF, Kleinovink JW, Christensen JR, Amidi M, Hennink WE, et al. Polymeric nanoparticles for co-delivery of synthetic long peptide antigen and poly IC as therapeutic cancer vaccine formulation. J Control Release 2015;203:16-22.
[18] Xiang SD, Scholzen A, Minigo G, David C, Apostolopoulos V, Mottram PL, et al. Pathogen recognition and development of particulate vaccines: Does size matter? Methods 2006;40:1-9.
[19] Winzler C, Rovere P, Rescigno M, Granucci F, Penna G, Adorini L, et al. Maturation stages of mouse dendritic cells in growth factor-dependent long-term cultures. J Exp Med 1997;185:317-328.
[20] Oyewumi MO, Kumar A, Cui Z. Nano-microparticles as immune adjuvants: correlating particle sizes and the resultant immune responses. Exp Rev Vaccines 2010;9:1095-1107.
[21] Silva JM, Vandermeulen G, Oliveira VG, Pinto SN, Rodrigues C, Salgado A, et al. Development of functionalized nanoparticles for vaccine delivery to dendritic cells: a mechanistic approach. Nanomedicine 2014;9:2639-2656.
[22] Sneh-Edri H, Likhtenshtein D, Stepensky D. Intracellular targeting of plga nanoparticles encapsulating antigenic peptide to the endoplasmic reticulum of dendritic cells and its effect on antigen cross-presentation in vitro. Mol Pharm 2011;8:1266-1275.
[23] Thiele L, Rothen-Rutishauser B, Jilek S, Wunderli-Allenspach H, Merkle HP, Walter E. Evaluation of particle uptake in human blood monocyte-derived cells in vitro. Does phagocytosis activity of dendritic cells measure up with macrophages? J Control Release 2001;76:59-71.
[24] Kreutz M, Tacken PJ, Figdor CG. Targeting dendritic cells-why bother? Blood 2013;121:2836-2844.
[25] Gutierro I, Hernandez RM, Igartua M, Gascon AR, Pedraz JL. Size dependent immune response after subcutaneous, oral and intranasal administration of BSA loaded nanospheres. Vaccine 2002;21:67-77.
[26] Johansen P, Storni T, Rettig L, Qiu Z, Der-Sarkissian A, Smith KA, et al. Antigen kinetics determines immune reactivity. Proc Natl Acad Sci U S A 2008;105:5189-5194.
[27] Demento SL, Cui W, Criscione JM, Stern E, Tulipan J, Kaech SM, et al. Role of sustained antigen release from nanoparticle vaccines in shaping the T cell memory phenotype. Biomaterials 2012;33:4957-4964.
[28] Mueller M, Schlosser E, Gander B, Groettrup M. Tumor eradication by immunotherapy with biodegradable PLGA microspheres-an alternative to incomplete Freund's adjuvant. Int J Cancer 2011;129:407-416.
[29] Mata E, Igartua M, Hernandez RM, Rosas JE, Patarroyo ME, Pedraz JL. Comparison of the adjuvanticity of two different delivery systems on the induction of humoral and cellular responses to synthetic peptides. Drug Deliv 2010;17:490-499.

[30] Couvreur P, Puisieux F. Nanoparticles and microparticles for the delivery of polypeptides and proteins. Adv Drug Deliv Rev 1993;10:141-162.
[31] Cohen S, Yoshioka T, Lucarelli M, Hwang L, Langer R. Controlled delivery systems for proteins based on poly(lactic glycolic acid) microspheres. Pharm Res 1991;8:713-720.
[32] Noh Y, Jang Y, Ahn K, Lim YT, Chung BH. Simultaneous in vivo tracking of dendritic cells and priming of an antigen-specific immune response. Biomaterials 2011;32:6254-6263.
[33] Uto T, Akagi T, Toyama M, Nishi Y, Shima F, Akashi M, et al. Comparative activity of biodegradable nanoparticles with aluminum adjuvants: Antigen uptake by dendritic cells and induction of immune response in mice. Immunol Lett 2011;140:36-43.
[34] Koppolu B, Zaharoff DA. The effect of antigen encapsulation in chitosan particles on uptake, activation and presentation by antigen presenting cells. Biomaterials 2013;34:2359-2369.
[35] Tel J, Lambeck AJA, Cruz LJ, Tacken PJ, de Vries IJM, Figdor CG. Human plasmacytoid dendritic cells phagocytose, process, and present exogenous particulate antigen. J Immun 2010;184:4276-4283.
[36] Akagi T, Baba M, Akashi M. Biodegradable nanoparticles as vaccine adjuvants and delivery systems: regulation of immune responses by nanoparticle-based vaccine. Polymers in Nanomedicine 2012;247:31-64.
[37] Trombetta ES, Mellman I. Cell biology of antigen processing in vitro and in vivo. Annu Rev Immunol 2005;23:975-1028.
[38] Davis ID, Chen W, Jackson H, Parente P, Shackleton M, Hopkins W, et al. Recombinant NY-ESO-1 protein with ISCOMATRIX adjuvant induces broad integrated antibody and CD4(+) and CD8(+) T cell responses in humans. Proc Natl Acad Sci U S A 2004;101:10697-10702.
[39] Shen LJ, Sigal LJ, Boes M, Rock KL. Important role of cathepsin S in generating peptides for TAP-independent MHC class I crosspresentation in vivo. Immunity 2004;21:155-165.
[40] Mant A, Chinnery F, Elliott T, Williams AP. The pathway of cross-presentation is influenced by the particle size of phagocytosed antigen. Immunol 2012;136:163-175.
[41] Foged C, Brodin B, Frokjaer S, Sundblad A. Particle size and surface charge affect particle uptake by human dendritic cells in an in vitro model. Int J Pharm 2005;298:315-322.
[42] Froehlich E. The role of surface charge in cellular uptake and cytotoxicity of medical nanoparticles. Int J Nanomedicine 2012;7:5577-5591.
[43] Rao DA, Forrest ML, Alani AWG, Kwon GS, Robinson JR. Biodegradable plga based nanoparticles for sustained regional lymphatic drug delivery. J Pharm Sci 2010;99:2018-2031.
[44] Panyam J, Zhou WZ, Prabha S, Sahoo SK, Labhasetwar V. Rapid endo-lysosomal escape of poly(DL-lactide-co-glycolide) nanoparticles: implications for drug and gene delivery. Faseb Journal 2002;16:UNSP 0892-6638/02/0016-1217.
[45] Manolova V, Flace A, Bauer M, Schwarz K, Saudan P, Bachmann MF. Nanoparticles target distinct dendritic cell populations according to their size. Eur J Immunol 2008;38:1404-1413.
[46] Reddy ST, van der Vlies AJ, Simeoni E, Angeli V, Randolph GJ, O'Neill CP, et al. Exploiting lymphatic transport and complement activation in nanoparticle vaccines. Nat Biotechnol 2007;25:1159-1164.
[47] Randolph GJ, Angeli V, Swartz MA. Dendritic-cell trafficking to lymph nodes through lymphatic vessels. Nat Rev Immunol 2005;5:617-628.
[48] Ochando JC, Yopp AC, Yang Y, Garin A, Li YS, Boros P, et al. Lymph node occupancy is required for the peripheral development of alloantigen-specific Foxp3(+) regulatory T cells. J Immunol 2005;174:6993-7005.
[49] Thomas SN, Vokali E, Lund AW, Hubbell JA, Swartz MA. Targeting the tumor-draining lymph node with adjuvanted nanoparticles reshapes the anti-tumor immune response. Biomaterials 2014;35:814-824.

CHAPTER 7

Summary and Perspectives

Immunotherapy of cancer is a rapidly emerging and groundbreaking approach in cancer treatment that makes use of various immune-regulating macromolecules to fight cancer [1,2]. Among these immunotherapeutics are therapeutic peptides and proteins (including antibodies) and nucleic acids. These immunotherapeutic agents are sensitive to degradation by proteases and nucleases upon *in vivo* administration and therefore require multiple injections which in turn would increase the risk of toxicity. Furthermore, the complex tumor environment with multiple immunosuppressive mechanisms might result in tolerance which sabotages the success of immunotherapy [3,4]. Sustained release delivery systems based on biodegradable polymers have been developed to tackle these issues, particularly to increase the efficacy of the treatment and limit the toxicity.
This thesis investigates two strategies towards using particulate carrier systems based on poly(lactic-co-hydroxymethylglycolic acid) (pLHMGA) in immunotherapy of cancer: therapeutic cancer vaccines and local delivery of immunomodulatory antibodies.

Cancer vaccines
Cancer vaccines usually comprise of tumor-specific antigens and adjuvants and intend to induce a strong and durable tumor-specific CD8+ T cell immune response capable of eradicating the tumor. Cancer vaccines target antigen presenting cells (especially dendritic cells, (DCs)), which are capable of processing and efficient antigen cross-presentation via MHC class I to CD8+ T cells [5,6].
Recently a new class of tumor antigens -synthetic long peptides (SLPs)- has been developed for cancer treatment. SLPs are usually 15-35 amino acid long and exhibit a very strong T cell response as compared to minimum peptide epitopes [7]. These minimum peptide epitopes (short peptides) can easily bind to MHC class I molecules on the surface of all nucleated cells (including DCS and macrophages) [8]. This direct binding causes a short-lived T cell response [9] and consequently leads to T cell tolerance and lack of immunological memory [10,11]. In contrast to short peptides, SLPs cannot directly bind to MHC class I molecules and therefore in order to present their epitope, they have to be taken up and processed by the DCs [8]. This takes away the possibility of direct binding of epitopes to MHC molecules. Importantly, SLPs are more efficiently processed by DCs and induce a stronger T cell immune response as compared to protein antigens [12]. Human papillomavirus (HPV) SLPs are among the SLPs that have been studied extensively in (pre)clinical models with promising results [13-15]. However, upon administration, free SLPs can be degraded by peptidases and proteases before their uptake and formation of MHC-binding epitopes [16]. By encapsulation of SLPs, they are protected against enzymatic degradation, and this increases the stability of the vaccine, its uptake by DCs and therefore its efficacy [17].
Encapsulation of antigens and adjuvants in particulate systems can address many other challenges. Biodegradable polymeric particles offer controlled delivery of the components of the vaccines and ability to deliver large amounts of antigens and adjuvants as their uptake by cells is more efficient than soluble vaccines. Moreover, using particles, co-delivery of multiple antigens and adjuvants is possible. By co-encapsulating TLR ligands, a strong tumor-specific CD8+ T cell response can be achieved which is desired for cancer immunotherapy [18]. Active targeting of particulate cancer vaccines is possible by decorating the surface of the particles with various antibodies or targeting ligands to secure the delivery of the payload to the right cell [19]. Lastly, particles could decrease the risk of side effects as compared to soluble antigens or those formulated in commonly used water-in-oil (W/O) emulsions such as incomplete Freund's adjuvant (IFA) and Montanide emulsions. W/O emulsions are prepared by emulsification of soluble antigen/adjuvant in a mixture of mineral oils and surfactants. However, these formulations are pharmaceutically not well-defined and therefore

antigen/adjuvant release kinetics are poorly reproducible. Moreover, their administration is associated with severe local side effects such as inflammation, granuloma, pain and swelling [15,20,21].

Immunomodulatory antibodies

Immunomodulatory antibodies enhance the anti-tumor immune response by altering the stimulatory or inhibitory signals on DCs and T cells [22-24]. The systemic administration of these antibodies in their soluble form has however been associated with severe toxicity and autoimmune reactions [25-27]. To overcome these drawbacks, sustained release formulations of these antibodies based on IFA or Montanide have been developed for local administration. However, as mentioned earlier in this chapter, W/O emulsions based on IFA or Montanide are associated with adverse effects and are therefore not the desirable formulations. Polymeric particles can provide safe and well-defined formulations with tailorable release kinetics. When aiming to release an immunotherapeutic agent locally, particles in micrometer range (>10 μm) are desired [28]. Such microparticles (MPs) will not be taken up by APCs and therefore they are able to deliver the cargo at the injection site without the therapeutic antibody being deactivated by APCs. Similar to NPs, co-delivery of multiple therapeutic agents is possible for MPs.

Controlled release delivery systems based on aliphatic polyesters

Poly(lactic-co-glycolic acid) (pLGA) is an aliphatic polyester and is the most extensively used polymer for delivery of peptides and proteins [29,30], but there are several stability issues regarding encapsulation of these molecules in pLGA [31].

Acidification inside the particles upon degradation can induce chemical modification, aggregation and incomplete release of the payload which consequently is responsible for adverse effects and reduced efficacy [32]. To overcome this drawback of pLGA, in our department, a hydrophilic polyester, poly(lactide-co-hydroxymethyl glycolic acid) (pLHMGA) has been developed [33]. pLHMGA has been successfully used for encapsulation of various peptides and proteins [34-36]. Moreover, it was shown that upon degradation, pLHMGA shows no pH drop inside the particles and as a result less chemical modification and aggregation was observed. pLHMGA particles have shown complete release of their cargo and are therefore considered "protein and peptide friendly" [35-37]. In addition, these particles are biocompatible *in vivo* [38] and therefore were chosen as carrier systems in this thesis.

In this thesis, ovalbumin (OVA) loaded pLHMGA nanoparticles (NPs) were initially evaluated as model vaccines i*n vitro* and *in vivo* with promising results. Encouraged by these results, a therapeutic cancer vaccine was designed based on human papillomavirus oncoprotein (HPV16 E7) which has shown promise in clinical trials [14,15]. A HPV SLP antigen derived from HPV16 E7, and poly IC (TLR3 ligand-adjuvant) were encapsulated in pLHMGA NPs and the therapeutic efficacy of the vaccine was evaluated in mice. For delivery of antibodies, pLHMGA MPs were loaded with antiCD40 and antiCTLA4 and the antitumor effects of these formulations were evaluated in tumor-bearing mice. Therapeutic efficacy of particulate formulations was compared to that of IFA emulsions in order to evaluate the particles as substitutes for IFA.

Chapter 1 gives an overview of clinically used cancer treatment modalities and briefly discusses the challenges in delivery of immunotherapeutics. Further the potential of biodegradable polymers as carriers for immunotherapeutics is addressed.

Chapter 2 reviews the application of particulate carrier systems based on aliphatic polyesters (particularly poly(lactic-co-glycolic acid)(pLGA)) in cancer immunotherapy. Delivery of immunotherapeutics is especially challenging due to sensitivity of these macromolecules to degradation *in vivo,* weak and short-lived immune responses and immune-suppression in the tumor environment that results in immunological tolerance. Particulate systems based on pLGA and similar polymers have great potential to overcome these challenges. In this review, important parameters for the design and development of a successful particulate delivery system are discussed. The effect of the immunotherapeutic agent, particle size, charge etc. and their effect on the type and magnitude of the immune response is reviewed and several examples of these systems for immunotherapy of cancer including cancer vaccines and immunomodulatory antibodies are given.

The feasibility of the use of pLHMGA carrier systems was evaluated in **Chapter 3** by encapsulating the model antigen ovalbumin (OVA) in pLHMGA NPs. To be able to track these particles in real time *in vivo,* two near-infrared dyes (NIR dye) were used to label OVA and the particles. To do so, an alkyne-bearing poly(d,l lactic acid) (alkyne-pDLLA) was synthesized and the azide-functionalized NIR dye was coupled to alkyne-pDLLA by click chemistry. NHS chemistry was used to label OVA with another NIR dye. The double emulsion-solvent evaporation technique was used to prepare spherical particles of 300-400 nm (DLS measurements). The particles showed a low burst release followed by sustained release of OVA in 30 days up to approximately 70% of the loaded content. The low burst release observed with pLHMGA NPs is preferred because it avoids premature release of the antigen before being taken up by the DCs. *In vitro* studies on DCs showed cytocompatibility of both the empty and OVA loaded NPs and proved that the labeling does not cause toxicity. *In vitro* studies using Alexa647-OVA pLHMGA NPs showed that NPs were efficiently taken up by DCs after 16 hours incubation at 37°C. Subsequently the ability of the OVA NPs to cross-present the antigen to T cells was evaluated *in vitro* using OVA-specific B3Z hybridoma T cells. The obtained results showed a dose dependent and strong T cell activation induced by OVA NPs, while soluble OVA was not able to activate T cells even at high doses. Additionally, the dual labelled NPs were as efficient in T cell activation as the unlabeled NPs, again proving that labeling does not affect the ability of NPs to induce an immune response. To study the fate of the model nanoparticulate vaccine *in vivo*, dual labeled NPs were injected into the tail base of mice and the signals of two NIR dyes were monitored simultaneously for more than 14 days. OVA and NPs showed similar NIR signal patterns at the injection site as well as in the lymph nodes suggesting that the antigen is being transported mostly in the form of NPs. The clearance of NPs from the injection site and accumulation in the lymph nodes- where the immune response initiates- was more gradual than soluble OVA protein. This prolonged supply of antigen to the lymph nodes secures a strong immune response which was observed in an *in vivo* T cell proliferation test performed by adoptive transfer of OT-1 T cells. OVA NPs showed superior antigen cross-presentation to OVA-specific CD8+ T cells in the lymph nodes and spleen as compared to soluble OVA. Taken together, this study showed the potential of pLHMGA NPs as antigen delivery systems for inducing cellular immune responses.

Encouraged by the results obtained by the study discussed in **Chapter 3**, we aimed to develop a therapeutic cancer vaccine based on pLHMGA NPs to treat HPV-induced cancer.

Many studies have focused on vaccination with minimal peptide epitopes of HPV16 E6 and E7 oncoproteins with limited success. On the other hand, increasing the length of the peptide vaccines has resulted in development of synthetic long peptides (SLPs) which have shown promising results in preclinical studies as well as in clinical trials. These peptides have been commonly formulated in IFA. Administration of IFA formulations is associated with severe local and long lasting side effects. Therefore in **Chapter 4** in order to develop a substitute for IFA emulsions, pLHMGA NPs loaded with a HPV SLP (derived from HPV16 E7 oncoprotein) with or without a toll like receptor 3 (TLR3) ligand (poly IC) were prepared. The particles were spherical with size around 400-500 nm (DLS measurements). The zeta potential of the HPV SLP NPs was negative due to the carboxylic acid end groups of the polymer. The HPV SLP + poly IC NPs showed an even more negative zeta potential which is likely due to surface associated negatively-charged poly IC molecules. The therapeutic efficacy of the NPs was compared to IFA emulsion in TC-1 tumor-bearing mice using a prime-boost vaccination regimen. The therapeutic efficacy of the NPs formulations containing HPV SLP and poly IC (either co-encapsulated or in soluble form) was comparable to that of HPV SLP and poly IC formulated in IFA. All formulations containing HPV SLP and poly IC (including NPs and IFA emulsion) significantly increased the survival of the tumor-bearing mice by three weeks. While HPV SLP NPs (without poly IC) delayed the tumor growth, they could not significantly prolong the survival of the mice. Survival of the mice treated with poly IC was comparable to that of the untreated group. In blood of mice 9 days after the prime dose, the population of HPV-specific CD8+ T cells was significantly enhanced when combined with poly IC either co-encapsulated with the antigen or in its soluble form and this HPV-specific T cell expansion in blood could successfully predict the outcome of the tumor study. Interestingly, no significant difference was observed between the effect of co-encapsulation of poly IC and co-administration of poly IC in the NPs. This could be due to the relatively high dose of the TLR ligand used that might have masked the expected superiority of the co-encapsulated TLR ligand as has been observed in previous studies. Nevertheless, administration of poly IC in soluble form can cause systemic toxicity and autoimmunity and is therefore not recommended. Subcutaneous administration of NPs -as opposed to IFA- did not show any adverse effects at the side of injection and therefore it was concluded that the (HPV SLP + poly IC) NPs are the preferred formulation since have the best safety profile among other formulations tested while exhibiting comparable therapeutic efficacy.

In **Chapter 5** the potential of the pLHMGA microparticles (MPs) was evaluated for local and sustained delivery of immunomodulatory antibodies. Given the important role of CD40-CD40L in DC activation and maturation and CTLA4 in immunosuppression, we chose two antibodies, antiCD40 and antiCTLA4 which were encapsulated in pLHMGA MPs. Because of the limited availability and laborious and costly preparation of the antibodies, the optimization of the formulation was done using polyclonal human IgG. This model IgG was labelled with a NIR dye to increase the sensitivity of quantification. In order to obtain a particle formulation suitable for local delivery of antibodies, we chose pLHMGA with a 50/50 initial monomer ratio. This polymer contains 25% of the hydrophilic BMMG monomer and it was hypothesized that using a more hydrophilic pLHMGA would be more "antibody friendly". Moreover it has been shown in previous studies that particles based on this polymer degrade in about 30 days, which is considered as a suitable timeframe to release an entrapped antibody for obtaining the desired antitumor effect. By altering the polymer concentration during particle preparation, different formulations were prepared and the size and morphology of the particles as well as IgG in vitro release kinetics were studied. It was observed that by increasing the polymer concentration from 10% to 30% the particle size increased from around 12 to 25 μm, sizes suitable to avoid unwanted uptake by antigen

presenting cells such as DCs and macrophages. The particles were spherical and IgG was encapsulated with high loading efficiency (>80%). Particles made with a polymer solution with a concentration of 10% showed the highest burst release (35% of the loading), followed by sustained release of the antibody up to 90% by day 7. An increase in polymer concentration resulted in decrease in burst release and a longer release time: the formulation made with polymer solution of 30% showed a burst release of only 1% and a sustained release of 50% of the loading in 35 days. The formulation prepared with polymer concentration of 15% showed a low burst release (12 %) but also a sustained release of the IgG up to 75% for 35 days *in vitro* and because of the favorable release characteristics was selected for further *in vivo* studies. Equal doses of IgG in PBS, IFA or in MPs were administered subcutaneously to mice and the serum antibody levels were monitored in time. IgG dissolved in PBS resulted in high levels of serum IgG for 6 days. Upon administration of MPs antibody serum levels were at least 10 times lower than the soluble form for a duration of 6 days after administration. This was encouraging since the locally administered MPs indeed release IgG in a sustained manner and the serum levels are likely sufficiently low to avoid systemic toxicity. Next, antiCD40 and antiCTLA4 were loaded in the optimized formulation. These particles showed similar characteristics in terms of size, morphology, loading efficiency and *in vitro* release kinetics as those prepared using the polyclonal IgG. The therapeutic efficacy of the MPs was compared to that of IFA formulations in mice inoculated with colon carcinoma tumor model (MC-38). The survival of mice treated with IFA formulations was comparable to that treated with MPs: 30% survival after 45 days when treated with antiCTLA-4 and 60% survival after 55 days in case of antiCD40 treatment. Importantly, the MPs did not show any local adverse effects and no remnants of the MPs were found at the injection site 60 days after particle injection, whereas inflammatory depots were observed in mice treated with IFA formulations. Additionally, and in agreement with data obtained from polyclonal IgG MPs, the antibody serum levels upon administration of MPs were lower than levels observed with IFA formulations. In conclusion, pLHMGA microparticles are systems that provide long-lasting and non-toxic antibody therapy for immunotherapy of cancer.

Although polymeric particles have shown promising results as carrier systems in cancer immunotherapy -specifically as cancer vaccines- the optimum particle size to secure efficient uptake by DCs is under debate, and therefore in **Chapter 6** the effect of particle size on the uptake of particles by DCs was investigated. In this study, NIR labelled (Cy5) pLHMGA particles loaded with Alexa488-OVA with different sizes (300 nm, and 1 and 2 μm) were prepared and characterized for the extent of their uptake by DCs in vitro. In flow cytometry studies, DCs showed higher cell binding and uptake upon incubation with NPs as compared to MPs. Confocal laser scanning microscopy using dual-labeled particles showed that OVA was released in the cytosol of DCs after 24 hours of incubation with NPs. This suggests that the antigen could be cross-presented via MHC class I molecules to CD8+ T cells to induce a cellular immune response which is particularly desired in cancer immunotherapy. Similar co-localization studies performed with MPs (2 μm) showed that the fluorescence signals of particles and OVA were mainly co-localized with the lysosomes. This indicates that the OVA is likely to be processed and presented via MHC class II which per se does not result in a strong T cell response.

In summary, this thesis discusses various applications of nano- and microparticulate carrier systems based on a hydrophilic aliphatic polyester, poly(lactic-co-hydroxymethyl glycolic acid), pLHMGA, in immunotherapy. Antigens, adjuvants and antibodies were encapsulated in pLHMGA nano- and microparticles by double emulsion solvent evaporation technique. Particles with various characteristics (size, release kinetics) were obtained by varying different

formulation and processing parameters. These particles have shown *in vitro* cytocompatibility and are well tolerated *in vivo*. Furthermore, the therapeutic efficacy of formulations based on pLHMGA polymers were comparable to commonly used W/O IFA emulsions in tumor-bearing mice.
As part of the "Cancer Vaccine Tracking" project, conducted by CTMM (Center for Translational Molecular Medicine), this research successfully 1-Optimized protocols for preparation of nano-and microparticles loaded with immunotherapeutic agents 2-Studied the immunological activity of particles *in vivo* in tumor models and 3-Correlated *in vivo* imaging of a model nanoparticulate vaccine to T cell immune responses. This model vaccine was further developed into Human papillomavirus synthetic long peptide therapeutic cancer vaccine.

Promises, potentials and challenges of pLHMGA particles in cancer immunotherapy

Promises and potentials

-pLHMGA has been successfully used in earlier studies for delivery of several peptides and proteins. The versatility of this polymer and its suitability for encapsulation of various molecules lies in its flexibility. The hydrophilicity of the polymer can be tailored by changing the ratio between d,l lactide and benzyloxymethyl methyl glycolide (BMMG). Doing so, various hydrophilic and hydrophobic molecules have been successfully encapsulated using this polymer [39,40]. Furthermore it was shown in **Chapter 5** and in previous studies that one could easily obtain different release rates with changing parameters such as polymer concentration.
-The particles were prepared by double emulsion solvent evaporation technique which is a relatively simple method and easy to scale up. Versatility of the method provides several parameters that can be altered to optimize a particle formulation. As an example for the preparation of particulate cancer vaccines, using this method and by changing a few parameters such as polymer concentration and volume fraction of the internal aqueous phase, a wide range of particle sizes can be obtained. Different particle sizes give us a means of passive targeting to DCs. It has been shown that upon hind footpad injection (a combination of intradermal and subcutaneous [41]) small nanoparticles (< 200 nm) freely drain to the lymph nodes and target lymph node-resident DCs which have been proposed as attractive targets for cancer vaccines [42], while larger NPs (> 500 nm) need be taken up by the DCs at the injection site and target skin-derived DCs. In addition and as suggested in **Chapter 6** particle size affects the antigen (cross-)presentation pathways which in turn define the type of the immune response [43]. Therefore, by engineering the size of the particles distinct immune responses can be achieved [44].
-Importantly pLHMGA has shown biodegradability and biocompatibility in preclinical studies in mice.
-pLHMGA particles can be freeze-dried after production and be stored at room temperature without stability concerns, whereas IFA solutions need to be made on spot due to instability and storage issues.

Challenges regarding development of a suitable formulation for clinical use

-pLHMGA and its hydrophilic precursor monomer (BMMG) are not commercially available and therefore their synthesis and scale up should be optimized.
-GMP (aseptic) production of the monomer, polymer and the formulation should be facilitated for clinical use.
-Co-encapsulation of multiple components requires multiple optimization steps.

Future work

Despite the promising results obtained in this thesis and previous studies, there are several complementary studies needed to provide a formulation suitable for clinical use. Future work on development of particulate carrier systems based on pLHMGA for immunotherapy of cancer can be divided in two aspects:

-Development and optimization of the formulation

-Employing multiple strategies to fight cancer

1-Development and optimization of the formulation

Cancer vaccine

In order to develop a cancer vaccine formulation for clinical use, many formulations consisting of SLPs and TLR ligands or other adjuvants can be developed (either co-encapsulated or encapsulated individually). In order to optimize the particle size, additional *in vitro* uptake and *in vitro* and *in vivo* T cell activation studies can be performed to investigate the mechanism of particle uptake and its relation to antigen cross presentation and T-cell activation. Further to enhance the particle uptake by DCs the surface of the particles can be decorated with targeting ligands such as mannan, antiCD40 or TLR (2,4,6,7) ligands [45,46].

Antibody delivery

To reach the clinics with these antibody delivery systems, monodisperse microparticulate formulations of antibodies can be developed to minimize the particle uptake by APCs, several other immunomodulatory antibodies can be encapsulated in the MPs such as antiPD1 (programmed cell death -1) [2].

Additionally, the effect of immunotherapeutic release kinetics from the particles on the strength of the immune response and possible side effects should be evaluated. Alternative strategies for encapsulation of immunotherapeutics can be explored, such as spray drying, solid-in-oil-in-oil (S/O/O) and solid-in-oil-in-water (S/O/W) in order to increase the stability of the encapsulated material. More in depth biocompatibility studies should be conducted such as evaluation of autoimmunity (systemic toxicity) and histology (local adverse effects) and optimal dosage and administration intervals should be investigated.

2-Employing multiple strategies to fight cancer

There are various regulatory mechanisms in the tumor environment that cause T cell tolerance and tumor-induced immunosuppression is a significant challenge in cancer treatment. Particulate delivery systems are capable of inducing strong immune responses and are therefore attractive systems for use in cancer immunotherapy. Further investigation using combinatorial therapy opens doors to successful tumor eradication and combination of immunotherapy and chemotherapy has already been investigated with promising results [47-50]. Alternatively, combination of multiple immunotherapy strategies is an interesting option. As a logical future step we suggest combination of particulate cancer vaccines and local delivery of immunomodulatory antibodies as an appealing approach in cancer immunotherapy.

Conclusion

The research described in this thesis shows the potential of pLHMGA particles as promising systems for safe and controlled delivery of immunotherapeutics and demonstrates that pLHMGA particles are suitable substitutes for IFA.

References

[1] Palucka K, Banchereau J. Cancer immunotherapy via dendritic cells. Nat Rev Cancer 2012;12:265-277.
[2] Weiner LM, Murray JC, Shuptrine CW. Antibody-based immunotherapy of cancer. Cell 2012;148:1081-1084.
[3] Shafer-Weaver K, Anderson M, Malyguine A, Hurwitz AA. T cell tolerance to tumors and cancer immunotherapy. Immune-Mediated Diseases: from Theory to Therapy 2007;601:357-368.
[4] de Visser KE, Schumacher TNM, Kruisbeek AM. CD8(+) T cell tolerance and cancer immunotherapy. J Immunother 2003;26:1-11.
[5] Finn OJ. Cancer vaccines: Between the idea and the reality. Nat Rev Immunol 2003;3:630-641.
[6] Timmerman JM, Levy R. Dendritic cell vaccines for cancer immunotherapy. Annu Rev Med 1999;50:507-529.
[7] Melief CJM, van der Burg SH. Immunotherapy of established (pre) malignant disease by synthetic long peptide vaccines. Nat Rev Cancer 2008;8:351-360.
[8] Bijker MS, van den Eeden SJE, Franken KL, Melief CJM, van der Burg SH, Offringa R. Superior induction of anti-tumor CTL immunity by extended peptide vaccines involves prolonged, DC-focused antigen presentation. Eur J Immunol 2008;38:1033-1042.
[9] Bennett SRM, Carbone FR, Toy T, Miller JFAP, Heath WR. B cells directly tolerize CD8(+) T cells. J Exp Med 1998;188:1977-1983.
[10] Toes REM, Blom RJJ, Offringa R, Kast WM, Melief CJM. Enhanced tumor outgrowth after peptide vaccination - Functional deletion of tumor-specific CTL induced by peptide vaccination can lead to the inability to reject tumors. J Immunol 1996;156:3911-3918.
[11] Bijker MS, van den Eeden SJF, Franken KL, Melief CJM, Offringa R, van der Burg SH. CD8(+) CTL priming by exact peptide epitopes in incomplete Freund's adjuvant induces a vanishing CTL response, whereas long peptides induce sustained CTL reactivity. J Immunol 2007;179:5033-5040.
[12] Rosalia RA, Quakkelaar ED, Redeker A, Khan S, Camps M, Drijfhout JW, et al. Dendritic cells process synthetic long peptides better than whole protein, improving antigen presentation and T-cell activation. Eur J Immunol 2013;43:2554-2565.
[13] van Duikeren S, Fransen MF, Redeker A, Wieles B, Platenburg G, Krebber W, et al. Vaccine-induced effector-memory CD8(+) T cell responses predict therapeutic efficacy against tumors. J Immunol 2012;189:3397-3403.
[14] Welters MJP, Kenter GG, de Vos van Steenwijk,Peggy J., Löwik MJG, Berends-van der Meer DMA, Essahsah F, et al. Success or failure of vaccination for HPV16-positive vulvar lesions correlates with kinetics and phenotype of induced T-cell responses. PNAS USA 2010;107:11895-11899.
[15] Kenter GG, Welters MJP, Valentijn ARPM, Lowik MJG, Berends-van der Meer DMA, Vloon APG, et al. Vaccination against HPV-16 oncoproteins for vulvar intraepithelial neoplasia. NEJM 2009;361:1838-1847.
[16] Falo LD, Colarusso LJ, Benacerraf B, Rock KL. Serum Proteases alter the antigenicity of peptides presented by class-i major histocompatibility complex-molecules. PNAS USA 1992;89:8347-8350.
[17] Danhier F, Ansorena E, Silva JM, Coco R, Le Breton A, Preat V. PLGA-based nanoparticles: An overview of biomedical applications. J Control Release 2012;161:505-522.
[18] Serda RE. Particle platforms for cancer immunotherapy. Int J Nanomedicine 2013;8:1683-1696.
[19] Conniot J, Silva JM, Fernandes JG, Silva LC, Gaspar R, Brocchini S, et al. Cancer immunotherapy: nanodelivery approaches for immune cell targeting and tracking. Frontiers in chemistry 2014;2:105-105.
[20] Gupta R, Relyveld E, Lindblad E, Bizzini B, Benefraim S, Gupta C. Adjuvants - a Balance between Toxicity and Adjuvanticity. Vaccine 1993;11:293-306.
[21] Graham BS, McElrath MJ, Keefer MC, Rybczyk K, Berger D, Weinhold KJ, et al. Immunization with cocktail of HIV-derived peptides in montanide ISA-51 is immunogenic, but causes sterile abscesses and unacceptable reactogenicity. PLoS One 2010;5:e11995.
[22] Fransen MF, Arens R, Melief CJM. Local targets for immune therapy to cancer: Tumor draining lymph nodes and tumor microenvironment. Int J Cancer 2013;132:1971-1976.
[23] Kyi C, Postow MA. Checkpoint blocking antibodies in cancer immunotherapy. FEBS Lett 2014;588:368-376.
[24] Weiner LM, Surana R, Wang S. Monoclonal antibodies: versatile platforms for cancer immunotherapy. Nat Rev Immunol 2010;10:317-327.
[25] Vonderheide RH, Glennie MJ. Agonistic CD40 antibodies and cancer therapy. Clin Cancer Res 2013;19:1035-1043.
[26] Fransen MF, Ossendorp F, Arens R, Melief CJM. Local immunomodulation for cancer therapy Providing treatment where needed. Oncoimmunol 2013;2:e26493.
[27] Sanderson K, Scotland R, Lee P, Liu D, Groshen S, Snively J, et al. Autoimmunity in a phase I trial of a fully human anti-cytotoxic T-lymphocyte antigen-4 monoclonal antibody with multiple melanoma peptides and montanide ISA 51 for patients with resected stages III and IV melanoma. J Clin Oncol2005;23:741-750.
[28] Doshi N, Mitragotri S. Macrophages Recognize Size and Shape of Their Targets. Plos One 2010;5:e10051.
[29] Lue J, Wang X, Marin-Muller C, Wang H, Lin PH, Yao Q, et al. Current advances in research and clinical applications of PLGA-based nanotechnology. Exp Rev Mol Diag 2009;9:325-341.
[30] Silva JM, Videira M, Gaspar R, Preat V, Florindo HF. Immune system targeting by biodegradable nanoparticles for cancer vaccines. J Control Release 2013;168:179-199.
[31] van de Weert M, Hennink WE, Jiskoot W. Protein instability in poly(lactic-co-glycolic acid) microparticles. Pharm Res 2000;17:1159-1167.
[32] Ding AG, Schwendeman SP. Acidic Microclimate pH Distribution in PLGA Microspheres Monitored by Confocal

Laser Scanning Microscopy. Pharm Res 2008;25:2041-2052.
[33] Leemhuis M, van Nostrum C, Kruijtzer J, Zhong Z, ten Breteler M, Dijkstra P, et al. Functionalized poly(alpha-hydroxy acid)s via ring-opening polymerization: Toward hydrophilic polyesters with pendant hydroxyl groups. Macromolecules 2006;39:3500-3508.
[34] Samadi N, van Nostrum CF, Vermonden T, Amidi M, Hennink WE. Mechanistic Studies on the Degradation and Protein Release Characteristics of Poly(lactic-co-glycolic-co-hydroxymethylglycolic acid) Nanospheres. Biomacromolecules 2013;14:1044-1053.
[35] Ghassemi AH, van Steenbergen MJ, Talsma H, van Nostrum CF, Jiskoot W, Crommelin DJA, et al. Preparation and characterization of protein loaded microspheres based on a hydroxylated aliphatic polyester, poly (lactic-co-hydroxymethyl glycolic acid). J Control Release 2009;138:57-63.
[36] Ghassemi AH, van Steenbergen MJ, Barendregt A, Talsma H, Kok RJ, van Nostrum CF, et al. Controlled release of octreotide and assessment of peptide acylation from poly(D,L-lactide-co-hydroxymethyl glycolide) compared to PLGA microspheres. Pharm Res 2012;29:110-120.
[37] Liu Y, Ghassemi AH, Hennink WE, Schwendeman SP. The microclimate pH in poly(D,L-lactide-co-hydroxymethyl glycolide) microspheres during biodegradation. Biomaterials 2012;33:7584-7593.
[38] Kazazi-Hyseni F, Zandstra J, Popa ER, Goldschmeding R, Lathuile AAR, Veldhuis GJ, et al. Biocompatibility of poly(d,l-lactic-co-hydroxymethyl glycolic acid) microspheres after subcutaneous and subcapsular renal injection. Int J Pharm 2015;482:99-109.
[39] Ghassemi A. Microspheres based on biodegradable functionalized poly(alpha-hydroxy) acids for the controlled release of bioactive proteins and peptides, PhD thesis, Utrecht University 2011.
[40] Samadi N. Biodegradable nanoparticles based on aliphatic polyesters; towards targeted intracellular delivery of protein therapeutics, PhD thesis, Utrecht University 2014.
[41] Kamala T. Hock immunization: A humane alternative to mouse footpad injections. J Immunol Methods 2007;328:204-214.
[42] Thomas SN, Vokali E, Lund AW, Hubbell JA, Swartz MA. Targeting the tumor-draining lymph node with adjuvanted nanoparticles reshapes the anti-tumor immune response. Biomaterials 2014;35:814-824.
[43] Mant A, Chinnery F, Elliott T, Williams AP. The pathway of cross-presentation is influenced by the particle size of phagocytosed antigen. Immunol 2012;136:163-175.
[44] Manolova V, Flace A, Bauer M, Schwarz K, Saudan P, Bachmann MF. Nanoparticles target distinct dendritic cell populations according to their size. Eur J Immunol 2008;38:1404-1413.
[45] Hamdy S, Haddadi A, Shayeganpour A, Samuel J, Lavasanifar A. Activation of antigen-specific t cell-responses by mannan-decorated PLGA nanoparticles. Pharm Res 2011;28:2288-2301.
[46] Rosalia RA, Cruz LJ, van Duikeren S, Tromp AT, Silva AL, Jiskoot W, et al. CD40-targeted dendritic cell delivery of PLGA-nanoparticle vaccines induce potent anti-tumor responses. Biomaterials 2015;40:88-97.
[47] Muller AJ, Prendergast GC. Marrying immunotherapy with chemotherapy: why say I do? Cancer Res 2005;65:8065-8068.
[48] Ramakrishnan R, Assudani D, Nagaraj S, Hunter T, Cho H, Antonia S, et al. Chemotherapy enhances tumor cell susceptibility to CTL-mediated killing during cancer immunotherapy in mice. J Clin Invest 2010;120:1111-1124.
[49] Lake RA, Robinson BWS. Opinion - Immunotherapy and chemotherapy - a practical partnership. Nat Rev Cancer 2005;5:397-405.
[50] Nowak AK, Robinson BWS, Lake RA. Synergy between chemotherapy and immunotherapy in the treatment of established murine solid tumors. Cancer Res 2003;63:4490-4496.

CHAPTER 8

Appendices

Nederlandse Samenvatting
List of Publications
List of abbreviations
Affiliation of collaborating authors
Acknowledgments
Curriculum Vitae

Nederlandse Samenvatting

Immuuntherapie tegen kanker is een snel opkomende en baanbrekende kankerbehandelingsaanpak die gebruik maakt van verscheidene immunoregulerende macromoleculen. Onder deze immunotherapeutica vallen therapeutische peptides, eiwitten (inclusief antilichamen) en nucleïnezuren. Deze therapeutica zijn gevoelig voor enzymatische degradatie door proteases en nucleases na *in vivo* toediening, en vereisen daarom meerdere injecties hetgeen het risico op toxiciteit zou kunnen verhogen. Daarnaast kan de complexe tumoromgeving, met meerdere immuunsuppressieve mechanismen, resulteren in immunologische tolerantie die het succes van immuuntherapie ondermijnt. Langdurige afgiftesystemen gebaseerd op biologisch afbreekbare polymeren zijn ontwikkeld om deze problemen aan te pakken, in het bijzonder om de effectiviteit van de behandeling te verhogen en de toxiciteit te beperken.

Dit proefschrift behandelt en onderzoekt twee strategieën voor het gebruik van afgiftesystemen die gebaseerd zijn op poly(lactic-co-hydroxymethylglycolic acid) (pLHMGA) voor de immuuntherapie tegen kanker: therapeutische kankervaccins en lokale toediening van immunomodulatoire antilichamen.

Kankervaccins

Kankervaccins bestaan gebruikelijk uit tumorspecifieke antigenen en immuun-versterkende adjuvanten en zijn bedoeld om een sterke en duurzame tumorspecifieke CD8+ T cel immuunrespons uit te lokken die in staat is om een tumor te elimineren. Kankervaccins richten zich op antigeenpresenterende cellen, in het bijzonder dendritische cellen (DCs), die in staat zijn om CD8+ T cellen te activeren door het antigeen efficiënt aan de T cellen te presenteren in MHC klasse I moleculen die aanwezig zijn op het oppervlak van de DC. Recentelijk is er een nieuwe klasse van tumorantigeen - synthetische lange peptides (SLPs) - ontwikkeld voor de behandeling van kanker. SLPs bestaan uit 15-35 aminozuren en laten een zeer sterke T celrespons zien in vergelijking met minimale peptide epitopen. Deze minimale peptide epitopen (korte peptides) kunnen zich makkelijk binden aan MHC klasse I moleculen op het oppervlak van alle antigeenpresenteerde cellen (inclusief DCs en macrofagen). Deze directe binding leidt tot een kortstondige T celrespons die op zijn beurt leidt tot T celtolerantie en gebrek aan immunologisch geheugen. In tegenstelling tot korte peptides kunnen SLPs zich niet direct binden aan MHC class I moleculen, en daarom moeten zij opgenomen en verwerkt worden door de DCs om hun epitoop te kunnen presenteren. Dit neemt de mogelijkheid weg van directe binding van epitopen aan MHC moleculen. Van belang is dat SLPs op een efficiëntere manier verwerkt worden door DCs en een sterkere T cel-immuunrespons induceren dan volledige eiwitten. Humaan papillomavirus (HPV) SLPs behoren tot de SLPs die intensief bestudeerd zijn in (pre)klinische modellen, met veelbelovende resultaten. Echter, na toediening kunnen vrije SLPs afgebroken worden door peptidases en proteases voordat ze zijn opgenomen en verwerkt tot MHC-bindende epitopen. Door encapsulatie worden SLPs beschermd tegen enzymatische afbraak, waardoor de stabiliteit, en daarmee de opname door DCs en de effectiviteit van het vaccin toenemen. De encapsulering van antigenen en adjuvanten in deeltjes biedt voor veel andere problemen een oplossing. Biologisch afbreekbare polymere deeltjes bieden zowel een gecontroleerde toediening van de componenten van vaccins, als de mogelijkheid tot toediening van grote hoeveelheden antigenen en adjuvanten, aangezien de opname in cellen meer efficiënt is dan die van oplosbare vaccins. Daarnaast is door het gebruik van deeltjes een gezamenlijke toediening mogelijk van meerdere antigenen en adjuvanten. Door middel van gezamenlijke encapsulering van TLR liganden kan een sterkere tumorspecifieke CD8+ T celrespons worden bereikt, wat wenselijk is voor immuuntherapie tegen kanker. Actieve targeting van op deeltjes gebaseerde

kankervaccins wordt mogelijk gemaakt door verschillende antilichamen of andere targeting moleculen aan te brengen op het deeltjesoppervlak, teneinde te verzekeren dat de lading terecht komt bij de juiste cel. Afsluitend, vergeleken met oplosbare antigenen, of antigenen geformuleerd in gebruikelijke water-in-olie (W/O) emulsies zoals Incomplete Freund's Adjuvant (IFA) en Montanide emulsies, zouden polymere deeltjes het risico op bijwerkingen kunnen verkleinen. W/O emulsies worden bereid door emulgering van oplosbaar antigeen/adjuvant in een mengsel van minerale olieën en surfactanten. Deze formuleringen zijn echter farmaceutisch niet goed gedefiniëerd, en daarom is de afgifte-kinetiek van antigeen/adjuvant slecht reproduceerbaar. Daarnaast kan de toediening van deze emulsies gepaard gaan met ernstige lokale bijwerkingen zoals ontstekingen, granulomen, pijn, en zwellingen.

Immunomodulatoire antilichamen

Immunomodulatoire antilichamen versterken de anti-tumorimmuunrespons door de stimulerende of inhiberende signalen op DCs en T cellen te wijzigen. De systemische toediening van deze antilichamen in oplosbare vorm kan echter gepaard gaan met hevige toxiciteit en auto-immuun reacties. Om deze nadelen te overkomen zijn formuleringen die hun inhoud langdurig afgeven voor lokale toediening van deze antilichamen ontwikkeld, gebaseerd op IFA of Montanide. W/O emulsies gaan echter gepaard met bijwerkingen, zoals eerder vermeld in deze samenvatting, en zijn daarom geen wenselijke formuleringen. Polymere deeltjes bieden de mogelijkheid voor de vervaardiging van veilige en goed gedefiniëerde formuleringen, met aanpasbare afgifte-kinetiek. Om een immunotherapeutische stof lokaal vrij te geven zijn deeltjes in de orde van grootte van micrometers (>10 μm) wenselijk. Zulke microdeeltjes worden niet opgenomen door APCs en zijn daarom in staat hun lading op de plek van injectie af te geven zonder dat de therapeutische antilichamen daarbij worden geïnactiveerd door APCs. Net als bij NPs, is bij MPs de gezamenlijke toediening van meerdere therapeutische moleculen mogelijk.

Controlled release delivery systems gebaseerd on aliphatische polyesters

Poly(lactic-co-glycolic acid) (pLGA) is een alifatische polyester en is het meest gebruikte polymeer voor de toediening van peptides en eiwitten, maar er zijn verscheidene stabiliteitsproblemen met de encapsulering van deze moleculen.

Verzuring in de deeltjes tijdens hun afbraak kan chemische veranderingen, aggregatie, en incomplete afgifte van de lading veroorzaken, waardoor daarna bijwerkingen en gereduceerde effectiviteit optreden. Om dit nadeel van pLGA te overkomen, is in onze afdeling een hydrofiele polyester ontwikkeld genaamd pLHMGA. pLHMGA is met succes gebruikt voor encapsulering van verscheidene peptides en eiwitten. Daarnaast is het aangetoond dat pLHMGA na degradatie geen verlaging van de pH binnenin de deeltjes vertoont, met als resultaat dat er minder chemische verandering en aggregatie van de ingesloten eiwitten optreden. pLHMGA deeltjes vertonen een complete vrijgave van hun lading en worden daarom gezien als "eiwit- en peptidevriendelijk." Daarnaast zijn deze deeltjes biocompatibel *in vivo* en daarom werden ze geselecteerd als draagsysteem in dit proefschrift.

In dit proefschrift werden initieel pLHMGA nanodeeltjes beladen met ovalbumine (OVA) geëvalueerd als modelvaccins, en werden ze *in vitro* en *in vivo* bestudeerd. Gebaseerd op veelbelovende resultaten van dit onderzoek werd een therapeutisch kankervaccin ontworpen, op basis van een onco-eiwit van humaan papillomavirus genaamd HPV16 E7, dat goede resultaten heeft laten zien in klinische proeven. Een HPV SLP verkregen uit E7 (antigeen) en poly IC (TLR3 ligand) als adjuvant werden geëncapsuleerd in pLHMGA nanodeeltjeswaarna de therapeutische effectiviteit van het vaccin in muizen geëvalueerd werd. Voor de toediening van antilichamen werden pLHMGA microdeeltjes beladen met antiCD40 en antiCTLA4 waarna de antitumoreffecten van deze formuleringen geëvalueerd werden in tumordragende muizen. De therapeutische effectiviteit van deze nano- en microdeeltjes werd vergeleken met die van IFA emulsies om de deeltjes als alternatief voor IFA te evalueren.

Als onderdeel van het "Cancer vaccine tracking" project, uitgevoerd door CTMM (Center for translational molecular medicine), zijn in dit onderzoek op succesvolle wijze 1- De protocollen voor de bereiding van nano- en microdeeltjes beladen met immunotherapeutische agenten geoptimaliseerd 2- De immunologische activiteit van deeltjes *in vivo* in tumormodellen bestudeerd en 3- De *in vivo* imaging van een modelnanodeeltjesvaccin gecorreleerd aan T celimmuunresponsen. Dit modelvaccin is verder ontwikkeld tot een Humaan papillomavirus therapeutisch SLP vaccin tegen kanker.

Hoofdstuk 1 geeft een overzicht van kankerbestrijdingsmodaliteiten in klinisch gebruik, en geeft een korte uiteenzetting van de uitdagingen in de toediening van immunotherapeutica. Daarnaast wordt het potentieel van biologisch afbreekbare polymeren als dragers van immunotherapeutica behandeld.

Hoofdstuk 2 bediscussieert de toepassing van deeltjessystems gebaseerd op alifatische polyesters (in het bijzonder pLGA) in immuuntherapie tegen kanker. Toediening van immunotherapeutica is een uitdaging in het bijzonder door de gevoeligheid van deze macromoleculen *in vivo,* de zwakke en kortstondige immuunresponsen en de immuunsuppressieve werking van de tumoromgeving, die resulteert in immunologische tolerantie. Deeltjessystemen gebaseerd op pLGA en vergelijkbare polymeren hebben een groot potentieel deze problemen te overwinnen. In dit overzicht worden belangrijke parameters voor het ontwerp en de ontwikkeling van een succesvol deeltjes afgiftesysteem behandeld. Het effect van de immunotherapeutische stof, deeltjesgrootte, lading, enz. en hun effect op het type en de omvang van de immuunrespons worden getoetst, en er worden verscheidene voorbeelden gegeven van deze systemen voor immuuntherapie tegen kanker, inclusief kankervaccins en immunomodulatoire antilichamen.

In **Hoofdstuk 3** werd de haalbaarheid van het gebruik van pLHMGA dragersystemen geëvalueerd door middel van de encapsulering van het modelantigeen ovalbumine (OVA) in pLHMGA nanodeeltjes. Om deze deeltjes *in vivo* te kunnen traceren werden twee near infra-red dyes (NIR dye) gebruikt om OVA en de deeltjes te markeren. Hiertoe werd een alkyne-dragend poly(d,l lactic acid) (alkyne-pDLLA) gesynthetiseerd en werd de azide-gefunctionaliseerde NIR dye gekoppeld aan alkyne-pDLLA door middel van click chemie. NHS chemie werd gebruikt om OVA met een andere NIR dye te markeren. De dubbele emulsie oplosmiddelverdampings techniek werd gebruikt om bolvormige deeltjes van 300-400 nm te bereiden. De deeltjes lieten een lage burst afgifte zien gevolgd door een langdurige afgifte van OVA in 30 dagen tot 70% van de inhoud. De lage burst afgifte waargenomen bij pLHMGA NPs verdient de voorkeur omdat deze de voortijdige afgiftevan het antigeen, voordat dit opgenomen wordt door de dendritische cellen, voorkomt. *In vitro* studies van DCs lieten cytocompatibiliteit zien van zowel de lege als de met OVA beladen nanodeeltjes en hebben bewezen dat de markering geen toxiciteit tot gevolg heeft. *In vitro* studies gebruikmakend van Alexa647-OVA pLHMGA OVA nanodeeltjes lieten zien dat NPs op efficiënte wijze werden opgenomen door dendritische cellen (DCs) na een incubatie van 16 uur bij 37°C. Daarna werd de mogelijkheid van de OVA NPs tot kruispresentatie van het antigeen aan T cellen *in vitro* geëvalueerd, gebruikmakend van OVA-specifieke B3Z hybridoom T cellen. De verkregen resultaten lieten een doseringsafhankelijke en sterke T celactivering zien geïnduceerd door OVA nanodeeltjes, terwijl oplosbaar OVA niet in staat was om T cellen te activeren, zelfs niet bij hoge doseringen. Daarnaast waren de "dual labeled" nanodeeltjes even efficiënt in T celactivering als de ongemarkeerde nanodeeltjes, daarmee nogmaals bewijzend dat markering geen invloed heeft op de mogelijkheid van nanodeeltjes om een immuunrespons te induceren. Om de uitkomst van het model-nanodeeltjesvaccin *in vivo* te bestuderen werden "dual labelled" nanodeeltjes in de staartbasis van muizen geïnjecteerd en werden de signalen van twee NIR kleurstoffen gedurende meer dan 14 dagen gelijktijdig bekeken.

OVA en nanodeeltjes lieten dicht bij elkaar liggende NIR signaalpatronen zien, zowel op de plaats van injectie als in de lymfeklieren, wat suggereert dat het antigeen getransporteerd wordt in de vorm van nanodeeltjes. De verplaatsing van de nanodeeltjes uit de plek van injectie en ophoping in de lymfeklieren - waar de immuunrespons opgestart wordt - was meer geleidelijk dan bij oplosbaar OVA eiwit. Deze geprolongeerde bevoorrading van antigeen naar de lymfeklieren verzekert een sterke immuunrespons, die geobserveerd werd in een *in vivo* T cel proliferatietest uitgevoerd door adoptive transfer van OT-1 T cellen. OVA nanodeeltjes lieten een superieure antigeen-kruispresentatie aan OVA-specifieke CD8+ T cellen in de lymfeklieren en de milt zien, vergeleken met oplosbaar OVA. Samengevat toonde dit onderzoek het potentieel van pLHMGA nanodeeltjes als antigeentoedieningssystemen voor het induceren van immuunresponsen .

Aangemoedigd door de resultaten verkregen door het onderzoek behandeld in **Hoofdstuk 3** hebben we getracht een therapeutisch kankervaccin gebaseerd op pLHMGA nanodeeltjeste ontwikkelen voor de bestrijding van door HPV veroorzaakte kanker. Veel onderzoeken hebben de nadruk gelegd op vaccinatie met minimale peptide epitopen van HPV16 E6 en E7 onco-eiwitten; deze waren echter weinig succesvol. Het verlengen van peptide vaccins daarentegen heeft de ontwikkeling van synthetische lange peptides (SLPs) tot gevolg gehad, die veelbelovende resultaten hebben laten zien in zowel preklinische onderzoeken als in klinische proeven. Deze peptides worden gewoonlijk geformuleerd in IFA, wat geassocieerd is met ernstige en langdurige lokale bijwerkingen. Daarom werden in **Hoofdstuk 4**, teneinde een vervanging voor IFA emulsies te ontwikkelen, pLHMGA nanodeeltjes beladen met een HPV SLP (verkregen uit HPV16 E7 oncoproteïne) met of zonder een toll like receptor 3 (TLR3) ligand (poly IC)vervaardigd. De deeltjes waren bolvorming met afmetingen rond 400-500 nm (gemeten door "dynamic light scattering' (DLS)). De zeta potentiaal van de HPV SLPs was negatief door de carbonzuur eindgroepen van het polymeer. De HPV SLP + poly IC NPs vertoonden een nog meer negatieve zeta potentiaal dat waarschijnlijk veroorzaakt wordt door oppervlakte-geassocieerde negatief geladen poly IC moleculen. De therapeutische effectiviteit van de NP formuleringen met HPV SLP en poly IC (danwel co-geëncapsuleerd, danwel in oplosbare vorm) was vergelijkbaar met die van HPV SLP en poly IC geformuleerd in IFA. Alle formuleringen die HPV SLP en poly IC bevatten (inclusief NPs en IDA emulsie) zorgden voor een significante toename van de levensduur van tumordragende muizen (drie weken). Hoewel HPV SLP nanodeeltjes (zonder poly IC) de groei van tumoren vertraagde, konden ze niet significant de levensduur van muizen verlengen, en het effect van poly IC op zichzelf was vergelijkbaar met de waarnemingen voor de onbehandelde groep. In het bloed van muizen 9 dagen na de eerste vaccinatie was de populatie van HPV-specifieke CD8+ T cellen significant toegenomen indien gecombineerd met poly IC, danwel co-geëncapsuleerd met het antigeen, danwel in zijn oplosbare vorm, en met deze HPV-specifieke T celexpansie in het bloed kon het resultaat van het tumoronderzoek met succes voorspeld worden. Interessant is dat tussen de effecten van co-encapsulering van poly IC , en co-administratie van poly IC in de nanodeeltjesgeen significant verschil gevonden is. Het zou kunnen dat dit komt door de relatief hoge dosering van de gebruikte TLR ligand, dat misschien de verwachte superioriteit van de co- geëncapsuleerde TLR ligand gemaskeerd heeft, welke waargenomen is in eerdere onderzoeken. Niettemin kan de toediening van poly IC in oplosbare vorm systematische toxiciteit en autoimmuniteit veroorzaken; dit wordt daarom niet aangeraden. Onderhuidse toediening van nanodeeltjes - in tegenstelling tot IFA - vertoonde geen bijwerkingen op de injectieplek, en daarom werd er geconcludeerd dat (HPV SLP + poly IC) nanodeeltjes de geprefereerde formulering zijn, aangezien deze het beste veiligheidsprofiel hebben onder de geteste formuleringen terwijl ze een vergelijkbare therapeutische effectiviteit vertonen.

In **Hoofdstuk 5** werd het potentieel van de pLHMGA microdeeltjes voor lokale en langdurige toediening van immunomodulatoire antilichamen geëvalueerd. Vanwege de

belangrijke rol van CD40-CD40L in zowel DC activatie als rijping, en die van CTLA4 in immuunsuppressie, hebben we twee antilichamen gekozen, antiCD40 en antiCTLA4, die werden geëncapsuleerd in pLHGMA microdeeltjes. Vanwege de beperkte beschikbaarheid en de arbeidsintensieve en kostbare bereiding van de antilichamen, werd voor de optimalisatie van de formulering gebruik gemaakt van polyclonaal humaan IgG. Dit model IgG werd gekenmerkt met een NIR kleurstof om de gevoeligheid van kwantificering te verhogen. Teneinde een deeltjesformulering bruikbaar voor de lokale toediening van antilichamen te verkrijgen, hebben we gekozen voor pLHMGA met een 50/50 monomeer ratio. Dit polymeer bevat 25% van het hydrofiele BMMG monomeer, en de hypothese was dat het gebruik van een meer hydrofiel pLHMGA meer "antilichaamvriendelijk" zou zijn. Daarnaast hebben voorgaande onderzoeken aangetoond dat deeltjes gebaseerd op dit polymeer binnen ongeveer 30 dagen afbreken, wat wordt gezien als een passende tijdsspanne om een ingesloten antilichaam vrij te geven, en om daardoor het gewenste antitumoreffect te bereiken. Door de polymeerconcentratie gedurende de bereiding van de deeltjes te veranderen werden verschillende formuleringen bereid, en werden de afmetingen en morfologie van de deeltjes bestudeerd, alsmede de IgG *in vitro* afgifte-kinetiek. Er werd waargenomen dat door de polymeerconcentratie van 10% tot 30% te verhogen, de deeltjesgrootte toenam van rond 12 tot 25 µm, passende afmetingen om ongewenste opname te voorkomen door antigeenpresenterende cellen zoals dendtritische cellen en macrofagen. De deeltjes waren bolvormig en IgG werd geëncapsuleerd met een hoge ladingsefficiëntie (>80%). Deeltjes bereid met een polymeeroplossing met een concentratie van 10% vertoonden de hoogste burst release (35% van de lading), gevolgd door een langdurige afgiftevan het antilichaam tot 90% na 7 dagen. Een toename van de polymeerconcentratie had een afname in de burst release en een langere afgiftetijd tot resultaat: de formulering bereid met een polymeeroplossing van 30% vertoonde een burst afgifte van slechts 1% en een langdurige afgifte van 50% van de lading in 35 dagen. De formulering bereid met een polymeerconcentratie van 15% vertoonde een lage burst afgifte(12%) maar ook een langdurige afgiftevan het IgG tot 75% gedurende 35 dagen *in vitro*, en werd vanwege de gunstige afgiftekarakteristieken geselecteerd voor verder *in vivo* onderzoek. Gelijke doseringen van IgG in PBS, IFA of in microdeeltjes werden onderhuids bij muizen toegediend waarna de serum-antilichaamniveaus werden bekeken. IgG opgelost in PBS resulteerde gedurende 6 dagen in hoge IgG serumniveaus. Met de toediening van microdeeltjes waren de antilichaam-serumniveaus minstens 10 keer lager dan voor de oplosbare vorm gedurende 6 dagen na toediening. Dit was gunstig aangezien de lokaal toegediende microdeeltjes inderdaad IgG op een vertraagde manier vrijgeven, en de serumniveaus zijn waarschijnlijk laag genoeg om systemische toxiciteit te voorkomen. Daarna werden antiCD40 en antiCTLA4 geladen in de geoptimaliseerde formulering. Deze deeltjes vertoonden, voor wat betreft grootte, morfologie, ladingsefficiëntie en *in vitro* afgifte-kinetiek, karakteristieken gelijkend aan deeltjes bereid gebruik makend van polyclonaal IgG. De therapeutische effectiviteit van de microdeeltjes werd vergeleken met die van IFA formulerinegn, in muizen geïnoculeerd met darm carcinoom tumormodel (MC-38). Het overlevingspercentage van muizen behandeld met IFA formuleringen was vergelijkbaar met dat van muizen behandeld met de microdeeltjes: 30% overleving na 45 dagen wanneer behandeld met antiCTLA4 and 60% overleving na 55 dagen wanneer behandeld met antiCD40. Het is belangrijk om op te merken dat de microdeeltjesgeen lokale bijwerkingen veroorzaakten, en dat er geen overblijfselen van de deeltjes gevonden werden op de injectieplek 60 dagen na deeltjesinjectie, terwijl ontstoken ophopingen geobserveerd werden in muizen behandeld met IFA formuleringen. Ook waren de antilichaam-serumniveaus na toediening van microdeeltjes lager dan de niveaus geobserveerd met IFA formuleringen, overeenkomstig met data verkregen met polyclonal IgG .

Hoewel polymere deeltjes veelbelovende resultaten hebben laten zien als draagsystemen in immuuntherapie tegen kanker - specifiek als kankervaccins - staat de optimale deeltjesgrootte

om efficiënte opname door DCs te garanderen nog ter discussie, daarom is in **Hoofdstuk 6** het effect van deeltjesgrootte op de opname door DCs onderzocht. In dit onderzoek werden (Cy5) pLHMGA deeltjes gemerkt met NIR en beladen met Alexa488-OVA, met verschillende afmetingen (300 nm, and 1 and 2 µm), bereid en gekarakteriseerd op in hoeverre ze opgenomen worden door DCs *in vitro*. In flow-cytometrie studies lietenDCs een hogere mate van celbinding en opname na incubatie met nanodeeltjes zien, in vergelijking met microdeeltjes. Confocale laser scanning microscopie gebruikmakend van dubbel gelabelde deeltjes heeft laten zien dat OVA afgegeven werd in het cytoplasma van DCs na 24 uur incubatie met nanodeeltjes . Dit suggereert dat het antigeen gekruispresenteerd kan worden via MHC klasse I moleculen naar CD8+ T cellen om een cellulaire immuunrespons te induceren, die bijzonder gewenst is in immuuntherapie tegen kanker. Gelijkende co-localisatie onderzoeken uitgevoerd met microdeeltjes (2 µm) hebben laten zien dat de fluorescentiesignalen van deeltjes en OVA hoofdzakelijk co-gelocaliseerd zijn met de lysosomen. Dit doet vermoeden dat de OVA verwerkt en gepresenteerd wordt via MHC klasse I moleculen, wat niet per se een sterke T celrespons tot resultaat heeft.

Samenvattend bediscussieert dit proefschrift verscheidene toepassingen van nano- en microdeeltjesdragersystemen gebaseerd op een hydrofiel alifatisch polyester, poly(lactic-co-hydroxymethyl glycolic acid), pLHMGA, in immuuntherapie. Antigenen, adjuvanten en antilichamen werden geëncapsuleerd door middel van de dubbele emusie oplosmiddelverdampings techniek. Deeltjes met verschillende karakteristieken (grootte, afgifte-kinetiek) werden verkregen door variaties in formulerings- en verwerkingsparameters. Deze deeltjes vertoonden *in vitro* cytocompatibiliteit en worden *in vivo* goed getolereerd. Daarnaast is de therapeutische effectiviteit van formulering gebaseerd op pLHMGA polymeren vergelijkbaar met gebruikelijke W/O IFA emulsies in tumordragende muizen.

List of Publications

Particulate systems based on poly(lactic-co-glycolic)acid (pLGA) for immunotherapy of cancer
Rahimian S, Fransen MF, Kleinovink JW, Amidi M, Ossendorp F and Hennink WE.
Current Pharmaceutical Design, 2015 *In Press.*

Polymeric microparticles for sustained and local delivery of antiCD40 and antiCTLA-4 in immunotherapy of cancer
Rahimian S, Fransen MF, Kleinovink JW, Amidi M, Ossendorp F and Hennink WE.
Biomaterials, 2015; 61:33-40.

Polymeric nanoparticles for co-delivery of synthetic long peptide antigen and poly IC as therapeutic cancer vaccine formulation
Rahimian S, Fransen MF, Kleinovink JW, Christensen JR, Amidi M, Hennink WE and Ossendorp F.
Journal of Controlled Release, 2015; 203:16-22.

Near-infrared labelled, ovalbumin loaded polymeric nanoparticles based on a hydrophilic polyester as model vaccine: In vivo tracking and evaluation of antigen-specific CD8+ T cell immune response
Rahimian S, Kleinovink JW, Fransen MF, Mezzanotte L, Gold H, Wisse P, Overkleeft H, Amidi M, Jiskoot W, Löwik CW, Ossendorp F and Hennink WE.
Biomaterials, 2014; 37:469-477.

Computer modeling assisted design of monodisperse PLGA microspheres with controlled porosity affords zero order release of an encapsulated macromolecule for three months
Kazazi-Hyseni F, Landin M, Lathuile A, Veldhuis GJ, Rahimian S, Hennink WE, Kok RJ, and van Nostrum CF.
Pharmaceutical Research, 2014; 31(10):2844-2856.

Covalent attachment of a three-dimensionally printed thermoplast to a gelatin hydrogel for mechanically enhanced cartilage constructs
Boere KWM, Visser J, Seyednejad H, Rahimian S, Gawlitta D, van Steenbergen MJ, Dhert WJA, Hennink WE, Vermonden T and Malda J.
Acta Biomaterialia 2014;10(6):2602-2611.

The effect of lauryl capping group on protein release and degradation of poly(d,l-lactic-co-glycolic acid) particles
Samadi N, Abbadessa A, Di Stefano A, van Nostrum CF, Vermonden T, Rahimian S, Teunissen EA, van Steenbergen MJ, Amidi M and Hennink WE.
Journal of Controlled Release 2013; 172(2):436-443.

List of Abbreviations

Abu	Aminobutyric acid
ACN	Acetonitrile
APC	Antigen presenting cell
BMMG	Benzyl-protected hydroxymethyl methyl glycolide
BnOH	Benzyl alcohol
$CDCl_3$	Deuterated chloroform
CTL	Cytotoxic T cell
CTLA4	Cytotoxic T lymphocyte antigen 4
DC	Dendritic cell
DCM	Dichloromethane
DMF	Dimethylformamide
DLS	Dynamic light scattering
DMSO	Dimethylsulfoxide
DNA	Deoxyribonucleic acid
DSC	Differential scanning calorimetry
GPC	Gel permeation chromatography
HPLC	High performance liquid chromatography
HPV	Human papillomavirus
IFA	Incomplete Freund's adjuvant
L%	Loading percentage
LE	Loading efficiency
LiCl	Lithium chloride
Mn	Number average molecular weight
Mw	Weight average molecular weight
MHC	Major histocompatibility complex
MP	Microparticle
NaN_3	Sodium azide

NHS	N-hydroxysuccinimide
NIR	Near-infrared
NMR	Nuclear magnetic resonance spectroscopy
OVA	Ovalbumin
NP	Nanoparticle
PBS	Phosphate buffer saline
Pd/C	Palladium on carbon
PDI	Polydispersity index
PDLLA	poly (D,L lactic acid)
PEG	poly(ethylene glycol)
PLA	poly(lactic acid)
PLBMGA	poly(lactic acid-ran-benzyloxymethyl glycolic acid)
PLHMGA	poly(lactic-co-hydroxymethyl glycolic acid)
PLGA	poly(lactic-co-glycolic acid)
Poly IC	polyinosinic:polycytidylic acid
PVA	polyvinyl alcohol
SDS	Sodium dodecyl sulfate
SEM	Scanning electron microscopy
SLP	Synthetic long peptide
$SnOct_2$	Stannous octoate
TCR	T cell receptor
TEM	Transmission electron microscopy
TFA	Trifluoro acetic acid
THF	Tetrahydrofuran
TLR ligand	Toll like receptor ligand
Tg	Glass transition state
UV	Ultra violet

Affiliation of collaborating authors

Maryam Amidi
Department of Pharmaceutics, Utrecht Institute for Pharmaceutical Sciences, Utrecht University, Utrecht, The Netherlands

Jonatan Riis Christensen
Department of Pharmaceutics, Utrecht Institute for Pharmaceutical Sciences, Utrecht University, Utrecht, The Netherlands

Joep van den Dikkenberg
Department of Pharmaceutics, Utrecht Institute for Pharmaceutical Sciences, Utrecht University, Utrecht, The Netherlands

Rachid El Khoulati
Department of Biology, Utrecht University, Utrecht, the Netherlands

Marieke F Fransen
Department of Immunohematology and Blood Transfusion, Leiden University Medical Center, Leiden, The Netherlands

Henrik Gold
Leiden Institute of Chemistry, Leiden University, Leiden, The Netherlands

Wim E Hennink
Department of Pharmaceutics, Utrecht Institute for Pharmaceutical Sciences, Utrecht University, Utrecht, The Netherlands

Wim Jiskoot
Division of Drug Delivery Technology, Leiden Academic Centre for Drug Research, Leiden University, The Netherlands

Jan Willem Kleinovink
Department of Immunohematology and Blood Transfusion, Leiden University Medical Center, Leiden, The Netherlands

Dandan Li
Department of Pharmaceutics, Utrecht Institute for Pharmaceutical Sciences, Utrecht University, Utrecht, The Netherlands

Bo Lou
Department of Pharmaceutics, Utrecht Institute for Pharmaceutical Sciences, Utrecht University, Utrecht, The Netherlands

Clemens W. Löwik
Department of Radiology, Leiden University Medical Center, Leiden, The Netherlands

Sabrina S. Oliveira
Department of Biology, Utrecht University, Utrecht, the Netherlands

Ferry Ossendorp
Department of Immunohematology and Blood Transfusion, Leiden University Medical Center, Leiden, The Netherlands

Hermen Overkleeft
Leiden Institute of Chemistry, Leiden University, Leiden, The Netherlands

Laura Mezzanotte
Department of Radiology, Leiden University Medical Center, Leiden, The Netherlands

Dusan Popov-Celeketic
Department of Biology, Utrecht University, Utrecht, the Netherlands

Patrick Wisse
Leiden Institute of Chemistry, Leiden University, Leiden, The Netherlands

There is absolutely no way that I can "***acknowledge***" you here the way that I want. I very much would like to do this in person! This is just the tip of the iceberg.

Dear Professor Hennink, Oh no! I mean Dear Wim, the fact that I got a PhD position and finished it, I owe to you, and let's not forget, also to Professor Werner Heisenberg! I am grateful for everything that you taught me, and I truly appreciate your generosity in sharing your knowledge.

Professor Ossendorp, dear Ferry, I am grateful for your patience and for your kind guidance and critical comments. This project opened a new door to me, thank you!

Maryam aziz, I am extremely lucky to have you as a supervisor and as a friend, I learned so much from you both in science and in life! Thank you for your great support during the difficult times and for the happy memories. You are truly an inspiration to me! May we always be friends and go to concerts together!

Dear Marieke, Right from the start, we faced a lot of challenges during the course of this project…precious antibodies leaking from particles full of holes… but your positive attitude, expertise and kindness helped us overcome them. Being in the lab with you was always fun regardless of the result! It was a pleasure to work with you. Thank you!

Professor Jiskoot, dear Wim, I am grateful for all the fruitful discussions and collaborations.

Professor Schiffelers, dear Raymond, thank you for your support with the statistical analysis and for your uplifting spirit.

My dear colleagues and friends!
Thank you for sharing your life and occasionally lab equipment, helping me, and tolerating my singing. Well a lot of you are not colleagues anymore, we just happened to meet at the work place!

Mehrnoush, for your motherly care and friendship,
Burcin, for all the good chats and great moments full of sugar and laughter.
Luis! first of all for Portuguese food, but I also have to say I admire your devotion, wisdom and wit in research and in promoting everything about Portugal!
Kristel, for all the nice talks and helping me practice Dutch.
Farshad, for the great discussions about languages and cultures.
Mazda for sharing all the concerns in our projects.
Neda, Negar and Marzieh for occasional private tea breaks and pleasant talks,
Yang, for being so smart!
Amr for crashing into a bus one evening in my street and teaching me a lesson: It can always get worse than this!
Yvonne for your generous help with last minute experiments, I got to use rare equipments!
Sytze and Niels for sharing postdoc top secrets on how to perform an experiment like a real scientist! Niels you won and I have to admit I am thrilled for you!
Andhyk, for being there to rescue, always!
Edu, Gracia y las chiquis I am so happy to have met you, a family of genius and excellence y con mucho gezelligheid!
Filis jan, right from my first days in this department you have not been anything but kind,

sweet and helpful, but that was just the beginning! We shared so much from recipes to make particles! to recipes to make cakes! Low points and high points, Thanks for being such a sweet friend!
My dear Mereltje! Such a long history we have together sitting back to back for four years! So many sweet moments (especially in Spain) and so many rainy days, Thank you!
Dear Melody, How can you manage to be so cool and at the same time so caring?
Isil jan! I admire your energy and passion in whatever you do and the smile you never lose! Thank you for the great talks and good times together.
Dear Steffen, every time you passed my desk, I felt better and learned something new! Thank you!

The uptake team!
Half of our department plus many other colleagues and friends were helping me with this last small chapter;
Dandan, Bo, Dusan, Rachid, Sabrina, Nahid, Gerdien, Joep, Antoinette, Nataschja and last but not least Marcel who saved my life when no D1 cells were to be spotted in the horizon!
I appreciate your kindness in the last days of my PhD, your help meant a lot to me.

I learned a lot supervising students! I hope they learned as much as I did! Emily, Madeleine and Jonatan, Thank you for dedicating your time and energy!

Mies and Joep, being your neighbour was great fun and also a privilege. Mies thank you for all the help in the lab plus teaching me Dutch words that no one else did!
Joep thanks for all the great discussions about …everything on the way to the Kruyt building.

Barbara! I appreciate your friendly attitude and great help during past 5 years!

To my pLHMGA buddies; Jeffrey and Lucia, Wish you beautiful crystalline monomers and white fluffy polymers! Good luck with everything.

Many thanks to Gijs (Ruud) for connecting the two world of formulation in Utrecht and tumor immunology in Leiden and taking care of my beautiful and colourful particles!

My old friend Antonis, great times we had together, It seems to me the weather was better when you were here! Thank you for bringing the sun from Greece and making my early months in this country happier!

…and all the old and new colleagues + old and new friends: Kimberley, Anna, Shima, Marina, Jan Jaap, Roy, Gregorz, Amirs, Audrey, Ana Silva, Francesca, Meriem, Laura, Sun, Maria, Rachel, Yinan, Markus, Orn, Oil, Roberta, Albert, Erik, Anastasia, Alessandra, Lisa, Marc, Fariba, Jean-Michel, Inge, Louann, Heili, James, Emmy, Ebel, Ethlinn, Georgi, Kim, Louis, Reka, Feilong, Maripaz, Ellen, Mohammad, Violeta, Bas, Rocio, Jonas, Davide, Maarten, Jos, Vera, Hans and Albert!

See what a huge team of supporters I had?
I might have forgotten to mention some of you here but I will never forget how you made me feel home there!

Maman azizam, The kindest, Shafigh-tarin rafigh! Thanks for your immense love and support and for caring for me more than I do. Never seen such a self-sacrificing person in my life!

Dear dad! Babayi! your passion for science made me end up here! We had so many nerdy and unusual toys at home, you encouraged the curiosity and creativity in me!

Saman juni! You and I (Esba va Rua) are not typical sisters but you are always there for me when I need you and I try to do the same! Tara maun!

Farid khan, Atousa jun and Yasmin aziz! I cannot thank you enough for taking care of me all these years and making me feel home here in the second Mazandaran!

Parisa and Bahar my artist and intellectual friends! Talking to you is always good, you know what is important in life!

Poupak azizam, your friendship means a world to me. Thank you so much for the kind and sympathetic messages and motivating talks late at night or early in the morning!

Amir jan, our occasional talks and meet ups during these years were so great, made me feel young again!

Siamak jan, our friendship had a lot of ups and downs, right from the start probably at the age of 4! Let's blame it on the war and not us!

Layla junam, my dear childhood friend, your visits to Utrecht were delightful, so were our trips together! Thanks for all those days full of fun and poetry. But that was not all, you were the first young generation scientist in our group of friends (86!) Layla khanum!

(E)Scott jan, you were the witness to everything, thank you so much for being there for me and being the king of spontaneity!

Dear Jeske, We shared a lot of exciting moments of our lives together. Thanks for all the encouraging and exciting talks and great moments (including the window talks)!

Jan Willem jan! friend/colleague/paranymph… TODOS! You are present in all the lines of this book! I am so fortunate to have such a great scientist friend! OLE!

Dear Sarah, My life-long and dearest friend, my paranymph/saghdush! I learned so much from you, courage and kindness, You are my OSTAD! Salud to our friendship and thanks a lot for everything!

Emiel, Esmile, Tahmures khan and Tomas jan! Mi cariño! azizem! My favourite person in the whole world! A million thanks to you for "being".
Let's go… listen to more music!

"Vedi, non è lontano, Partiam, ben mio, da qui...
Andiam! andiam mio bene, a ristorar le pene, d'un innocente amor!
Vorrei e non vorrei..."

Don Giovanni, Mozart

Sima
Spring / Utrecht

Curriculum Vitae

Sima Rahimian was born in1982 in Iran. In 2000 she obtained her high school diploma from National Organization for Development of Exceptional Talents-NODET) and started studying pharmacy at Tehran University of Medical Sciences. She defended her thesis in medicinal chemistry in January 2007 and worked at Sobhan Oncology on development of liposomal formulations for delivery of docetaxel. From 2007 till 2009 she worked at hospitals affiliated with Semnan University of Medical Sciences as the responsible pharmacist. In 2010 she joined the department of Pharmaceutics at Utrecht University to work on development of cross-linkable polyesters for tissue engineering purposes. In January 2011 she started her PhD project on polymeric particulate systems for immunotherapy of cancer. The results of this project are presented in this book.